Influence of viscosity on the diffusion of charges

Kaouthar Ahmouda

Touhami Lanez

Acknowledgment

First and foremost I would like to thank god الله for giving me the strength and for keeping me healthy throughout the course of the project.

I would like to think it is an honor for me to preside the jury.

I would like to think Mr Settou Nouredine, professor in university Kasdi Merbah of Ouargla, Mr Saidi Mokhtar, professor in university Kasdi Merbah of Ouargla, Mr Ladjel Segni, professor in university Kasdi Merbah of Ouargla, and Mr Terki Belgacem, associate professor in university Kasdi Merbah of Ouargla, for agreeing to review my work.

I would like to thank my dear husband Mounir, without your support I would never done this, I could not have ask for a better husband- thank you.

I would like to thank my two families for being understood, without their support I would never continue this work.

I would like to show my gratitude to my third family, the family of my uncle, Said Mohamed Salah for all the support.

I would like to thank the entire research group for being like my family.

Finally, I would like to thank VTRS and University centre of El-Oued for allowing me to use my research in its laboratory.

Table of Contents

Acknowledgment *2*

Table of Contents *3*

Introduction *7*

Chapter 01 Voltammetry techniques, cyclic and rotating disc electrode *20*

1. Introduction *20*

2. Voltammetry technique *21*

2.1. Indicator electrode **21**

2.1.1. Mercury electrodes 22

2.1.2. Carbon electrodes 22

2.1.3. Metal electrodes 22

2.2. Reference electrode **22**

2.2.1. The saturated calomel electrode (SCE) 23

2.2.2. The silver/silver chloride electrode 23

2.3. Counter electrode **23**

2.4. The solvent **24**

2.5. The supporting electrolyte **24**

3. Unsteady state technique voltammetry *25*

3.1. Cyclic voltammetry **25**

3.1.1. Description 25

3.1.2. Principle 26

4. Theory of cyclic voltammetry *27*

4.1. Irreversible system **27**

4.2. Quasi reversible system **28**

4.3. Reversible system **29**

4.3.1. Generals Current –potential curves 32

4.3.2. Cyclic voltammetric curve 33

5. Hydrodynamic, steady state technique voltammetry *36*

5.1. Rotating indicator electrode voltammetry **37**

5.2. Current-Potential Curve **38**

5.2.1. Reversible system 38

5.2.2. Irreversible system 40

6. Electrical Double Layer *40*

6.1. Diffusion layer thickness **42**

7. Conclusion *43*

Chapter 02 Mass transfer by diffusion and the viscosity of liquid mixtures *44*

1. Introduction *44*

2. Diffusion mass principle *45*

2.1. Fick's Laws **46**

2.1.1. Fick’s first low 46

2.1.2. Fick’s second low 47

3. Diffusion Coefficients *48*

3.1. Estimation of Diffusion Coefficients in Dilute Liquid Mixtures **49**

3.1.1. Einstein stocks equation 49

3.1.2. Wilke and Chang correlation 49

3.2. Estimation of Diffusion Coefficients in concentrated Liquid Mixtures **50**

3.3. Caldwell and Babb equation **50**

3.4. Vignes equation **50**

4. Diffusion equations *50*

4.1. Diffusion equations solutions **51**

4.1.1. Steady-State Diffusion 51

4.1.2. Non-Steady-State Diffusion 51

4.2. Diffusion equation solution in electrochemical problem **53**

4.2.1. Boundary Conditions electrochemical Problem 53

4.2.2. Error Function Concentration Distribution 54

4.2.3. Diffusion profile for a diffusion couple 55

5. The Film Theory *56*

5.1. Concentration boundary layer **56**

6. Liquid mixture viscosity *57*

6.1. Viscosity definition **57**

6.1.1. Macroscopic viscosity definition 57

6.1.2. Microscopic viscosity definition 58

6.2. Kinematic viscosity **59**

6.3. Viscosity dependence on Temperature **59**

6.3.1. Arrhenius method 59

6.3.2. Duhne Representation 59

6.3.3. Qung-Fang et al. Equation 60

6.3.4. Lee and Wei Approach 60

7. Viscosities of Solutions and Mixtures *62*

7.1. Viscosities of Solutions **62**

7.1.1. Faulkenhagen Relations 62

7.1.2. Jones-dole equation 63
7.1.3. Kern rule 63

7.2. Liquid mixture viscosity 63
7.2.1. Method of Grunberg and Nissan 63
7.2.2. Unifac-Visco Method 65
7.2.3. Kendall and Monroe Relation 68
7.2.4. Arrhenius Equation 68
7.2.5. Method of Teja and Rice 68

8. Conclusion 71

Chapter 03 Effect of kinematic viscosity on the diffusion of charges 72

1. Introduction 72

2. Chemicals and materials 73

2.1. Chemicals 73

2.2. Materials 73

2.3. The properties of ferrocene, ferrocenyl methyl aniline and N-(ferrocenyl methyl)-2-nitro aniline 74
2.3.1. The properties of ferrocene 74
2.3.2. The properties of Ferrocenyl methyl aniline 75
2.3.3. The properties of N-(ferrocenyl methyl)-2-nitro aniline 75

3. General Process for preparation of studied solutions 76

4. Calculation of the kinematic viscosity of studied solutions at 25^0C 77

4.1. Calculation of dynamic viscosity of KCl aqueous solution 78

4.2. Calculation of the dynamic viscosity of fluids mixture 78
4.2.1. Calculation of interaction parameter 78
4.2.2. Calculation of critical volume 80
4.2.3. Calculation of critical volume of the mixture 80
4.2.4. Calculation of critical temperature, critical volume product 81
4.2.5. Calculation of critical temperature of the mixture 81
4.2.6. Calculation of dynamic viscosity of constituent in T_R 82
4.2.7. Calculation of parameter **ε** 83
4.2.8. Calculation of mixture viscosity of potassium chloride solution and ethanol in 25^0C 84

4.3. Calculation of dynamic viscosity of solution after adding the solute 84

4.4. Calculation of the kinematic viscosity of the medium 85

5. Study of electrochemical behavior and calculation of diffusion coefficients of charges 90

5.1. Study of electrochemical behavior of the supporting electrolyte 91

5.2. Study of electrochemical behavior and calculation of diffusion coefficients of ferrocene/ferrocenium couple 94
5.2.1. Study of electrochemical behavior of ferrocene 94

5.2.2. Calculation of diffusion coefficients of ferrocene/ferrocenium couple and diffusion layer thicknesses _____ 112

5.3. The electrochemical behavior of ferrocenyl methyl aniline and calculation of diffusion coefficient of ferrocenyl methyl aniline/ferrocenium 118

5.3.1. The electrochemical behavior of ferrocenyl methyl aniline _____ 118

5.3.2. The calculation of diffusion coefficient of ferrocenyl methyl aniline/ferrocenium couple and diffusion layer thicknesses _____ 137

5.4. The electrochemical behavior of N-(ferrocenyl methyl)-2-nitro aniline and calculation of diffusion coefficients of N-(ferrocenyl methyl)-2-nitro aniline/ferrocenium couple 142

5.4.1. The electrochemical behavior of N-(ferrocenyl methyl)-2-nitro aniline _____ 143

5.4.2. The calculation of diffusion coefficient of N-(ferrocenyl methyl)-2-nitro aniline /ferrocenium couple and diffusion layer thicknesses _____ 161

6. Discussion of results ***166***

7. Conclusion ***169***

Conclusion ***164***

Bibliography ***165***

Appendix ***171***

Introduction

The study of the effect of viscosity on the diffusion of ferrocene/ferrocenium, ferrocenyl methyl aniline/ferrocenium and of N-(ferrocenyl methyl)-2-nitro aniline/ferrocenium couples within medium containing aqueous ethanol at different percentages as the solvent, potassium of chloride as the electrolyte support is the aim of this work.

A small amount ferrocene, ferrocenyl methyl aniline, N-(ferrocenyl methyl)-2-nitro aniline was dissolved in a chosen volume of ethanol to prepare the principle solution (3mM) of each molecule, 5 ml of the principle solution was removed and it was replaced with 5ml of potassium chloride aqueous solution ($0.3M$) to prepare the first solution will be analyze (2.7mM, 90% aqueous ethanol), with the same process, the second solution(81% aqueous ethanol), the third solution (73% aqueous ethanol), the forth solution (66% aqueous ethanol), and the fifth solution (59% aqueous ethanol) solution for each molecule were prepared.

The electrochemical behavior and diffusion coefficients of studied couples in aqueous ethanol at different percentages, are investigated using two voltammetry techniques, One of the most well known technique of electrochemistry is the voltammetry which is a dynamic, microanalysis, Controlled-potential potentiostatic techniques, associated with the measurement and interpretation of current-potential (I-E) relationships [3]. in cyclic voltammetry technique, which is the most known, the calculation of diffusion coefficients is based on the extraction of current peaks densities(I_{Pa}, I_{Pc}) and using Randles-Sevcik relation to plot current peak densities as a function of the square root of scan rate which varied from 25, 50, 75, 100, to 150 mV/s. In rotating disc electrode voltammetry, the calculation of diffusion coefficients is based on the extraction of the limit current density (I_{lim}) and using levich relation to plot current limit density as a function of the square root of angular velocity, which varied from 1200, 1600, 1800, to 2000 rpm, at scan rate equals to 100 mV/s.

The dynamic viscosity of each prepared mixture is calculated using the most adequate models, of Faulkenhagen and of Teja –Rice.

This manuscript is organized as follows, we started by the theoretical part that consists of two chapters, the first is about the voltammetry techniques; cyclic and

rotating disc electrode voltammetry. The second is about the transfer of mass by diffusion and the viscosity of liquid mixtures and solutions. The experimental part is detailed in the third chapter, where we describe: firstly, done experiences. Secondly, the constructed VBA program which calculates the kinematic viscosity of mixtures. Thirdly, the study of electrochemical behavior of studied molecules using cyclic and rotating disc electrode voltammetry, on two different indicator electrode materials (GC, Pt), and calculation of diffusion coefficients and diffusion layer thicknesses in aqueous ethanol at different percentages on two different indicator electrode materials. Finally , discussion of the obtained results and conclusion.

Chapter 01

Voltammetry techniques, cyclic and rotating disc electrode

1. Introduction

Electrochemistry plays important roles in developing new areas of science and technology and makes essential contributions to solving global energy and environmental problems, deals with the phenomena associated with charge separation and charge transfer, which occur homogeneously in solutions or heterogeneously at electrode/solution interface [1], only redox active species present at the interface can undergo this electron transfer [2].

The electrochemical reaction at the interface makes the composition in the nearby solution different from the bulk of the solution further away. Because the solution tends to become homogeneous, redox active species diffuse between the bulk and the perturbed zone, in which the reactant is depleted. Convection due to heating or stirring makes the solution rapidly more homogeneous, thus reducing this zone from about 100 μm to less than 1 μm [2].

One of the most well known technique of electrochemistry is the voltammetry which is a dynamic, microanalysis, Controlled-potential potentiostatic techniques, associated with the measurement and interpretation of current-potential (I-E) relationships. [3] are become popular since 1940, Randles and Sevcik reported the

first cyclic voltammetric studies in 1948 , while the 1950s and 1960s saw the wide spread use of hydrodynamic techniques such as rotating-disc electrode (RDE) voltammetry and alternating current (AC) pulse and square -wave voltammetry [4][5].

The 1970s and early 1980s then witnessed the wide-spread use of microelectrodes, initially under slow scan rate near steady-state conditions then under extremely fast scan rate, transient DC voltammetric techniques. by the beginning of this millennium, an extensive range of voltammetric techniques have been made available and can be applied to redox active species in solution, solid and gas phases using conventional conducting electrodes, semiconducting electrodes and even poorly conducting materials and chemically modified electrodes[2].

2. Voltammetry technique

Within an electrolytic cell, the reactions of interest occur at the surface of the indicator electrode [1]. Therefore, we are interested in controlling the potential drop across the interface between the surface of the indicator electrode and the solution. [3]However, it is impossible to control or measure this interfacial potential without placing another electrode in the solution. Thus, two interfacial potentials must be considered, neither of which can be measured independently. Hence, one requirement for this counter electrode is that its interfacial potential remains constant, so that any changes in the cell potential produce identical changes in the indicator electrode interfacial potential, the interfacial potential of the counter electrode varies as the current is passed through the cell. This problem is over come by using a three-electrodes system, the influence of iR-drop is eliminated considerably with three-electrode instruments, if the tip of the reference electrode is placed near the surface of the indicator electrode, using a luggin capillary [6].

2.1. Indicator electrode

The oxidation/reduction reaction occurs at indicator stationary or rotating disk electrode’s surface, it should provide high signal to-noise characteristics, as well as a reproducible response [1], two factors depend on the selection of indicator electrode’s material: the redox behavior of the analyte and the background current over the potential region required for the measurement [2]. Other considerations include the

potential window, electrical conductivity, surface reproducibility, geometry, mechanical properties, cost, availability and toxicity [4].

2.1.1. Mercury electrodes

The dropping mercury electrode (DME), the hanging mercury drop electrode (HMDE), and the mercury film electrode (MFE) are the most frequently used for electrochemistry in aqueous solution [2]. have major advantages such as, greatly extend the cathodic potential window and possesses a highly reproducible, readily renewable, and smooth surface, roughness factor is equal to one . However the Disadvantages of the use of mercury are its limited anodic range, and toxicity [5].

2.1.2. Carbon electrodes

Solid electrodes based on carbon are currently in widespread use in electroanalysis, primarily because of their broad potential window, low background current, rich surface chemistry, low cost, chemical inertness, and suitability for various sensing and detection applications. In contrast, electron transfer rates observed at carbon surfaces are often slower than those observed at metal electrodes. **(**Glassy carbon electrode**,** carbon paste electrode**,** carbon fiber electrode, diamond electrode) [7].

2.1.3. Metal electrodes

Platinum and gold are the most widely used metallic electrodes, offer very favorable electron transfer kinetics and a large anodic potential range. In contrast, the low hydrogen overvoltage at these electrode limits the cathodic potential window [2], the high background currents associated with the formation of surface oxide or adsorbed hydrogen layers strongly alter the kinetics of the electrode reaction, leading to irreproducible data , other metals such as copper, nickel, or silver, have been used as electrode materials in connection with specific applications, such as the detection of amino acids or carbohydrates in alkaline media (copper and nickel) and cyanide or sulfur compounds (silver) [8].

2.2. Reference electrode

The reference electrode provides a stable and reproducible potential against which the potential of the indicator electrode is compared [2]. The saturated hydrogen electrode **(SHE)** is **primary referenced electrode** from which all other electrode reversible

potentials are derived, the SHE is so difficult to operate experimentally, and not particularly safe because it involves elemental hydrogen gas [6], that we avoid the SHE if it is at all possible [9], instead two electrodes, the calomel **(SCE)** and silver-silver chloride electrodes-are defined as secondary reference electrodes [10].

2.2.1. The saturated calomel electrode (SCE)

The saturated calomel electrode (SCE) **Hg/Hg_2Cl_2**, used to be widely used, the following equation illustrates the half cell reaction:

$$\frac{1}{2}\, Hg_2Cl_2(solid) + e^- \leftrightarrow Hg(liquid) + Cl^-(solution)$$

If the activity of the chloride ion is maintained at a constant level, then *SCE* will also have a constant value, which explains why this couple is the basis for a reference electrode [3]. The activity of chloride ion is best maintained by employing a constant *surplus* of KCl/NaCl crystals at the foot of the tube to ensure saturation, an SCE not having a thick crust of KCl/NaCl crystals should be avoided, since its potential might not be known [7].

2.2.2. The silver/silver chloride electrode

Today the saturated silver-silver chloride electrode Ag/AgCl is the most popular secondary reference electrode [2], the following equation illustrates the half cell reaction:

$$AgCl + (solid) + e^- \leftrightarrow Ag(solid)Cl^-(solution)$$

The saturated Ag/AgCl electrode is operationally similar to the calomel electrode but is more rugged [3]. Many other forms of reference electrode are used: Ag/Ag^+ (silver salt) electrodes, Ag or Pt wire quasi-reference electrodes [11]. The reference electrode should be separated from the electrolytic solution and indicator electrode by a salt bridge, take on consideration minimize junction potential [2].

2.3. Counter electrode

The counter electrode usually consists of a piece of platinum or carbon, of large surface area placed directly in the test solution Since current flows through the counter electrode [11], it must have a sufficiently large surface area relative to the

indicator electrode to prevent limitation of the current flowing in the total circuit, the current measured flows between the indicator and counter electrode [12].

2.4. The solvent

Three types of liquid substances, molecular liquids, ionic liquids and atomic liquids, can serve as solvents [1].They dissolve solutes that are solid, liquid or gaseous and form solutions [5]. Molecular liquid solvents are the most common and include besides water, many organic solvents and some inorganic solvents [6]. When a chemical reaction takes place in solution, the solvent is usually in so much excess that its concentration does not change appreciably as the reaction proceeds [9], and is therefore, not involved in the rate expression. The solvent must be appropriate for each measurement because it have significant effects on electrode processes [10].

- The electroactive species under study and the reaction products must dissolve and remain sufficiently stable in the solvent [13].
- A polar solvent of weak acidity is suitable for an electrode reaction that occurs at negative potentials or whose measurement is affected by acidic solvents.
- A polar solvent of weak basicity is suitable for an electrode reaction that occurs at positive potentials or whose measurement is affected by basic solvents.
- The solvent should be easy to purify, low in toxicity, benign to the environment, reasonable in price and should dissolve enough supporting electrolyte [14].
- Solvents of low viscosity will generally give electrolyte solutions with greater conductivities [15].

2.5. The supporting electrolyte

The supporting electrolyte plays various roles, to make the electrolytic solution conductive, to eliminate migration current that may flow in its absence, and to control reaction conditions by varying acid–base property [1], and complexing ability of the solution and by changing the double-layer structure at the electrode. The selection of supporting electrolyte must be carefully carried out, just as the selection of solvents. The supporting electrolyte can be base, acid, salt [11].

- It should be soluble in the solvent under study and should dissociate into ions to give enough conductivity to the solution.

- It should be resistant to oxidation and reduction and should give a wide potential window [1].
- It does not have an unfavorable effect on the electrode reaction to be measured [16].

3. Unsteady state technique voltammetry

Transient techniques involve a potential perturbation is applied to the Indicator electrode and the resulting current response associated with the reduction or oxidation reaction of interest is measured as a function of potential (time) [3].

The specification of voltammetry technique (linear, cyclic, square wave …) is given by the interpretation of the diagram, $E = f(t)$.

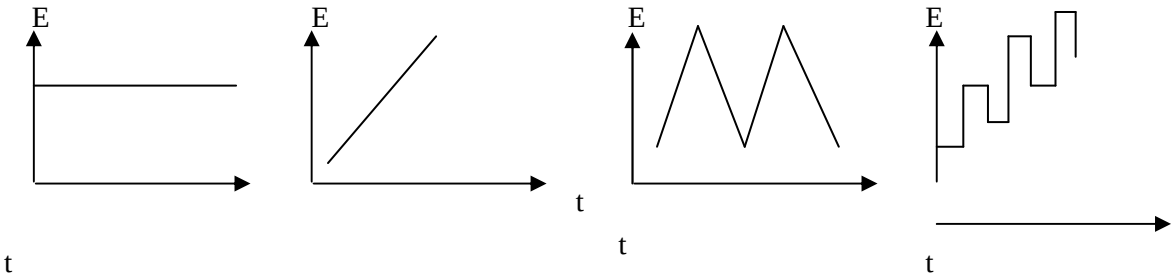

Figure I-1: voltage applied between the indicator electrode and the reference electrode.

3.1. Cyclic voltammetry

3.1.1. Description

Cyclic voltammetry is the most widely used technique for acquiring quantitative, qualitative information about electrochemical reactions [2]. Its power results from its ability to rapidly provide considerable information on the thermodynamics of redox processes and kinetics of heterogeneous electron transfer reaction and on coupled chemical reaction or adsorption processes and offers a rapid location for redox potentials of electroactive species and convenient evaluation of the effect of media on the redox processes [11].

3.1.2. Principle

The cyclic voltammetry technique consists of scanning linearly as function of time, the potential imposed on stationary indicator electrode, using triangular potential waveform depending on the information sought, single or multiple cycles can be used, Starts at value E_1,to a value E_2 (switching potential) with scan rate ν (V/s) [1], where the direction of scan is reversed and the stationary indicator potential reversed to its original value E1 .the starting potential is usually selected so that the chemical species under investigation are not initially oxidized or reduced and the switching potential is usually selected so that the potential interval E_1-E_2 contains an oxidation or reduction process of interest [17].

The plot of current flowing thought the stationary indicator electrode as function of the applied potential is termed a **cyclic voltammogram** [1]. The cyclic voltammogram is a complicated, time dependent function of a large number of physical and chemical parameters [4].

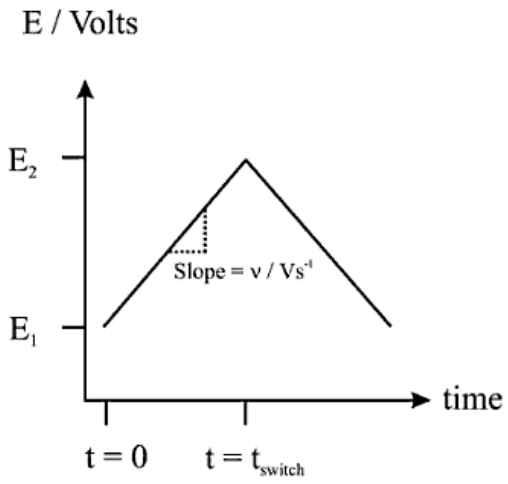

Figure I-2 the potential waveform applied to the indicator electrode in the cyclic voltammetry experiment [4].

Forward sweep: $E(t) = E_1 - \nu t \qquad 0 < t \leq \lambda$

Reverse sweep: $E(t) = -E_1 - 2\nu\lambda + \nu t \qquad t > \lambda$

4. Theory of cyclic voltammetry

4.1. Irreversible system

Charge transfer at the electrode is extremely slow .depending on the potential, only one of the cathodic or anodic heterogeneous reactions has a measurable rate, thus, the current is largely controlled by the rate of the charge transfer reaction [4].since the surface concentration at the electrode are dependent on the heterogeneous reaction and are far removed from thermodynamic equilibrium, one speaks of an irreversible process. Under such conditions, the Nernst equation does not apply, furthermore this means that measured potential value cannot be compared with thermodynamics equilibrium potentials [18].

- There is no reverse peak in an irreversible cyclic voltammogram because the reverse electron-transfer process does not occur at a measurable rate.
- The peak current, in amperes, at 25°C for an irreversible oxidation process is given by the expression,

$$I_P^{Ox} = (2.99 * 10^5) n(\alpha n_a)^{\frac{1}{2}} A D_A^{\frac{1}{2}} v^{\frac{1}{2}} [A_0] \qquad (I-1).$$

I_P^{Ox}: Peak current (mA/cm^2).

n : Total number of electrons transferred.

α: Charge –transfer coefficient (dimensionless).

n_a: Number of electrons transferred before the rate limiting electron transfer step.

A: Area of indicator electrode (cm^2).

D_A: diffusion coefficient of species A (cm^2/s).

v: scan rate (mV/s).

$[A_0]$: Concentration of species A, at the surface of the indicator electrode, (mol/cm^3).

- The peak potential is a function of scan rate, unlike the case for a reversible process when the peak potentials are independent of scan rate. As the scan rate increases, oxidation peak potential shifts to more positive potentials [4].

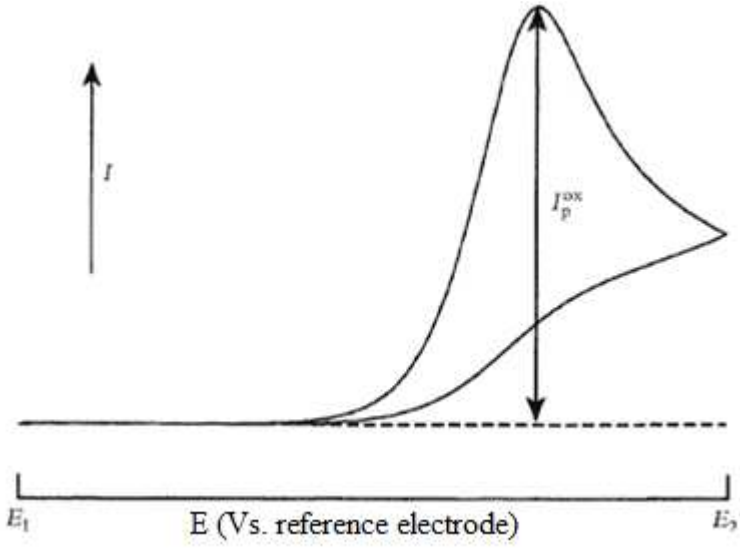

Figure I-3: Cyclic voltammogram obtained for an electrochemically irreversible one-electron oxidation process [4].

4.2. Quasi reversible system

Both the charge transfer and the mass transport determine the current. The Nernst equation is only approximately satisfied. The charge transfer is there for termed quasi reversible.

The scan rate can have a considerable effect on the nature of the observed cyclic voltammogram. At sufficiently slow scan rates, quasi-reversible processes appear to be fully reversible. However, as the scan rate is increased, the kinetics of electron transfer are not fast enough to maintain (Nernstian) equilibrium. In the scan rate region, when the process is quasi-reversible, the following observations can be made [4].

- The separation of the forward and reverse peaks ΔE_P is larger than the value of 59/n mV associated with a reversible process at 25°C. Importantly, ΔE_P increases with increasing scan rate and the value of the standard rate constant for the electron-transfer process, k^0, may be calculated from the separation of the peaks in a quasi-reversible process, provided voltammograms are corrected for solution resistance and background current effects.
- The peaks become broader as the scan rate increases, and the peak current is below the value expected for a reversible electron-transfer process.
- The magnitude of ratio of the peak currents is equal to unity for a quasi-reversible system when α= 0.5.

4.3. Reversible system

An example of an electrochemical reversible system is the simplest possible one-electron oxidation or reduction of a chemical species in solution at the indicator electrode. The rate of heterogeneous charge transfer is so high that a dynamic equilibrium is established at the phase boundary. Butler - Volmer equation is reduced to the Nernst equation [2], i.e, the surface concentrations depend only on the actual electrode potential and are no longer influenced by heterogeneous kinetic effects. The current, as a measurable quantity for the charge flux at the electrode surface, is influenced solely by mass transport; the slowest step (diffusion control).the characteristic shape of the cyclic voltammogram is a result of the potential-dependent changes in the surface concentration of the redox system and the simultaneous diffusion processes.

Matsuda and Ayabe proposed the following regimes in order to define whether an electron-transfer process will be observed to be reversible, quasi-reversible or irreversible [4]:

- Reversible: $k^0 \geq 0.3v^{1/2}cm.s^{-1}$.
- Quasi-reversible : $0.3v^{1/2} > k^0 > (2.10^5)v^{\frac{1}{2}}\,cm.s^{-1}$.
- Irreversibile: $k^0 \leq (2.10^5)v^{\frac{1}{2}}\,cm.s^{-1}$.

k^0: The standard rate constant for the electron-transfer process($cm.s^{-1}$).

v: The potential scan rate.

In reversible system we can write [19],

$$j_A(0,t) = \frac{i}{nFA} \qquad (I-2)$$

$$= C_A(0,t)k^0 exp\left[-\frac{\alpha nF}{RT(E-E^0)}\right] - C_B(0,t)k^0 exp\left[(1-\alpha)\frac{nF}{RT(E-E^0)}\right]$$

$$E = E^0 - \frac{RT}{nF}\,lnQ$$

i: the current.

n: electron transferred number.

F: faraday constant.

A: indicator electrode area.

R: gas constant.

T: absolute temperature.

α: Charge –transfer coefficient (dimensionless).

$j_A(0,t)$: Flux of species A at the surface of the indicator electrode, at time t.

$C_A(0,t)$: Concentration of species A at the surface of the indicator electrode, at time t.

$C_B(0,t)$: Concentration of species B at the surface of the indicator electrode, at time t [20].

Mass transfer to an electrode is governed by the Nernst –plank equation, written for one dimensional mass transfer along the x-axis as:

$$J_j(x,t) = -D_j \frac{\partial C_j(x,t)}{\partial x} - \frac{z_j F D_j C_j}{RT} \frac{\partial \emptyset(x,t)}{\partial x} + C_j(x,t)V(x,t) \qquad (\mathrm{I}-3)$$

$D_j \frac{\partial C_j(x,t)}{\partial x}$: represents the diffusion term.

$\frac{z_j F D_j C_j}{RT} \frac{\partial \emptyset(x,t)}{\partial x}$: represents the migration term.

$C_j(x,t)V(x,t)$: represents the convection term.

Only diffusion along the positive x-axis perpendicular to the electrode surface need be considered,

The NERNEST PLANK equation becomes,

$$J(x,t) = -D \frac{\partial C(x,t)}{\partial x} \qquad (\mathrm{I}-4)$$

The current (*I*) is directly proportional to the flux and the surface area (*A*)

$$\mathrm{I} = -\mathrm{nFAJ} \qquad (\mathrm{I}-5)$$

So;

$$I = nFAD \frac{\partial C(x,t)}{\partial x} \qquad (\mathrm{I}-6)$$

Hence, the current (at any time) is proportional to the concentration gradient of the electroactive species, as indicated by the equations above; the diffusional flux is time-dependent.

$$\frac{\partial C(x,t)}{\partial t} = D\frac{\partial^2 C(x,t)}{\partial x^2} \qquad (\mathrm{I}-7)$$

The diffusion equation is applied to species Ox and Red:

$$\frac{\partial Cox\ (x,t)}{\partial t} = Dox\frac{\partial^2 Cox(x,t)}{\partial x^2} \qquad (\mathrm{I}-8)$$

$$\frac{\partial C_{Red}(x,t)}{\partial t} = D_{Red}\frac{\partial^2 C_{Red}(x,t)}{\partial x^2} \qquad (\mathrm{I}-9)$$

- The solution is initially homogeneous , the initial concentrations of ox and Red are:

$t = 0 \qquad x \geq 0 \qquad c(x,o)_{ox} = c_{ox_0}^{*} \qquad c(x,0)_{Red} = 0$

- The electrolysis cell is large enough that the bulk concentrations of o and R are unchanged during the time of an experiment.

$t > 0 \qquad x \to \infty \qquad c(x,t)_{ox} = c_{ox_0}^{*} \qquad c(x,t)_{Red} = 0$

- For every ox molecule consumed, an Red molecule is formed at the electrode surface

$t > 0 \qquad x = 0 \qquad D_{ox}\frac{\partial [c_{ox}]_0}{\partial x} = -D_{Red}\frac{\partial [c_{Red}]_0}{\partial x}$

- The electron-transfer reaction is very fast so that 0 and R are always in equilibrium at the electrode surface with the concentration ratio given by the Nernst equation:

$t > 0 \qquad x = 0 \qquad \frac{C(0,t)_{ox}}{C(0,t)_{Red}} = \exp[(E - E0')\,nF/RT$

Ox, Red concentrations profiles are defined by the following equations respectively:

$$C_{0x}(x,t) = C_{0x}^{*}\frac{\varepsilon\theta + \mathrm{erf}\,(x/2\sqrt{D_0 t})}{1+\varepsilon\theta}$$

$$C_{Red}(x,t) = C_{0x}^{*}\frac{\varepsilon[1-\mathrm{erf}\,(x/2\sqrt{D_{Red}t})]}{1+\varepsilon\theta}$$

Where,

$\varepsilon = \sqrt{D_{0x}/D_{Red}}$,$\theta = \frac{C_{0x}(0,t)}{C_{Red}(0,t)}$

$$C_{0x}(0,t) = C_{0x}^{*}\frac{\varepsilon\theta}{1+\varepsilon\theta} \qquad (\mathrm{I}-10)$$

$$C_{Red}(0,t) = C_{0x}^{*}\frac{\varepsilon}{1+\varepsilon\theta} \qquad (\mathrm{I}-11)$$

$C_{0x}(0,t)$:concentration of the oxidized spicies at the surface of the indicator eletrode.

$C_{Red}(0,t)$:concentration of the reduced spicies at the surface of the indicator eletrode.

C_{0x}^{*}: bulk concentration of the oxidized spicies [21].

4.3.1. Generals Current –potential curves

The net current is proportional to the flux of Ox at the electrode,

$$I = -nFAJ_{0x}(0,t) \qquad (\mathrm{I}-12)$$

The flux is given by Fick's first law,

$$J_{0x}(x,t) = -D_{0x}\frac{\partial C_{Ox}(x,t)}{\partial x} \qquad (\mathrm{I}-13)$$

So,

$$J_{Ox}(x,t) = -C_{Ox}\frac{\sqrt{D_{Ox}/\pi t}}{1+\varepsilon\theta}exp\frac{-x^{2}}{4D_{0x}t} \qquad (I-14)$$

Setting $x = 0$, we have the flux at the electrode surface;

$$J_{Ox}(o,t) = -C_{Ox}^{*}\frac{\sqrt{D_{Ox}/\pi t}}{1+\varepsilon\theta} \qquad (\mathrm{I}-15)$$

Substituting equation (I-14) into equation (I-11), we obtain

$$I = nFAC_{0x}^{*}\frac{\sqrt{D_{Ox}/\pi t}}{1+\varepsilon\theta} \qquad (\mathrm{I}-16)$$

When the electrode potential is large and negative, E «E_0, θ and C_{ox} (0, t) are very small. In this case, every ox molecule that arrives at the electrode will be reduced. Making the potential more negative cannot make the current any larger because it is limited by the rate of diffusion of ox to the electrode. Setting θ= 0, then gives the limiting diffusion current [19]:

$$I_D = nFAC_{Ox}^{*}\sqrt{D_{Ox}/\pi t} \qquad (\mathrm{I}-17)$$

called the Cottrell equation The potential dependence of the current is most clearly seen if we eliminate time and the other parameters of by dividing by $i_{D:}$

$$\frac{I}{I_D} = \frac{1}{1+\varepsilon\theta} \qquad (\mathrm{I}-18)$$

Rearranging and substituting for ε and θ , we obtain a form which bears a superficial resemblance to the Nernst equation [20] :

$$E = E^{0} - \frac{RT}{nF} ln\sqrt{D_{ox}/D_{Red}} + \frac{RT}{nF} ln\frac{I_D - I}{I} \qquad (\mathrm{I}-19)$$

The first two terms on the right-hand side of equation (I-18) are usually lumped together to define a new parameter, called the *half-wave potential*,

$$E_{1/2} = E^{O} - \frac{RT}{2nF} ln\frac{D_{Ox}}{D_{Red}} \qquad (\mathrm{I}-20)$$

So;

$$E = E_{1/2} + \frac{RT}{nF} ln\frac{I_D - I}{I} \qquad (\mathrm{I}-21)$$

(I-20) called the Heyrovsky - Ilkovic equation [21].

4.3.2. Cyclic voltammetric curve

We will need to find the concentrations of Ox and Red, $C_{Ox}(x,t)$, and $C_{Red}(x,t)$, as functions of time and distance from the electrode, the problem is define by the same specifications 1-3 and just the forth must be recognized as having a time-dependent form [22],

$$\frac{c(0,t)_{ox}}{c(0,t)_{Red}} = f(t) = \exp[(E_1 - \nu t - E0')\, nF/RT]$$

with the Laplace transformation, the boundary condition can be written:

$$\frac{c(0,t)_{ox}}{c(0,t)_{Red}} = \theta e^{-\sigma t} = \theta S(t)$$

$$S(t) = e^{-\sigma t}, \theta = \exp[(E_1 - E0')\, nF/RT], \sigma = (\frac{nF}{RT})\nu$$

Laplace transformation of the diffusion equations and application of the initial and semi-infinite conditions leads to;

$$\bar{C}_{ox}(x,s) = \frac{C^*_{ox}}{s} + A(s)\exp\left[-\sqrt{\left(\frac{s}{D_{Ox}}\right)}x\right]$$

The transform of the current is given by;

$$\bar{I}(s) = nFAD_{ox}[\frac{\partial}{\partial x}\bar{C}_{ox}(x,s)]_{x=0}$$

Combining (I-13) with (I-14) we obtain,

$$C_{ox}(0,t) = C^*_{Ox} - [nFA(\sqrt{\pi D_{ox}})]^{-1}$$

by letting

$$f(\tau) = \frac{I(\tau)}{nFA}\int_o^t I(t-\tau)^{-1/2}d\tau$$

(I-15) can be written;

$$C_{ox}(0,t) = C^*_{Ox} - (\sqrt{\pi D_{ox}})^{-1}\int_o^t f(t-\tau)^{-1/2}d\tau$$

Similarly from an expression for C_R (0, x) can be obtained (assuming R is initially absent),

$$C_{Red}(0,t) = (\sqrt{\pi D_{ox}})^{-1}\int_o^t f(t-\tau)^{-\frac{1}{2}}d\tau$$

From these equations and the boundary condition we obtain;

$$\int_o^t f(t-\tau)^{-1/2}d\tau = \frac{C^*_{Ox}}{[\theta s(t)(\pi D_{Red})^{-\frac{1}{2}} + (\pi D_{Ox})^{-\frac{1}{2}}]}$$

$$\int_o^t I(t-\tau)^{-1/2}d\tau = \frac{nFA\pi^{1/2}D_{ox}^{1/2}C_{ox}^*}{[\theta s(t)\varepsilon + 1]}$$

Whereas before $\varepsilon = \sqrt{D_{0x}/D_{Red}}$

So the current equation is [23],

$$I = nFAC_{ox}^*(\pi D_{ox}\sigma)^{\frac{1}{2}}x(\sigma t) \qquad (\mathrm{I}-22)$$

The obtained voltammogram will have the following shape:

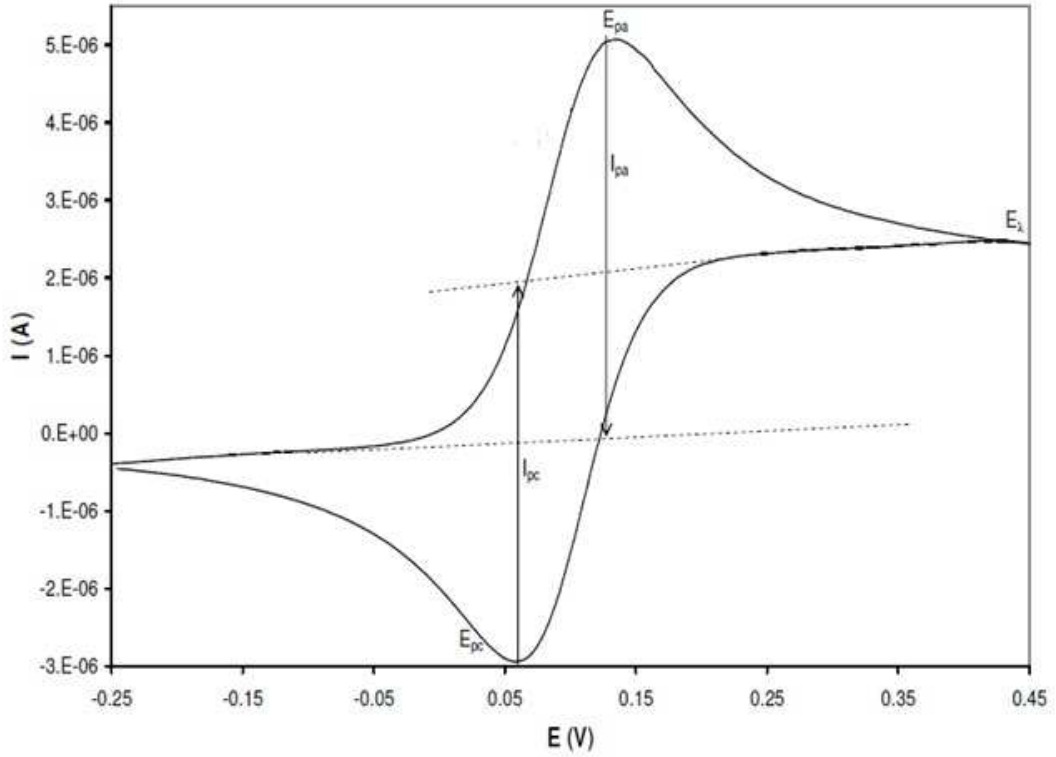

Figure I -4: cyclic voltammetric curve of reversible charge transfer obtained to show how the CV parameters [2].

Were evaluated E_λ = switching potential, $E_{1/2}$ =half wave potential , E_{Pa}, E_{Pc} = anodic,cathodic peak potential ,I_{Pa}, I_{Pc} = anodic, cathodic peak current.

The most important parameters are the two peaks potential E_{Pa}, E_{Pc} as well as the two peaks currentI_{Pa}, I_{Pc}.

For reversible charge transfer ($\alpha = 0.5$), without coupled chemical reaction [3]:

- $\frac{I_{Pa}}{I_{Pc}} = 1$
- $\Delta E_P = \left|E_{P,C} - E_{P,a}\right| = \frac{0.059}{n}\ V,\ (25\ ^0\mathrm{C})$.

- The peak current for a reversible couple (25°C) is given by the Randles–Sevcik equation:

$$I_P = 0.4463 \left(\frac{F^3}{RT}\right)^{1/2} n^{3/2} A C D^{1/2} v^{1/2} \qquad (I-23)$$

The multiplied constant 0.4463 is found with numerical simulation, it corresponds to the maximal value saved at the resolution of the theoretical equations which are drive to this relation [7].

F: faraday constant (C/mol).
R: gas constant (J/mol. K).
T: absolute temperature (K).
n: number of transferred electrons.
A: area of indicator electrode (cm^2).
C: the concentration in the bulk solution (mol/cm^3).
D: diffusion coefficient (cm^2/s).
ν : scan rate (mV/s).

- $E_{P,C}, E_{P,a}$ are independent on scan rate ,The half wave potential for a reversible couple is centered between$E_{P,C}$ and $E_{P,a}$ [6]:

$$\mathrm{E}_{1/2} = \frac{E_{P,C} + E_{P,a}}{2} \qquad (I-24)$$

- If Ox and Red have equal diffusion coefficients, $E_{1/2}$ is identical to the formal reversible potentialE_f^0. Otherwise, E_f^0 is related to$E_{1/2}$ by the expression,[23].

$$E_{1/2} = E_f^0 + \left(\frac{RT}{nF}\right) \ln(D_{Ox}/D_{Red})^{1/2} \qquad (I-25)$$

5. Hydrodynamic, steady state technique voltammetry

Hydrodynamic methods involve convective mass transport of reactants and products; there are many electrochemical techniques in which the indicator electrode moves with respect to the solution [2]. These involve systems where the indicator electrode is itself in motion (e.g., rotating disks, rotating wires, streaming mercury electrodes, rotating mercury electrodes, vibrating electrodes) or ones where there is forced solution flow past a stationary electrode (conical, tubular, screen, and packed-bed electrodes in fluid streams, channel electrodes, bubbling electrodes) ,with

hydrodynamic methods, a steady state is attained rather quickly and measurements can be made with high precision, at steady state, double-layer charging does not enter the measurement. Also, the rates of mass transfer at the electrode surface in these methods are typically larger than the rates of diffusion alone, so that the relative contribution of mass transfer to electron-transfer kinetics is often smaller [6].

The concentration distributions of each species in the electrode reaction mechanism are assumed to be temporally invariant at each applied potential, the effective time-scale of a near steady-state process is determined by the rate at which material reaches the electrode surface. This time-scale may be varied in a number of ways:

- Altering the convective rate of transport, for example, by changing the rotation frequency of a RDE.
- Decreasing the size of the electrode so that the ratio of radial to linear diffusion of material to the electrode surface is enhanced [3].

5.1. Rotating indicator electrode voltammetry

The indicator, rotating disk electrode (RDE) is circular disc of metal, graphite or another Conductor [2], vertically mounted in the shaft of a synchronous controllable-speed motor and rotated with constant angular velocity (ω) about an axis perpendicular to the plain disk surface the fluid in an adjacent layer develops a radial velocity that moves it away from the disk center [8], this fluid is replenished by a flow normal to the surface. Hence, the RDE can be viewed as a pump that draws a fresh solution up from the bulk solution (figure I-5) [9].

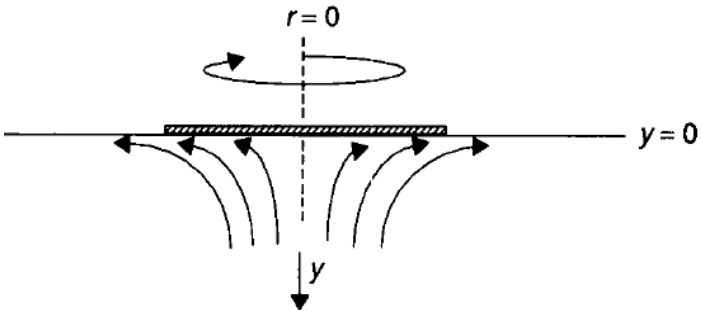

Figure I-5: Schematic representation of the fluid flow from the solution bulk and toward the face of an RDE (y = 0). Where the disc is spun about $r = 0$ at a frequency w.

5.2. Current-Potential Curve

5.2.1. Reversible system

Solutions to the mass transport equations are combined with the Nernst equation to obtain the reversible response shown in figure I-6, the steady-state convective-diffusion equation, written in terms of cylindrical coordinates, becomes [10]:

$$v_r\left(\frac{\partial C_{ox}}{\partial r}\right)+\frac{v_\emptyset}{r}\left(\frac{\partial C_{ox}}{\partial \emptyset}\right)+v_y\left(\frac{\partial C_{ox}}{\partial y}\right)=D_{ox}\left(\frac{\partial^2 C_{ox}}{\partial y^2}+\frac{\partial^2 C_{ox}}{\partial r^2}+\frac{1}{r}\frac{\partial C_{ox}}{\partial r}+\frac{1}{r^2}\left(\frac{\partial^2 C_{ox}}{\partial \emptyset^2}\right)\right)$$

After considerable simplifications, the equation becomes,

$$v_y\left(\frac{\partial C_{ox}}{\partial y}\right)=D_{ox}\frac{\partial^2 C_{ox}}{\partial y^2}$$

After mathematical treatment we obtain:

$$C_{0x}^{*}=\left(\frac{\partial C_{ox}}{\partial y}\right)_{y=0}0.8934\left(\frac{3D_{ox}\omega^{-\frac{3}{2}}\nu^{\frac{1}{2}}}{0.51}\right)^{\frac{1}{3}} \qquad (\mathrm{I}-26)$$

The current is the flux at the electrode surface, that is,

$$I=nFAD_{ox}\left(\frac{\partial C_{ox}}{\partial y}\right)_{y=0} \qquad (\mathrm{I}-27)$$

Where, under the chosen current conditions, we obtain the Levich equation:

$$I_{L,C}=-0.62nFAD_{ox}^{2/3}\omega^{1/2}\nu^{-1/6}C_{ox}^{*} \qquad (I-28)$$

$$I_{L,a}=0.62nFAD_{Red}^{2/3}\omega^{1/2}\nu^{-1/6}C_{Red}^{*} \qquad (\mathrm{I}-29)$$

$I_{L,C}$: limit cathodic current (mA).

$I_{L,a}$: limit anodic current (mA).

n: electron transferred number.

F: faraday constant (c/mol).

A: indicator electrode area (cm^2).

D_{ox}: diffusion coefficient of oxidized species (cm^2/s).

D_{Red}: diffusion coefficient of reduced species (cm^2/s).

ω: angular velocity (rad/s).

ν : Kinematic viscosity of medium (cm^2/s).

C ox: concentration of oxidized species (mol/cm3).

C Red: concentration of reduced species (mol/cm3).

With, $$E = E_{1/2} + \frac{RT}{nF} ln \frac{i_{l,c} - i}{i_{l,a} - i} \qquad (I - 30)$$

Where $$E_{1/2} = E_f^0 + \left(\frac{RT}{nF}\right) \ln(D_{Ox}/D_{Red})^{2/3} \qquad (I - 31)$$

The obtained polarogram will have the following shape,

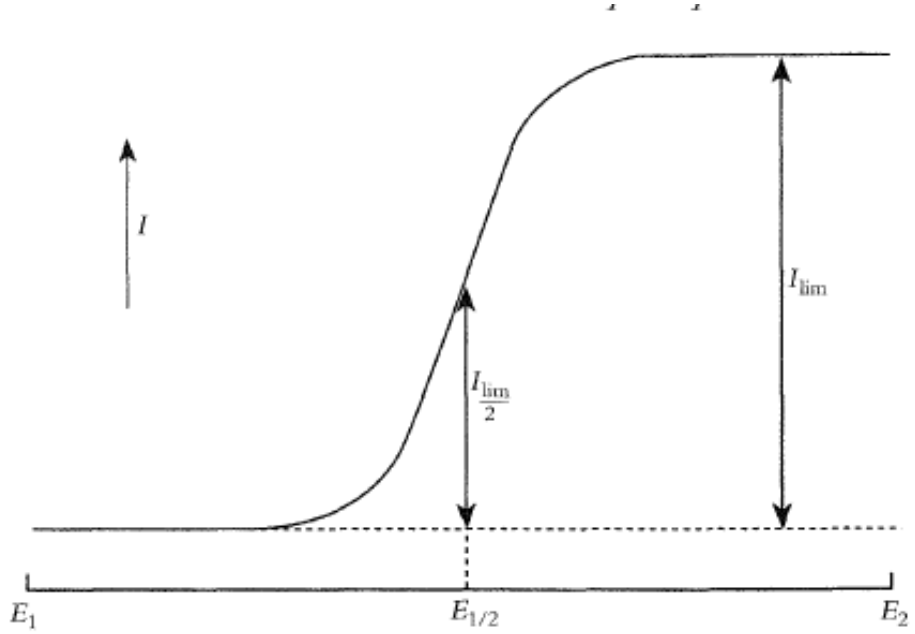

Figure I-6: polarogram obtained for a simple reversible one-electron transfer process at a hydrodynamic electrode [4].

The most important parameters are I_{lim} and$E_{1/2}$, for a reversible electron-transfer process a plot of E, versus $log_{10}[(I_{Lim} - I)/I]$ so-called 'log plot', will have a slope of;

- $E_{1/4} - E_{3/4} = 2.303RT/nF = \frac{0.059}{n}$ V, 25 ^{0}C.
- If Ox and Red have equal diffusion coefficients, $E_{1/2}$ is identical to the formal reversible potentialE_f^0, and it independent to ω (angular velocity).
- The shape of the wave for a reversible reaction is independent of ω. Thus, since i_l varies as $\omega^{1/2}$, i at any potential should also vary as $\omega^{1/2}$[8].

5.2.2. Irreversible system

For a totally irreversible one-step, one-electron reaction, the disk current is defined by Koutecky-Levich equation [9],

$$\frac{1}{i} = \frac{1}{i_k} + \frac{1}{i_{l,c}} = \frac{1}{i_k} + \frac{1}{0.62nFAD_{ox}^{2/3}\omega^{1/2}\nu^{-1/6}C_{ox}^{*}} \qquad (I-32)$$

$i_k = FAk_f(E)C_{Ox}^{*}$, with, $k_f(E) = k^0 exp[-\alpha f(E - E^{0\prime})]$

i_k,represents the current in the absence of any mass-transfer effects, that is, the current that would flow under the kinetic limitation if the mass transfer were efficient enough to keep the concentration at the electrode surface equal to the bulk value, regardless of the electrode reaction[12].

A comparison between a reversible and irreversible polarograms, one electron oxidation process, us illustrated in (figure I-7).

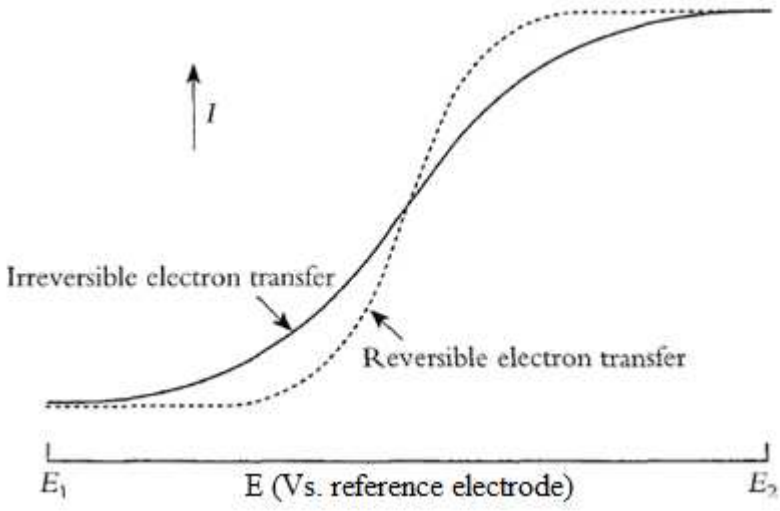

Figure I-7: Comparison of polarograms obtained for a reversible and irreversible one-electron oxidation process at a hydrodynamic electrode having equal half-wave potentials. [4]

6. Electrical Double Layer

The interface between an electrolyte solution and an electrode has come to be known as the electrical double layer [2]. The double layer is much thinner than the diffusion

layer because it is only a few molecular layers thick. Under the applied potential, the liquid and solid layers are charged at their interface. Heterogeneity is a common thread binding all electroanalytical methods. The act of placing an electrode in contact with a solution creates a phase boundary that differentiates identical solute molecules into two types; those at a distance from the electrode and those close enough to participate in the fascinating mutual interactions known collectively as electrochemistry. This is not a trivial distinction, for often it is the bulk-phase properties alone which are of analytical concern [3].

The electrical double layer reflects the ionic zones formed in the solution [1], has a complex structure of several distinct parts. the first layer is the inner Helmholtz plane (IHP), contains solvent molecules and specifically adsorbed ions, the next layer, the *outer Helmholtz plane* (OHP), reflects the imaginary plane passing through the center of solvated ions at their closest approach to the surface The solvated ions are nonspecifically adsorbed and are attracted to the surface by long range coulombic forces. The outer layer referred to as the *diffuse layer* (or *Gouy layer*), the equilibrium between these two opposing effects, indicates that the concentration of ionic species at a given distance from the surface, $C(x)$, decays exponentially with the ratio between the electrostatic energy and the thermal energy, the potential drops are a linear increase until the OHP and an exponential one within the diffuse layer [8] (Figure I-8).

The simplest reactions involve only mass transfer of a reactant to the electrode. Heterogeneous electron transfer involving non adsorbed species and mass transfer of the product to the bulk solution [2]. The movement of material from one location in solution to another arises either from differences in electrical or chemical potential at the two locations or from movement of a volume element of solution .the modes of mass transfer are:

- Diffusion (transport through a chemical potential gradient).
- Electric migration (transport through an electric potential gradient).
- Convection may occur either through gravity operating on a density gradient (natural convection) or through stirring of the solution or motion of the electrode (forced convection) [3].

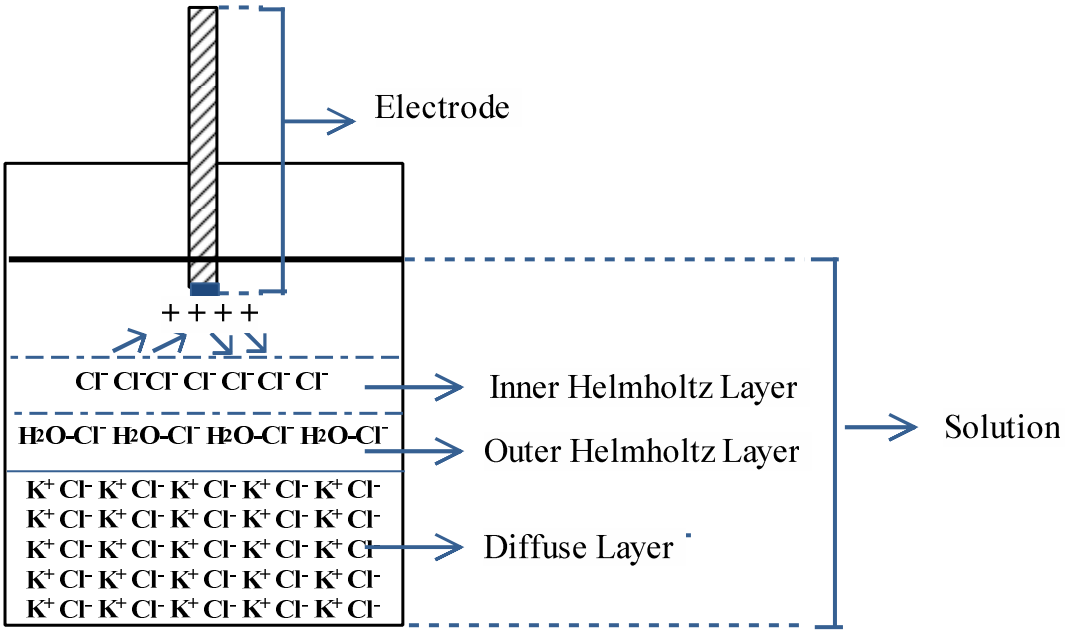

Figure I-8: Schematic representation of the electrical double layer.

6.1. Diffusion layer thickness

The diffusion layer is a layer near the electrode surface in which the solution is depleted of electroactive material [7]. We define the thickness of this depleted layer δ as the distance over which a linear concentration gradient would produce the same flux at the electrode surface as calculated from an exact solution to the diffusion equation. If the diffuser is deposited initially onto the surface of a sample and spreads into one half-space, the expression of diffusion layer thickness at stationary electrode is given by [8],

$$\delta = \sqrt{D_{Ox}t} \qquad (I-33)$$

δ: Diffusion layer thickness (cm).

D_{Ox}: Diffusion coefficient (cm^2/s).

t: the time (s).

The expression of diffusion layer thickness at rotating disc electrode is given by,

$$\delta_{ox} = 1.61 D_{ox}^{1/3} \omega^{-1/2} \nu^{1/6} \qquad (I-34)$$

δ_{ox}: Diffusion layer thickness.

D_{Ox}: Diffusion coefficient (cm^2/s).

ω: Angular velocity (rad/s).

ν: Kinematic viscosity of the medium (cm^2/s)

7. Conclusion

Rotated disk voltammetry is similar to cyclic voltammetry in that the indicator electrode potential is (slowly) swept back and forth across the formal potential of analyte [8]. It differs significantly in that the working electrode itself is rotated at a very high speed. This rotational motion sets up a well defined flow of solution towards the surface of the rotating disk electrode. The flow pattern is akin to a vortex that literally sucks the solution towards the electrode [19].

For qualitative studies of homogeneous reactions coupled to an electron-transfer process, cyclic voltammetry is by far the most commonly used technique [2]. It has the advantages of steady-state voltammetry in resolving a feature from each electrode couple as well as the advantages of the reversal techniques of chronoamperometry and chronopotentiometry that a single experiment often reveals the nature of the system. For quantitative measurements the other methods are often more accurate, but, with care, cyclic voltammetry can provide useful kinetic data with high sensitivity, selectivity toward electroactive species, a wide linear range, portable and low-cost instrumentation, speciation capability, and a wide range of electrodes that allow assays of unusual environments [11].

The RDE voltammetry provides an efficient and reproducible mass transport and hence analytical measurements can be made with high sensitivity and precision [1]. Such well-defined behavior greatly simplifies interpretation of the measurement. The convective nature of the electrode results also in very short response times, as a steady state is attained rather quickly, moreover, at steady state; double-layer charging does not enter the measurement. Also, the rates of mass transfer at the electrode surface in these methods are typically larger than the rates of diffusion alone, so that the relative contribution of mass transfer to electron-transfer kinetics is often smaller [6].

Chapter 02

Mass transfer by diffusion and the viscosity of liquid mixtures

1. Introduction

Mass transfer has a long and distinguished history dating to the 19th century, The development of mass transfer theory based on the film concept, which began in the 1920s and continued during two decades of intense activity, The 1950s and the decades that followed saw a second shift in emphasis, signaling a return to a more fundamental approach to the topic. Mass transfer was now seen as part of the wider basin of transport phenomena [23].

Most kinetic processes in ponderable media require the redistribution of mass, energy, momentum or charge, over macroscopic distances, occurs through a random process called diffusion, its macroscopic description rests on a particular differential equation called the diffusion equation [24].

Mass transfer is a fascinating subject as central our daily lives as it is to chemical industry, mass transfer equations describe the transport in living cells, the efficiency of distillation, and the dispersal of pollutants, mass transfer is responsible for gas absorption, for the fog formed by rain on snow, for dyeing of wool and for dissolution of sugar added to cup of tea [25].

many other procedures such as evaporation of petrol in carburetor, the liquid petrol is evaporated by sucked air at pressure lower than atmosphere, evaporation of liquid ammonia in the atmosphere of hydrogen in Electrolux refrigerator, humidification of air in cooling tower, or cooler air is cooling by using its heat to evaporate water, problems like those are easy to identify and fun to study [26]. Viscous friction forces control mass transfer and Resistances to mass transfer can occur [27][28] so, the concept of an effective film thickness, which lumps the resistance to transport into a fictitious thin film adjacent to a boundary or interface must be understood. Transport takes place through this film driven by the linear driving force across it and impeded by a resistance [23].

Mass transport is a process of transfer of mass due to the concentration difference of species in mixtures. The mixture may have one or more of species whose concentrations vary from point to point. The species having such variation of concentrations start transporting themselves from the region of higher concentration to lower concentration so long there is concentration difference of species, mass transfer will occur [25]. The atoms are randomly distributed in liquid and they are much closer together as a result the collisions are much more complicated many body interactions rather than simple two body- collisions the atoms or molecules in liquid are surrounded by other atoms or molecules which form a cage an atom or molecule moves within its cage, depends on momentum and velocity between an atom and other atoms or molecules with which it collides, three mechanisms are responsible to the mass transfer migration ,convection and diffusion [29].

2. Diffusion mass principle

Mass transfer by diffusion is the transport of substance at molecular or microscopic level, takes place from higher concentration region to lower concentration region of any substance in a mixture or system, it occurs when a substance diffuses through a layer of stagnant fluid, in case diffusing substance is in turbulent motion, then eddy diffusion occurs and mass transport of substance increases as compared to diffusion by only molecular diffusion [25].

2.1. Fick's Laws

At about the same time that Maxwell was developing his kinetic theory of gases, Thomas Graham, Adolf Fick, and others were attempting to uncover the basic diffusion equations through experimental studies involving binary mixtures, the result of Fick's work was the "law" that now bears his name (Fick, 1855)[30].

2.1.1. Fick's first low

Random Walk and Diffusion

From a microscopic viewpoint, diffusion occurs by the Brownian motion of atoms or molecules. In many instance we must may be unconcerned with the discrete nature of matter, the diffusing atoms are dissolved in low concentrations and that they move by jumping from an interstitial site to a neighboring one with a jump length λ, and with frequency Γ, We suppose a concentration gradient along the $x$direction, Without a driving force, forward and backward hops occur with the same jump rate and the net flux J from plane 1 to 2 is [24][29]:

$$J = \Gamma n_1 - \Gamma n_2 \qquad (\text{II} - 1)$$

The quantities n_1 and n_2 are related to the volume concentrations of diffusing atoms via:

$$C_1 = \frac{n_1}{\lambda}\,, C_2 = \frac{n_2}{\lambda} \qquad (II - 2)$$

$C(x.t)$ Changes slowly as a function of the distance variable x in terms of inter atomic distances.

From a Taylor expansion of the concentration-distance function keeping only the first term we get:

$$C_1 - C_2 = -\lambda \frac{\partial C}{\partial x} \qquad (\text{II} - 3)$$

Inserting equations (II-2) and (II-3) into (II-1) we arrive at,

$$J = -\lambda^2 \Gamma \frac{\partial C}{\partial x} = \boldsymbol{J(x,t) = -D\frac{\partial C}{\partial x}} \qquad (\text{II} - 4)$$

This equation is called Fick's first low Cartesian coordinates one-dimensional by comparison with Fick's first law we obtain for the diffusion coefficient: $D = \lambda^2 \Gamma$.

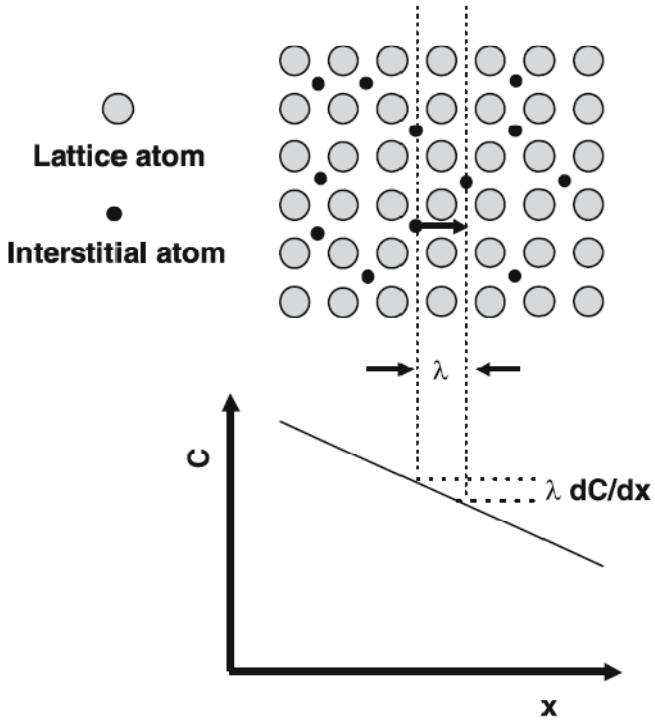

Figure II-1: Schematic representation of unidirectional diffusion of atoms in a lattice [29].

2.1.2. Fick's second low

Fick's first law equation (II-4) and the equation of continuity can be combined to give an equation which is called Fick's second law or sometimes also called the diffusion equation [28]:

$$\frac{\partial C}{\partial t} = \nabla.(D\nabla C) \qquad (II-5)$$

It is non-linear if D depends on concentration, but if the diffusivity is independent of concentration, it simplifies to,

$$\frac{\partial C}{\partial t} = D\Delta C \qquad (II-6)$$

This form of Fick's second law is sometimes also called the *linear diffusion equation*. It is a linear second-order partial differential equation for the concentration field $C(x.y.z.t)$. Where $\nabla^2 = \Delta$ is

The laplacian operator, defined as : $\nabla^2 = \frac{\partial^2}{\partial x^2} + \frac{\partial^2}{\partial y^2} + \frac{\partial^2}{\partial z^2}$.

The Laplacian operator on the right-hand side of equation (II-6) has different representations in different coordinate systems. Using these representations we get for isotropic diffusion the following forms of the linear diffusion equation [29].

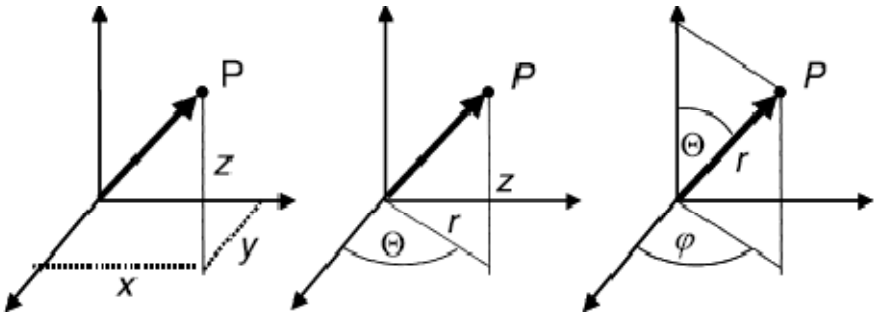

Figure II-2: Cartesian (left), cylindrical (middle), and spherical (right) coordinates [31].

Cartesian coordinates x, y, z:

$$D\nabla^2 C = \frac{\partial C}{\partial t} = D\left(\frac{\partial^2 C}{\partial x^2} + \frac{\partial^2 C}{\partial y^2} + \frac{\partial^2 C}{\partial z^2}\right)$$

Cylindrical coordinates r, θ, z:

$$D\nabla^2 C = \frac{\partial C}{\partial t} = D\left(\frac{1}{r}\frac{\partial\left(r\frac{\partial C}{\partial r}\right)}{\partial r} + \frac{1}{r^2}\frac{\partial^2 C}{\partial \theta^2} + \frac{\partial^2 C}{\partial Z^2}\right)$$

Spherical coordinates r, θ, ϕ:

$$D\nabla^2 C = \frac{\partial C}{\partial t} = D\left(\frac{1}{r^2}\frac{\partial\left(r^2\frac{\partial C}{\partial r}\right)}{\partial r} + \frac{1}{\mathrm{r^2}\sin\theta}\frac{\partial\left(\sin\theta\frac{\partial C}{\partial \theta}\right)}{\partial \theta} + \frac{1}{\mathrm{r^2}\sin^2}\frac{\partial^2 \mathrm{C}}{\theta\,\partial\phi^2}\right)$$ [25].

3. Diffusion Coefficients

Gas molecules spend most of their time in transit between collisions and are only modestly affected by intermolecular forces. In liquids these forces are the dominant factor that determines the mobility of the molecules. They are notoriously difficult to quantify, and as a consequence, the prediction of liquid diffusivities has lagged behind theories describing the motion of gas molecules. Diffusion coefficients in binary liquid mixtures are of the order $10^{-9} m^2/s$. Unlike the diffusion coefficients in ideal gas mixtures, those for liquid mixtures can be strong functions of concentration [30][31].

3.1. Estimation of Diffusion Coefficients in Dilute Liquid Mixtures

3.1.1. Einstein stocks equation

The Stokes-Einstein equation is a purely theoretical method of estimating D_{AB}^{0}, viewed the diffusion process as a hydrodynamic phenomenon in which the thermal motion of the molecules is resisted by a Stokesian drag force subsequent modification by Sutherland and Eyring, established the following proportionality for the diffusion coefficient, so that the diffusion coefficient is related to the viscosity by [24] :

$$D_{AB}^{0}\left(\frac{cm^2}{s}\right) = K_B \frac{T}{6\pi\mu_B r_A} \qquad (\text{II}-7)$$

This simple relation is valid only if the molecules of the diffusing species are very large compared to the solvent molecules (V_A > 500 cm^3/mol) [28], that diffusivity varies inversely with the viscosity of the solvent [30] and the molecular dimension of the diffusion molecule [31].

K_B : Boltzmann constant (1.38048J/K).
T: absolute temperature (K).
μ_B : dynamic viscosity of the solvent (cp)
r_A: Hydrodynamic radius of solute A.

3.1.2. Wilke and Chang correlation

One of the best known methods of semi empirical correlations of infinite dilution diffusivities proposed by Wilke and Chang has been reasonably successful in predicting diffusion coefficients of small molecules in aqueous and organic systems at normal temperatures. It has the form:

$$D_{AB}^{0}\left(\frac{cm^2}{s}\right) = 7.4 * 10^{-8}(\phi M_B)^{1/2}\frac{T}{\mu_B V_A^{0.6}} \qquad (\text{II}-8)$$

Where D is the diffusion coefficient of solute A, B incm^2/s; M_B is the molecular weight of solvent B in Daltons; T is the temperature in K; μ_B is the viscosity in centipoises; and V_A is the molar volume of the solute, incm^3/mol [32]. The empirical

parameter ϕ is 1 for most organic solvents, 1.5 for alcohols, and 2.6 for water. This result is widely used for fast estimates [33].

3.2. Estimation of Diffusion Coefficients in concentrated Liquid Mixtures

Most methods for predicting *D* in concentrated solutions attempt to combine the infinite dilution coefficients D_{AB}^{0} and D_{BA}^{0} in a simple function of composition [34].

3.3. Caldwell and Babb equation

The simplest expression proposed by Caldwell and Babb is recommended by Danner and Daubert.

$$D_{AB} = x_A D_{BA}^{0} + x_B D_{AB}^{0} \qquad (\text{II} - 9)$$

x_A, x_B : Mole fractions.

3.4. Vignes equation

Vignes suggested that the composition dependence of *D* can be expressed by a relation of the form:

$$D_{AB} = {D_{AB}^{0}}^{x_2} * {D_{BA}^{0}}^{x_1} \qquad (\text{II} - 10)$$

x_1, x_2 : Mole fractions.

This formula is recommended by Reid et al. (1987). The Vignes equation is less successful for mixtures containing an associating component (e.g., an alcohol). Alternative prediction methods need to be developed for such systems [30][35].

4. Diffusion equations

The diffusion equation is derived from Fick's first law by adding conservation of matter, the diffusion equations without convection in nonreactive systems are summarized below [29].

Unsteady state $\qquad \frac{\partial C}{\partial t} = \nabla^2 \mathrm{C} \qquad \mathrm{C} = \mathrm{f}(\mathrm{x}, \mathrm{t})$

Steady state $\nabla^2 C = 0$ $C = f(x)$

4.1. Diffusion equations solutions

4.1.1. Steady-State Diffusion

At steady state, there is no change of concentration with time. Steady-state diffusion is characterized by the condition [37]:

$$\frac{\partial C}{\partial t} = 0 \qquad (II - 11)$$

Table II-1: One dimensional, steady state diffusion in simple geometries

Geometry	**Mass flow rate (kg/s)**	**$R_{diffusion}$ (s/m^3)**	**Concentration distribution**
Plane membrane	$M_A = \frac{C_{A1} - C_{A2}}{\frac{L}{D_A A}}$	$\frac{L}{D_A A}$	$\frac{C_A - C_{A1}}{C_{A2} - C_{A1}} = \frac{X}{L}$
Cylindrical shell	$M_A = \frac{C_{A1} - C_{A2}}{\frac{ln\frac{r_2}{r_1}}{2\pi D_A L}}$	$\frac{ln\frac{r_2}{r_1}}{2\pi D_A L}$	$\frac{C_A - C_{A1}}{C_{A2} - C_{A1}} = \frac{ln\frac{r}{r_1}}{ln\frac{r_2}{r_1}}$
Spherical shell	$M_A = \frac{C_{A1} - C_{A2}}{\frac{\frac{1}{r_1} - \frac{1}{r_2}}{4\pi D_A}}$	$\frac{\frac{1}{r_1} - \frac{1}{r_2}}{4\pi D_A}$	$\frac{C_A - C_{A1}}{C_{A2} - C_{A1}} = \frac{\frac{1}{r} - \frac{1}{r_1}}{\frac{1}{r_1} - \frac{1}{r_2}}$

For the special geometrical settings mentioned, this leads to different *stationary concentration* distributions, table II-1, for linear flow we get:

$$D\frac{\partial^2 C}{\partial x^2} = 0 \qquad (\mathrm{II} - 12)$$

So the concentration distribution is of the form:

$$C(x) = a + Ax \qquad (\mathrm{II} - 13)$$

Where a and A denote constants, a constant concentration gradient and a linear distribution of concentration is established under linear flow steady-state conditions, if the diffusion coefficient is a constant [29][36].

4.1.2. Non-Steady-State Diffusion

Solutions of equation (II-6), giving the concentration as a function of time and position, can be obtained by various means once the boundary and initial conditions have been specified. In certain cases, the conditions are geometrically highly symmetric. Then it is possible to obtain explicit analytic solutions.

Such solutions comprise either Gaussians, error functions and related integrals, or they are given in the form of Fourier series,

$$\frac{\partial C(x,t)}{\partial t} = D\frac{\partial^2 C(x,t)}{\partial x^2} \qquad (\mathrm{II}-14)$$

Thin-Film Solution

An initial condition at t = 0, which is encountered in many one-dimensional diffusion problems, is the following: $C(x.0) = M\delta(x)$ .The diffusing species is deposited at the plane x = 0 and allowed to spread for t > 0. M denotes the number of diffusing particles per unit area and δ (x) the Dirac delta function. This initial condition is also called instantaneous planar source [38]. The solution equation (II-13) is according to the geometry.

Sandwich geometry

If the diffusant (or diffuser) is allowed to spread into two material bodies occupying the half-spaces $0 < x < \infty$ *and* $-\infty < x < 0$, which have equal and constant diffusivity, the solution is denoted as Gaussian solution,

$$C(x.t) = \frac{M}{2\sqrt{\pi Dt}}\exp\left(-\frac{x^2}{4Dt}\right) \qquad (II-15)$$

Thin-film geometry

If the diffuser is deposited initially onto the surface of a sample and spreads into one half-space, the solution is denoted as *Gaussian solution*,

$$C(x.t) = \frac{M}{\sqrt{\pi Dt}} \exp\left(-\frac{x^2}{4Dt}\right) \qquad (II-16)$$

The quantity $2\sqrt{Dt}$ is a characteristic *diffusion length*, which occurs frequently in diffusion problems [38].

4.2. Diffusion equation solution in electrochemical problem

In solving the mass-transfer part of an electrochemical problem, a diffusion equation is written for each dissolved species O, R.

$$\frac{\partial C_O(x,t)}{\partial t} = D_O \frac{\partial^2 C_O(x,t)}{\partial x^2} \qquad (\text{II}-17)$$

$$\frac{\partial C_R(x,t)}{\partial t} = D_R \frac{\partial^2 C_R(x,t)}{\partial x^2} \qquad (II-18)$$

4.2.1. Boundary Conditions electrochemical Problem

Initial Conditions

The initial condition express solution homogeneity before the experiment starts at,

$$t = 0, C_O(x,0) = C_O^*$$

The initial condition express that R, is initially absent from the solution,

$$C_R(x,0) = 0$$

Semi-infinite Boundary Conditions

The semi-infinite condition is an assertion that regions distant from the electrode are unperturbed by the experiment.

$$\lim_{x\to\infty} C_O(x,t) = C_O^* \,, \lim_{x\to\infty} C_R(x,t) = 0$$

Electrode Surface Boundary Conditions

The third condition, expresses the condition at the electrode surface after the potential transition, and it embodies the particular experiment we have at hand.

$$C_O(0,t) = f(E),$$

$$\frac{C_O(0,t)}{C_R(0,t)} = f(E)$$

$f(E)$ is some function of the electrode potential derived from the general current potential characteristic or one of its special cases (e.g., the Nernst equation).After Laplace transformation of (II-7), the application of conditions (II-8) and (II-9) yields,

$$\overline{C_O}(x,s) = \frac{C_o^*}{s} + A(s)e^{-\sqrt{s/D_o}x}$$

By applying the third condition, the function *A(s)* can be evaluated, and then $C_o = (x,t)$can be inverted to obtain the concentration profile for species Ox. Transforming of equation (II-7) gives:

$$\overline{C_O}(x,0) = 0$$

This implies that:

$$\overline{C_O}(x,s) = \frac{C_o^*}{s} + \frac{C_o^*}{s}e^{-\sqrt{s/D_o}x}$$

Inversion of this equation gives:

$$C_O(x.t) = C_o^*\left\{1 - erfc\left[\frac{x}{2\sqrt{D_O t}}\right]\right\}$$

as time goes by, the diffusion layer expands (to $\delta_2$andδ_3 at t_2 and t_3), and hence the concentration gradient decreases [8].

4.2.2. Error Function Concentration Distribution

The other important solution to the one-dimensional diffusion equation is used when the surface concentration stays constant, as during deposition onto the surface, that is during pre-dep [28]. The solution in this case is given by the complementary error function:

$$C(x.t) = C_S erfc\left(\frac{x}{2\sqrt{Dt}}\right)$$

where the complementary error function is defined in terms of the error function as:

$$erfc(z) = 1 - \text{erf}\,(z)$$

the error function is an integral of the Gaussian probability distribution function:

$$\mathrm{erf}(z) = \frac{2}{\sqrt{\pi}} \int_0^z \exp(-\eta^2)\, d\eta$$

These functions are important in statistical analysis, which is where the name comes from [39].

4.2.3. Diffusion profile for a diffusion couple

The flux into the surface depends on the concentration gradient at the surface, and this decreases with time,

$$J_{x=0} = -D\left(\frac{dC}{dx}\right)_{x=0} = \sqrt{\frac{D}{\pi t}}\, C_S \qquad (\mathrm{II}-19)$$

The same formal solution applies for a diffusion couple, where the two dissimilar materials are joined at x = 0, [28] as illustrated in figure II-3.

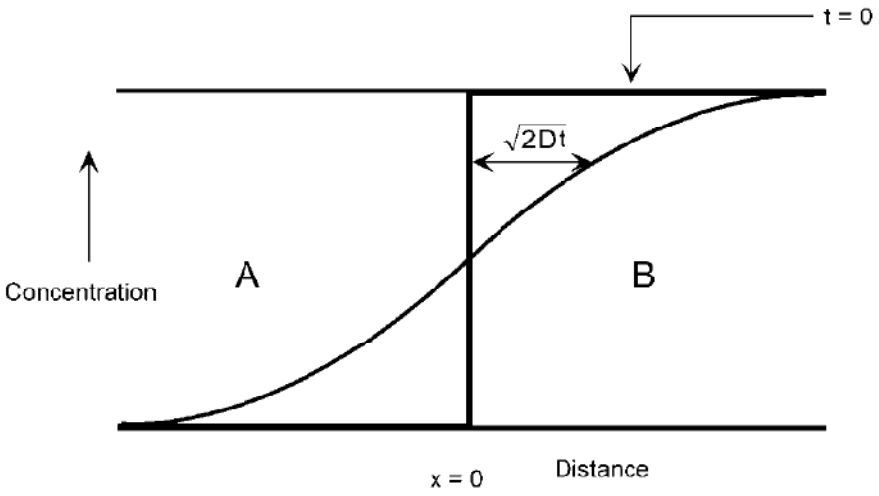

Figure II-3: Diffusion profile for a diffusion couple

5. The Film Theory

5.1. Concentration boundary layer

The simplest theory for interfacial mass transfer, assumes that a stagnant film exists near every interface. This film, also called an unstirred layer, when the fluid in motion and the solid surface are at different concentrations, a consequence of fluid-surface interaction is the development of a region in the fluid through which the concentration varies from zero at the surface to a finite value in the fluid, is almost always hypothetical, for fluid motions commonly occur right up to even a solid interface. Nonetheless, such a hypothetical film, suggested first by Nernst in 1904, gives the simplest model of the interfacial region [29].

it provides simple physical insight into mass transfer, for it shows in very simple terms how resistance to mass transfer might occur near an interface ,In the film model, we imagine that all of the resistance to mass transfer is concentrated in a thin film, or layer, adjacent to the phase boundary [30].

Also that transfer occurs within this film either by turbulent fluid flow then the solute concentration within this region will be constant and mass transfer will be by the reaction rate at the interface, or by steady-state molecular diffusion if the boundary layer involves laminar flow, then a concentration gradient will develop between the solid surface and the bulk fluid, so the mass transfer will be controlled by diffusion, by boundary layer. And it often accurately predicts changes in mass transfer caused by other factors, like chemical reaction or concentrated solution [40][41].

The concentration boundary layer is the region of the fluid in which concentration gradient exists, and its thickness δ_c , is defined as the value of y for witch $[(C_{AS} - C_A)/(C_{AS} - C_{A\infty})] = 0.99$, (figure II-4), [38] with increasing distance from leading edge the effects of species transfer penetrate further more in the bulk fluid and the concentration boundary layer grows.

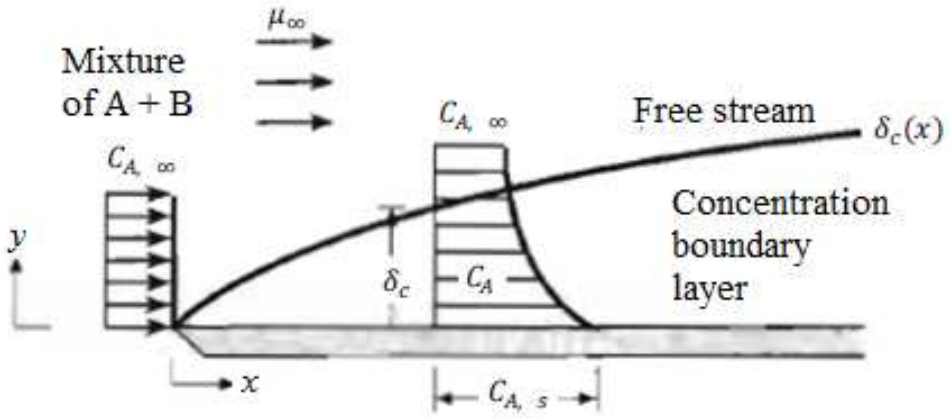

Figure II-4: species concentration boundary layer development on a flat plate

6. Liquid mixture viscosity

The need for properties is ever increasing to make processes more economical. A good survey of the viscosity data, its critical evaluation and correlation would help design engineers, scientists and technologists in their areas of interest [42]. All liquids and gases have a *viscosity*, is expressed as an internal friction when the shape of the fluid is changed. Particularly viscous liquids are honey, glycerin, and thick oils [27]. Although the viscosities of both liquids and gases change with temperature and pressure, they affect the viscosity in a different manner [42][43].

6.1. Viscosity definition

Viscosity is a fundamental property of fluid due to cohesion and interaction between molecules [42], offers resistance to flow or shear. Viscosity can also be termed as a drag force and is a measure of the frictional properties of the fluid. It is a function of temperature, pressure and molecule proprieties. The inverse of viscosity is called the fluidity [44][45].

6.1.1. Macroscopic viscosity definition

Stationary Newtonian fluid flow is between two plates infinite parallels with each other separated by, in the direction perpendicular to$y$, one plate held fixed the other plate moves parallel to itself at a constant speed V_0 along ox direction [25], the fluid is driven by the motion (figure II-5), at steady state motion the fluid velocity varies linearly from 0 to V_0 from plate to the other:

$$V_x(y) = V_0 \frac{y}{a}$$

The flow realized is called the simple shear flow or the plane coquette flow, proportionality between the friction forces F opposed to relative plate motion and the change of speed to plate to another is given by Newton's second law:

$$\sigma = \frac{F_x}{S} = \mu \frac{V_0}{L} = -\mu \frac{\partial V_x}{\partial y} \qquad (\text{II} - 20)$$

The report$\sigma = \frac{F_x}{S}$, is called shear stress and it has pression unity [27][46].

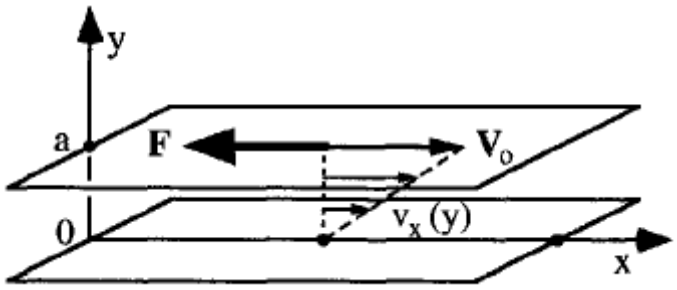

Figure II-5: simple shear flow geometry

6.1.2. Microscopic viscosity definition

The shear stress due to the velocity gradient promotes the jump of the particle from its cage to the neighboring cage, which it ensured by the activation thermal energy $K_B T$, so the jump's frequency satisfies Max well equation; the shear stress is given by the following equation [27]:

$$\sigma = \frac{h}{\alpha} \exp\left(\frac{\Delta g_0}{K_B T}\right) \frac{\partial V_x}{\partial y}$$

$$\mu = \frac{h}{\alpha} \exp\left(\frac{\Delta g_0}{K_B T}\right) \qquad (II - 21)$$

h: Plank constant,$6.62.10^{-34}$ (J/s).

Δg_0: Activation energy.

$K_B T$: Thermal energy.

$\frac{\partial V_x}{\partial y}$: Velocity gradient.

The constant materialμ, is called dynamic viscosity.

6.2. Kinematic viscosity

Kinematic viscosity is the transport of momentum by diffusion, plays a fundamental role in determining the fluid's motion, that is due to viscous stresses is determined by ν rather than byμ. Kinematic viscosity , ν, governs flow's stability, increases, flow's stability increases too [46], the kinematic is the dynamic viscosity to mass density ratio [47]:

$$\nu = \frac{\mu}{\rho} \qquad (\mathrm{II}-22)$$

6.3. Viscosity dependence on Temperature

The liquid viscosity decreases as the temperature increases, several methods have been proposed for the estimation of pur liquid viscosity from a variety of input information [48].

6.3.1. Arrhenius method

Arrhenius proposed the following relation to calculate the pur liquid viscosityμ [49]:

$$\mu = \frac{h}{\frac{V}{N}} \exp\left(3.8\frac{T_e}{T}\right) \qquad (II-23)$$

h: Plank constant, $6.62.10^{-34}$ (J.s).
v: mole volume (m^3/mol).
N: Avogadro Ampere number, $6.023.10^{23}$.
T_e: boiling temperature.

6.3.2. Duhne Representation

Duhne presented his relation in the logarithmic form as [49]:

$$ln\mu = A + \left(\frac{B}{T}\right) \qquad (\mathrm{II}-24)$$

A, B: are constants given by Duhne.

6.3.3. Qung-Fang et al. Equation

Qung-Fung et al proposed the following equation to calculate the pur liquid viscosity [49]:

$$\mu = \frac{hN}{V}\exp\left(\frac{\Delta G^*}{T}\right) \qquad (I-25)$$

h: plank constant, $6.62.10^{-34}$ (J.s).
v: mole volume (m^3/mol).
N: Avogadro Ampere number, $6.023.10^{23}$.
ΔG^*: Activation energy in boiling temperature.

6.3.4. Lee and Wei Approach

Lee and Wei proposed a corresponding states model applicable to the calculation of the viscosity of liquids using oxygen (r_1), octane (r_2) and water (r_3) as three reference fluids [49]. The corresponding states model based on three reference fluids can be written as:

$$\mu_R(T_R, P_R) = \mu_R^{r_1} + \frac{\alpha-\alpha^{r_1}}{\alpha-\alpha^{r_2}}\left[\mu_R^{r_1}-\mu_R^{r_2}\right] + \beta^*\left[\mu_R^{r_3} - \left(\mu_R^{r_1} + \frac{\alpha-\alpha^{r_1}}{\alpha-\alpha^{r_2}}\right)\left(\mu_R^{r_1}-\mu_R^{r_2}\right)\right]$$

With

$$\mu_R = ln\left(\frac{\mu}{\mu^*}+1\right) ;\mu^* = \frac{M^{1/2}{P_C}^{2/3}}{(RT_C)^{1/6}N^{1/3}}$$

$$T_R = T/T_C\theta; P_R = P/P_C; \beta^* = \beta/\beta^{r_3}$$

Where *N* is the Avogadro's number and the parameters are: α (radius of gyration), θ (energy correction factor) and β* (an empirical dimensionless polar/association parameter relative to water) that characterize the size/shape and polar/hydrogen-bonding effects. As already mentioned, the reference fluids selected are: oxygen, octane, and water. The reduced viscosity of the chosen reference fluids can be expressed as:

$$\mu_R^i = A_0 + (A_1/T_R) + A_2T_R + A_3T_R^2 + A_4P_R + A_5P_R^{0.5} + A_6T_RP_R \text{ (II}-26)$$

The value of the parameterθ as unity. The coefficients of the equation for the reference fluids (chosen) are listed in the following Table.

Table II-2: The coefficients of the equation for the reference fluids

Substance	Oxygen	Octane	Water
A_0	-6.65720	-5.10800	-44.7450
A_1	2.63270	2.72726	10.4698
A_2	11.4927	9.14020	75.4262
A_3	-6.41400	-5.52700	-43.8460
A_4	0.00392	-0.03138	-0.05814
A_5	0.00920	0.01440	0.00130
A_6	0.0910	0.0883	0.12030

The method provides for the calculation of the dynamic viscosity from a knowledge of the model parameters (T_C, P_C, α, θ and β*). While θ can be estimated from the following equation with the coefficients given for each class of compounds, β* has to be calculated from a knowledge of the viscosity of the fluid at one known temperature and pressure.

$$\theta = B_0 + (B_1/Z_C) + B_2 T_C^{0.5}$$

Z_C is the critical compressibility factor and T_C is the critical temperature in K. The coefficients of this for different classes of organic compounds are given in the following Table.

Table II-3: Coefficients of the generalized equation for θ for different classes of substances

Substance class	B_0	B_1	B_2
Alkanes	1.1403	-0.11630	0.01366
Alkenes	0.6985	0.10294	-0.00513
Alicyclics	3.2093	-0.47549	-0.01465
Alkylbenzenes	2.2787	-0.34340	-
Alkylhalids	0.4126	-	0.03202
Alcohols	5.2358	-0.30248	-0.11702
Ethers	0.6162	0.10376	-
Ketones	0.8327	0.04376	-
Carboxylic acids	1.1199	0.00584	-
Esters	1.5208	-0.11563	-
Nitriles, Amines, etc.	2.2758	-0.00428	-0.04924
Benzene derivatives	0.2938	0.18358	-

Pure liquid viscosities are predicted with an average absolute deviation of about 5 to 7%, depending on the types of substances and the temperature and pressure conditions [49].

7. Viscosities of Solutions and Mixtures

Viscosities of solutions meaning homogeneous products of dissolution of solids or gases in liquids, and fluid mixtures meaning homogeneous mixtures resulting out of mixing of two or more fluids are often needed for the design of the different unit operations and processes involved, While it will be ideal to measure the viscosities of the solutions and mixtures at the conditions of interest [46][50].

7.1. Viscosities of Solutions

7.1.1. Faulkenhagen Relations

Faulkenhagen from his theoretical analysis proposed equations [44] for the estimation of the viscosity of dilute as well as concentrated electrolyte solutions, for dilute solutions the viscosity can be calculated from using the relation:

$$\frac{\eta_S}{\eta_0} = 1 + A\sqrt{C} \qquad (\mathrm{II} - 27)$$

η_S: The viscosity of the solution.
η_0: The viscosity of the solvent.
C: The concentration of the solute.

A is a constant> 0, dependent on the electrostatic forces between the ions.

$$A = \frac{0.517z^2}{L^{\infty}\eta_0\sqrt{\varepsilon_0 T}} \qquad (II - 28)$$

Faulkenhagen model enables the calculation of the constant A for the case of equal ionic valencies ($z_1 = z_2 = z$) and equal ionic mobilities ($L_1{}^{\infty} = L_2{}^{\infty} = L^{\infty}$)

L^{∞}: Ionic mobility at infinite dilution.

ε_0: The dielectric constant of the solvent.

T: absolute temperature.

7.1.2. Jones-dole equation

For more concentrated solutions the equation becomes [38]:

$$\frac{\eta_S}{\eta_0} = 1 + A\sqrt{C} + BC \qquad (II - 29)$$

And for still higher concentrated solutions, up to 1 mol per litter, the equation becomes:

$$\frac{\eta_S}{\eta_0} = 1 + A\sqrt{C} + BC + Cc^2 \qquad (\text{II} - 30)$$

The values of the constants of the three-constant equation are given by Kaminsky [40].

7.1.3. Kern rule

Kern[5] suggests that viscosity twice that for water should be used for salts in water whose concentration is below (-30 % when syrupy type solutions are not formed. A solution of sodium hydroxide in water should be considered syrupy even when it is dilute. The implication of this rule is [42]:

$$(\eta_{solution} < 2\eta_{water})_{c<30\%} \qquad (\text{II} - 31)$$

7.2. Liquid mixture viscosity

Rarely the data are readily available at the conditions that are necessary for design of the equipment or for other calculations. Therefore, the data must be interpolated or extrapolated using the existing literature data and using appropriate correlations or models [42].

7.2.1. Method of Grunberg and Nissan

In this procedure, the low-temperature liquid viscosity for mixtures is given as,

$$ln\eta_m = \sum_i x_i ln\eta_i + \frac{1}{2}\sum_{i=1}^{n}\sum_{j=i}^{n} x_i x_j G_{ij} \qquad (\text{II} - 32)$$

or, for a binary of 1 and 2, G_{ii}=0,

$$ln\eta_m = x_1 ln\eta_1 + x_2 ln\eta_2 + x_1 x_2 G_{12} \qquad (\text{II} - 33)$$

η_m: Dynamic viscosity of the mixture (cp).

η_i: Dynamic viscosity of the constituent i (cp).

x_i, x_j: liquid mole fractions of the constituents i, j respectively.

G_{ij}: Interaction parameter, is a function of the components *i* and *j* as well as the temperature (and, in some cases, the composition). To calculate it, there are four steps as follow:

1- For a binary of *i* and *j*, select *i* by following the priority rules below. (then becomes the second component.)
   i _ an alcohol, if present.
   i _ an acid, if present.
   i _ the component with the most carbon atoms.
   i _ the component with the most hydrogen atoms.
   i _ the component with the most —CH_3 groups.
   Gij =0 if none of these rules establish a priority.

2- Once the decision has been made which component is *i* and which is *j*, calculate $\sum \Delta_i$ and $\sum \Delta_j$ from the group contributions in Table II-4.

3- Determine the parameter *W*. (If either *i* or *j* contains atoms other than carbon and hydrogen, set *W* = 0 and go to step 4.) Let the number of carbon atoms in *I* be *Ni* and that in *j* be *Nj*.

$$W = \frac{(0.3161)(N_i - N_j)^2}{N_i + N_j} - (0.1188)\left(N_i - N_j\right) \qquad (II - 34)$$

4- Calculate *Gij* from,

$$G_{ij} = \sum \Delta_i - \sum \Delta_j + W \qquad (II - 35)$$

This technique yields quite acceptable estimates of low-temperature liquid mixture viscosities for many systems, but Table does not allow one to treat many types of compounds. Also, the method does not cover aqueous mixtures [45].

Table II-4: group contribution for $\mathbf{G_{ij}}$at 298 K

Group	**Notes**	**Value of Δ_i**
$-CH_3$		-0.100
$> CH_2$		0.096
$> CH -$		0.204
$> C <$		0.433
Benzen ring substitutions :		
Ortho		0.174
Metha		-
Para		0.154
Cyclohexane ring		0.887
$-OH$	methanol	0.887
	ethanol	-0.023
	Higher aliphatic alcohol	-0.443
$> C = O$	ketones	1.046
$-Cl$		$0.653 - 0.161N_{cl}$
$-Br$		-0.116
$-COOH$	Acids with :	
	Nonassociated liquids	$-0.411 + 0.06074N_c$
	ketones	1.130
	Formic acid with ketones	0.167

7.2.2. Unifac-Visco Method

Gaston-Bonhomme, Petrino and Chevalier have modified the UNIFAC activity coefficient method to predict viscosities. In this method, viscosity is calculated by [45];

$$ln\eta_m = \sum_i x_i \, ln(\eta_i V_i) - lnV_m + \frac{\Delta^* g^{EC}}{RT} + \frac{\Delta^* g^{ER}}{RT} \qquad (\text{II} - 36)$$

η_m: Dynamic viscosity of the mixture (cp).

η_i: Dynamic viscosity of the constituent i (cp).

x_i: Mole fraction of the constituent i.

V_i: Mole volume of constituent i (cm^3/mol).

V_m: Mole volume of the mixture (cm^3/mol).

R: gas constant (8.32 J/mol.K).

T: absolute temperature (K).

The combinatorial term is calculated by,

$$\frac{\Delta^* g^{EC}}{RT} = \sum_i x_i \, ln \frac{\emptyset_i}{x_i} + \frac{z}{2} \sum_i q_i x_i ln \frac{\emptyset_i}{\theta_i} \qquad (II-37)$$

Z: The coordinate number =10.

θ_i: Molecular surface area fraction.

$\emptyset_i$: Molecular volume fraction.

$$\emptyset_i = \frac{x_i r_i}{\sum_j x_j r_j} \qquad (II-38)$$

$$\theta_i = \frac{x_i q_i}{\sum_j x_j q_j} \qquad (II-39)$$

where q_i , the van der Waals' surface area, and r_i , the van der Waals' volume of component *i*, are found by summation of the corresponding group contributions. Thus, if n^i_k is the number of groups of type *k* in the molecule *i*,

$$q_i = \sum_K n_K^i Q_K \qquad (II-40)$$

$$r_i = \sum_K n_K^i R_K \qquad (II-41)$$

Where, Q_K and R_K are the constants representing the group surface and size and are given in table II-5 [46][48].

Table II-5: UNIFAC-VISCO, Group Volume and Surface Area Parameters

Group K	$\boldsymbol{R_K}$	$\boldsymbol{Q_K}$
CH_2, CH_{2cy}	0.6744	0.540
CH_3	0.9011	0.848
CH_{ar}	0.5313	0.400
Cl	0.7910	0.724
CO	0.7713	0.640
COO	1.0020	0.880
OH	1.0000	1.200
CH_3OH	1.4311	1.432

UNIFAC-VISCO, Group Volume and Surface Area Parameters are summarized in the table II-5.

$$\frac{\Delta^* g^{ER}}{RT} = -\sum x_i ln\gamma_i^{*R} \qquad (II-42)$$

$$ln\gamma_i^{*R} = \sum_K n_K^i \left[ln\gamma_K^* - ln\gamma_K^{*i}\right] \qquad (II-43)$$

γ_K^*: Activity coefficient of group K in a mixture of groups in the actual mixture.

γ_K^{*i}: Activity coefficient of group K in a mixture of groups formed from the groups in pure component i.

$$ln\gamma_K^* = Q_K\left[1 - \ln\left(\sum_m \emptyset_m \Psi_{mK}^*\right) - \sum_m \frac{\emptyset_m \Psi_{Km}^*}{\sum_n \emptyset_n \Psi_{nm}^*}\right] \qquad (II-44)$$

$$\emptyset_m = \frac{Q_m X_m}{\sum_K X_K Q_K} \qquad (II-45)$$

$\emptyset_m$: The surface area fraction in the mixture of groups.

X_m: The mole fraction in the mixture of groups.

Ψ_{nm}^*: Interaction parameter,

$$\Psi_{nm}^* = \exp\left(-\frac{\alpha_{nm}}{298}\right) \qquad (II-46)$$

α_{nm} is given in the table II-6

Table II -6: UNIFAC-VISCO group interaction parameter: $\boldsymbol{\alpha_{nm}}$

	CH_2	**CH_3**	**CH_{2y}**	**CH_{ar}**	**Cl**	**CO**	**COO**	**OH**	**CH_3OH**
CH_2	0	66.53	224.6	406.7	60.30	859.5	1172.0	498.6	-219.7
CH_3	-709.5	0	-130.7	-119.5	82.41	-125.4	-172.4	594.4	-228.7
CH_{2Y}	-58.1	187.3	0	8.958	215.4	128.4	-165.7	694.4	-381.53
CH_{ar}	-623.7	237.2	50.89	0	177.2	128.4	-49.85	419.3	-88.81
Cl	-710.3	375.2	-163.3	-139.8	0	-404.3	-525.4	960.2	-165.4
CO	586.3	-21.75	740.6	-117.9	-4.145	0	29.20	221.5	55.52
COO	541.6	-44.25	416.2	-36.17	240.5	22.92	0	186.8	69.62
OH	-634.5	1209.0	-138	197.7	195.7	664.1	68.35	0	416.0
CH_3OH	-526.1	653.1	751.3	51.31	-140.9	-22.59	-286.2	-23.91	0

The UNIFAC-VISCO method was the only one that demonstrated any success in predicting viscosities of mixtures of compounds with large size differences. The method has also been successfully applied to ternary and quaternary alkanes systems [46].

7.2.3. Kendall and Monroe Relation

Kendall and Monroe proposed the following relation for mixture viscosity [42]:

$$\mu_m^{1/3} = x_1\mu_1^{1/3} + x_2\mu_2^{1/3} \qquad (II-47)$$

μ_m: Dynamic viscosity of the mixture (cp).

$\mu_1,\ \mu_2$: dynamic viscosity of component 1,2 respectively (cp).

x_1, x_2: mole fractions of component 1,2 respectively.

It holds good for several cases of mixtures consisting of non-polar and non-associated liquids.

7.2.4. Arrhenius Equation

Arrhenius suggested the following equation:

$$log\eta_m = x_1 log\eta_1 + x_2 log\eta_2 \qquad (\text{II}-48)$$

μ_m: Dynamic viscosity of the mixture (cp).

μ_1, μ_2: Dynamic viscosity of component 1,2 respectively (cp).

x_1, x_2: Mole fractions of component 1,2 respectively.

Arrhenius equation to be applicable, it is necessary that the two liquids constituting the mixture be of similar structure, non-polar and non-associated or one of the components should be present in dominant quantity in the mixture. Further, the difference between the viscosities of the two pure components making up the mixture should be small (below 15 cP) [43].

7.2.5. Method of Teja and Rice

Method of Teja –Rice is based on a corresponding-states treatment for mixture compressibility factors, Teja and Rice proposed an analogous form for liquid mixture viscosity, Per binary pair in the mixture [46].

$$ln(\Upsilon_m \varepsilon_m) = ln(\Upsilon\varepsilon)^{R_1} + [ln(\Upsilon\varepsilon)^{R_2} - ln(\Upsilon\varepsilon)^{R_1}]\frac{\omega_m - \omega^{R_1}}{\omega^{R_2} - \omega^{R_1}} \qquad (II-49)$$

Where the superscripts $R_1$and R_2 refer to two reference fluids.

ω, The acentric factor, and ε is a parameter defined as:

$$\varepsilon = \frac{V_c^{2/3}}{(T_c M)^{1/2}} \qquad (II-50)$$

The variable of composition is introduced in four places: the definitions of $\omega_m, V_{cm}, T_{cm} M_m$.the rules suggested by the authors to compute these mixture parameters are:

$$V_{cm} = \sum_i \sum_j x_i x_j V_{cij} \qquad (II-51)$$

$$T_{cm} = \frac{\sum_i \sum_j x_i x_j T_{cij} V_{cij}}{V_{cm}} \qquad (II-52)$$

$$M_m = \sum_i x_i M_i \qquad (II-53)$$

$$\omega_m = \sum_i x_i \omega_i \qquad (II-54)$$

$$V_{cij} = \frac{\left(V_{ci}^{1/3} + V_{cj}^{1/3}\right)^3}{8} \qquad (II-55)$$

$$T_{cij} V_{cij} = \psi_{ij}\left(T_{ci} T_{cj} V_{ci} V_{cj}\right)^{1/2} \qquad (II-56)$$

ψ_{ij} : is an interaction parameter (mPa$^{1/2}$).

ω_m: Acentric factor of the mixture.

V_{cm}: Critical volume of the mixture.

T_{cm}: Critical temperature of the mixture.

M_m: Molar mass of the mixture.

The equation (II-45) can simplify to be:

$$ln(\mu_m \varepsilon_m) = x_1 ln(\mu\varepsilon)_1 + x_2 ln(\mu\varepsilon)_2 \qquad (II-57)$$

μ_m : Dynamic viscosity of the mixture (cp).

μ_1, μ_2: Dynamic viscosity of reference (1), (2) respectively (cp).

$x_1,\ x_2$: mole fraction of reference (1), (2) respectively.

It must take into account ,

μ_1 is to be evaluated at $T[(T_c)^{R1}/T_{cm}]$and $\mu_2$at. $T[(T_c)^{R2}/T_{cm}]$

They correlated the reference fluid viscosities with an Andrade type equation:

$$\ln(\mu\varepsilon) = A + \frac{B}{T_R} \qquad (II-58)$$

Where $T_R = T[(T_c)^R/T_{cm}]$ (II − 59)

And A, B are constants of the components 1, 2.

Teja and Rice method gives good results for many mixtures ranging from strictly nonpolar to highly polar aqueous-organic systems. For nonpolar mixtures, errors averaged about 1%. For nonpolar-polar and polar-polar mixtures, the average rose to about 2.5%, whereas for systems containing water, an average error of about 9% was reported.

In comparison with the Grunberg-Nissan correlation with G_{ij}found by regressing data, Teja and Rice method shows that about the same accuracy is achieved for both methods for nonpolar-nonpolar and nonpolar-polar systems, but their technique was significantly more accurate for polar-polar mixtures, and particularly for aqueous solutions for which Grunberg and Nissan's form should not be used [46].

The Binary interaction parameter

The binary interaction parameter based on cohesive adhesive Vander walls interaction is given by the following relation [51][52]:

$$\psi_{ij} = \frac{\sigma_{ij}}{(0.25 * \delta_i * \delta_j)} \qquad (II-60)$$

and

$$\sigma_{ij} = \frac{\sigma_{ii} + \sigma_{jj}}{2} \qquad (II-61)$$

where

$$\sigma_{ii} = 0.25 * \delta_i^2 \qquad (\text{II} - 62)$$

and

$$\sigma_{jj} = 0.25 * \delta_j^2 \qquad (\text{II} - 63)$$

σ_{ii}, σ_{jj} : Cohesive forces (mPa).

σ_{ij}: Interaction forces (mPa).

δ: Solubility parameter and it can be calculated by the following relation:

$$\delta = \sqrt{[(\Delta H_V - RT)/V_m]} \qquad (\text{II} - 64)$$

ΔH_V: Enthalpy of vaporization (J/mol.K).

R: gas constant (8.32 J/mol.K).

T: absolute temperature (K).

V_m: mole volume (cm^3/mol).

8. Conclusion

Liquid mass transfer mechanism is a very important to treat, it can due to only by diffusion, We have considered mass diffusion in a stationary or unmixed medium, which has led to the use of Fick's law and an linear concentration profile is obtained across the concentration boundary layer whereas a Gaussian concentration profile is obtained when equation diffusion unsteady state is solved [32], When a stirred or turbulent medium was involved , Navier- stokes system equations are presented to describe the laminar velocity boundary layer, and in nonisotherm state energy equation is presented to describe heat transfer process, whereas concentration equation is presented to describe mass transfer process [33]. Mass transfer coefficient can be calculated, equality the analogues Newton law with Fick's diffusion equation at the boundary layer edge ($y = 0$) or by using correlations depend on the geometry (tube, circular, plate flat ….), the convection type (natural, forced), local or average mass transfer coefficient and so on [34].

The viscosity is a measure of the resistance to the flow so to the mass transfer process, it can be calculate using viscometers such as orifices viscometers, capillary viscometers, high temperature high shear rate viscometers, ultrasonic viscometers,

vibrational viscometers, rotational viscometers ,falling ball viscometers and so on, it also can be calculate using correlations [42][44].

To calculate the solution viscosity Faulkenhagen relations are used, dilute solution, more concentration solution and still higher concentration solution up to 1 mol per liter. To calculate liquid mixture viscosity many methods are exist such as, Gruenberg and Nissan method, Arrhenius method, UNIFAC -VISCO method, Kendall and Monroe method and Teja-Rice method and so on, each method has conditions take on consideration after choice it, several other recent methods have been published since 1987 for specific situations include those for hydrocarbon mixtures for solutions with suspended particles and for phosphorus [44][45].

Chapter 03

Effect of kinematic viscosity on the diffusion of charges

1. Introduction

The experimental part consists of the preparation of 05 solutions of each studied molecule which are ferrocene, ferrocenyl methyl aniline, N-(ferrocenyl_methyl)-2-nitro aniline, each medium contains aqueous ethanol as the solvent, and KCl as the supporting electrolyte. the electrochemical behavior of ferrocene, ferrocenyl methyl aniline, N-(ferrocenyl methyl)-2-nitro aniline were investigated using cyclic voltammetry on different indicator electrode material (glassy carbon, platinum) at scan rates vary from 25, 50, 75, 100 to 150 mV/s and rotating disc electrode voltammetry on different indicator electrode material (glassy carbon, platinum) at angular velocities vary from 1200, 1600, 1800 to 2000 rpm (revolution per minute), at scan rate equals to 100 mV/s. The diffusion coefficients of ferrocene/ferrocenium, ferrocenyl methyl aniline/ferrocenium and N-(ferrocenyl methyl)-2-nitro aniline/ferrocenium couples in aqueous ethanol at different percentages are obtained using Randles-Sevcik, levich relations respectivelly.

At another side the dynamic viscosity of each studied medium was calculated using the most adequate models, of Faulkenhagen and of Rice - Teja, the effect of the Viscosity on the diffusion of ferrocene/ferrocenium, ferrocenyl methyl

aniline/ferrocenium and N-(ferrocenyl methyl)-2-nitro aniline/ferrocenium couples in aqueous ethanol at different percentages has been studied.

2. Chemicals and materials

2.1. Chemicals

Ferrocene (98%, Acros organics), Ferrocenyl methyl aniline (98%) and N-(ferrocenyl methyl) -2-nitro aniline (98%) present the electroactive molecules, ethanol (99%, Biochem) presents the solvent of the electroactive species, and potassium chloride (98%, Biochem) in distilled water presents the supporting electrolyte. All the freshly prepared solutions were degassed under nitrogen gas flow before experiments.

2.2. Materials

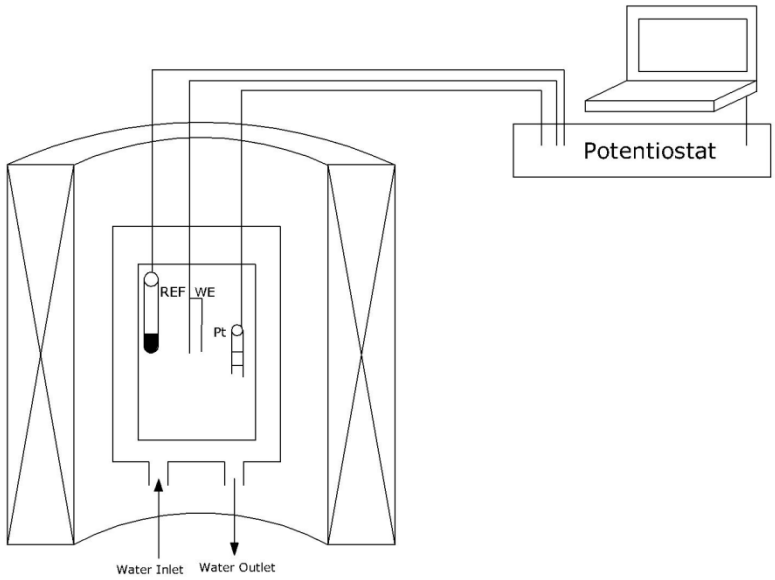

Figure III- 1: the schematic experimental apparatus.

To study the electrochemical behavior of electroactive molecules, we used: Potentiostate/ Galvanostat PGZ 301 VoltaLab 40 model with VoltaMaster 4 software. Platinum electrode (Pt) as auxiliary electrode. Glassy carbon electrode (GC ,0.05 cm^2) and platinum electrode (Pt ,0.03 cm^2) as the indicator electrodes and saturated calomel electrode (SCE) as reference electrode.(figure III-1)

Cyclic voltammograms and polarograms were displayed using Origin 8.0 software. $I_P = f(\sqrt{v})$ and $I_{lim} = f(\sqrt{\omega})$ plots are plotted using MS Excel software. The

kinematic viscosity of prepared mediums was calculated employing visual basic for application (VBA) programming language.

2.3. The properties of ferrocene, ferrocenyl methyl aniline and N-(ferrocenyl methyl)-2-nitro aniline

2.3.1. The properties of ferrocene

Bis**(**cyclopentadienyl**)**iron(II) or ferrocene is one of the most studied organometallic molecules [51]. It has a sandwich structure with the iron sandwiched between two cyclopentadienyl rings. Additionally, it is a well established [52][53] one-electron donor (n = 1).The independently 1951 discovery of ferrocene by Pauson and Miller revolutionized the area of organometallic chemistry [54][55][56]. The 1973 Nobel Prize in Chemistry was awarded to, Wilkinson and Fischer for elucidation of its structure [51] figure (III-1). This led to greater interest in d-block metal-carbon bonds and brought about the development of organometallic chemistry.

The properties of ferrocene are the following [57]:

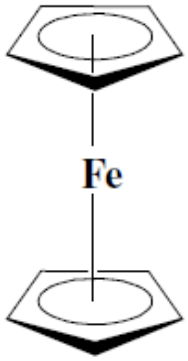

Figure III- 2: chemical structure of ferrocene.

IUPAC name	ferrocene,bis(η^5-cyclopentadienyl)iron
Molecular formula	$C_{10}H_{10}Fe$
Molar mass	186.04 g/mol
Density	1.107g/cm^3(0 ^{0}C), 1.490g/cm^3(20 ^{0}C)
Melting point	$173-174$ ^{0}C
Boiling point	249 ^{0}C
Solubility	0,1mg/ml (21 ^{0}C) in water, 100 mg/ml (19.5 ^{0}C) in

	DMSO.
Appearance	Light orange crystalline powder
The spectrums	The spectrums of ferrocene are presented in the appendix

2.3.2. The properties of Ferrocenyl methyl aniline

The properties of ferrocenyl methyl aniline are the following [58]:

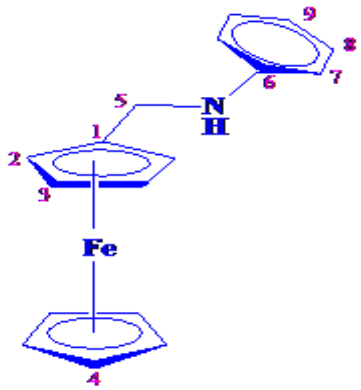

Figure III- 3 : Chemical structure of ferrocenyl methyl aniline.

IUPAC name	Ferrocenyl methyl amine-2- phenyl
Molecular formula	$Fc - CH_2 - NH - C_6H_5$
Molar mass	$291 g/mol$
Boiling point	$85 - 86\ ^0C$
appearance	Yellow crystalline powder
The spectrums	The spectrums of ferrocenyl methyl aniline are presented in the appendix

2.3.3. The properties of N-(ferrocenyl methyl)-2-nitro aniline

The properties of N-(ferrocenyl methyl)-2-nitro aniline which were found are the following [59]:

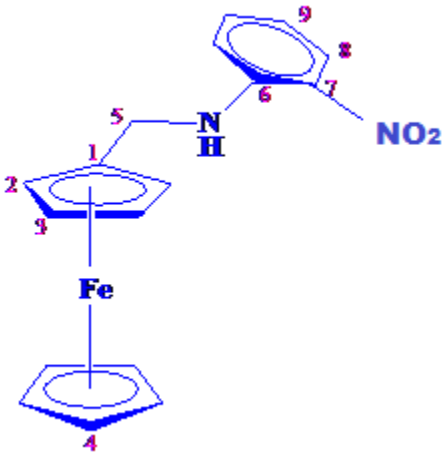

Figure III- 4 : Chemical structure of N-(ferrocenyl methyl)-2-nitro aniline.

IUPAC name	Ferrocenyl methyl amine-2- nitrophenyl.
Molecular formula	$Fc - CH_2 - NH - C_6H_4 - NO_2$
Molar mass	$336\ g/mol$
Melting point	$110 - 115\ ^0$C
appearance	Red cinnabar crystalline powder
The spectrums	The spectrums of N-(ferrocenyl methyl)-2-nitro aniline, are presented in the appendix

3. General Process for preparation of studied solutions

A small amount of studied molecule was dissolved in a chosen volume of ethanol ($50ml$),so that the final concentration of the principle solution is $3.10^{-3}M$, at another side $0.3M$ of KCl aqueous solution was prepared by dissolving 2.235 g of KCl in $100\ ml$ of distilled water. $5\ ml$ of the primary solution was removed and it was replaced by $5\ ml$ of KCl aqueous solution to obtain the first solution of each species will be analyze, has concentration of $2{,}70.10^{-3}$ M (90 % aqueous ethanol),with the same process to prepare the second ,the third ,the forth, and the fifth solution.

The composition of the prepared solutions of ferrocene, ferrocenyl methyl aniline and N-(ferrocenyl methyl)-2-nitro aniline obtained are summarized in the table III-1.

Table III- 1 : composition of the prepared solutions of ferrocene, ferrocenyl methyl aniline, N-(ferrocenyl methyl)-2-nitro aniline

Mass of must be dissolved in 50 ml of ethanol		**Principle solution** (mol/cm^3)	**studied solutions**	**Concentration** (mol/cm^3)	**Aqueous ethanol %**
electroactive specie	**Weight** (g)				
Ferrocene:	0.0264	3.10^{-6}	1	$2,70.10^{-6}$	90
Ferrocenyl methyl aniline:	0.043		2	$2,43.10^{-6}$	81
N-(ferrocenyl methyl)-2nitro aniline:	0.050		3	$2,19.10^{-6}$	73
			4	$1,97.10^{-6}$	66
			5	$1,77.10^{-6}$	59

4. Calculation of the kinematic viscosity of studied solutions at 25^0C

The calculation of the kinematic viscosity of each solution is based on four steps:

- The first step consists of the use of Faulkenhagen model to calculate the dynamic viscosity of KCl aqueous solution.
- The second step consists of the use of Rice-Teja model to calculate the dynamic viscosity of fluids mixture after mixing KCl aqueous solution with C_2H_5OH using the following model:

$$ln(\eta_m \varepsilon_m) = x_1 ln(\eta\varepsilon)_1 + x_2 ln(\eta\varepsilon)_2$$

Teja –Rice method is a binary data model, calculates the dynamic viscosity of mixture fluids system. In our case, we should calculate the dynamic viscosity of $(KCl, H_2O)(R_1)$, C_2H_5OH (R_2) mixture.It must be taking account that, η_1 is to be evaluated at $T_R = T[(T_c)^{R1}/T_{cm}]$, and $\eta_2$at $T_R = T[(T_c)^{R2}/T_{cm}]$, using an Andrade type equation:

$$\ln(\mu\varepsilon) = A + B/T_R$$

With

$$\varepsilon = \frac{V_c^{2/3}}{(T_c M)^{1/2}}$$

- The third step consists of the calculation of the dynamic viscosity of the mixture after adding the solute using Faulkenhagen model.
- The forth step consists of the calculation of the volume density of mixture to calculate its kinematic viscosity.

To make the calculation easy, a Visual Basic for Application (VBA) program was constructed, it demands data corresponding to KCl,H_2O, C_2H_5OH, and electroactive molecules, this program consists of many parts.

4.1. Calculation of dynamic viscosity of KCl aqueous solution

The first step consists of the calculation of dynamic viscosity of KCl aqueous solution employing Faulkenhagen model.

```
Public Function mu_solution1(mu0 As Double, z As Double,
     c As Double, eps0 As Double, L As Double, T As Double)
   Dim A As Double
   A = (0.517 * z ^ (2)) / (L * mu0 * eps0 ^ (0.5) * T)
   mu_solution1 = mu0 * (1 + A * (c * 0.001) ^ (0.5))
End Function
```

4.2. Calculation of dynamic viscosity of fluids mixture

The second step consists of the use of Rice-Teja model to calculate the dynamic viscosity of fluids mixture after mixing KCl aqueous solution withC_2H_5OH; many parts of VBA program were constructed to calculate it.

4.2.1. Calculation of interaction parameter

The first part calculates the interaction parameterψ_{ij}, The calculation of the binary interaction parameter based on cohesive adhesive Vander walls interactions is given by the following relations:

$$\psi_{ij} = \frac{\sigma_{ij}}{(0.25 * \delta_i * \delta_j)}$$

and

$$\sigma_{ij} = (\sigma_{ii} + \sigma_{jj})/2$$

where

$$\sigma_{ii} = 0.25 * \delta_i^2$$

and

$$\sigma_{jj} = 0.25 * \delta_j^2$$

$\delta$is the solubility parameter and it can be calculated by the following relation:

$$\delta = \sqrt{[(\Delta H_V - RT)/V_m]}$$

```
Public Function solubilutyparameter(deltahvap As Double,
           T As Double, volumemolaire As Double) As Double
   solubilutyparameter = ((deltahvap - 8.32 *
                  (T + 273.15))/ volumemolaire) ^ (1 / 2)
End Function
```

```
Public Function gamma(sigma As Double)
  gamma = 0.25 * sigma ^ 2
End Function
```

```
Public Function interaction_parameter_psiab(deltahvapa As Double,
deltahvapb As Double, T As Double, volma As Double, volmb As
Double) As Double
  Dim sigmaa As Double
  Dim sigmab As Double
  sigmaa = solubilutyparameter(deltahvapa, T, volma)
  sigmab = solubilutyparameter(deltahvapb, T, volmb)
  Dim gammaa As Double
  Dim gammab As Double
  gammaa = gamma(sigmaa)
  gammab = gamma(sigmab)
  Dim gammaab As Double
  gammaab = (gammaa + gammab) / 2
  interaction_parameter_psiab=gammaab/(0.25*sigmaa*sigmab)
End Function
```

4.2.2. Calculation of critical volume

The second part calculatesV_{Cij}. The calculation of V_{Cij} is based on the following relation:

$$V_{cij} = \frac{\left(V_{ci}^{1/3} + V_{cj}^{1/3}\right)^3}{8}$$

```
Public Function Vc_ij(Vc1 As Double, Vc2 As Double, i As Integer,
j As Integer) As Double
   If (i < 0) Or (i > 2) Or (j < 0) Or (j > 2) Then
     Vc_ij = -1
     Exit Function
   End If
   If i = 1 And j = 1 Then
       Vc_ij = Vc1
   ElseIf (i = 1 And j = 2) Or (i = 2 And j = 1) Then
       Vc_ij = ((Vc1 ^ (1 / 3) + Vc2 ^ (1 / 3)) ^ 3) / 8
   ElseIf i = 2 And j = 2 Then
       Vc_ij = Vc2
   End If
End Function
```

4.2.3. Calculation of critical volume of mixture

The calculation of V_{Cm} is based on the following relations:

$$V_{cm} = \sum_i \sum_j x_i x_j V_{cij}$$

```
Public Function Vcm(x1 As Double, x2 As Double, Vc1 As Double, Vc2
As Double) As Double
    Dim x(2) As Double
    x(0) = x1
    x(1) = x2

    Dim v As Double
    Dim i As Integer
    Dim j As Integer

    v = 0
```

```
    For i = 0 To 1
        For j = 0 To 1
          v= v +x(i)*x(j) * Vc_ij(Vc1, Vc2, i + 1, j + 1)
        Next j
    Next i
    Vcm = v
End Function
```

4.2.4. Calculation of critical temperature, critical volume product

The forth part calculatesT_{cij} V_{cij} :

$$T_{cij}V_{cij} = \psi_{ij}\left(T_{ci}T_{cj}V_{ci}V_{cj}\right)^{\frac{1}{2}}$$

```
Public Function Tcij_Vcij(Tc1 As Double, Tc2 As Double, Vc1 As
Double, Vc2 As Double, deltahvap1 As Double, deltahvap2 As Double,
T As Double, volm1 As Double, volm2 As Double, i As Integer, j As
Integer) As Double

  If (i < 0) Or (i > 2) Or (j < 0) Or (j > 2) Then
    Tcij_Vcij = -1
    Exit Function
  End If

  If i = 1 And j = 1 Then
      Tcij_Vcij = Tc1 * Vc1
  ElseIf (i = 1 And j = 2) Or (i = 2 And j = 1) Then
      Tcij_Vcij=interaction_parameter_psiab(deltahvap1,
        deltahvap2,T,volm1,volm2)*((Tc1*Tc2*Vc1*Vc2)^(1/2))
  ElseIf i = 2 And j = 2 Then
      Tcij_Vcij = Tc2 * Vc2
  End If
End Function
```

4.2.5. Calculation of critical temperature of the mixture

The fifth part calculatesT_{cm}:

$$T_{cm} = \frac{\sum_i \sum_j x_i x_j T_{cij} V_{cij}}{V_{cm}}$$

```
Public Function Tcm(x1 As Double, x2 As Double, Tc1 As Double, Tc2
   As Double, Vc1 As Double, Vc2 As Double, deltahvap1 As Double,
   deltahvap2 As Double, T As Double, volm1 As Double, volm2 As
   Double) As Double
    Dim x(2) As Double
    x(0) = x1
    x(1) = x2
    Dim tcmt As Double
    Dim i As Integer
    Dim j As Integer
    tcmt = 0
    For i = 0 To 1
        For j = 0 To 1
          tcmt = tcmt + x(i) * x(j) * Tcij_Vcij(Tc1, Tc2, Vc1,
               Vc2, deltahvap1, deltahvap2, T, volm1, volm2, i + 1,
               j + 1)
        Next j
    Next i
    Tcm = tcmt / Vcm(x1, x2, Vc1, Vc2)
End Function
```

4.2.6. Calculation of dynamic viscosity of constituent in T_R

The sixth part calculates the dynamic viscosity of constituentμ_i. The calculation of μ_i is based on Andrade model:

$$\ln(\mu\varepsilon) = A + B/T_R$$

$$T_R = T\left[(T_c)^{Ri}/T_{cm}\right]$$

```
Public Function mu(A As Double, B As Double, _
            x1 As Double, x2 As Double, Tc1 As Double, Tc2 As
Double, Vc1 As Double, Vc2 As Double, _
          deltahvap1 As Double, deltahvap2 As Double, T As
Double, volm1 As Double, volm2 As Double, rang As Integer) As
Double
    Dim ln_mu As Double
    Dim TR As Double
    Dim Tc As Double
```

```
    If rang = 1 Then
        Tc = Tc1
    ElseIf rang = 2 Then
        Tc = Tc2
    Else
        MsgBox "Pour calculer mu, le rang doit etre 1 ou 2"
        Exit Function
    End If

    TR = (T + 273.15) * Tc / Tcm(x1, x2, Tc1, Tc2, Vc1,
            Vc2, deltahvap1, deltahvap2, T, volm1, volm2)
    ln_mu = A + B / TR

    mu = Exp(ln_mu)

End Function
```

4.2.7. Calculation of parameter ε

The seventh part calculates$\varepsilon_i, \varepsilon_m$. The parameter ε is based on the following relation:

$$\varepsilon = \frac{V_c^{2/3}}{(T_c M)^{1/2}}$$

The calculation of the mole mass of the mixture is based on the following relation:

$$M_m = \sum_i x_i M_i$$

```
Public Function Epsilon(Vc As Double, Tc As Double, M As Double)
As Double
    Epsilon = Vc ^ (2 / 3) / (Tc * M) ^ (1 / 2)
End Function
```

```
Public Function EpsilonMix(x1 As Double, x2 As Double, Tc1 As
    Double, Tc2 As Double, Vc1 As Double, Vc2 As Double,
    deltahvap1 As Double, deltahvap2 As Double, T As Double, volm1
    As Double, volm2 As Double, _
    Mm1 As Double, Mm2 As Double) As Double

    Dim Vvcm As Double
    Dim Vtcm As Double
    Dim VMmix As Double
```

```
    Vvcm = Vcm(x1, x2, Vc1, Vc2)
    Vtcm = Tcm(x1, x2, Tc1, Tc2, Vc1, Vc2, deltahvap1, deltahvap2,
           T, volm1, volm2)
    VMmix = x1 * Mm1 + x2 * Mm2

    EpsilonMix = Vvcm ^ (2 / 3) / (Vtcm * VMmix) ^ (1 / 2)
End Function
```

4.2.8. Calculation of mixture viscosity of potassium chloride solution and ethanol in 25^0C

The eighth part calculates $\mu_{(kcl+H_2O),C_2H_5OH}$ (25^0C)

```
Public Function mu_mix2(mu1 As Double, x1 As Double, x2 As Double,
Tc1 As Double, Tc2 As Double, Vc1 As Double, Vc2 As Double,
deltahvap1 As Double deltahvap2 As Double, T As Double, volm1 As
Double, volm2 As Double,Mm1 As Double, Mm2 As Double, A2 As
Double, B2 As Double) As Double
    Dim mu2, eps1, eps2, epsMix As Double    mu2 = mu(A2, B2, x1,
       x2, Tc1, Tc2, Vc1, Vc2, deltahvap1, deltahvap2, T, volm1,
       volm2, 2)
    eps1 = Epsilon(Vc1, Tc1, Mm1)
    eps2 = Epsilon(Vc2, Tc2, Mm2)
    epsMix = EpsilonMix(x1, x2, Tc1, Tc2, Vc1, Vc2, deltahvap1,
            deltahvap2, T, volm1, volm2, Mm1, Mm2)
    mu_mix2 = (Exp(x1)*mu1*eps1+Exp(x2)*mu2*eps2)/epsMix
End Function
```

4.3. Calculation of dynamic viscosity of solution after adding the solute

The third step consists of the calculation of the dynamic viscosity of the solution μ_{sol} after adding the solute, based on relation of Faulkenhagen.

$$\frac{\mu_S}{\mu_0} = 1 + A\sqrt{C}$$

$$A = \frac{0.517z^2}{L^{\infty}\eta_0\sqrt{\varepsilon_0 T}}$$

The calculation of the ionic mobility of solute is based on Nernst relation [63]:

$$L^{\infty} = \frac{DF^2|Z|}{RT}$$

D : diffusion coefficient (m^2/s).

F: Faraday constant (c/mol).

Z: ionic valencies.

R: gas constant (8.32J/mol.K).

T: absolute temperature (K).

The calculation of the absolute permittivity of the solvent is based on the following relation [1]:

$$\varepsilon_s = (y_{kcl} + y_{H_2o})\varepsilon_{H_2O} + y_{C_2H_5OH}\varepsilon_{C_2H_5OH}$$

```
Public Function mu_solution(mu0 As Double, z As Double, n As
Double, c As Double, fvol1 As Double, fvol2 As Double,eps1 As
Double, eps2 As Double, pente As Double)
        Dim eps_solvant, A As Double
        Dim diff As Double
        diff=pente^2/((269000#)^2*n^3*(c*0.001)^2)
eps_solvant = fvol1 * eps1 + fvol2 * eps2
A=(0.517*z^(2)*8.314)/(z*96500*diff*eps_solvant^(0.5)*mu0)
        mu_solution = mu0 * (1 + A * (c * 0.001) ^ (0.5))
End Function
```

4.4. Calculation of kinematic viscosity of mixture

The forth step consists of the calculation of kinematic viscosity of mixture, ν_m based on the following relation:

$$\nu_m = \frac{\mu_m}{\rho_m}$$

With $$\rho_m = \rho_{(H_2O+KCl)}y_{(H_2O+Kcl)} + \rho_{C_2H_5OH}y_{C_2H_5OH}$$

ρ_m: Volume density of the mixture.

$\rho_{(H_2O+KCl)}$: Volume density of KCl aqueous solution.

$\rho_{C_2H_5OH}$: Volume density of ethanol.

$y_{(H_2O+Kcl)}$: Volume fraction of KCl aqueous solution in the mixture.

$y_{C_2H_5OH}$: Volume fraction of ethanol in the mixture.

```
Public Function densityMix(v1 As Double, v2 As Double, ro1 As
       Double, ro2 As Double) As Double
    densityMix = v1 * ro1 + v2 * ro2  / (v1 + v2 )
End Function
```

```
Public Function nu_kinvis_mix(x1 As Double, x2 As Double, Tc1 As
     Double, Tc2 As Double, Vc1 As Double, Vc2 As Double,
     deltahvap1 As Double, deltahvap2 As Double, T As Double, volm1
     As Double, volm2 As Double, Mm1 As Double, Mm2 As Double, A1
     As Double, B1 As Double, A2 As Double, B2 As Double, v1 As
     Double, v2 As Double, ro1 As Double, ro2 As Double) As Double
Dim vnu_mix, vro_mix As Double
 vnu_mix=mu_mix(x1,   x2,   Tc1,   Tc2,   Vc1,   Vc2,   deltahvap1,
        deltahvap2, T, volm1, volm2, Mm1, Mm2, A1, B1, A2, B2)
   vro_mix = densityMix(v1, v2,ro1, ro2)
    nu_kinvis_mix = vu_mix / vro_mix
End Function
```

To can be applied the program, the mole fractions and the volume fractions of the constituents must be calculated, and additionally it needs some data corresponding constituents.

The calculation of mole fraction of the constituent (i) is based on the following relation:

$$x_i = \frac{number\ of\ mole\ of\ constituent\ i}{total\ mole\ number\ of\ constituents}$$

(H_2O, KCl) Solution

The calculation was carried out using 04 decimals and the results are reported with 02 decimals

Table III- 2: The mole fractions of$\boldsymbol{KCl}$ and of $\boldsymbol{H_2O}$ in aqueous potassium chloride solution

Mole fractions	$\boldsymbol{x_1(H_2O)}$	$\boldsymbol{x_2(KCl)}$
(H_2O, KCl) solution (0.3 M)	$\frac{(100 * 1)/18}{5.55 + 0.03} = 0.99$	$\frac{0.3 * 0.1}{5.55 + 0.03} = 0.01$

$(KCl + H2O)$, C_2H_5OH mixture

The calculation of the mole fractions is based on the volumes of the constituents in the mixture.

Table III- 3 : Mole fractions of($\boldsymbol{KCl + H2O}$), C_2H_5OH in the mixture

Aqueous ethanol %	$\boldsymbol{V_{H_2O+KCl}}$ $(\boldsymbol{ml})$	$\boldsymbol{V_{C_2H_5OH}}$ $(\boldsymbol{ml})$	$\boldsymbol{x_{KCl}}$
90	5.00	45.00	(5*10^{-3}*0.3)/1.04=0.0014
81	9.50	40.50	(9.5*10^{-3}*0.3)/1.21=0.0023
73	13.55	36.45	(13.55*10^{-3}*0.3)/1.37=0.0029
66	17.19	32.80	(17.195*10^{-3}*0.3)/1.51=0.0034
59	20.47	29.52	(20.4755*10^{-3}*0.3)/1.64=0.0037

$\boldsymbol{x_{H_2O}}$	$\boldsymbol{x_{C_2H_5OH}}$	$\boldsymbol{x_{KCl+H_2O}}$
((5*1)/18)/1.04= 0.26	((45*0.78)/46)/1.04= 0.73	0.00143+0.26=0.26
((9.5*1)/18)/1.21= 0.43	((40.5*0.78)/46)/1.21= 0.56	0.00234+0.43= 0.43
((13.55*1)/18)/1.37= 0.54	((36.45*0.78)/46)/1.37=0.44	0.002956+0.54= 0.55
((17.195*1)/18)/1.51= 0.62	((32.805*0.78)/46)/1.51=0.36	0.003401+0.62= 0.63
((20.4755*1)/18)/1.64= 0.69	((29.5245*0.78)/46)/1.64=0.30	0.003735+0.69= 0.69

The calculation of volume fraction of the constituent (i) is based on the following relation:

$$y_i = \frac{the\ volume\ of\ the\ constitent\ i}{total\ volume}$$

The calculation was carried out using 04 decimals and the results are reported with 02 decimals.

Table III- 4: Volume fractions of (KCl+H_2O), C_2H_5OH in the mixture

Aqueous ethanol %	$\boldsymbol{V_{H_2O+Kcl}}$ **(ml)**	$\boldsymbol{V_{C_2H_5OH}}$ **(ml)**	$\boldsymbol{y_{Kcl+H_2o}}$	$\boldsymbol{y_{C_2H_5OH}}$
90	5.00	45.00	0.10	0.90
81	9.50	40.50	0.19	0.81
73	13.55	36.45	0.27	0.72
66	17.19	32.81	0.34	0.65
59	20.47	29.53	0.40	0.59

Table III- 5 : Data corresponding to KCl solution [60][61][62]

$\boldsymbol{\mu_{H_2O}}$ **(25 ^{0}C)** $(\boldsymbol{mPas.s})$	$\boldsymbol{Z}$	$\boldsymbol{C}$ $(\boldsymbol{mol/cm^3})$	$\boldsymbol{L_{\infty K^+,cl^-}}$ $(\boldsymbol{m^2/Vs})$	$\boldsymbol{\varepsilon_{H_2O}}$ **(25 ^{0}C)**
0.89	1	0,3.10^{-3}	7,70.10^{-8}	78,39

constituent	x_1	x_2	V_{c1} (cm^3/mol)	V_{c2} (cm^3/mol)	T (K)	T_{C1} (K)	T_{C2} (K)
H_2O,KCl	0,99	0,0053	55,95	625	298.15	647,14	3470

M_{m1} (g/mol)	M_{m2} (g/mol)	T_{Cm} (K)	V_{cm} (cm^3/mol)
18	74,5	707,98	57,89

ΔH_{V1} $(J/mol.K)$	ΔH_{V2} $(J/mol.K)$	V_{m1} (cm^3/mol)	V_{m2} (cm^3/mol)
4,07E+04	7,17E+05	18,07	37,55

Table III- 6: The data corresponding to (KCl+H2O), C_2H_5OH [43][61]

constituent	V_{c1} (cm^3/mol)	V_{c2} (cm^3/mol)	T_{C1} (K)	T_{C2} (K)	ΔH_{V1} $(J/mol.K)$
(KCl+H_2o),C_2H_5OH	57,89	167	707,98	513,92	4.43E+4

ΔH_{V2} $(J/mol.K)$	V_{m1} (cm^3/mol)	M_{m1} (g/mol)	M_{m2} (g/mol)	A_2	B_2
3,86E+04	18.174	18.30	46	-6.21	1614

ε_{H_2O}	$\varepsilon_{C_2H_5OH}$	ρ_{H_2O} (g/cm^3)	$\rho_{C_2H_5OH}$ (g/cm^3)	V_{m2} (cm^3/mol)
78,39	24,6	0.999	0.78	58,606

The calculated kinematic viscosity of aqueous KCl solution and the calculated kinematic viscosity of(KCl/H_2O), C_2H_5OH the constituents of the medium are summarized in the table III-7.

Table III- 7: Kinematic viscosity of Kcl solution and of$(Kcl + H_2O)$, C_2H_5OH mixture

Aqueous ethanol %	Concentration (mol/cm^3)	x_1 $(Kcl + H_2O)$	x_2 C_2H_5OH	μ_{kcl+H_2o}(25 ^{0}C) (cp)	T_{cm} (K)
90	2.70E-06	0.267	0.732	1.381	577.67
81	2.43E-06	0.435	0.564		617.05
73	2.19E-06	0.550	0.449		642.66
66	1.97E-06	0.633	0.366		660.10
59	1.77E-06	0.695	0.304		672.26

Aqueous ethanol %	T_R **(K)**	$\mu_{kcl+H_2o}\ (T_R)$ (cp)	$\mu_{C_2H_5OH}\ (T_R)$ (cp)	$\mu_{kcl,,H_2o,C_2H_5oH}$ **(25 ^{0}C)** (cp)
90	92.25	1.127	0.882	3.166
81	68.93	1.204	1.336	4.241
73	55.30	1.254	1.749	5.129
66	46.62	1.288	2.102	5.838
59	40.84	1.311	2.390	6.387

The kinematic viscosities of solutions of ferrocene dissolving in aqueous ethanol at different percentages are shown in the table III-8.

Table III- 8 : Kinematic viscosities of solutions of ferrocene within aqueous ethanol at different percentages

Aqueous ethanol %	C (mol/cm^3)	**volume fractions**		$\varepsilon_{solvent}$
		y_{H_2O+Kcl}	$y_{C_2H_5OH}$	
90	2.70E-06	0.10	0.9	0.1*78.39+0.9*24.6=29.98
81	2.43E-06	0.19	0.81	34.82
73	2.19E-06	0.27	0.72	39.18
66	1.97E-06	0.34	0.65	43.09
59	1.77E-06	0.40	0.59	46.63

$\mu_{(kcl,H_2O,C_2H_5OH,Fr)}$ **(25 ^{0}C)** (cp)	V_{H_2O+Kcl} (ml)	$V_{C_2H_5OH}$ (ml)	y_{Kcl+H_2o}	$y_{C_2H_5OH}$	ρ_{Kcl+H_2O} (g/ml)
3.166	5.00	45.00	0.10	0.90	(100+2.23)/100 =1.0223
4.241	9.50	40.50	0.19	0.81	
5.129	13.55	36.45	0.27	0.72	
5.838	17.19	32.80	0.34	0.65	
6.387	20.47	29.52	0.40	0.59	

ρ_m (g/ml)	$\nu_{solution}$ **(25 ^{0}C)** (cm^2/s)
0.808	$3.91 .10^{-5}$
0.830	$5.10.10^{-5}$
0.849	$6.04.10^{-5}$
0.866	$6.73.10^{-5}$
0.882	$7.24.10^{-5}$

The kinematic viscosities of solutions of ferrocenyl methyl aniline in aqueous ethanol at different percentages are shown in the table III-9.

Table III- 9: Kinematic viscosities of solutions of ferrocenyl methyl aniline within aqueous ethanol at different percentages

Aqueous ethanol %	C (mol/cm^3)	$\mu_{(kcl,H_2O,C_2H_5OH,m2)}$ **(cp)**	$\nu_{solution}$ **(25 ^{0}C)** (cm^2/s)
90	2.70E-06	3.166	$3.91.10^{-5}$
81	2.43E-06	4.241	$5.10.10^{-5}$
73	2.19E-06	5.129	$6.04.10^{-5}$
66	1.97E-06	5.838	$6.73.10^{-5}$
59	1.77E-06	6.387	$7.24.10^{-5}$

And the kinematic viscosities of solutions of N-(ferrocenyl methyl)-2-nitro aniline in aqueous ethanol at different percentages are shown in table III-10.

Table III- 10: Kinematic viscosities of solutions of N-(ferrocenyl methyl)-2-nitro aniline within aqueous ethanol at different percentages

Aqueous ethanol %	C (mo/cm^3)	$\mu_{(kcl,H_2O,C_2H_5OH,m3)}$ **(cp)**	$\nu_{solution}$ **(25 ^{0}C)** (cm^2/s)
90	2.70E-06	3.166	$3.91.10^{-5}$
81	2.43E-06	4.241	$5.10.10^{-5}$
73	2.19E-06	5.129	$6.04.10^{-5}$
66	1.97E-06	5.838	$6.73.10^{-5}$
59	1.77E-06	6.387	$7.24.10^{-5}$

5. Study of electrochemical behavior and calculation of diffusion coefficients of charges

The oxido-reductive properties of ferrocene derivatives are studied employing the electrochemical methods [64][65]. Miller and Al. [66] are demonstrated employing cyclic voltammetry that the oxidation of some ferrocene derivatives drive with a reversible electrochemical process to ferrocenium cations such it shown in the following figure:

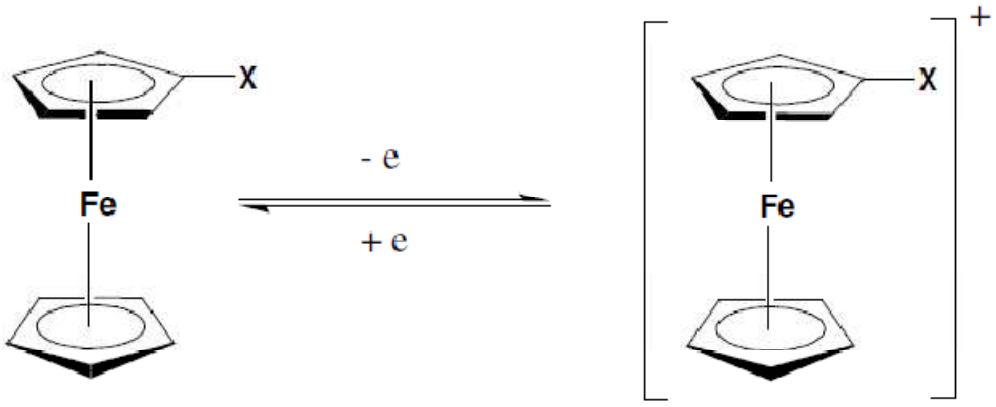

Figure III- 5 : the oxidation of ferrocene.

5.1. Study of electrochemical behavior of the supporting electrolyte

To confirm the non reactivity of the supporting electrolyte (KCl aqueous solution) in window potential of $0-600\,mV$, $1{,}12g$ of KCl was dissolved in $50\,ml$ of distilled water, to obtain an KCl aqueous solution has concentration of$0{,}3M$.

Cyclic voltammetry technique was employed in the electrochemical study of the KCl aqueous solution, at scan rate equals to$100\,mV/s$, the obtained voltammogram is raised from the residual current, so the supporting electrolyte is not reactive in window potential of$0-600\,mV$.

To compare the residual current and the faradic current obtained from the electrochemical reaction of ferrocene, ferrocenyl methyl aniline, N-(ferrocenyl methyl)-2-nitro aniline species, we superposed the voltammogram obtained from the supporting electrolyte and each one obtained from the studied species(Fig III-6, III-7, and III-8).

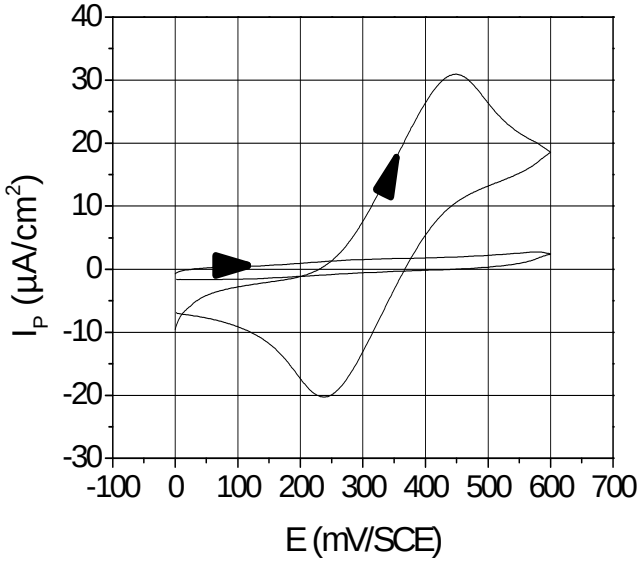

Figure III- 6: the overlays of the volatammogram of the supporting electrolyte and the volatammogram of ferrocene at100 mV/s, in aqueous ethanol (90%), in window potential of 0-600 mV (Vs/SCE), at 25^{0}C.

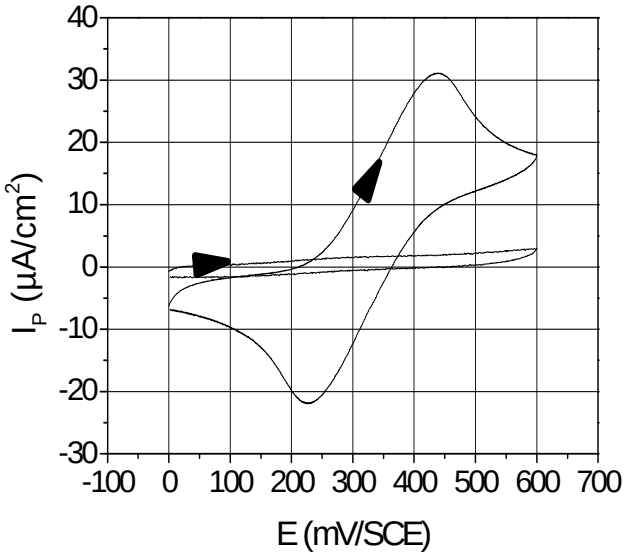

Figure III- 7 : the overlays of the volatammogram of the supporting electrolyte and the volatammogram of ferrocenyl methyl aniline at100 mV/s, in aqueous ethanol (90%), in window potential of 0-600 mV (Vs/SCE), at 25 ^{0}C.

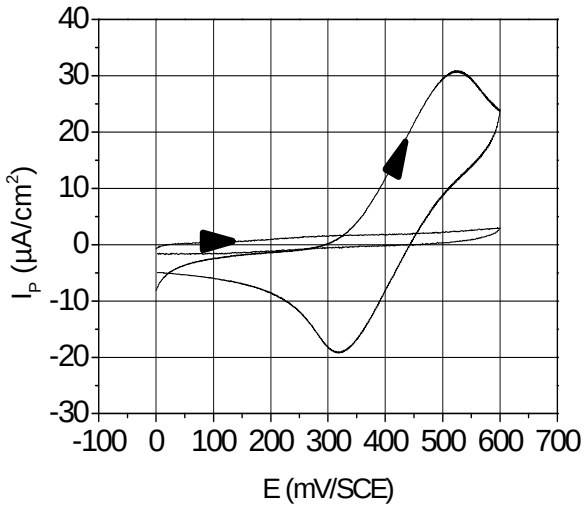

Figure III- 8 : the overlays of the volatammogram of the supporting electrolyte and the volatammogram of ferrocenyl methyl aniline at100 mV/s, in aqueous ethanol (90%), in window potential of 0-600 mV (Vs/SCE), 25 ^{0}C.

The overlays of the volatammogram of the supporting electrolyte and the volatammogram of ferrocene, ferrocenyl methyl aniline, N-(ferrocenyl methyl)-2-nitro aniline at 100mv/s, in aqueous ethanol (81%, 73%, 66%, and 59%) are presented in the appendix.

The voltammetry was used to study the electrochemical behavior of ferrocene, ferrocenyl methyl aniline and N-(ferrocenyl methyl)-2-nitro aniline molecules in aqueous ethanol at different percentages with known kinematic viscosity ν_m, Cyclic voltammetry was used as a type of transient voltammetry using two different indicator electrode materials (GC, Pt) and at different scan rates equal to 25, 50, 75, 100 and 150 mV/s, at another side rotating disc electrode voltammetry was used as a type of hydrodynamic voltammetry using also two different indicator electrode materials (GC, Pt) at different angular velocities equal to 1200, 1600, 1800 and 2000 rpm, at scan rate equals to 100 mV/s.

5.2. Study of electrochemical behavior and calculation of diffusion coefficients of ferrocene/ferrocenium couple

5.2.1. Study of electrochemical behavior of ferrocene

On platinum (Pt) indicator *fixed electrode*

Before the study of the electrochemical behavior of ferrocene in aqueous ethanol at different percentages, on Pt indicator electrode, the reactivity and the stability of the electroactive molecule must be confirmed, the reactivity of ferrocene in window potential of 0-600mV is confirmed with the obtaining of a cyclic voltammogram presents an anodic peak at 0.451 mV and an cathodic peak at 0.250 mV (fig III-9, (A)), those two peaks are corresponded to the oxidation and to the reduction of ferrocene/ferrocenium couple, and the superposed of multi-cycles voltammograms (in our case 05 cycles) indicates that the system is stable and do not change with the variation of the time (figure III-9, (B)).

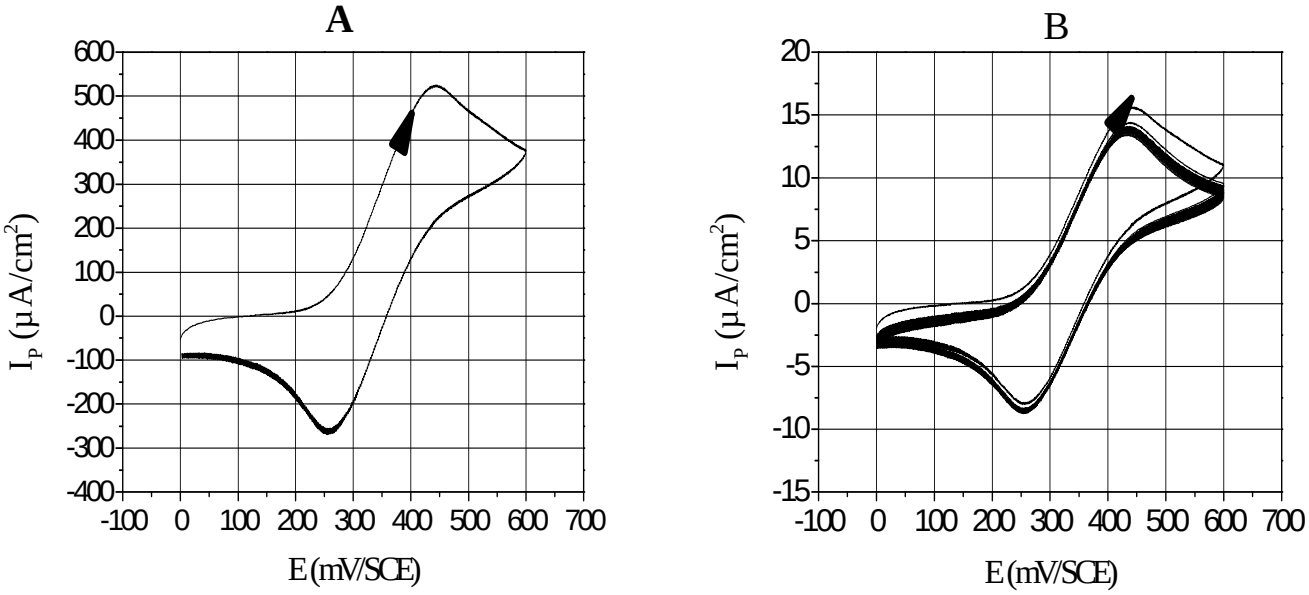

Figure III- 9 : cyclic voltammogram of ferrocene in aqueous ethanol (90%) at100 mV/s, on Pt indicator electrode. (A) one cycle, (B) five cycles, (Vs/SCE), 25 ^{0}C.

The cyclic voltammograms and the multi-cycles voltammograms of ferrocene in aqueous ethanol (81%, 73%, 66%, and 59%) on Pt fixed indicator electrode at scan rate of 100mV/s are presented in the appendix.

On the Pt indicator fixed electrode, the electrochemical behavior of ferrocene presented a rapid, reversible and one electron transferred electrochemical reaction in potential window of 0-600 mV (Vs/SCE), at different scan rates equal to 25, 50, 75, 100 and150 mV/s.

The electrochemical parameters of ferrocene/ferrocenium couple obtained on Pt fixed indicator electrode are summarized in the table III-11.

Table III- 11 : analysis of data obtained from cyclic voltammograms of ferrocene in aqueous ethanol at different percentages on Pt FIE

Aqueous ethanol %	**Scan rate** (mV/s)	E_a (mV)	E_c (mV)	$E_{1/2}$ (mV)	I_a (mA/cm^2)	I_c (mA/cm^2)	$\lvert I_a/I_c \rvert$
90	25	426.8	278.9	352.85	353E-03	-352E-03	1.0030
	50	443.6	271.3	357.45	420E-03	-419E-03	1.0025
	75	439.3	264.2	351.75	473E-03	-472E-03	1.0013
	100	441.4	257.1	349.25	521E-03	-520E-03	1.0026
	150	450.1	249.0	349.55	606E-03	-604E-03	1.0032
81	25	359.4	256.6	308.00	249E-03	-248E-03	1.0065
	50	355.0	253.3	304.15	316E-03	-315E-03	1.0038
	75	357.7	247.4	302.55	370E-03	-369E-03	1.0024
	100	359.4	245.7	302.55	417E-03	-414E-03	1.0059
	150	365.3	241.4	303.35	499E-03	-497E-03	1.0041
73	25	325.1	239.8	282.45	188E-03	-187E-03	1.0076
	50	319.7	239.2	279.45	255E-03	-253E-03	1.0076
	75	324.6	235.9	280.25	303E-03	-301E-03	1.0063
	100	326.2	233.8	280.00	342E-03	-341E-03	1.0042
	150	331.1	228.9	280.00	408E-03	-404E-03	1.0079
66	25	293.6	224.0	258.80	172E-03	-171E-03	1.0077
	50	293.0	220.7	256.85	219E-03	-219E-03	1.0011
	75	296.3	219.1	257.70	268E-03	-265E-03	1.0101
	100	299.0	218.6	258.80	296E-03	-295E-03	1.0040
	150	299.0	217.5	258.25	355E-03	-355E-03	1.0021
59	25	272.4	209.9	241.15	128E-03	-126E-03	1.0200
	50	276.7	206.0	241.35	181E-03	-180E-03	1.0080
	75	276.2	206.0	241.10	213E-03	-211E-03	1.0055
	100	280.0	205.0	242.50	239E-03	-238E-03	1.0074
	150	281.1	202.8	241.95	302E-03	-300E-03	1.0035

The values of $E_{1/2}$ are independents to scan rate variations, so the electrochemical reaction of ferrocene on Pt fixed indicator electrode is a rapid and reversible.

Mode of transfer electrochemical reaction of ferrocene on Pt FIE

To find the electrochemical reaction mechanism of ferrocene at Pt fixed indicator electrode, we plotted the intensity of the anodic and cathodic peaks current as a function of the square root of scan rate $I_P = f(\sqrt{v})$, in each case we obtained a straight line passes by the origin which indicates that the electrochemical reaction on Pt fixed indicator electrode is controlled by diffusion process.

On Pt rotating indicator electrode

On Pt rotating indicator electrode, the electrochemical behavior of ferrocene presented a rapid, reversible and one electron transferred electrochemical reaction in window potential of 0-600 mV, at scan rate equals to100 mV/s and at different angular velocities equal to 1200, 1600, 1800 and 2000 rpm.

Table III- 12 : analysis of data obtained from polarograms of ferrocene in aqueous ethanol at different percentages on Pt RIE

Aqueous ethanol %	**Angular velocities** rpm	I_{lim} (mA/cm^2)	$I_{lim/2}$ (mA/cm^2)	$E_{1/2}$ (mV)
90	1200	0.9306	0.46530	374.0
	1600	1.0970	0.54850	385.3
	1800	1.1820	0.59100	391.2
	2000	1.2710	0.63550	397.2
81	1200	0.8077	0.40385	311.4
	1600	0.9254	0.46270	319.5
	1800	0.9736	0.48680	319.7
	2000	1.0120	0.50600	320.0
73	1200	0.6205	0.31025	282.2
	1600	0.7113	0.35565	287.1
	1800	0.7466	0.37330	292.5
	2000	0.7862	0.39310	292.8
66	1200	0.5392	0.26960	251.5
	1600	0.6165	0.30825	255.8
	1800	0.6560	0.32800	256.3
	2000	0.6780	0.33900	257.4
59	1200	0.4329	0.21645	229.9
	1600	0.4975	0.24875	233.1
	1800	0.5259	0.26295	235.3
	2000	0.5546	0.27730	237.4

The electrochemical parameters of oxidation reaction of ferrocene obtained on Pt rotating indicator electrode are summarized in the table III-12.

The values of $E_{1/2}$ are independents to angular velocities variations, so the electrochemical reaction of ferrocene on Pt rotating indicator electrode is a rapid and reversible.

Mode of transfer electrochemical reaction of ferrocene on Pt RIE

To find the oxidation reaction mechanism of ferrocene to ferrocenium cation on Pt rotating indicator electrode, we plotted the variations in the intensity of the limit current as a function of the square root of angular velocity , $I_{lim} = f(\sqrt{\omega})$ .in each case we obtained a straight line passes by the origin which indicate that the oxidation reaction is controlled by diffusion process.

cyclic voltammogram of ferrocene on Pt fixed electrode at scan rates 25, 50, 75, 100 and 150 mV/s, the polarogram of ferrocene on Pt rotating electrode at angular velocities 1200, 1600, 1800 and 2000 rpm, at scan rate equals 100 mV/s, $I_P = f(\sqrt{v})$ plot and $I_{lim} = f(\sqrt{\omega})$ plot of ferrocene in aqueous ethanol (90%, 81%, 73%, 66%, 59%), on Pt indicator electrode in potential window of 0-600 mV (Vs/SCE), at 25 ^{0}C are presented in figure III-10 to figure III-14.

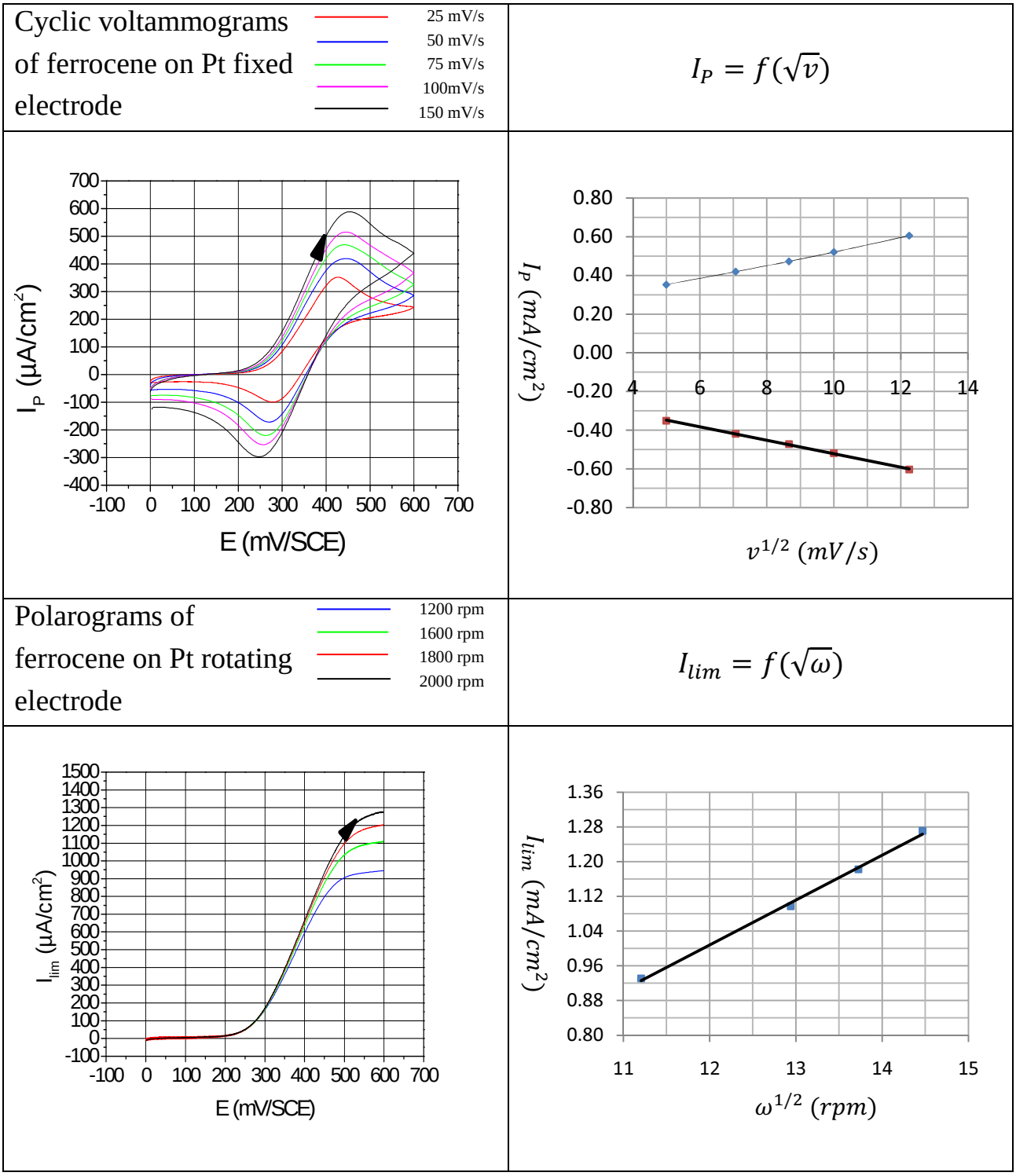

Figure III- 10: cyclic voltammogram of ferrocene on Pt fixed electrode at scan rates 25, 50, 75, 100 and 150 mV/s, the polarogram of ferrocene on Pt rotating electrode at angular velocities 1200, 1600, 1800 and 2000 rpm, $\boldsymbol{I_P = f(\sqrt{v})}$ plot and $\boldsymbol{I_{lim} = f(\sqrt{\omega})}$ plot of ferrocene in aqueous ethanol (90 %), on Pt indicator electrode in potential window of 0-600 mV (Vs/SCE), at 25 ^{0}C.

Cyclic voltammograms of ferrocene on Pt fixed electrode	$I_P = f(\sqrt{v})$
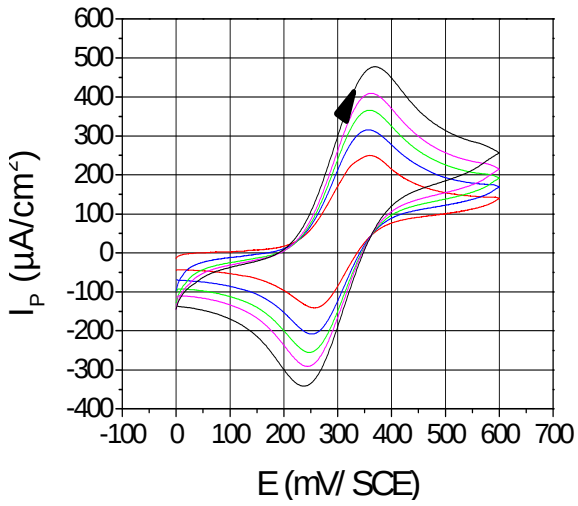	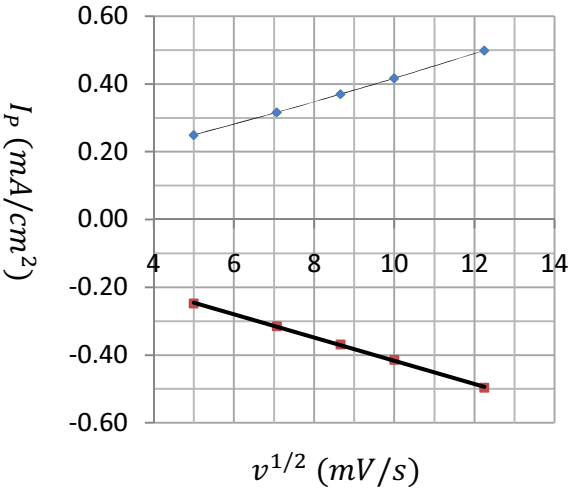
polarograms of ferrocene on Pt rotating electrode	$I_{lim} = f(\sqrt{\omega})$
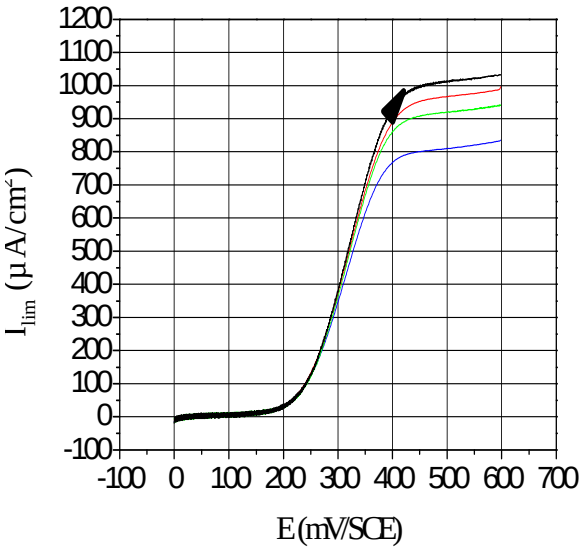	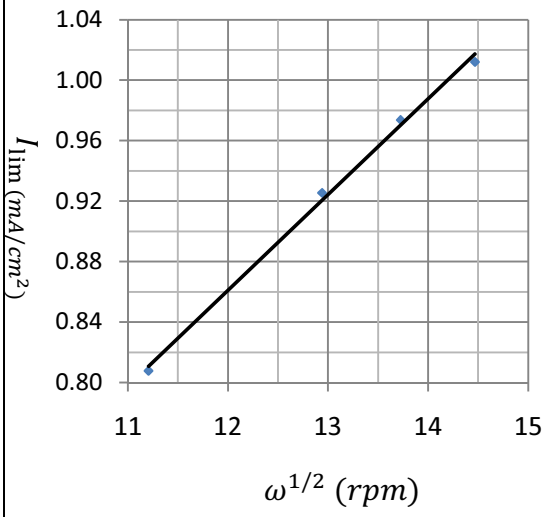

Figure III- 11: cyclic voltammogram of ferrocene on Pt fixed electrode at scan rates 25, 50, 75, 100 and 150 mV/s, the polarogram of ferrocene on Pt rotating electrode at angular velocities 1200, 1600, 1800 and 2000 rpm, $\boldsymbol{I_P = f(\sqrt{v})}$ plot and $\boldsymbol{I_{lim} = f(\sqrt{\omega})}$ plot of ferrocene in aqueous ethanol (81 %) on Pt indicator electrode in potential window of 0-600 mV (Vs/SCE), at 25 ^{0}C.

Cyclic voltammograms of ferrocene on Pt fixed electrode	$I_P = f(\sqrt{v})$
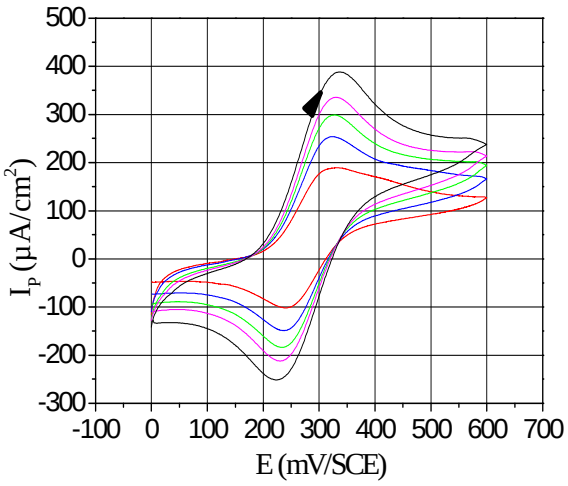	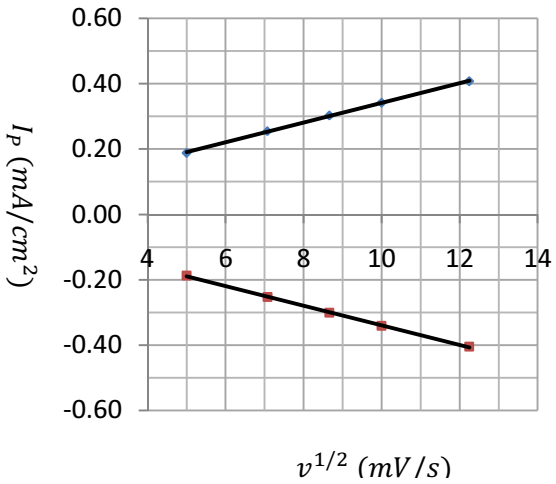
polarograms of ferrocene on Pt rotating electrode	$I_{lim} = f(\sqrt{\omega})$
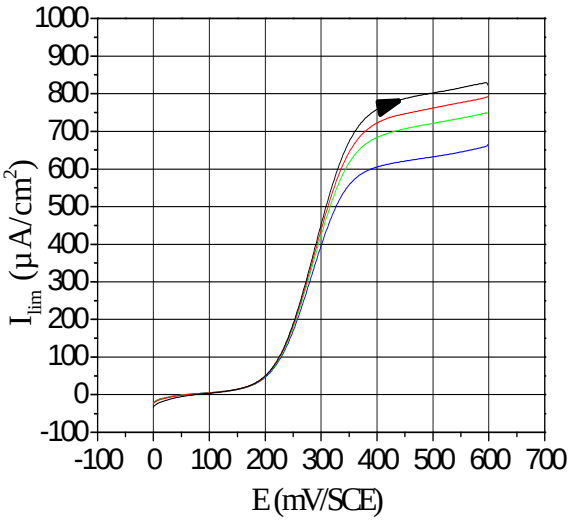	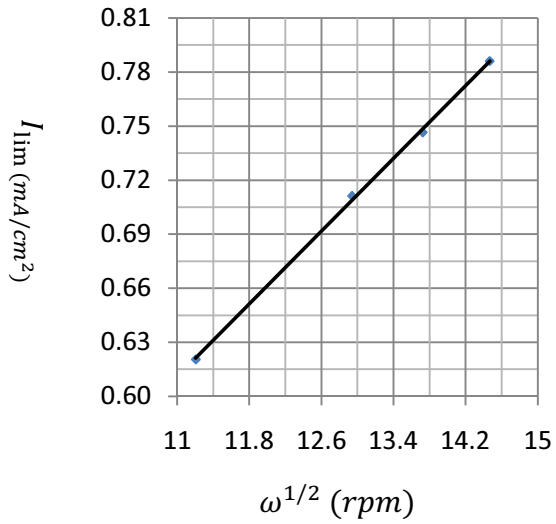

Figure III- 12 : cyclic voltammogram of ferrocene on Pt fixed electrode at scan rates 25, 50, 75, 100 and 150 mV/s, the polarogram of ferrocene on Pt rotating electrode at angular velocities 1200, 1600, 1800 and 2000 rpm, $\boldsymbol{I_P = f(\sqrt{v})}$ plot and $\boldsymbol{I_{lim} = f(\sqrt{\omega})}$ plot of ferrocene in aqueous ethanol (73 %) on Pt indicator electrode in potential window of 0-600 mV (Vs/SCE), at 25 ^{0}C.

Cyclic voltammograms of ferrocene on Pt fixed electrode	$I_P = f(\sqrt{v})$
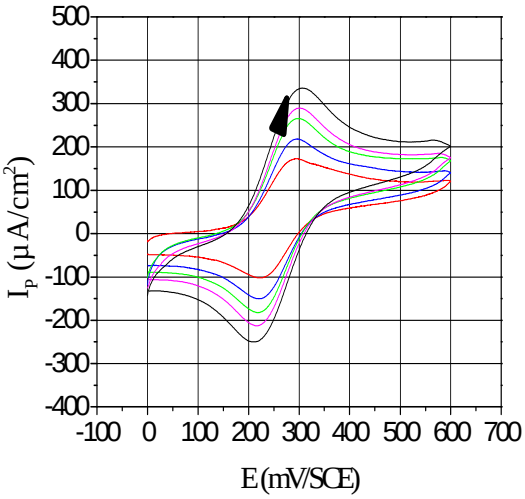	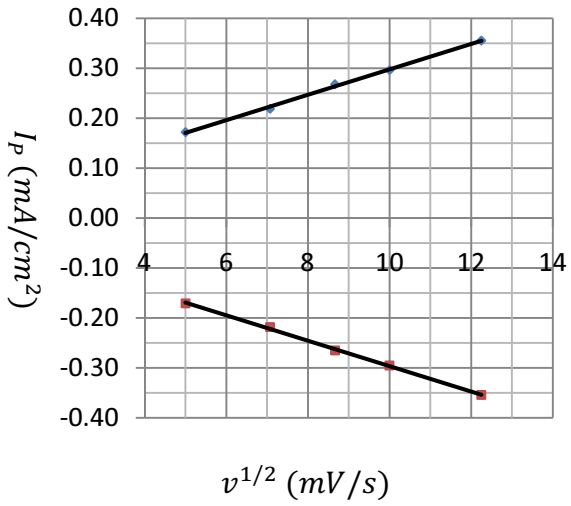
polarograms of ferrocene on Pt rotating electrode	$I_{lim} = f(\sqrt{\omega})$
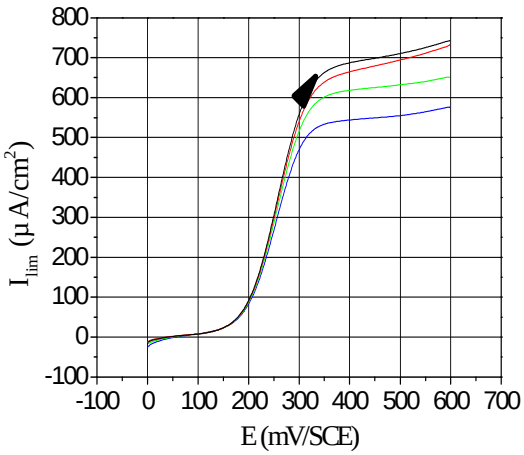	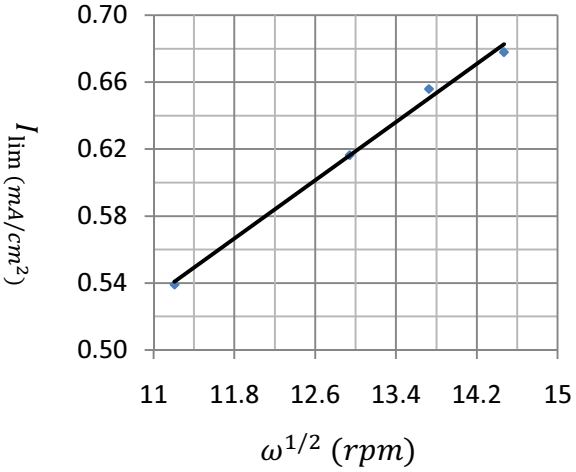

Figure III- 13 : cyclic voltammogram of ferrocene on Pt fixed electrode at scan rates 25, 50, 75, 100 and 150 mV/s, the polarogram of ferrocene on Pt rotating electrode at angular velocities 1200, 1600, 1800 and 2000 rpm, $\boldsymbol{I_P = f(\sqrt{v})}$ plot and $\boldsymbol{I_{lim} = f(\sqrt{\omega})}$ plot of ferrocene in aqueous ethanol (66 %) on Pt indicator electrode in potential window of 0-600 mV (Vs/SCE), at 25 ^{0}C.

Cyclic voltammograms of ferrocene on Pt fixed electrode	$I_P = f(\sqrt{v})$
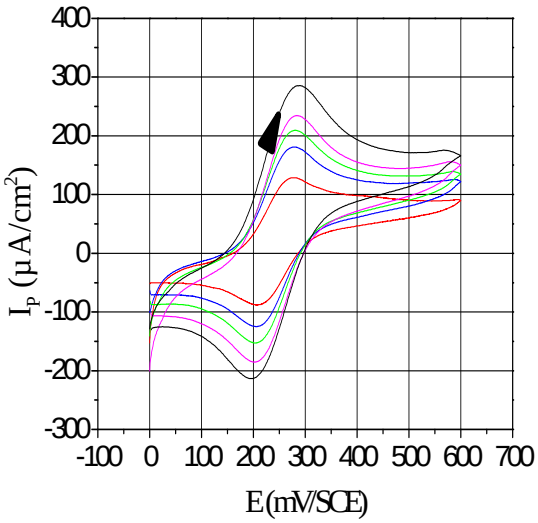	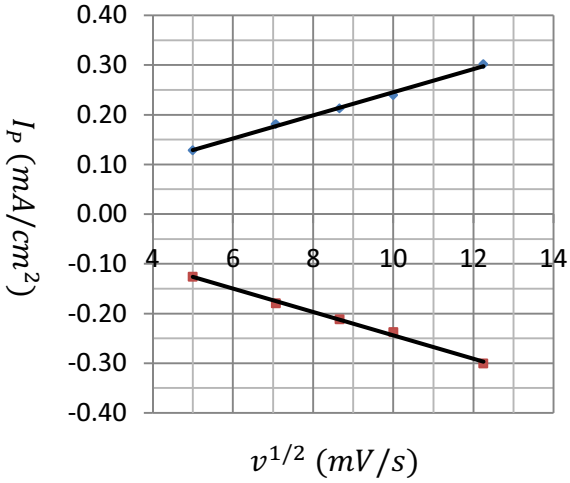
polarograms of ferrocene on Pt rotating electrode	$I_{lim} = f(\sqrt{\omega})$
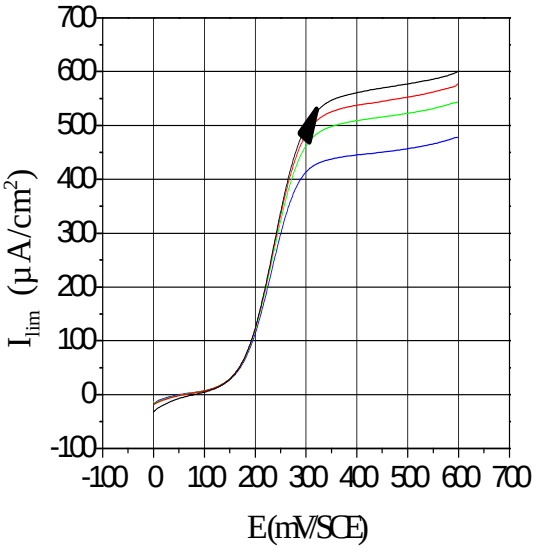	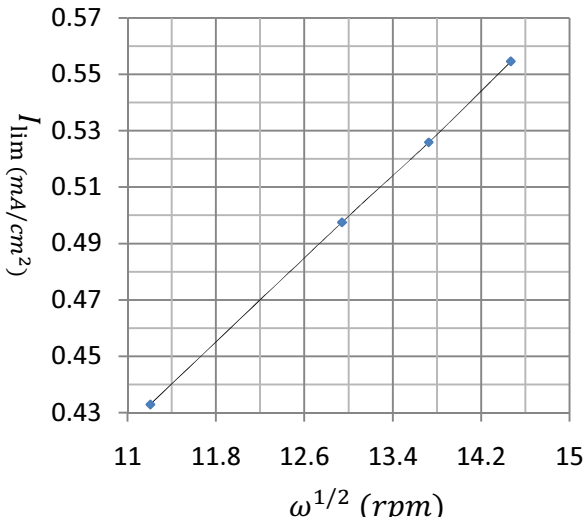

Figure III- 14 : cyclic voltammogram of ferrocene on Pt fixed electrode at scan rates 25, 50, 75, 100 and 150 mV/s, the polarogram of ferrocene on Pt rotating electrode at angular velocities 1200, 1600, 1800 and 2000 rpm, $\boldsymbol{I_P = f(\sqrt{v})}$ plot and $\boldsymbol{I_{lim} = f(\sqrt{\omega})}$ plot of ferrocene in aqueous ethanol (59 %) on Pt indicator electrode in potential window of 0-600 mV (Vs/SCE), at 25 ^{0}C.

On glassy carbon (GC) indicator fixed electrode

Before the study of the electrochemical behavior of ferrocene in aqueous ethanol at different percentages, on GC indicator electrode, the reactivity and the stability of the electroactive molecule must be confirmed, the reactivity of ferrocene in window potential of 0-600mV (Vs/SCE) is confirmed with the obtaining of a cyclic voltammogram presents an anodic peak at 0.450 mV and an cathodic peak at 0.250 mV (fig III-15, (A)), those two peaks are corresponded to the oxidation and to the reduction of ferrocene/ferrocenium couple, and the superposed of multi-cycles voltammograms (in our case 05 cycles) indicates that the system is stable and do not change with the variation of the time (fig III-15, (B)).

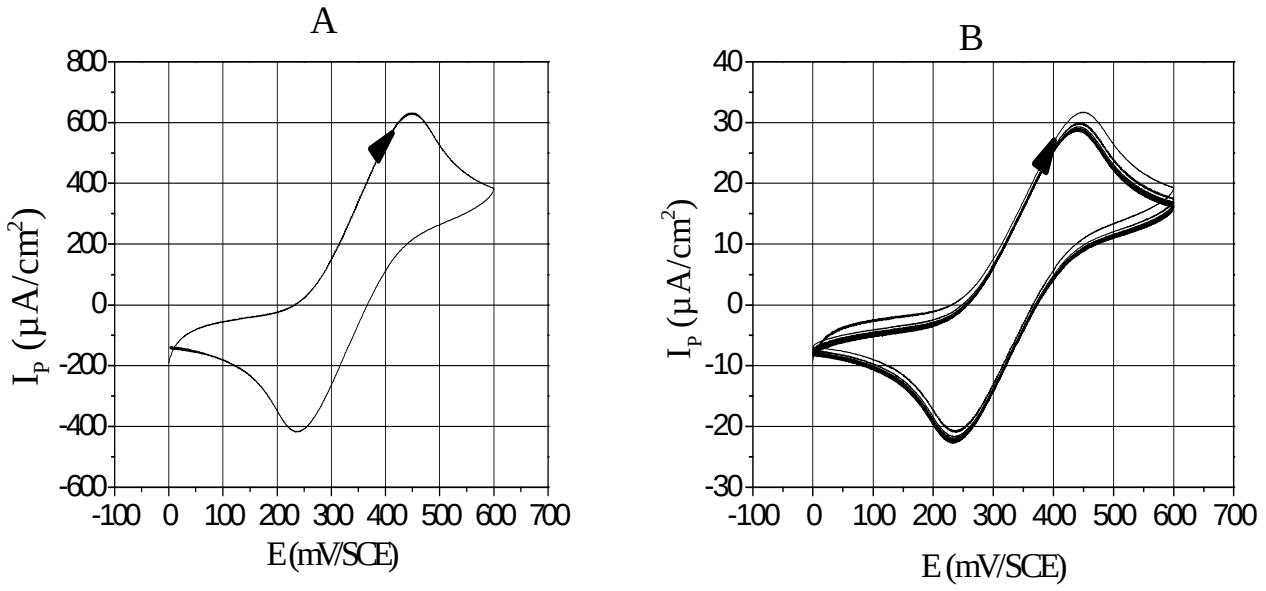

Figure III- 15: cyclic voltammogram of ferrocene in aqueous ethanol (90%) at100 mV/s, on GC indicator electrode (A) one cycle, (B) five cycles, (Vs/SCE), 25 ^{0}C.

The cyclic voltammograms and the multi-cycles voltammograms of ferrocene in aqueous ethanol (81%, 73%, 66%, and 59%) on GC indicator electrode are presented in the appendix.

On GC indicator fixed electrode, the electrochemical behavior of ferrocene presented a reversible; one electron transferred electrochemical reaction in potential window of 0-600 mV and at different scan rates equal to 25, 50, 75, 100, and150 mV/s.

The electrochemical parameters of ferrocene obtained on GC indicator electrode are summarized in the table III-13.

Table III- 13 : analysis of data obtained from cyclic voltammograms of ferrocene in aqueous ethanol at different percentages on GC FIE

Aqueous ethanol %	**Scan rate** (mV/s)	E_a (mV)	E_c (mV)	$E_{1/2}$ (mV)	I_a (mA/cm^2)	I_c (mA/cm^2)	$\lvert I_a/I_c \rvert$
90	25	421.9	265.3	343.60	399E-03	-397E-03	1.0072
	50	430.0	252.8	341.40	486E-03	-485E-03	1.0029
	75	441.4	244.6	343.00	566E-03	-563E-03	1.0053
	100	448.5	236.5	342.50	628E-03	-625E-03	1.0037
	150	461.6	226.7	344.15	732E-03	-729E-03	1.0033
81	25	369.1	252.1	310.60	333E-03	-332E-03	1.0043
	50	369.1	248.5	308.80	415E-03	-414E-03	1.0034
	75	371.9	242.5	307.20	469E-03	-466E-03	1.0046
	100	374.0	239.8	306.90	515E-03	-513E-03	1.0036
	150	381.6	233.2	307.40	621E-03	-620E-03	1.0018
73	25	325.1	240.3	282.70	239E-03	-237E-03	1.0078
	50	324.0	235.9	279.95	342E-03	-340E-03	1.0041
	75	329.5	234.9	282.20	398E-03	-397E-03	1.0046
	100	332.2	231.6	281.90	448E-03	-446E-03	1.0033
	150	334.9	226.6	280.75	539E-03	-537E-03	1.0034
66	25	299.0	225.6	262.30	199E-03	-197E-03	1.0082
	50	300.1	221.3	260.70	271E-03	-270E-03	1.0049
	75	302.8	219.6	261.20	335E-03	-333E-03	1.0062
	100	305.0	218.0	261.50	381E-03	-380E-03	1.0021
	150	309.3	216.4	262.85	465E-03	-465E-03	1.0002
59	25	273.5	207.1	240.30	201E-03	-200E-03	1.0071
	50	276.2	205.0	240.60	260E-03	-259E-03	1.0054
	75	277.3	205.0	241.15	306E-03	-305E-03	1.0036
	100	278.4	201.7	240.05	345E-03	-344E-03	1.0032
	150	281.1	201.7	241.40	422E-03	-421E-03	1.0041

The values of $E_{1/2}$ are independents to scan rate variations, so the electrochemical reaction of ferrocene on GC fixed indicator electrode is a rapid and reversible.

Mode of transfer electrochemical reaction of ferrocene on GC FIE

To find the redox reaction mechanism of ferrocene at the GC fixed indicator electrode, we plotted the intensity of the anodic and cathodic peaks current as a function of the square root of scan rate $I_P = f(\sqrt{v})$, in each case we obtained a straight line passes by the origin which indicates that the electrochemical reaction on the GC fixed indicator electrode is controlled by diffusion process.

On glassy carbon GC rotating indicator electrode

On the GC rotating indicator electrode, the electrochemical behavior of ferrocene presented a rapid, reversible, and one electron transferred electrochemical reaction in 0-600 mV potential window, at scan rate equals to100 mV/s and at different angular velocities equal to 1200, 1600, 1800 and 2000 rpm.

The electrochemical parameters of ferrocene obtained on GC rotating indicator electrode are summarized in the table III-14.

Table III- 14: analysis of data obtained from polarograms of ferrocene in aqueous ethanol at different percentages on GC RIE

Aqueous ethanol %	**Angular velocities** rpm	I_{lim} (mA/cm^2)	$I_{lim/2}$ (mA/cm^2)	$E_{1/2}$ (mV)
90	1200	1.371	0.6855	395.0
	1600	1.564	0.7820	403.6
	1800	1.650	0.8250	409.6
	2000	1.740	0.8700	416.3
81	1200	1.061	0.5305	327.0
	1600	1.214	0.6070	330.2
	1800	1.299	0.6495	335.1
	2000	1.376	0.6880	339.4
73	1200	0.885	0.4428	283.8
	1600	1.012	0.5060	287.6
	1800	1.069	0.5345	291.9
	2000	1.112	0.5560	293.0
66	1200	0.712	0.3561	256.3
	1600	0.819	0.4095	260.6
	1800	0.866	0.4334	263.3
	2000	0.916	0.4580	265.0
59	1200	0.614	0.3073	233.1
	1600	0.696	0.3482	234.7
	1800	0.727	0.3637	236.4
	2000	0.764	0.3820	239.6

The values of $E_{1/2}$ are independents to angular velocities variations, so the electrochemical reaction of ferrocene on GC rotating indicator electrode is a rapid and reversible.

Mode of transfer electrochemical reaction of ferrocene on GC RIE

To find the oxidation reaction mechanism of ferrocene to ferrocenium cation at GC rotating indicator electrode, we plotted the variations in the intensity of the limit current as a function to the square root of angular velocity , $I_{lim} = f(\sqrt{\omega})$ .in each case we obtained a straight line passes by the origin which indicates that the oxidation reaction is controlled by diffusion process.

cyclic voltammogram of ferrocene on GC fixed electrode at scan rates 25, 50, 75, 100 and 150 mV/s, the polarogram of ferrocene on GC rotating electrode at angular velocities 1200, 1600, 1800 and 2000 rpm, $\boldsymbol{I_P = f(\sqrt{v})}$ plot and $\boldsymbol{I_{lim} = f(\sqrt{\omega})}$ plot of ferrocene in aqueous ethanol (90%, 81%, 73%, 66%, 59%), on GC indicator electrode in potential window of 0-600 mV (Vs/SCE), are shown in figure III-16 to figure III-20.

Cyclic voltammograms of ferrocene on GC fixed electrode	$I_P = f(\sqrt{v})$
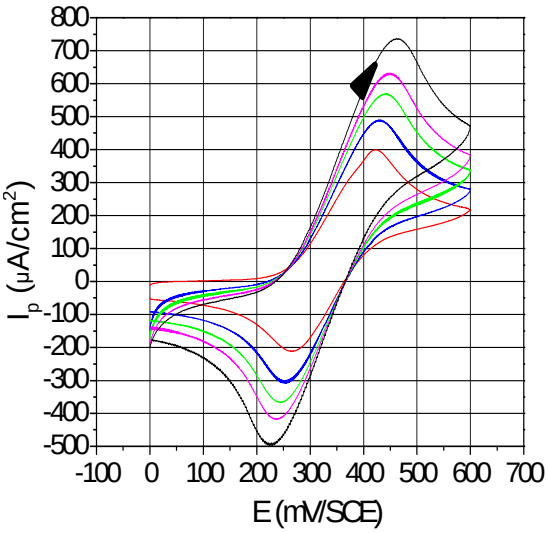	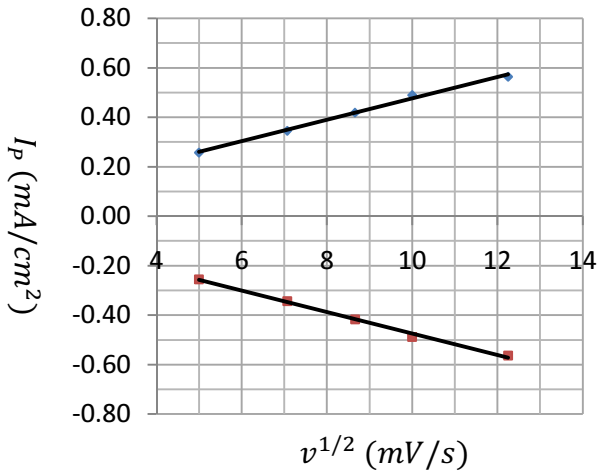
polarograms of ferrocene on GC rotating electrode	$I_{lim} = f(\sqrt{\omega})$
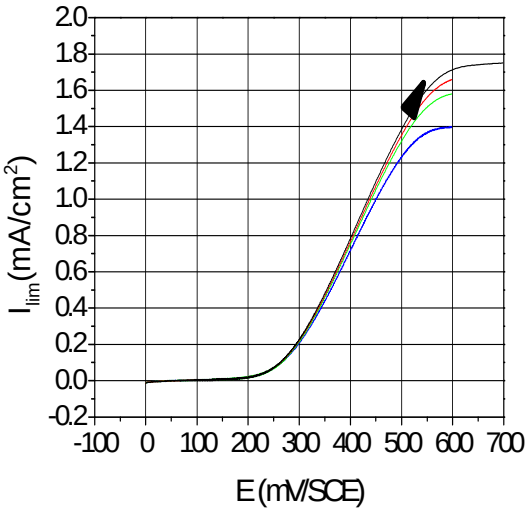	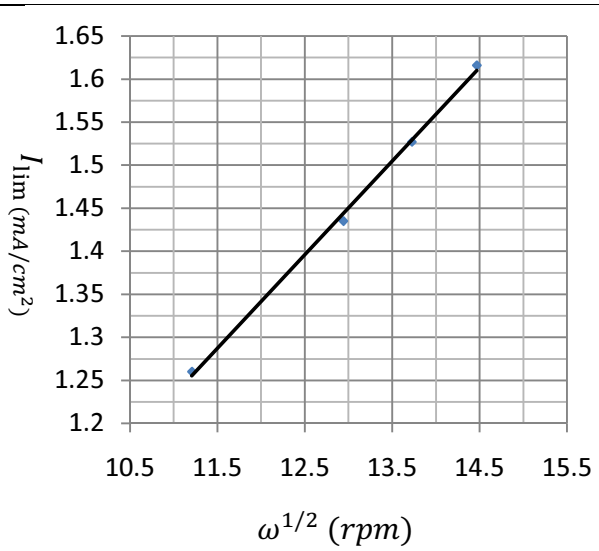

Figure III- 16 : cyclic voltammogram of ferrocene on GC fixed electrode at scan rates 25, 50, 75, 100 and 150 mV/s, the polarogram of ferrocene on GC rotating electrode at angular velocities 1200, 1600, 1800 and 2000 rpm, $\boldsymbol{I_P = f(\sqrt{v})}$ plot and $\boldsymbol{I_{lim} = f(\sqrt{\omega})}$ plot of ferrocene in aqueous ethanol (90 %), on GC indicator electrode in potential window of 0-600 mV (Vs/SCE), at 25 ^{0}C.

Cyclic voltammograms of ferrocene on GC fixed electrode	$I_P = f(\sqrt{v})$
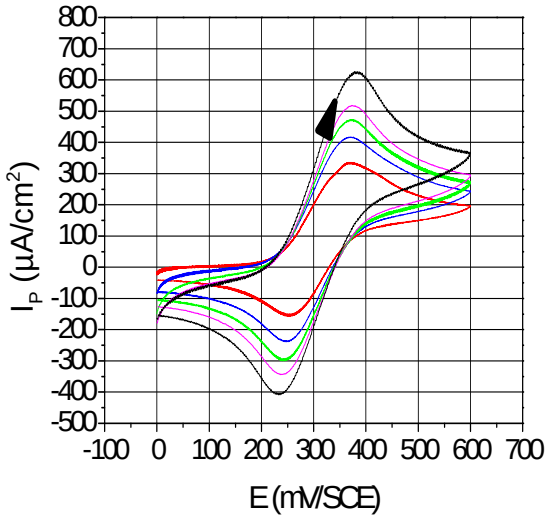	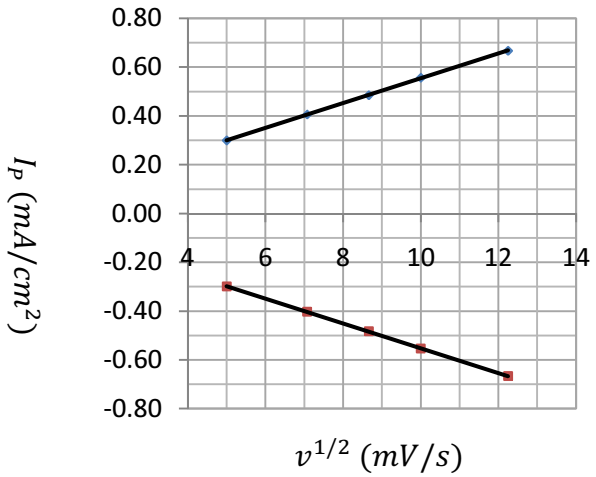
polarogram of ferrocene on GC rotating electrode	$I_{lim} = f(\sqrt{\omega})$
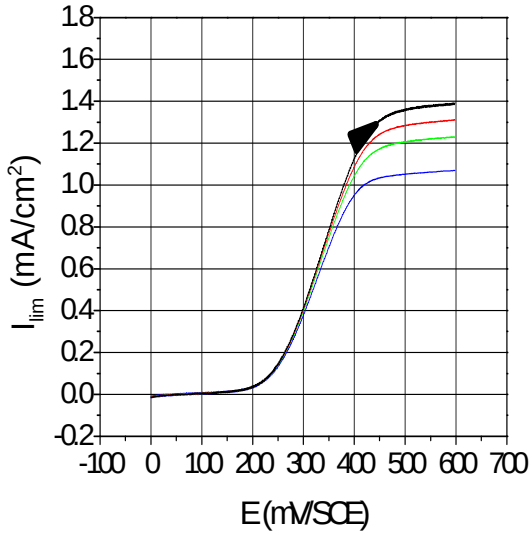	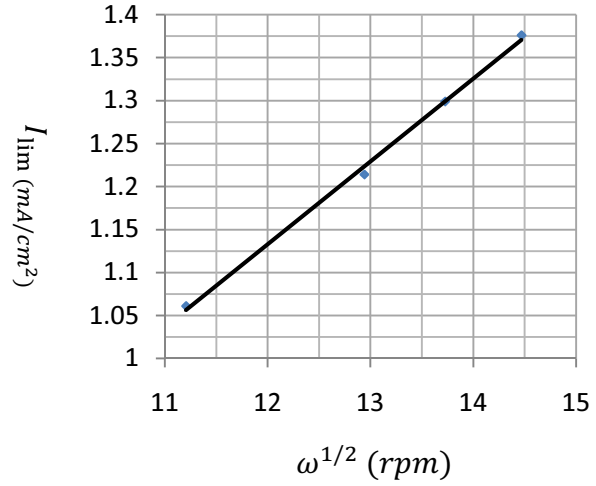

Figure III- 17 : cyclic voltammogram of ferrocene on GC fixed electrode at scan rates 25, 50, 75, 100 and 150 mV/s, the polarogram of ferrocene on GC rotating electrode at angular velocities 1200, 1600, 1800 and 2000 rpm, $\boldsymbol{I_P = f(\sqrt{v})}$ plot and $\boldsymbol{I_{lim} = f(\sqrt{\omega})}$ plot of ferrocene in aqueous ethanol (81 %) on GC indicator electrode in potential window of 0-600 mV (Vs/SCE), at 25 ^{0}C.

Cyclic voltammograms of ferrocene on GC fixed electrode	$I_P = f(\sqrt{v})$
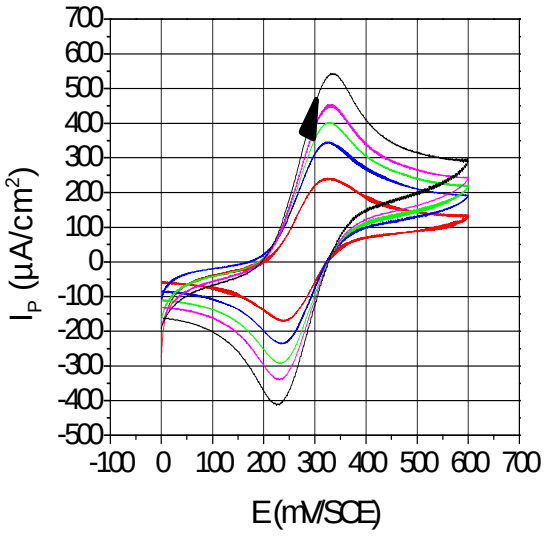	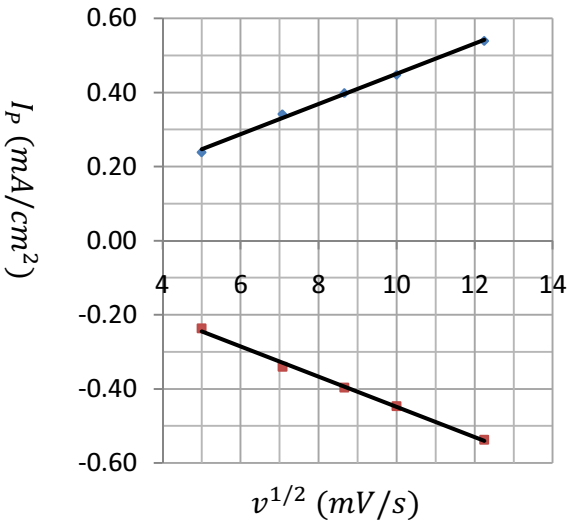
polarograms of ferrocene on GC rotating electrode	$I_{lim} = f(\sqrt{\omega})$
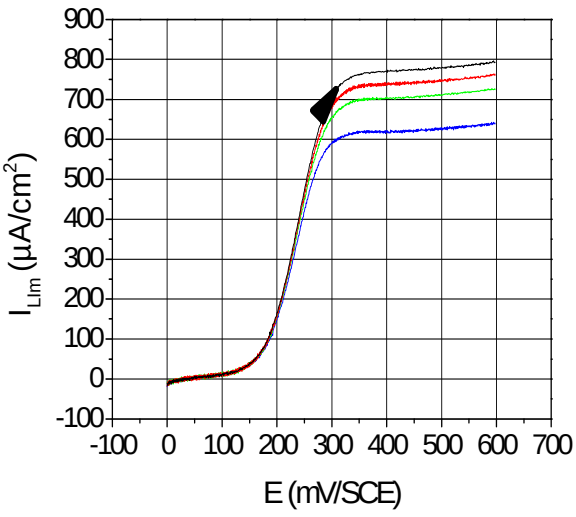	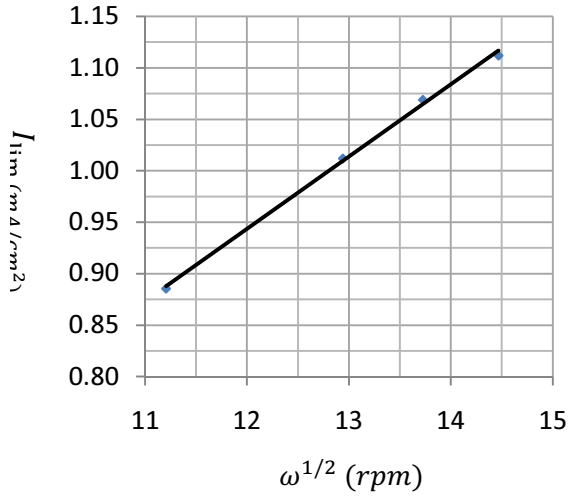

Figure III- 18: cyclic voltammogram of ferrocene on GC fixed electrode at scan rates 25, 50, 75, 100 and 150 mV/s, the polarogram of ferrocene on GC rotating electrode at angular velocities 1200, 1600, 1800 and 2000 rpm, $\boldsymbol{I_P = f(\sqrt{v})}$ plot and $\boldsymbol{I_{lim} = f(\sqrt{\omega})}$ plot of ferrocene in aqueous ethanol (73 %) on GC indicator electrode in potential window of 0-600 mV (Vs/SCE), at 25 ^{0}C.

Cyclic voltammograms of ferrocene on GC fixed electrode	$I_P = f(\sqrt{v})$
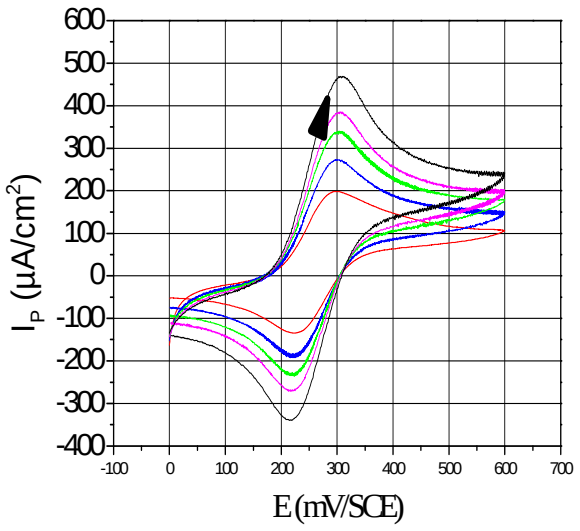	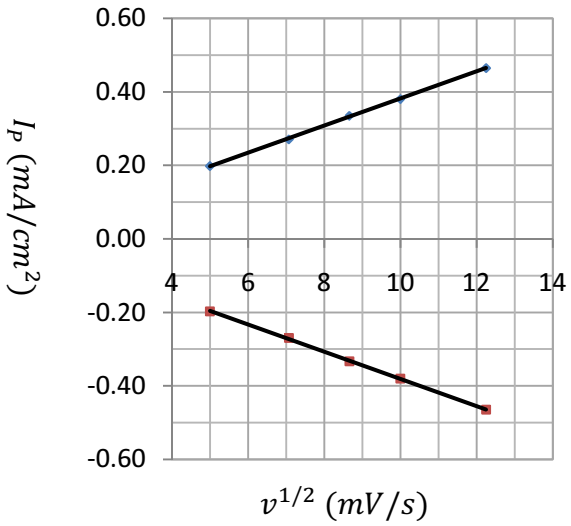
polarograms of ferrocene on GC rotating electrode	$I_{lim} = f(\sqrt{\omega})$
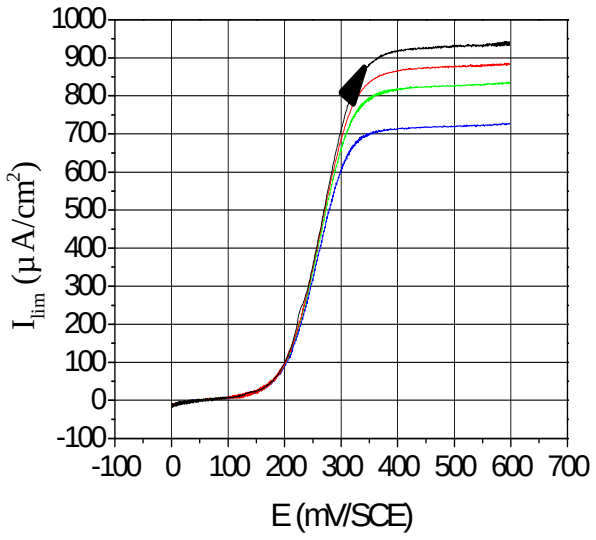	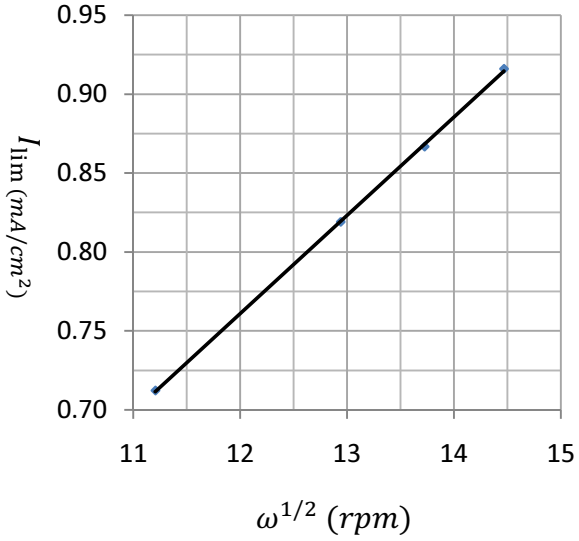

Figure III- 19 : cyclic voltammogram of ferrocene on GC fixed electrode at scan rates 25, 50, 75, 100 and 150 mV/s, the polarogram of ferrocene on GC rotating electrode at angular velocities 1200, 1600, 1800 and 2000 rpm, $\boldsymbol{I_P = f(\sqrt{v})}$ plot and $\boldsymbol{I_{lim} = f(\sqrt{\omega})}$ plot of ferrocene in aqueous ethanol (66 %) on GC indicator electrode in potential window of 0-600 mV (Vs/SCE), at 25 ^{0}C.

Cyclic voltammograms of ferrocene on GC fixed electrode	$I_P = f(\sqrt{v})$
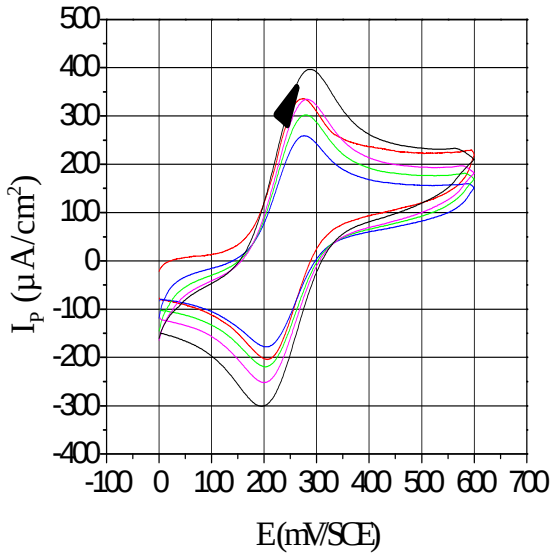	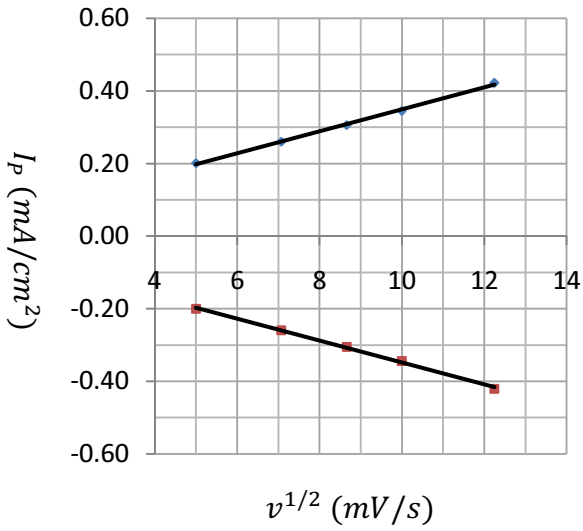
polarograms of ferrocene on GC rotating electrode	$I_{lim} = f(\sqrt{\omega})$
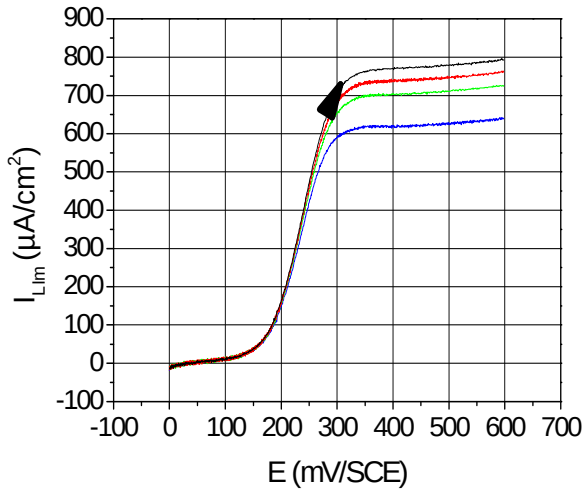	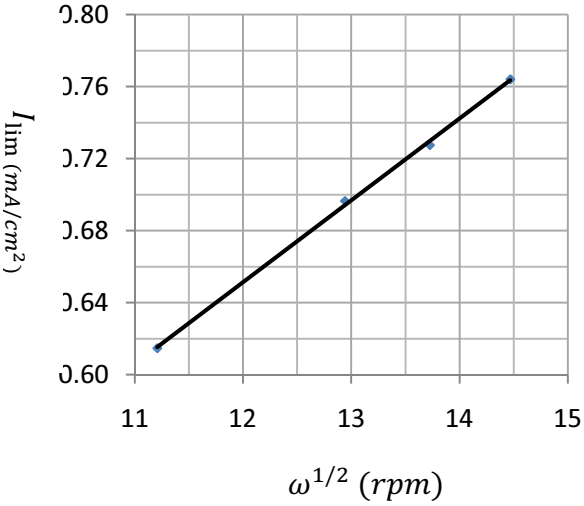

Figure III- 20 : cyclic voltammogram of ferrocene on GC fixed electrode at scan rates 25, 50, 75, 100 and 150 mV/s, the polarogram of ferrocene on GC rotating electrode at angular velocities 1200, 1600, 1800 and 2000 rpm, $\boldsymbol{I_P = f(\sqrt{v})}$ plot and $\boldsymbol{I_{lim} = f(\sqrt{\omega})}$ plot of ferrocene in aqueous ethanol (59 %) on GC indicator electrode in potential window of 0-600 mV (Vs/SCE), at 25 ^{0}C.

5.2.2. Calculation of diffusion coefficients of ferrocene/ferrocenium couple and diffusion layer thicknesses

On fixed Pt, GC indicator electrodes

The electrochemical reaction of ferrocene on Pt and GC fixed indicator electrodes is a reversible; one electron transferred electrochemical reaction, controlled by diffusion process. A VBA program was constructed to facilitate the calculation of the diffusion coefficients of all electroactive species in aqueous ethanol at different percentages.

The first part calculates the coefficient diffusion based on the following relations:

$$I_P = 0.4463 \left(\frac{F^3}{RT}\right)^{1/2} n^{3/2} A C D^{1/2} \nu^{1/2}$$

$$D = (the\ slope)^2 / ((26900)^2 * (C)^2)$$

```
Public Function coefficient_diffusion(pente As Double, n As
      Double, c As Double)
  Coefficient_diffusion = (pente^2)/((269000)^(2)*n^3*c^2)
End Function
```

The diffusion coefficients of ferrocene/ferrocenium couple in aqueous ethanol at different percentages obtained on Pt fixed indicator electrode are summarized in the table III-15, and the results are reported with 02 decimals.

Table III- 15: the diffusion coefficients of ferrocene in aqueous ethanol at different percentages on Pt FIE

Aqueous ethanol %	**Concentration** (mol/l)	**The slope**	D_{Fc} (m^2/s)	**The slope**	D_{Fc^+} (m^2/s)
90	$2{,}70.10^{-3}$	0.00348	2.30E-09	0.00348	2.30E-09
81	$2{,}43.10^{-3}$	0.00344	2.77E-09	0.00344	2.77E-09
73	$2{,}19.10^{-3}$	0.00302	2.64E-09	0.00302	2.64E-09
66	$1{,}97.10^{-3}$	0.00255	2.32E-09	0.00255	2.32E-09
59	$1{,}77.10^{-3}$	0.00233	2.39E-09	0.00233	2.39E-09

The diffusion layer of ferrocene, ferrocenyl methyl aniline and N (ferrocenyl methyl)2 nitro aniline, in aqueous ethanol solution at different percentages obtained on Pt, GC fixed indicator electrodes, at scan rate equals to 100 mV/s, in window potential of 0-600 mV/s, lives 6 s.

The diffusion layer thicknesses of ferrocene in aqueous ethanol solution at different percentages obtained on Pt fixed indicator electrode are summarized in table III-16.

Table III- 16: diffusion layer thicknesses of ferrocene in aqueous ethanol solution at different percentages obtained on Pt FIE

Aqueous ethanol %	C (mol/l)	D (m^2/s)	t (s)	$\delta = \sqrt{Dt}$ (cm)
90	$2.70 .10^{-3}$	$2.30 .10^{-9}$	1	0.004796
			2	0.006782
			3	0.008307
			4	0.009592
			5	0.010724
			6	0.011747
81	$2.43 .10^{-3}$	$2.77 .10^{-9}$	1	0.005263
			2	0.007443
			3	0.009116
			4	0.010526
			5	0.011769
			6	0.012892
73	$2.19 .10^{-3}$	$2.64 .10^{-9}$	1	0.005138
			2	0.007266
			3	0.008899
			4	0.010276
			5	0.011489
			6	0.012586
66	$1.97 .10^{-3}$	$2.32 .10^{-9}$	1	0.004817
			2	0.006812
			3	0.008343
			4	0.009633
			5	0.010770
			6	0.011798
59	$1.77 .10^{-3}$	$2.39 .10^{-9}$	1	0.004889
			2	0.006914
			3	0.008468
			4	0.009778
			5	0.010932
			6	0.011975

The diffusion coefficients of ferrocene/ferrocenium couple in aqueous ethanol at different percentages obtained on GC fixed indicator electrode are summarized in the table III-17, and the results are reported with 02 decimals.

Table III- 17: the diffusion coefficients of ferrocene/ferrocenium couple in aqueous ethanol at different percentages on GC FIE

Aqueous ethanol %	**Concentration** (mol/l)	**The slope**	D_{Fc} (m^2/s)	**The slope**	D_{Fc^+} (m^2/s)
90	$2{,}70.10^{-3}$	0.00462	4.05E-09	0.00462	4.05E-09
81	$2{,}43.10^{-3}$	0.00390	3.56E-09	0.00390	3.56E-09
73	$2{,}19.10^{-3}$	0.00407	4.79E-09	0.00407	4.79E-09
66	$1{,}97.10^{-3}$	0.00369	4.86E-09	0.00369	4.86E-09
59	$1{,}77.10^{-3}$	0.00303	4.04E-09	0.00303	4.04E-09

The diffusion layer thicknesses of ferrocene in aqueous ethanol solution at different percentages obtained on GC fixed indicator electrode are summarized in table III-18.

Table III- 18: diffusion layer thicknesses of ferrocene in aqueous ethanol solution at different percentages obtained on GC FIE

Aqueous ethanol %	C (mol/l)	D (m^2/s)	t (s)	$\delta = \sqrt{Dt}$ (cm)
90	$2.70\ .10^{-3}$	$4.05.\ 10^{-9}$	1	0.006364
			2	0.009000
			3	0.011023
			4	0.012728
			5	0.014230
			6	0.015588
81	$2.43.10^{-3}$	$3.56.\ 10^{-9}$	1	0.005967
			2	0.008438
			3	0.010334
			4	0.011933
			5	0.013342
			6	0.014615
73	$2.19.10^{-3}$	$4.79.\ 10^{-9}$	1	0.006921
			2	0.009788
			3	0.011987
			4	0.013842
			5	0.015476
			6	0.016953

Aqueous ethanol %	C (mol/l)	D (m^2/s)	t (s)	$\delta = \sqrt{Dt}$ (cm)
66	$1.97.10^{-3}$	$4.86.\ 10^{-9}$	1	0.006971
			2	0.009859
			3	0.012075
			4	0.013943
			5	0.015588
			6	0.017076
59	$1.77.10^{-3}$	$4.04.\ 10^{-9}$	1	0.006356
			2	0.008989
			3	0.011009
			4	0.012712
			5	0.014213
			6	0.015569

On rotating Pt, GC indicator electrodes

The reaction of oxidation of ferrocene to ferrocenium cation on Pt and GC rotating indicator electrodes is a reversible; one electron transferred electrochemical reaction, controlled by diffusion process. A VBA program was constructed to facilitate the calculation of the diffusion coefficients of the electroactive molecules in aqueous ethanol at different percentages.

The second part of VBA program calculates the coefficient diffusion on Pt and GC rotating indicator electrodes, based on the following relations:

$$I_{lim} = 0.62nFAD^{2/3}\omega^{1/2}\nu^{-1/6}c$$

$$D = (the\ slope)^{3/2}/((0.62 * F)^{3/2} * \nu^{-1/4} * (c)^{3/2})$$

```
Public Function coeff_diff_elec_tour(nu_kinvis_mix As Double,
              pente As Double, n As Double, c As Double)As Double
  coeff_diff_elec_tour=(pente^(3/2))/((062*96500)^(3/2)*c^(3/2)*
                       (nu_kinvis_mix)^(-1/4))
End Function
```

The diffusion coefficients of ferrocene in aqueous ethanol at different percentages obtained on Pt rotating indicator electrode are summarized in the table III-19, and the results are reported with 02 decimals.

Table III- 19: diffusion coefficients of ferrocene in aqueous ethanol at different percentages obtained on Pt RIE

Aqueous ethanol %	**Concentration** (mol/l)	**The slope**	D_{Fc} (m^2/s)
90	$2{,}70.10^{-3}$	0.01035	4.06E-08
81	$2{,}43.10^{-3}$	0.00633	2.43E-08
73	$2{,}19.10^{-3}$	0.00505	2.11E-08
66	$1{,}97.10^{-3}$	0.00435	2.03E-08
59	$1{,}77.10^{-3}$	0.00372	1.92E-08

The diffusion layer thicknesses of studied electroactive molecules in aqueous ethanol solutions at different percentages on Pt, GC rotating indicator electrode were calculated using a VBA Program based on the following relation:

$$\delta = 1.61 * {D_{ox}}^{(1/3)} * \omega^{(-1/2)} * \nu^{(1/6)}$$

```
Public Function epaisseur_diffusion_delta(n As Integer, w
         As Double, nusolution As Double, diffusioncoef As Double)

   epaisseur_diffusion_delta_ox = 1.61 * diffusioncoef ^ (1 / 3)*
                                  w^(-1/2) * nusolution^(1 6)
End Function
```

The diffusion layer thicknesses of ferrocene in aqueous ethanol solution at different percentages obtained on Pt rotating indicator electrode are summarized in table III-20

Table III- 20: diffusion layer thicknesses of ferrocene in aqueous ethanol solution at different percentages on Pt RIE

Aqueous ethanol %	C (mol/cm^3)	D (m^2/s)	ν_{sol} (25 ^{0}C) (cm^2/s)	ω (rad/s)	δ (cm)
90	$2.70.10^{-3}$	$4.06.10^{-8}$	$3.91\ .10^{-5}$	125.60	0.001217
				167.46	0.001054
				188.40	0.000994
				209.33	0.000943
81	$2.43.10^{-3}$	$2.43.10^{-8}$	$5.10.10^{-5}$	125.60	0.001072
				167.46	0.000929
				188.40	0.000876
				209.33	0.000831

Aqueous ethanol %	C (mol/cm^3)	D (m^2/s)	ν_{sol} (25 ^{0}C) (cm^2/s)	ω (rad/s)	δ (cm)
73	$2.19.10^{-3}$	$2.11.10^{-8}$	$6.04.10^{-5}$	125.60	0.001052
				167.46	0.000911
				188.40	0.000859
				209.33	0.000815
66	$1.97.10^{-3}$	$2.03.10^{-8}$	$6.73.10^{-5}$	125.60	0.001058
				167.46	0.000916
				188.40	0.000864
				209.33	0.000819
59	$1.77.10^{-8}$	$1.92.10^{-8}$	$7.24.10^{-5}$	125.60	0.001051
				167.46	0.000910
				188.40	0.000858
				209.33	0.000814

The diffusion coefficients of ferrocene in aqueous ethanol at different percentages obtained on GC rotating indicator electrode are summarized in table III-21, and the results are reported with 02 decimals.

Table III- 21 : the diffusion coefficients of ferrocene in aqueous ethanol at different percentages obtained on GC RIE

Aqueous ethanol %	**Concentration** (mol/l)	**The slope**	D_{Fc} (m^2/s)
90	$2,70.10^{-3}$	0.01126	4.60E-08
81	$2,43.10^{-3}$	0.00964	4.56E-08
73	$2,19.10^{-3}$	0.00702	3.46E-08
66	$1,97.10^{-3}$	0.00622	3.47E-08
59	$1,77.10^{-3}$	0.00455	2.60E-08

Diffusion layer thicknesses of ferrocene in aqueous ethanol at different percentages obtained on GC rotating indicator electrode are summarized in table III-22.

Table III- 22 : diffusion layer thicknesses ferrocene in aqueous ethanol solution at different percentages obtained on GC RIE

Aqueous ethanol %	C (mol/cm^3)	D (m^2/s)	ν_{sol} **(25 ^{0}C)** (cm^2/s)	ω (rad/s)	δ (cm)
90	$2.70\ 10^{-3}$	$4.60\ 10^{-8}$	$3.91\ 10^{-5}$	125.60	0.001269
				167.46	0.001099
				188.40	0.001036
				209.33	0.000983
81	$2.43\ 10^{-3}$	$4.56\ 10^{-8}$	$5.10\ 10^{-5}$	125.60	0.001323
				167.46	0.001145
				188.40	0.001080
				209.33	0.001024
73	$2.19\ 10^{-3}$	$3.46\ 10^{-8}$	$6.04\ 10^{-5}$	125.60	0.001241
				167.46	0.001075
				188.40	0.001013
				209.33	0.000961
66	$1.97\ 10^{-3}$	$3.47\ 10^{-8}$	$6.73\ 10^{-5}$	125.60	0.001265
				167.46	0.001095
				188.40	0.001033
				209.33	0.000980
59	$1.77\ 10^{-8}$	$2.60\ 10^{-8}$	$7.24.10^{-5}$	125.60	0.001163
				167.46	0.001007
				188.40	0.000949
				209.33	0.000901

5.3. Electrochemical behavior and calculation of diffusion coefficient of ferrocenyl methyl aniline/ferrocenium

5.3.1. Electrochemical behavior of ferrocenyl methyl aniline

On platinum (Pt) fixed indicator electrode

Before the study of the electrochemical behavior of ferrocenyl methyl aniline in aqueous ethanol at different percentages, on Pt fixed indicator electrode, the reactivity and the stability of the electroactive molecule must be confirmed, the

reactivity of ferrocenyl methyl aniline in window potential of 0-600mv (Vs/SCE) is confirmed with the obtaining of a cyclic voltammogram presents an anodic peak at 0.450 mV and an cathodic peak at 0.250 mV (fig III-21 (A)), those two peaks are corresponded to the oxidation and to the reduction of ferrocenyl group/ferrocenium couple, and the superposed of multi-cycles voltammograms, in our case 05 cycles, indicates that the system is stable and do not change with the variation of the time (figure III-21 (B)).

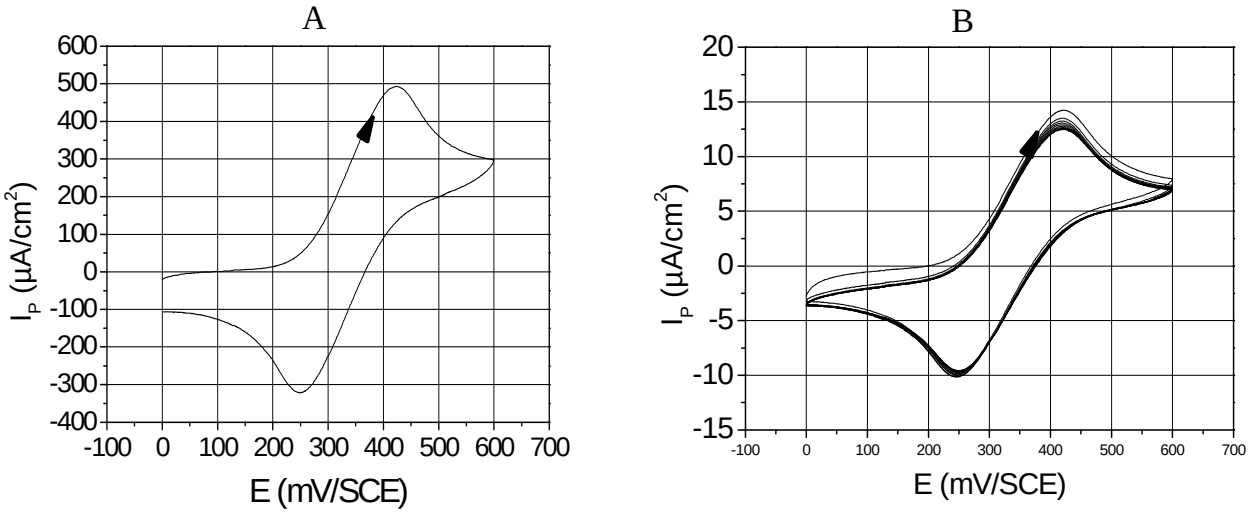

Figure III- 21 : cyclic voltammogram of ferrocenyl methyl aniline at 100mv/s on Pt indicator electrode in window potential of 0-600mV (Vs/SCE), (A) one cycle, (B) fives cycles, (Vs/SCE), 25 ^{0}C.

The cyclic voltammograms and the multi-cycles voltammograms of ferrocenyl methyl aniline in aqueous ethanol (81%, 73%, 66%, and 59%) on Pt indicator electrode are presented in the appendix.

On the Pt fixed indicator electrode, the electrochemical reaction of ferrocenyl methyl aniline in aqueous ethanol at different percentages presented a reversible; one electron transferred electrochemical reaction, in potential window of 0-600 mV (Vs/SCE) at scan rate equal to 25, 50, 75, 100, and150 mV/s.

The electrochemical parameters of ferrocenyl methyl aniline obtained on Pt fixed indicator electrode are summarized in the table III-23.

Table III- 23: analysis data obtained from cyclic voltammograms of ferrocenyl methyl aniline in aqueous ethanol at different percentages on Pt FIE

Aqueous ethanol %	**Scan rate** (mV/s)	E_a (mV)	E_c (mV)	$E_{1/2}$ (mV)	I_a (mA/cm^2)	I_c (mA/cm^2)	$\lvert I_a/I_c \rvert$
90	25	393.6	276.7	335.15	258E-03	-255E-03	1.0106
	50	405.0	265.3	335.15	346E-03	-344E-03	1.0061
	75	414.3	255.0	334.65	419E-03	-417E-03	1.0058
	100	423.5	250.6	337.05	490E-03	-488E-03	1.0047
	150	432.8	238.1	335.45	564E-03	-563E-03	1.0025
81	25	339.2	255.5	297.35	227E-03	-225E-03	1.0070
	50	347.9	251.7	299.80	299E-03	-297E-03	1.0065
	75	348.5	247.4	297.95	361E-03	-358E-03	1.0084
	100	352.8	246.8	299.80	410E-03	-410E-03	1.0008
	150	357.7	241.4	299.55	490E-03	-489E-03	1.0014
73	25	320.8	245.7	283.25	192E-03	-189E-03	1.0161
	50	323.5	242.5	283.00	261E-03	-259E-03	1.0082
	75	326.3	239.2	282.75	310E-03	-308E-03	1.0078
	100	327.8	238.1	282.95	349E-03	-347E-03	1.0049
	150	333.3	233.8	283.56	424E-03	-422E-03	1.0030
66	25	302.7	233.2	267.95	166E-03	-165E-03	1.0028
	50	303.4	231.6	267.50	215E-03	-214E-03	1.0048
	75	304.4	231.1	267.75	260E-03	-257E-03	1.0080
	100	305.5	229.4	267.45	302E-03	-299E-03	1.0094
	150	308.3	227.2	267.75	364E-03	-362E-03	1.0066
59	25	288.7	223.4	256.05	149E-03	-148E-03	1.0064
	50	291.4	223.4	257.40	192E-03	-189E-03	1.0167
	75	290.9	221.8	256.35	230E-03	-228E-03	1.0099
	100	292.5	221.3	256.90	263E-03	-261E-03	1.0079
	150	294.7	217.5	256.10	319E-03	-317E-03	1.0048

The values of $E_{1/2}$ are independents to scan rates variations, so the electrochemical reaction of ferrocenyl methyl aniline on Pt fixed indicator electrode is a rapid and reversible.

Mode of transfer reaction of Ferrocenyl methyl aniline on Pt FIE

To find the electrochemical reaction mechanism of ferrocenyl methyl aniline at Pt fixed indicator electrode, we plotted the intensity of the anodic and cathodic peaks current as a function of the square root of scan rate$I_P = f(\sqrt{v})$, in each case we obtained a straight line passes by the origin which indicates that the electrochemical reaction of ferrocenyl methyl aniline on Pt fixed indicator electrode is controlled by diffusion process.

On Pt rotating indicator electrode

On Pt rotating indicator electrode, the electrochemical behavior of ferrocenyl methyl aniline presented a rapid, reversible and one electron transferred electrochemical reaction in potential window of 0-600 mV, at scan rate equals to100 mV/s, at different angular velocities equal to 1200, 1600, 1800 and2000 rpm.

The electrochemical parameters of ferrocenyl methyl aniline obtained on Pt Rotating indicator electrode are summarized in the table III-24.

The values of $E_{1/2}$ are independents to angular velocities variations, so the electrochemical reaction of ferrocenyl methyl aniline on Pt rotating indicator electrode is a rapid and reversible.

Table III- 24 : analysis data obtained from polarograms of ferrocenyl methyl aniline in aqueous ethanol at different percentages on Pt RIE

Aqueous ethanol %	**Angular velocities** rpm	I_{lim} (mA/cm^2)	$I_{lim/2}$ (mA/cm^2)	$E_{1/2}$ (mV)
90	1200	0.95533	0.47766	358.8
	1600	1.08900	0.54450	373.4
	1800	1.13000	0.56500	373.9
	2000	1.18000	0.59000	373.9
81	1200	0.72180	0.03609	302.2
	1600	0.83130	0.41565	307.6
	1800	0.88320	0.44160	309.2
	2000	0.92720	0.46360	311.6
73	1200	0.60270	0.30135	274.4
	1600	0. 70540	0.35270	280.1
	1800	0.73800	0.36900	281.1
	2000	0.78560	0.39280	285.6
66	1200	0.50890	0.25445	255.8
	1600	0.57860	0.28930	260.6
	1800	0.61160	0.30580	261.7
	2000	0.63930	0.31965	262.3
59	1200	0.33050	0.16525	235.8
	1600	0.37640	0.18820	239.1
	1800	0.38690	0.19345	243.6
	2000	0.40260	0.20130	246.1

Mode of transfer reaction of Ferrocenyl methyl aniline on Pt RIE

To find the oxidation reaction mechanism of ferrocenyl methyl aniline to ferrocenium cation at Pt rotating indicator electrode, we plotted the variations in the intensity of the limit current as a function of the square root of angular velocity , $I_{lim} = f(\sqrt{\omega})$, in each case we obtained a straight line passes by the origin indicates that the oxidation reaction of ferrocenyl methyl aniline is controlled by diffusion process.

Cyclic voltammogram of ferrocenyl methyl aniline on Pt fixed electrode at scan rates 25, 50, 75, 100 and 150 mV/s, the polarogram of ferrocenyl methyl aniline on Pt rotating electrode at angular velocities 1200, 1600, 1800 and 2000 rpm, $I_P = f(\sqrt{v})$ plot and $I_{lim} = f(\sqrt{\omega})$ plot of ferrocenyl methyl aniline in aqueous ethanol (90%, 81%, 73%, 66%, 59%), on Pt indicator electrode in potential window of 0-600 mV (Vs/SCE), at 25 ^{0}C, are presented in figure III-22 to figure III-26.

Cyclic voltammograms of ferrocenyl methyl aniline on Pt fixed electrode	$I_P = f(\sqrt{v})$
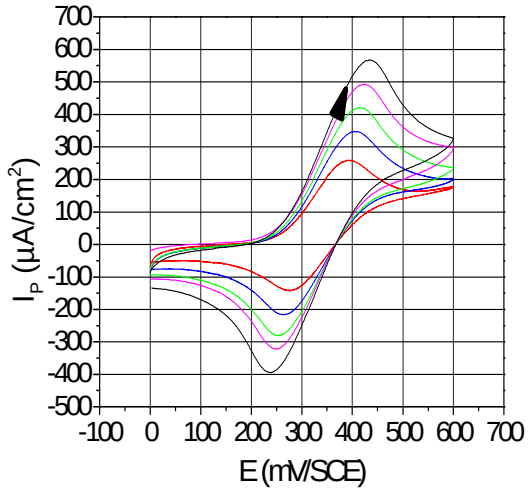	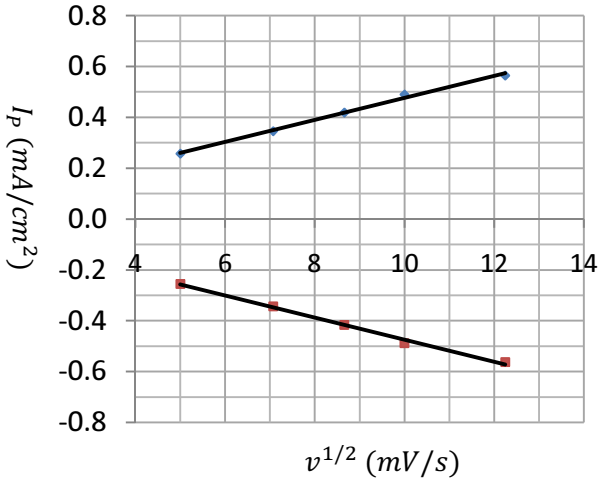
polarograms of ferrocenyl methyl aniline on Pt rotating electrode	$I_{lim} = f(\sqrt{\omega})$
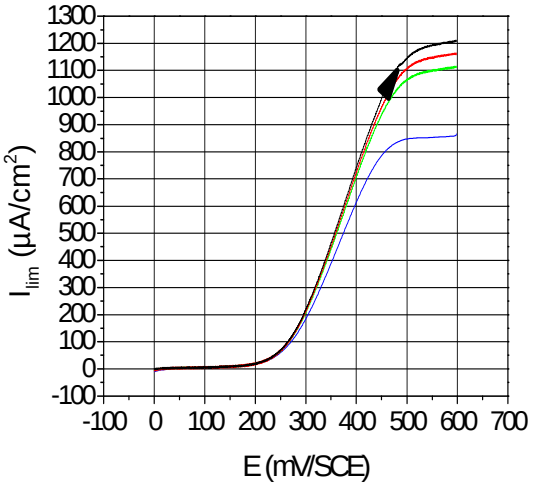	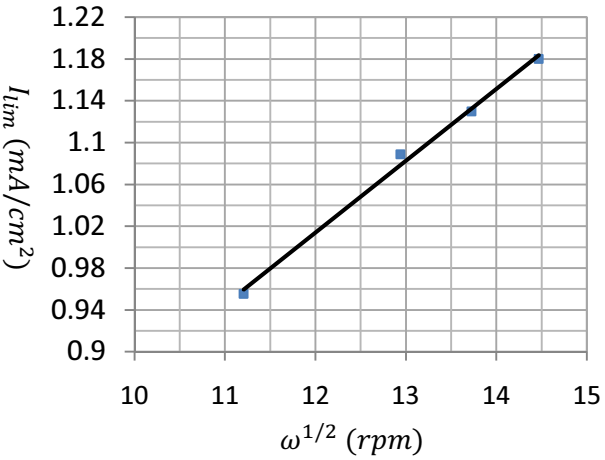

Figure III- 22 : cyclic voltammogram of ferrocenyl methyl aniline on Pt fixed electrode at scan rates 25, 50, 75, 100 and 150 mV/s, the polarogram of ferrocenyl methyl aniline on Pt rotating electrode at angular velocities 1200, 1600, 1800 and 2000 rpm, $\boldsymbol{I_P = f(\sqrt{v})}$ plot and $\boldsymbol{I_{lim} = f(\sqrt{\omega})}$ plot of ferrocenyl methyl aniline in aqueous ethanol (90%) on Pt indicator electrode in potential window of 0-600 mV (Vs/SCE), at 25 ^{0}C.

Cyclic voltammograms of ferrocenyl methyl aniline on Pt fixed electrode	$I_P = f(\sqrt{v})$
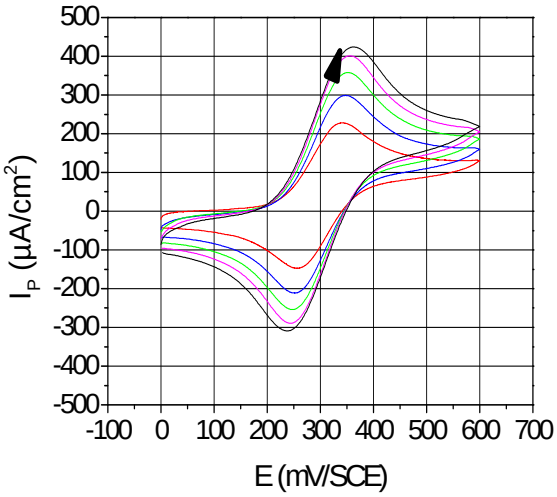	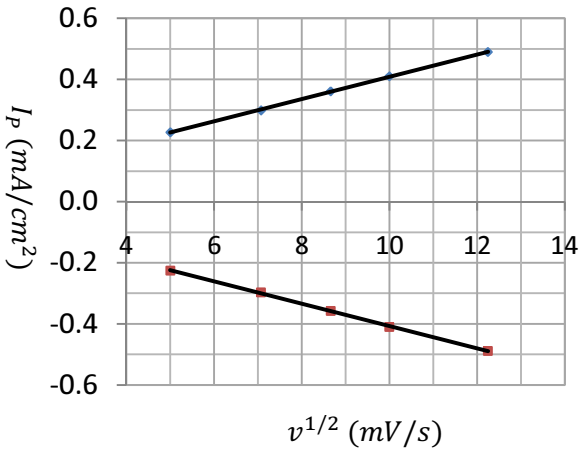
polarograms of ferrocenyl methyl aniline on Pt rotating electrode	$I_{lim} = f(\sqrt{\omega})$
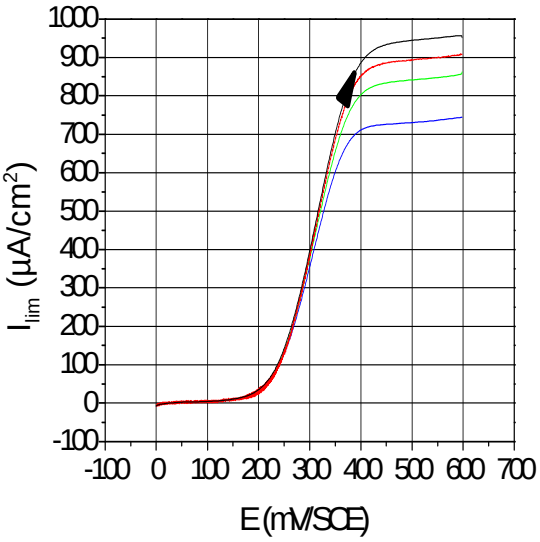	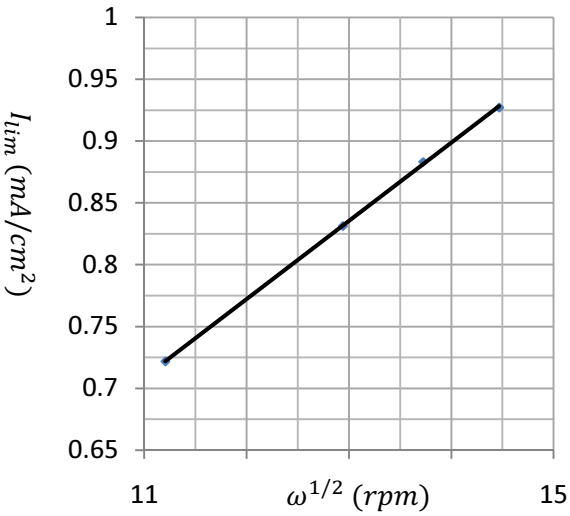

Figure III- 23: cyclic voltammogram of ferrocenyl methyl aniline on Pt fixed electrode at scan rates 25, 50, 75, 100 and 150 mV/s, the polarogram of ferrocenyl methyl aniline on Pt rotating electrode at angular velocities 1200, 1600, 1800 and 2000 rpm, $\boldsymbol{I_P = f(\sqrt{v})}$ plot and $\boldsymbol{I_{lim} = f(\sqrt{\omega})}$ plot of ferrocenyl methyl aniline in aqueous ethanol (81%) on Pt indicator electrode in potential window of 0-600 mV (Vs/SCE), at 25 ^{0}C.

Cyclic voltammograms of ferrocenyl methyl aniline on Pt fixed electrode	$I_P = f(\sqrt{v})$
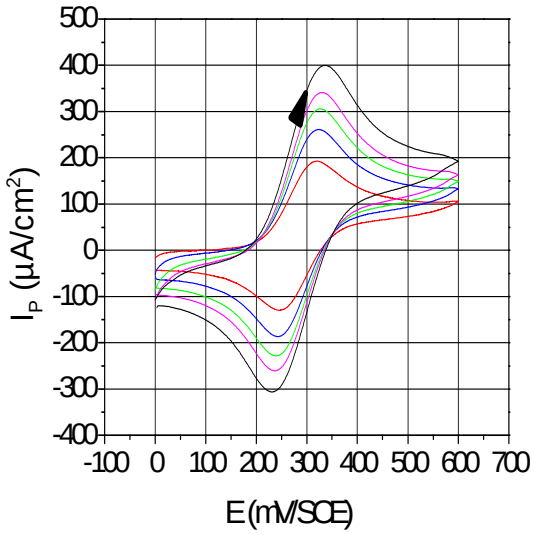	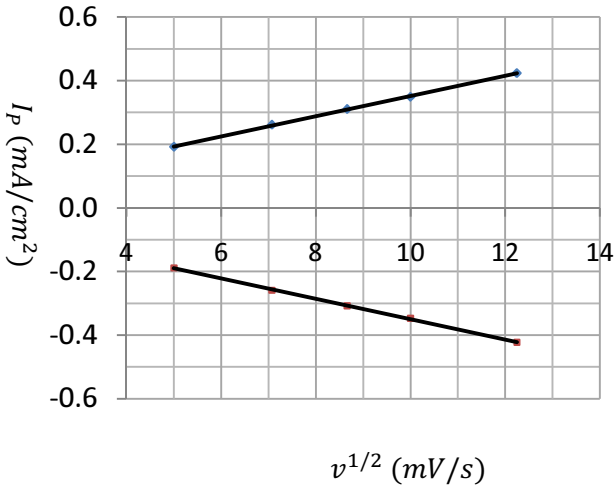
polarograms of ferrocenyl methyl aniline on Pt rotating electrode	$I_{lim} = f(\sqrt{\omega})$
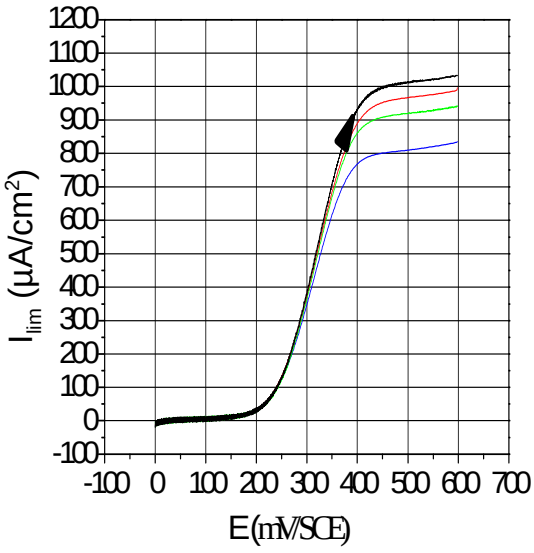	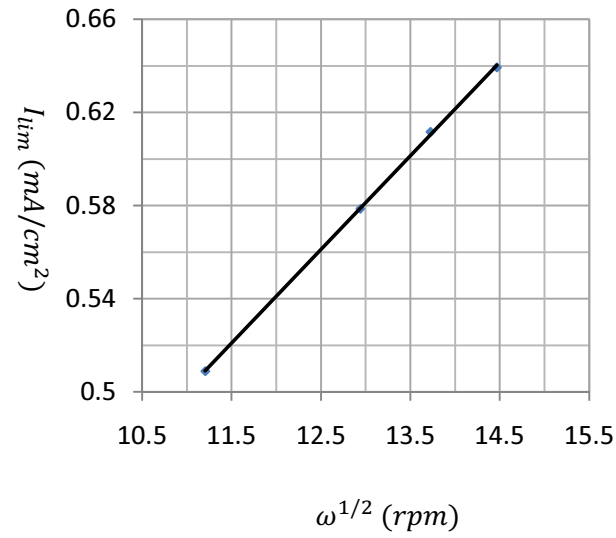

Figure III- 24: cyclic voltammogram of ferrocenyl methyl aniline on Pt fixed electrode at scan rates 25, 50, 75, 100 and 150 mV/s, the polarogram of ferrocenyl methyl aniline on Pt rotating electrode at angular velocities 1200, 1600, 1800 and 2000 rpm, $\boldsymbol{I_P = f(\sqrt{v})}$ plot and $\boldsymbol{I_{lim} = f(\sqrt{\omega})}$ plot of ferrocenyl methyl aniline in aqueous ethanol (73 %) on Pt indicator electrode in potential window of 0-600 mV (Vs/SCE), at 25 ^{0}C.

Cyclic voltammograms of ferrocenyl methyl aniline on Pt electrode	$I_P = f(\sqrt{v})$
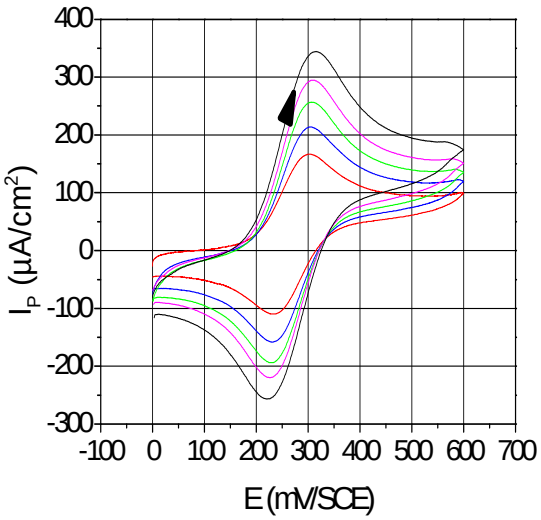	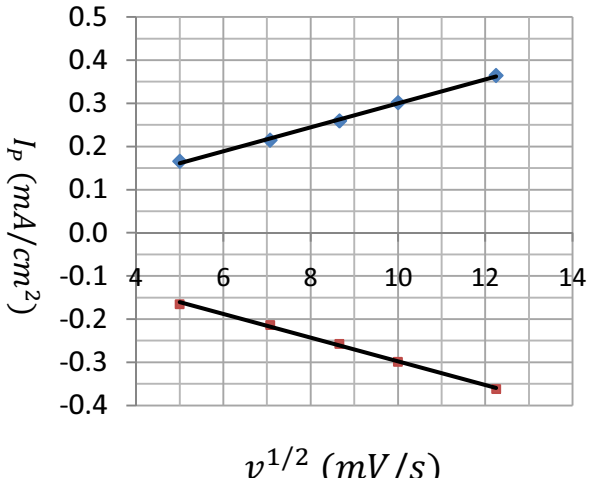
polarograms of ferrocenyl methyl aniline on Pt rotating electrode	$I_{lim} = f(\sqrt{\omega})$
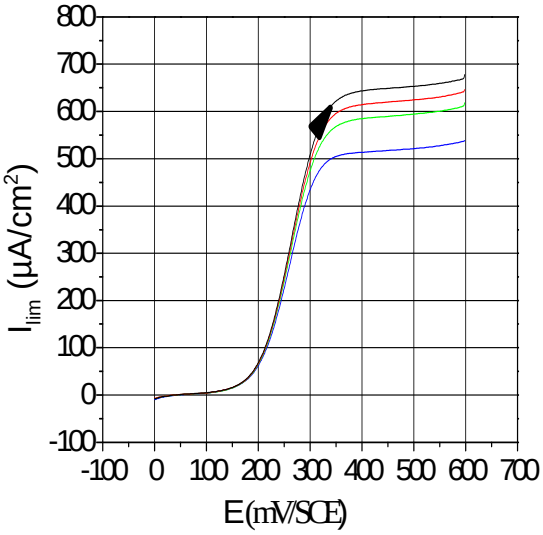	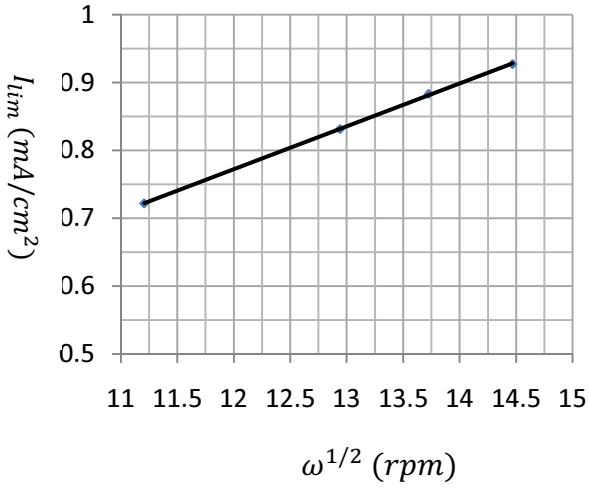

Figure III- 25: cyclic voltammogram of ferrocenyl methyl aniline on Pt fixed electrode at scan rates 25, 50, 75, 100 and 150 mV/s, the polarogram of ferrocenyl methyl aniline on Pt rotating electrode at angular velocities 1200, 1600, 1800 and 2000 rpm, $\boldsymbol{I_P = f(\sqrt{v})}$ plot and $\boldsymbol{I_{lim} = f(\sqrt{\omega})}$ plot of ferrocenyl methyl aniline in aqueous ethanol (66 %) on Pt indicator electrode in potential window of 0-600 mV (Vs/SCE), at 25 ^{0}C.

Cyclic voltammograms of ferrocenyl methyl aniline on Pt fixed electrode	$I_P = f(\sqrt{v})$
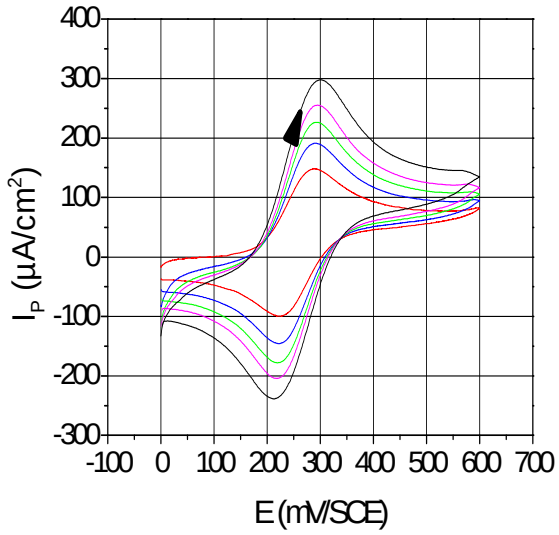	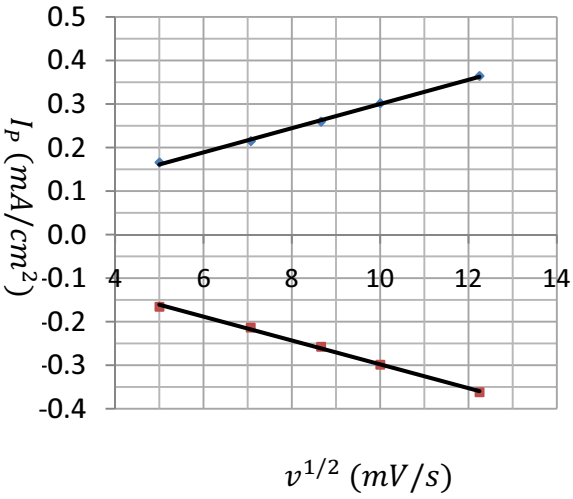
polarograms of ferrocenyl methyl aniline on Pt rotating electrode	$I_{lim} = f(\sqrt{\omega})$
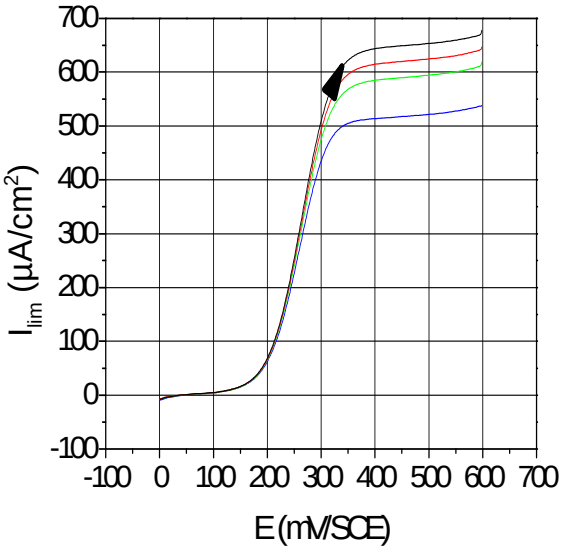	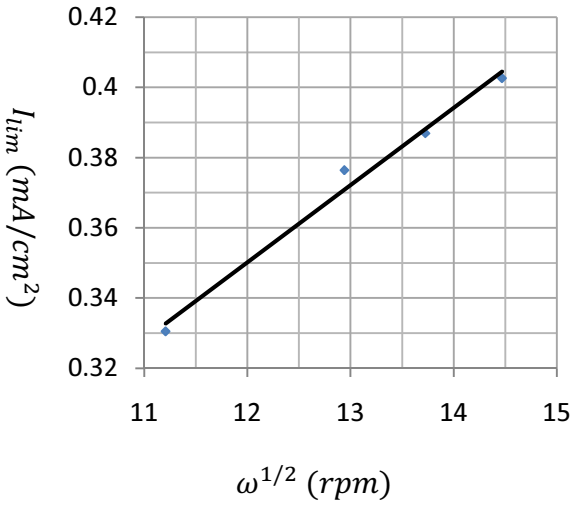

Figure III- 26 : cyclic voltammogram of ferrocenyl methyl aniline on Pt fixed electrode at scan rates 25, 50, 75, 100 and 150 mV/s, the polarogram of ferrocenyl methyl aniline on Pt rotating electrode at angular velocities 1200, 1600, 1800 and 2000 rpm, $\boldsymbol{I_P = f(\sqrt{v})}$ plot and $\boldsymbol{I_{lim} = f(\sqrt{\omega})}$ plot of ferrocenyl methyl aniline in aqueous ethanol (59 %) on Pt indicator electrode in potential window of 0-600 mV (Vs/SCE), at 25 ^{0}C.

On glassy carbon (GC) fixed indicator electrode

Before the study of the electrochemical behavior of ferrocenyl methyl aniline in aqueous ethanol at different percentages, on GC indicator electrode, the reactivity and the stability of the electroactive molecule must be confirmed, the reactivity of ferrocenyl methyl aniline in window potential of 0-600mv is confirmed with the obtaining of a cyclic volatammogram presents an anodic peak at 0.451 mV and an cathodic peak at 0.248 mV (fig III-27 (A)), those two peaks are corresponded to the oxidation and to the reduction of ferrocenyl group/ferrocenium couple , and the superposed of multi-cycles voltammograms (in our case 05 cycles), indicates that the system is stable and do not change with the variation of the time (figIII-27 (B)).

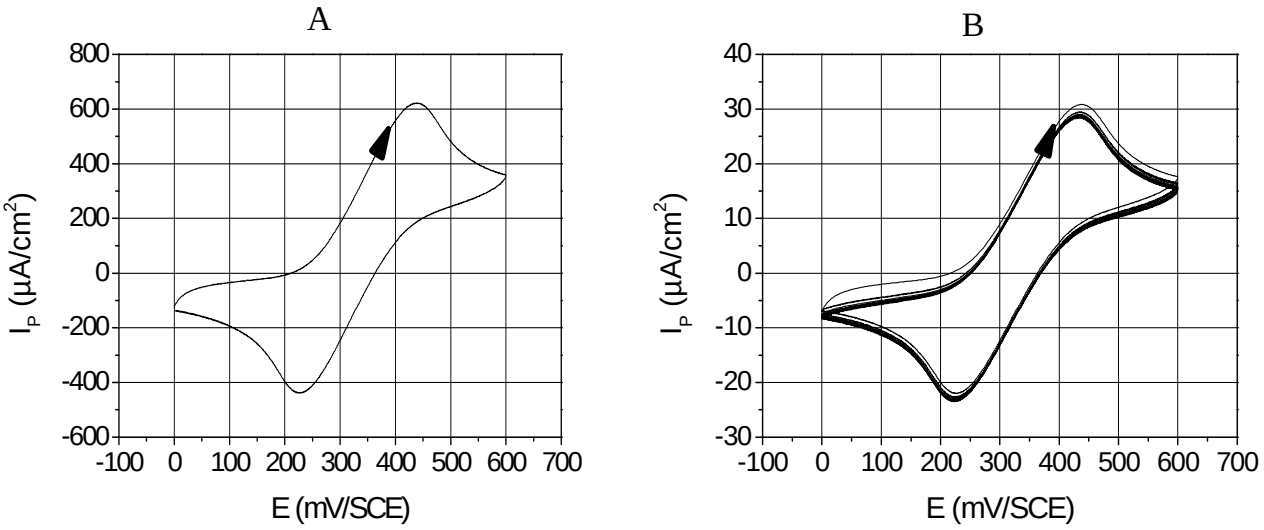

Figure III- 27 : cyclic voltammogram of ferrocenyl methyl aniline at100 mV/s, on GC FIE in window potential of 0-600 mV, (Vs/SCE), (A) one cycle, (B) five cycles, 25 ^{0}C.

The cyclic voltammograms and the multi-cycles voltammograms of ferrocenyl methyl aniline in aqueous ethanol (81%, 73%, 66%, and 59%) on GC indicator electrode, at scan rate equals to 100mV/s, are presented in the appendix.

On the GC fixed indicator electrode, the electrochemical behavior of ferrocenyl methyl aniline /ferrocenium couple presented a rapid, reversible and one electron transferred electrochemical reaction, in potential window of 0-600 mV at different scan rates equal to 25, 50, 75,100 and150 mV/s .

The electrochemical parameters of ferrocenyl methyl aniline obtained on GC fixed indicator electrode are summarized in the table III-25.

Table III- 25 : analysis data obtained from cyclic voltammograms of ferrocenyl methyl aniline in aqueous ethanol at different percentages on GC FIE

Aqueous ethanol %	**Scan rate** mV/s	E_a mV	E_c mV	$E_{1/2}$ mV	I_a mA/cm^2	I_c mA/cm^2	$\lvert I_a/I_c \rvert$
90	25	400.7	257.1	328.90	3.52E-02	-3.51E-02	1.0030
	50	416.8	244.1	330.45	4.65E-02	-4.62E-02	1.0063
	75	428.9	235.4	332.15	5.52E-02	-5.50E-02	1.0036
	100	437.1	227.8	332.45	6.22E-02	-6.18E-02	1.0050
	150	455.6	217.6	336.60	7.35E-02	-7.34E-02	1.0010
81	25	350.7	253.3	302.00	2.99E-02	-2.98E-02	1.0020
	50	360.0	245.7	302.85	4.05E-02	-4.03E-02	1.0060
	75	367.0	239.8	303.40	4.85E-02	-4.83E-02	1.0040
	100	370.8	235.9	303.35	5.56E-02	-5.54E-02	1.0043
	150	380.0	230.0	305.00	6.67E-02	-6.67E-02	1.0008
73	25	321.3	240.8	281.05	2.59E-02	-2.57E-02	1.0089
	50	325.1	237.6	281.35	3.43E-02	-3.42E-02	1.0026
	75	330.0	235.4	282.70	4.11E-02	-4.10E-02	1.0037
	100	332.3	232.1	282.20	4.70E-02	-4.68E-02	1.0027
	150	336.0	230.5	283.25	5.70E-02	-5.68E-02	1.0037
66	25	303.4	233.2	268.30	2.30E-02	-2.28E-02	1.0076
	50	305.5	229.4	267.45	3.11E-02	-3.09E-02	1.0068
	75	309.9	228.3	269.10	3.74E-02	-3.73E-02	1.0044
	100	312.1	227.2	269.65	4.28E-02	-4.26E-02	1.0047
	150	315.3	224.5	269.90	5.20E-02	-5.19E-02	1.0029
59	25	286.0	218.5	252.25	1.71E-02	-1.68E-02	1.0167
	50	287.6	219.6	253.60	2.41E-02	-2.40E-02	1.0029
	75	289.7	216.9	253.30	2.90E-02	-2.87E-02	1.0085
	100	291.9	216.4	254.15	3.38E-02	-3.36E-02	1.0060
	150	294.7	217.5	256.10	4.17E-02	-4.15E-02	1.0037

The values of $E_{1/2}$ are independents to scan rates variations, so the electrochemical reaction of ferrocenyl methyl aniline on GC fixed indicator electrode is a rapid and reversible.

Mode of transfer reaction of ferrocenyl methyl aniline on GC FIE

To find the electrochemical reaction mechanism of ferrocenyl methyl aniline at GC fixed indicator electrode, we plotted the intensity of the anodic and cathodic peaks current as a function of the square root of scan rate $I_P = f(\sqrt{v})$, in each case we

obtained a straight line passes by the origin which indicates that the electrochemical reaction on GC fixed indicator electrode is controlled by diffusion process.

On glassy carbon (GC) rotating indicator electrode

On the GC rotating indicator electrode, the electrochemical behavior of ferrocenyl methyl aniline/ferrocenium couple presented a rapid, reversible and one electron transferred electrochemical reaction in potential window of 0-600 mV, at scan rate equals to100 mV/s, at different angular velocities equal to 1200, 1600, 1800 and 2000 rpm.

The electrochemical parameters of ferrocenyl methyl aniline obtained on GC Rotating indicator electrode are summarized in the table III-26.

Table III- 26: analysis data obtained from cyclic voltammograms of ferrocenyl methyl aniline in aqueous ethanol at different percentages on GC RIE

Aqueous ethanol %	**Angular velocities** rpm	I_{lim} mA/cm^2	$I_{lim/2}$ mA/cm^2	$E_{1/2}$ mV
90	1200	1.260	0.6300	377.7
	1600	1.435	0.7175	389.3
	1800	1.527	0.7635	393.3
	2000	1.616	0.8080	401.5
81	1200	1.055	0.5275	316.8
	1600	1.190	0.5950	335.1
	1800	1.226	0.6130	335.4
	2000	1.254	0.6270	335.5
73	1200	0.819	0.4099	281.1
	1600	0.934	0.4673	297.0
	1800	0.989	0.4945	297.1
	2000	1.036	0.5180	297.2
66	1200	0.753	0.3769	263.9
	1600	0.864	0.4324	267.1
	1800	0.939	0.4697	269.3
	2000	1.010	0.5050	274.1
59	1200	0.566	0.2833	241.8
	1600	0.637	0.3185	245.5
	1800	0.666	0.3332	245.5
	2000	0.698	0.3490	246.6

The values of $E_{1/2}$ are independents to angular velocities variations, so the electrochemical reaction of ferrocenyl methyl aniline on GC rotating indicator electrode is a rapid and reversible.

Mode of transfer reaction of ferrocenyl methyl aniline on GC RIE

To find the oxidation reaction mechanism of ferrocenyl methyl aniline to ferrocenium cation at GC rotating indicator electrode, we plotted the variations in the intensity of the limit current as a function as the square root of angular velocity , $I_{lim} = f(\sqrt{\omega})$, in each case we obtained a straight line passes by the origin which indicates that the oxidation reaction is controlled by diffusion process.

cyclic voltammogram of ferrocenyl methyl aniline on GC fixed electrode at scan rates 25, 50, 75, 100 and 150 mV/s, the polarogram of ferrocenyl methyl aniline on GC rotating electrode at angular velocities 1200, 1600, 1800 and 2000 rpm, $\boldsymbol{I_P = f(\sqrt{v})}$ plot and $\boldsymbol{I_{lim} = f(\sqrt{\omega})}$ plot of ferrocenyl methyl aniline in aqueous ethanol (90%, 81%, 73%, 66%, 59%), on GC indicator electrode in potential window of 0-600 mV (Vs/SCE), at 25 ^{0}C, are presented in figure III-28 to figure III-32.

Cyclic voltammograms of ferrocenyl methyl aniline on GC fixed electrode	$I_P = f(\sqrt{v})$
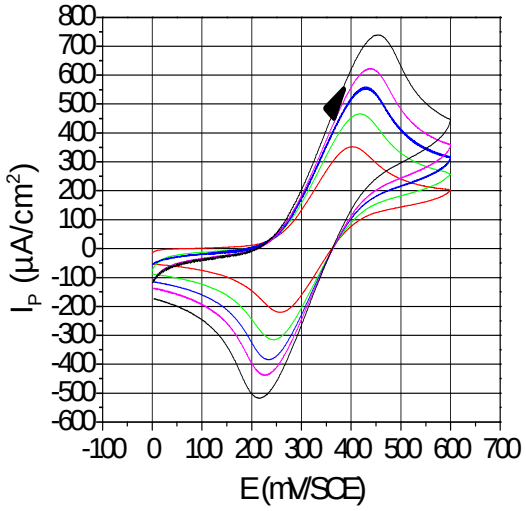	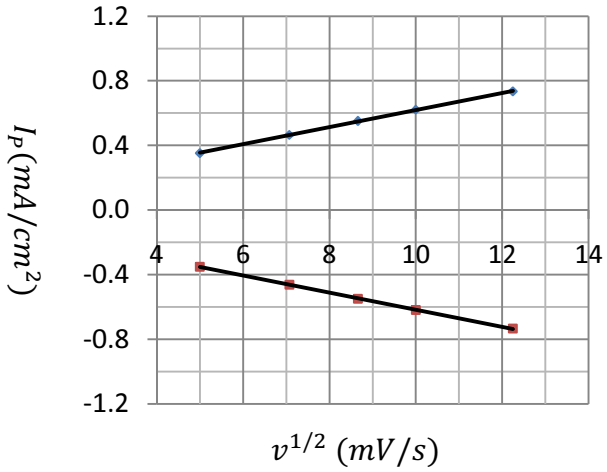
polarograms of ferrocenyl methyl aniline on GC rotating electrode	$I_{lim} = f(\sqrt{\omega})$
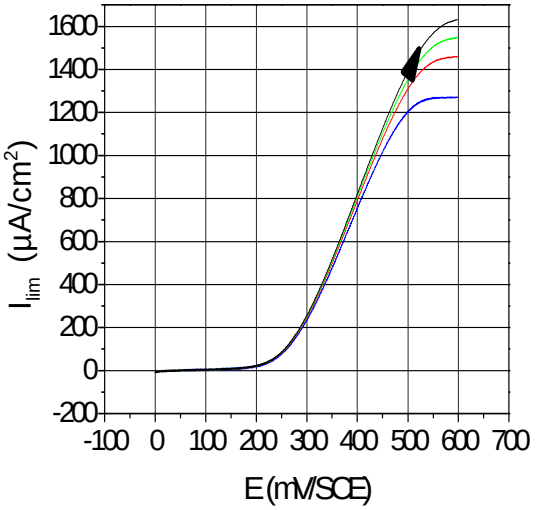	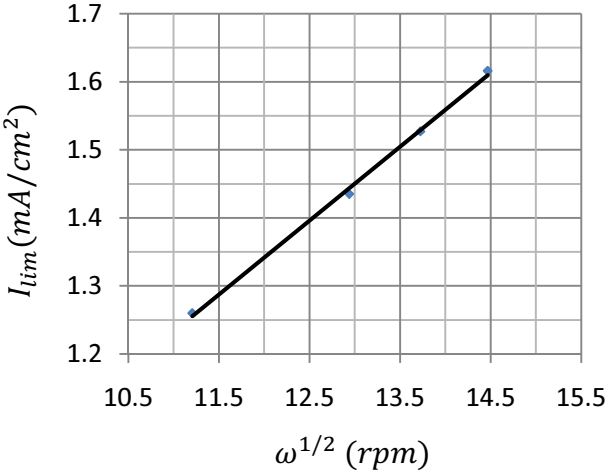

Figure III- 28 : cyclic voltammogram of ferrocenyl methyl aniline on GC fixed electrode at scan rates 25, 50, 75, 100 and 150 mV/s, the polarogram of ferrocenyl methyl aniline on GC rotating electrode at angular velocities 1200, 1600, 1800 and 2000 rpm, $\boldsymbol{I_P = f(\sqrt{v})}$ plot and $\boldsymbol{I_{lim} = f(\sqrt{\omega})}$ plot of ferrocenyl methyl aniline in aqueous ethanol (90 %) on GC indicator electrode in potential window of 0-600 mV (Vs/SCE), at 25 ^{0}C.

Cyclic voltammograms of ferrocenyl methyl aniline on GC fixed electrode	$I_P = f(\sqrt{v})$
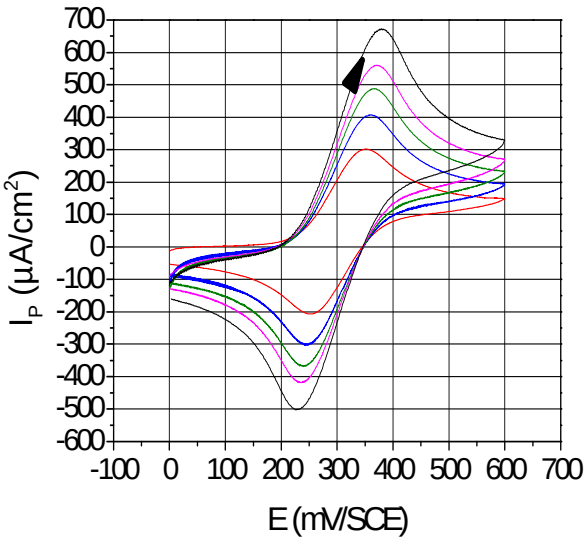	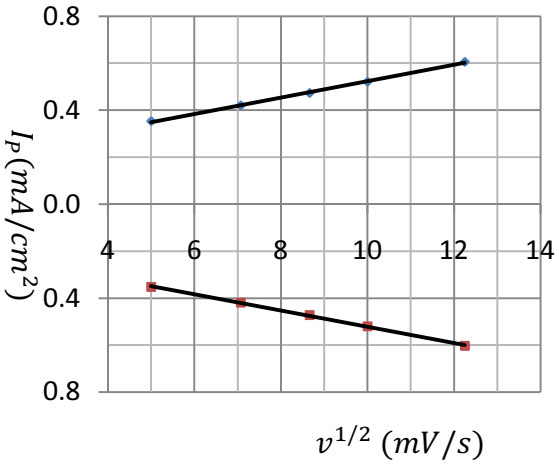
polarograms of ferrocenyl methyl aniline on GC fixed electrode	$I_{lim} = f(\sqrt{\omega})$
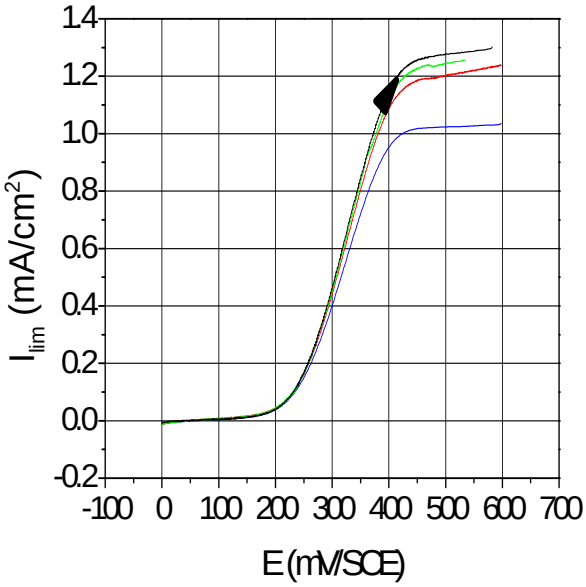	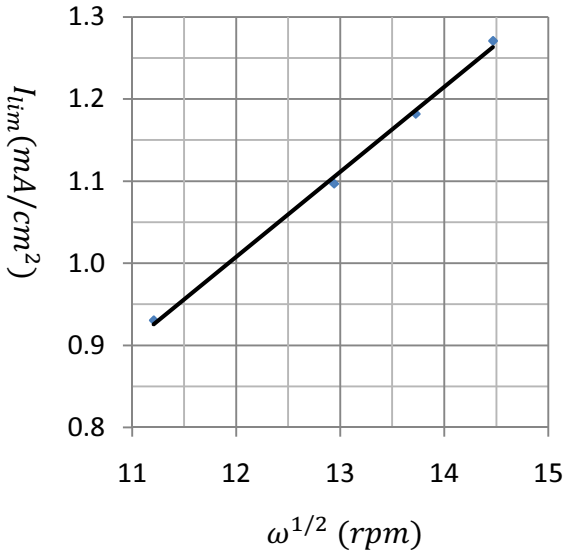

Figure III- 29 : cyclic voltammogram of ferrocenyl methyl aniline on GC fixed electrode at scan rates 25, 50, 75, 100 and 150 mV/s, the polarogram of ferrocenyl methyl aniline on GC rotating electrode at angular velocities 1200, 1600, 1800 and 2000 rpm, $\boldsymbol{I_P = f(\sqrt{v})}$ plot and $\boldsymbol{I_{lim} = f(\sqrt{\omega})}$ plot of ferrocenyl methyl aniline in aqueous ethanol (81%) on GC indicator electrode in potential window of 0-600 mV (Vs/SCE), at 25 ^{0}C.

Voltammograms of ferrocenyl methyl aniline on GC electrode	$I_P = f(\sqrt{v})$
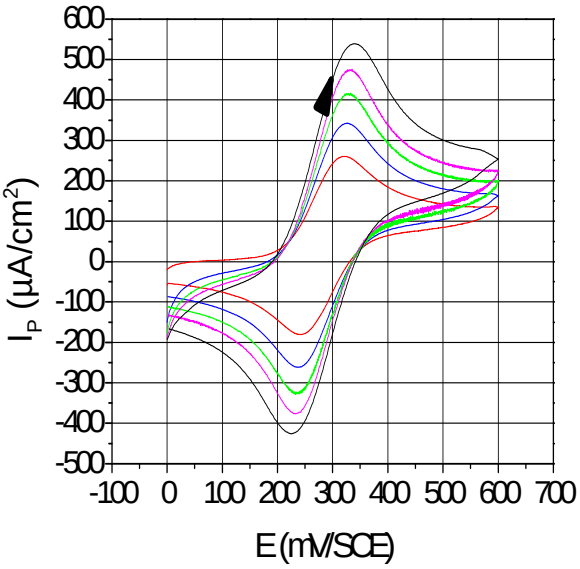	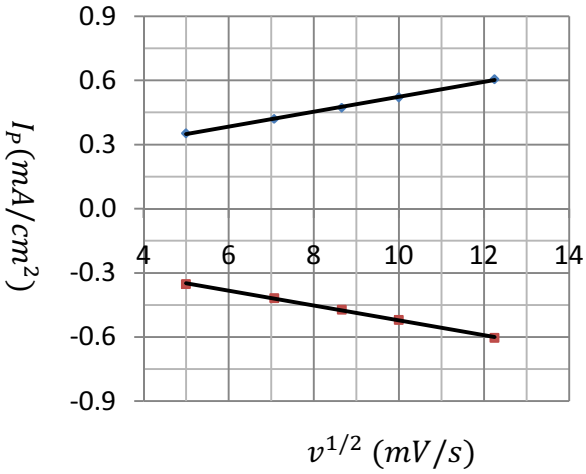
polarograms of ferrocenyl methyl aniline on GC electrode	$I_{lim} = f(\sqrt{\omega})$
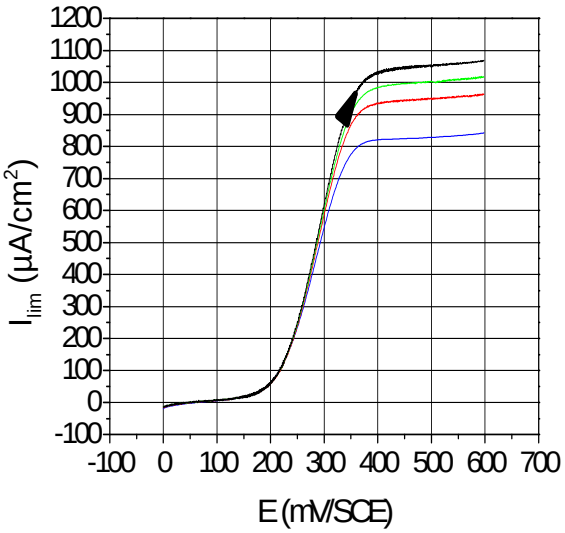	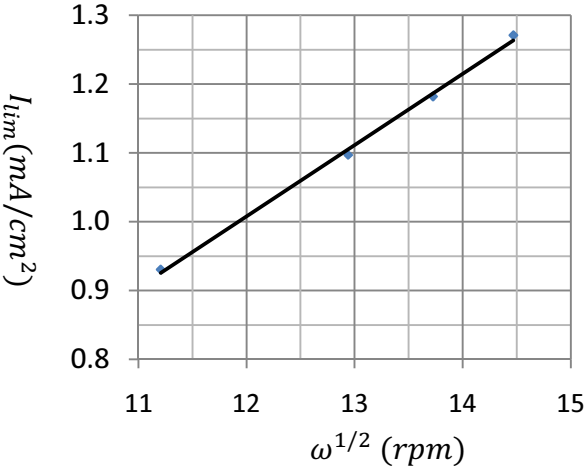

Figure III- 30 : cyclic voltammogram of ferrocenyl methyl aniline on GC fixed electrode at scan rates 25, 50, 75, 100 and 150 mV/s, the polarogram of ferrocenyl methyl aniline on GC rotating electrode at angular velocities 1200, 1600, 1800 and 2000 rpm, $\boldsymbol{I_P = f(\sqrt{v})}$ plot and $\boldsymbol{I_{lim} = f(\sqrt{\omega})}$ plot of ferrocenyl methyl aniline in aqueous ethanol (73%) on GC indicator electrode in potential window of 0-600 mV (Vs/SCE), at 25 ^{0}C.

Cyclic voltammograms of ferrocenyl methyl aniline on GC fixed electrode	$I_P = f(\sqrt{v})$
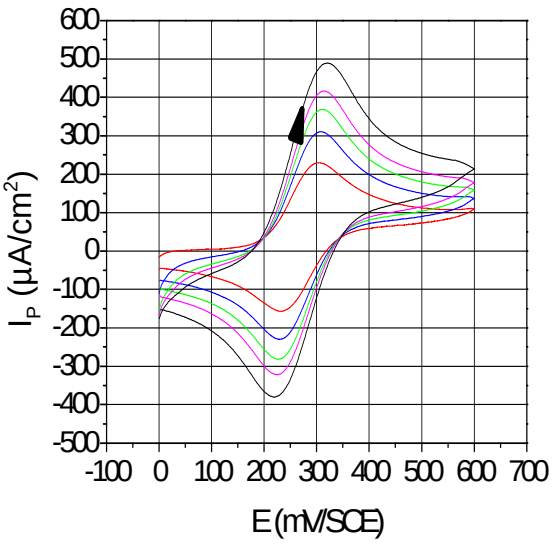	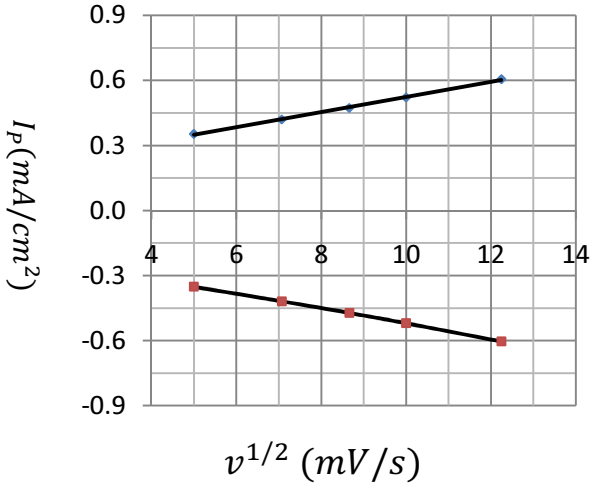
Polarograms of ferrocenyl methyl aniline on GC rotating electrode	$I_{lim} = f(\sqrt{\omega})$
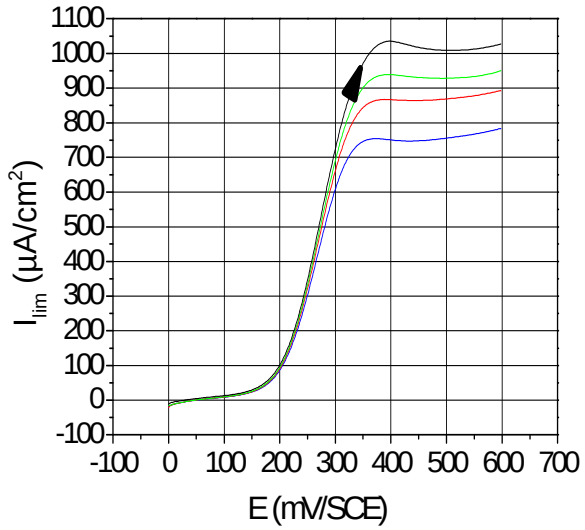	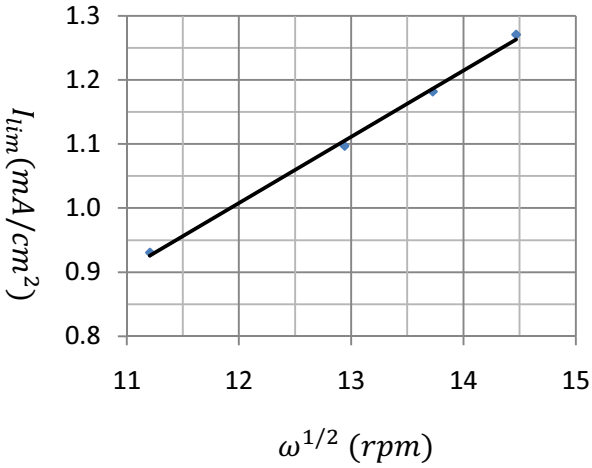

Figure III- 31 : cyclic voltammogram of ferrocenyl methyl aniline on GC fixed electrode at scan rates 25, 50, 75, 100 and 150 mV/s, the polarogram of ferrocenyl methyl aniline on GC rotating electrode at angular velocities 1200, 1600, 1800 and 2000 rpm, $\boldsymbol{I_P = f(\sqrt{v})}$ plot and $\boldsymbol{I_{lim} = f(\sqrt{\omega})}$ plot of ferrocenyl methyl aniline in aqueous ethanol (66 %) on GC indicator electrode in potential window of 0-600 mV (Vs/SCE), at 25 ^{0}C.

Cyclic voltammograms of ferrocenyl methyl aniline on GC fixed electrode	$I_P = f(\sqrt{v})$
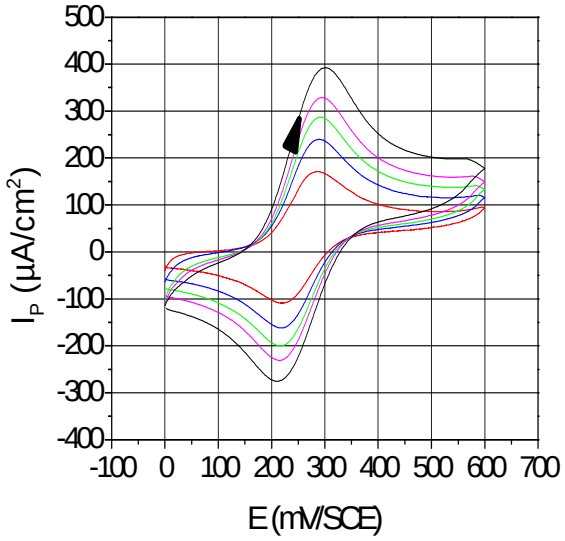	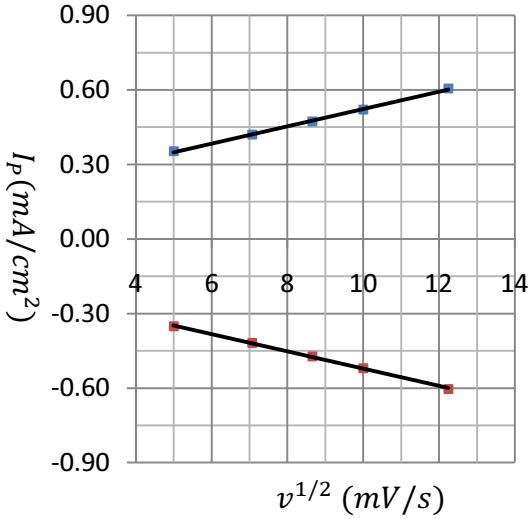
polarograms of ferrocenyl methyl aniline on GC rotating electrode	$I_{lim} = f(\sqrt{\omega})$
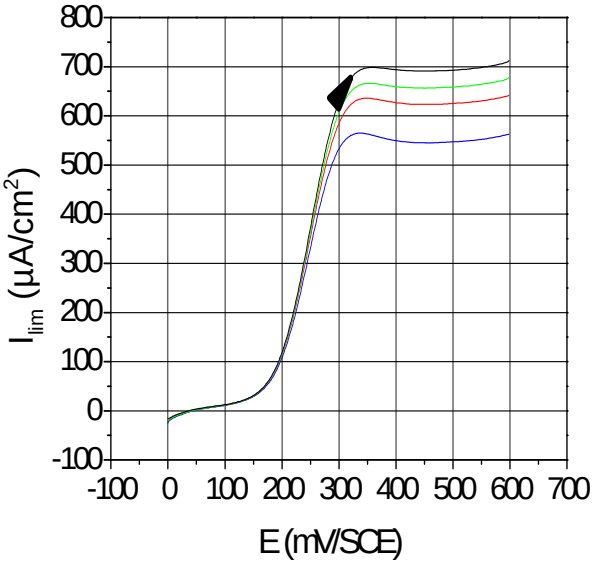	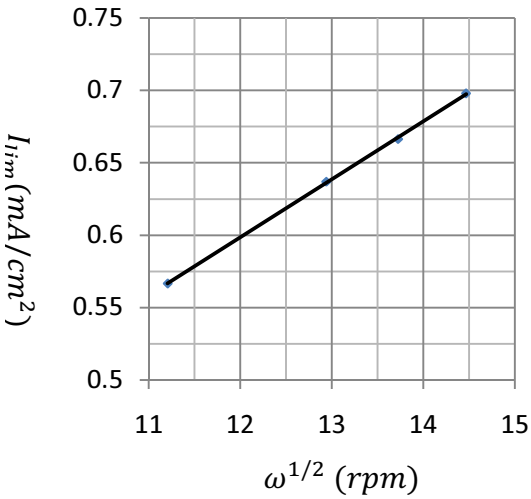

Figure III- 32 : cyclic voltammogram of ferrocenyl methyl aniline on GC fixed electrode at scan rates 25, 50, 75, 100 and 150 mV/s, the polarogram of ferrocenyl methyl aniline on GC rotating electrode at angular velocities 1200, 1600, 1800 and 2000 rpm, $\boldsymbol{I_P = f(\sqrt{v})}$ plot and $\boldsymbol{I_{lim} = f(\sqrt{\omega})}$ plot of ferrocenyl methyl aniline in aqueous ethanol (59 %) on GC indicator electrode in potential window of 0-600 mV (Vs/SCE), at 25 ^{0}C.

5.3.2. The calculation of diffusion coefficient of ferrocenyl methyl aniline/ferrocenium couple and diffusion layer thicknesses

On Pt, GC fixed indicator electrodes

The electrochemical reaction of ferrocenyl methyl aniline / ferrocenium couple on Pt and GC fixed indicator electrodes is a rapid, reversible and one electron transferred electrochemical reaction, controlled by diffusion process. The same VBA program was used to facilitate the calculation of the diffusion coefficients of ferrocenyl methyl aniline / ferrocenium couple.

The diffusion coefficients of ferrocenyl methyl aniline / ferrocenium couple obtained on Pt fixed indicator electrode are summarized in the table III-27, and the results are reported with 02 decimals.

Table III- 27: diffusion coefficients of ferrocenyl methyl aniline / ferrocenium couple in aqueous ethanol at different percentages on Pt FIE

Aqueous ethanol %	**Concentration** (mol/l)	**The slope**	D_{m2} (m^2/s)	**The slope**	D_{Fc^+} (m^2/s)
90	$2{,}70.10^{-3}$	0.00433	3.55E-09	0.00433	3.55E-09
81	$2{,}43.10^{-3}$	0.00367	3.15E-09	0.00367	3.15E-09
73	$2{,}19.10^{-3}$	0.00317	2.90E-09	0.00317	2.90E-09
66	$1{,}97.10^{-3}$	0.00277	2.73E-09	0.00277	2.73E-09
59	$1{,}77.10^{-3}$	0.00236	2.46E-09	0.00236	2.46E-09

The diffusion layer thicknesses of ferrocenyl methyl aniline in aqueous ethanol solution at different percentages obtained on Pt fixed indicator electrode are summarized in the table III-28.

The diffusion coefficients of ferrocenyl methyl aniline /ferrocenium couple in aqueous ethanol at different percentages obtained on GC fixed indicator electrode are summarized in the table III-29 and the results are reported with 02 decimals.

Table III- 28 : diffusion layer thicknesses of ferrocenyl methyl aniline in aqueous ethanol solution at different percentages on Pt FIE

Aqueous ethanol %	C (mol/l)	D (m^2/s)	t (s)	$\delta = \sqrt{Dt}$ (cm)
90	$2.70 .10^{-3}$	3.55E-09	1	0.005958
			2	0.008426
			3	0.010320
			4	0.011916
			5	0.013323
			6	0.014595
81	$2.43.10^{-3}$	3.15E-09	1	0.005612
			2	0.007937
			3	0.009721
			4	0.011225
			5	0.012550
			6	0.013748
73	$2.19.10^{-3}$	2.90E-09	1	0.005385
			2	0.007616
			3	0.009327
			4	0.010770
			5	0.012042
			6	0.013191
66	$1.97.10^{-3}$	2.73E-09	1	0.005225
			2	0.007389
			3	0.009050
			4	0.010450
			5	0.011683
			6	0.012798
59	$1.77.10^{-3}$	2.46E-09	1	0.004960
			2	0.007014
			3	0.008591
			4	0.009920
			5	0.011091
			6	0.012149

Table III- 29 : the diffusion coefficients of ferrocenyl methyl aniline /ferrocenium couple in aqueous ethanol at different percentages on GC FIE

Aqueous ethanol %	**Concentration** (mol/l)	**The slope**	D_{m2} (m^2/s)	**The slope**	D_{Fc^+} (m^2/s)
90	$2{,}70.10^{-3}$	0.00529	5.30E-09	0.00529	5.30E-09
81	$2{,}43.10^{-3}$	0.00509	6.06E-09	0.00509	6.06E-09
73	$2{,}19.10^{-3}$	0.00429	5.30E-09	0.00429	5.30E-09
66	$1{,}97.10^{-3}$	0.00401	7.09E-09	0.00401	7.09E-09
59	$1{,}77.10^{-3}$	0.00338	4.07E-09	0.00338	4.07E-09

The diffusion layer thicknesses of ferrocenyl methyl aniline in aqueous ethanol solution at different percentages obtained on GC fixed indicator electrode are summarized in the table III-30.

On Pt, GC rotating indicator electrodes

The reaction of oxidation of ferrocenyl methyl aniline to ferrocenium cation on Pt and GC rotating indicator electrode is a rapid, reversible and one electron transferred electrochemical reaction, controlled by diffusion process, the same VBA program was used to calculate the diffusion coefficients of ferrocenyl methyl aniline.

The diffusion coefficients of ferrocenyl methyl aniline in aqueous ethanol at different percentages obtained on Pt rotating indicator electrode are summarized in the table III-31, and the results are reported with 02 decimals.

Table III- 30: diffusion layer thicknesses of ferrocenyl methyl aniline in aqueous ethanol solution at different percentages obtained on GC FIE

Aqueous ethanol %	C (mol/l)	D (m^2/s)	t (s)	$\delta = \sqrt{Dt}$ (cm)
90	$2.70 .10^{-3}$	$5.30. 10^{-9}$	1	0.007280
			2	0.010296
			3	0.012610
			4	0.014560
			5	0.016279
			6	0.017833
81	$2.43.10^{-3}$	$6.06. 10^{-9}$	1	0.007785
			2	0.011009
			3	0.013483
			4	0.015569
			5	0.017407
			6	0.019068
73	$2.19.10^{-3}$	$5.30. 10^{-9}$	1	0.007280
			2	0.010296
			3	0.012610
			4	0.014560
			5	0.016279
			6	0.017833
66	$1.97.10^{-3}$	$7.09. 10^{-9}$	1	0.008420
			2	0.011908
			3	0.014584
			4	0.016840
			5	0.018828
			6	0.020625
59	$1.77.10^{-3}$	$4.07. 10^{-9}$	1	0.006380
			2	0.009022
			3	0.011050
			4	0.012759
			5	0.014265
			6	0.015627

Table III- 31: the diffusion coefficients of ferrocenyl methyl aniline in aqueous ethanol at different percentages on Pt RIE

Aqueous ethanol %	**Concentration** (mol/l)	**The slope**	D_{m2} (m^2/s)
90	$2{,}70.10^{-3}$	0.00687	2.19E-08
81	$2{,}43.10^{-3}$	0.00633	2.43E-08
73	$2{,}19.10^{-3}$	0.00553	2.42E-08
66	$1{,}97.10^{-3}$	0.00402	1.80E-08
59	$1{,}77.10^{-3}$	0.00220	8.73E-09

The diffusion layer thicknesses of ferrocenyl methyl aniline in aqueous ethanol solution at different percentages obtained on Pt rotating indicator electrode are summarized in the table III-32.

Table III- 32 : diffusion layer thicknesses of ferrocenyl methyl aniline in aqueous ethanol solution at different percentages on Pt RIE

Aqueous ethanol %	C (mol/cm^3)	D (m^2/s)	ν_{sol} (25 ^{0}C) (cm^2/s)	ω (rad/s)	δ (cm)
90	$2.70.10^{-3}$	$2.19.10^{-8}$	$3.91\ .10^{-5}$	125.60	0.000991
				167.46	0.000858
				188.40	0.000809
				209.33	0.000768
81	$2.43.10^{-3}$	$2.43.10^{-8}$	$5.10.10^{-5}$	125.60	0.001072
				167.46	0.000929
				188.40	0.000876
				209.33	0.000831
73	$2.19.10^{-3}$	$2.42.10^{-8}$	$6.04.10^{-5}$	125.60	0.001101
				167.46	0.000954
				188.40	0.000899
				209.33	0.000853
66	$1.97.10^{-3}$	$1.80.10^{-8}$	$6.73.10^{-5}$	125.60	0.001016
				167.46	0.000864
				188.40	0.000815
				209.33	0.000773
59	$1.77.10^{-8}$	$8.73.10^{-9}$	$7.24.10^{-5}$	125.60	0.000808
				167.46	0.000700
				188.40	0.000660
				209.33	0.000626

Table III- 33 : the diffusion coefficients of ferrocenyl methyl aniline in aqueous ethanol at different percentages on GC RIE

Aqueous ethanol %	**Concentration** (mol/l)	**The slope**	D_{m2} (m^2/s)
90	$2{,}70.10^{-3}$	0.01086	4.36E-08
81	$2{,}43.10^{-3}$	0.00622	2.37E-08
73	$2{,}19.10^{-3}$	0.00665	3.19E-08
66	$1{,}97.10^{-3}$	0.00778	4.86E-08
59	$1{,}77.10^{-3}$	0.00401	2.15E-08

Table III- 34 : diffusion layer thicknesses of ferrocenyl methyl aniline in aqueous ethanol solution at different percentages on GC RIE

Aqueous ethanol %	C (mol/cm^3)	D (m^2/s)	ν_{sol} **(25 ^{0}C)** (cm^2/s)	ω (rad/s)	δ (cm)
90	$2.70.10^{-3}$	$4.36.10^{-8}$	$3.91\ .10^{-5}$	125.60	0.001247
				167.46	0.001080
				188.40	0.001018
				209.33	0.000966
81	$2.43.10^{-3}$	$2.37.10^{-8}$	$5.10.10^{-5}$	125.60	0.001063
				167.46	0.000921
				188.40	0.000868
				209.33	0.000824
73	$2.19.10^{-3}$	$3.19.10^{-8}$	$6.04.10^{-5}$	125.60	0.001208
				167.46	0.001046
				188.40	0.000986
				209.33	0.000935
66	$1.97.10^{-3}$	$4.86.10^{-8}$	$6.73.10^{-5}$	125.60	0.001415
				167.46	0.001225
				188.40	0.001155
				209.33	0.001096
59	$1.77.10^{-8}$	$2.15.10^{-8}$	$7.24.10^{-5}$	125.60	0.001091
				167.46	0.000945
				188.40	0.000891
				209.33	0.000845

The diffusion layer thicknesses of ferrocenyl methyl aniline in aqueous ethanol solution at different percentages obtained on GC rotating indicator electrode are summarized in the table III-34.

The diffusion coefficients of ferrocenyl methyl aniline in aqueous ethanol at different percentages obtained on GC rotating indicator electrode are summarized in the table III-33, and the results are reported with 02 decimals.

5.4. Study of electrochemical behavior and calculation of diffusion coefficients of N-(ferrocenyl methyl)-2-nitro aniline/ferrocenium couple

5.4.1. The electrochemical behavior of N-(ferrocenyl methyl)-2-nitro aniline

On platinum (Pt) indicator fixed electrode

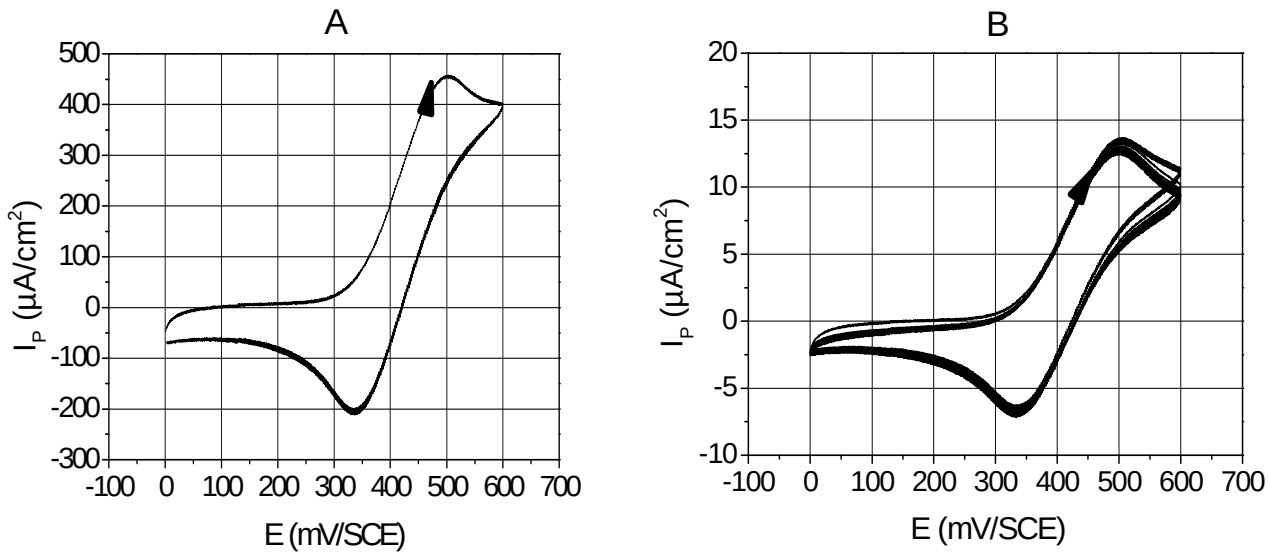

Figure III- 33 : cyclic voltammogram of N-(ferrocenyl methyl)-2-nitro aniline in aqueous ethanol (90%), on Pt indicator electrode in window potential of 0-600 mV , (Vs/SCE), (A) one cycle, (B) five cycles, 25 ^{0}C.

Before the study of the electrochemical behavior of N-(ferrocenyl methyl)-2-nitro aniline in aqueous ethanol at different percentages, on Pt indicator electrode, the reactivity and the stability of the electroactive molecule must be confirmed, the reactivity of N-(ferrocenyl methyl)-2-nitro aniline in window potential of 0-600mV is confirmed with the obtaining of a cyclic voltammogram presents an anodic peak at 0.490 mV and an cathodic peak at 0.350 mV (figure III-33 (A)), those two peaks are corresponded to the oxidation and to the reduction of ferrocenyl group/ferrocenium

couple , and the superposed of multi-cycles voltammograms (in our case 05 cycles), indicates that the system is stable and do not change with the variation of the time (figure III-33 (B)).

The cyclic voltammograms and the multi-cycles voltammograms of N-(ferrocenyl methyl)-2-nitro aniline in aqueous ethanol (81%, 73%, 66%, and 59%) on Pt indicator electrode at scan rate equals to 100 mV/s, are presented in the appendix.

Table III- 35: analysis data obtained from cyclic voltammograms of N-(ferrocenyl methyl)-2-nitro aniline in aqueous ethanol at different percentages on Pt FIE

Aqueous ethanol %	**Scan rate** (mV/s)	E_a (mV)	E_c (mV)	$E_{1/2}$ (mV)	I_a (mA/cm^2)	I_c (mA/cm^2)	$\lvert I_a/I_c \rvert$
90	25	496.6	353.9	425.25	3.27E-02	-3.26E-02	1.0011
	50	517.6	345.2	431.40	3.68E-02	-3.66E-02	1.0067
	75	503.4	340.9	422.15	4.07E-02	-4.05E-02	1.0062
	100	499.6	335.4	417.50	4.54E-02	-4.52E-02	1.0047
	150	512.1	328.4	420.25	5.27E-02	-5.25E-02	1.0042
81	25	422.4	338.7	380.55	2.14E-02	-2.11E-02	1.0124
	50	426.8	334.9	380.85	2.80E-02	-2.76E-02	1.0128
	75	430.6	330.5	380.55	3.36E-02	-3.32E-02	1.0118
	100	432.8	328.4	380.60	3.80E-02	-3.77E-02	1.0084
	150	438.2	324.0	381.10	4.57E-02	-4.55E-02	1.0035
73	25	400.1	325.1	362.60	1.68E-02	-1.67E-02	1.0057
	50	399.0	322.4	360.70	2.30E-02	-2.28E-02	1.0085
	75	401.2	320.8	361.00	2.71E-02	-2.68E-02	1.0128
	100	403.4	319.1	361.25	3.18E-02	-3.17E-02	1.0058
	150	406.7	315.9	361.30	3.75E-02	-3.75E-02	1.0005
66	25	376.8	307.5	342.15	1.00E-02	-9.77E-03	1.0249
	50	375.7	305.0	340.35	1.39E-02	-1.36E-02	1.0201
	75	374.0	306.1	340.05	1.66E-02	-1.63E-02	1.0162
	100	377.8	303.9	340.85	1.89E-02	-1.87E-02	1.0067
	150	377.3	304.4	340.85	2.29E-02	-2.28E-02	1.0053
59	25	401.2	310.8	356.00	7.22E-03	-6.98E-03	1.0346
	50	389.8	311.9	350.85	1.09E-02	-1.07E-02	1.0183
	75	395.2	315.3	355.25	1.41E-02	-1.39E-02	1.0091
	100	393.6	317.5	355.55	1.59E-02	-1.58E-02	1.0054
	150	398.0	319.1	358.55	2.13E-02	-2.11E-02	1.0086

On the Pt indicator fixed electrode, the electrochemical behavior of N-(ferrocenyl methyl)-2-nitro aniline presented a rapid, reversible and one electron transferred

electrochemical reaction in potential window of 0-600 mV, at different scan rates equal to 25, 50, 75,100 and 150 mV/s .

The electrochemical parameters of N-(ferrocenyl methyl)-2-nitro aniline obtained on Pt fixed indicator electrode are summarized in the table III-35.

The values of $E_{1/2}$ are independents to scan rates variations, so the electrochemical reaction of N-(ferrocenyl methyl)-2-nitro aniline on Pt fixed indicator electrode is a rapid and reversible.

Mode of transfer reaction of N-(ferrocenyl methyl)-2-nitro aniline on Pt FIE

To find the electrochemical reaction mechanism of N-(ferrocenyl methyl)-2-nitro aniline / ferrocenium couple on Pt fixed indicator electrode, we plotted the intensity of the anodic and cathodic peaks current as a function of the square root of scan rate $I_P = f(\sqrt{v})$, in each case we obtained a straight line passes by the origin which indicates that the electrochemical reaction of N-(ferrocenyl methyl)-2-nitro aniline on Pt fixed indicator electrode is controlled by diffusion process.

On Pt rotating indicator electrode

On Pt rotating indicator electrode, the electrochemical behavior of N-(ferrocenyl methyl)-2-nitro aniline presented a rapid, reversible and one electron transferred electrochemical reaction in potential window of 0-600 mV ,at scan rate equals to 100 mV/s at different angular velocities equal to 1200, 1600, 1800 and 2000 rpm .

The electrochemical parameters of N-(ferrocenyl methyl)-2-nitro aniline obtained on Pt Rotating indicator electrode are summarized in the table III-36.

The values of $E_{1/2}$ are independents to angular velocities variations, so the electrochemical reaction of N-(ferrocenyl methyl)-2-nitro aniline on Pt rotating indicator electrode is a rapid and reversible.

Table III- 36: analysis data obtained from polarograms of N-(ferrocenyl methyl)-2-nitro aniline in aqueous ethanol at different percentages on Pt RIE

Aqueous ethanol %	**Angular velocities** rpm	I_{lim} (mA/cm^2)	$I_{lim/2}$ (mA/cm^2)	$E_{1/2}$ (mV)
90	1200	0.7825	0.03912	438.7
	1600	0.8990	0.4495	445.9
	1800	0.9660	0.4830	448.4
	2000	1.0260	0.5130	452.2
81	1200	0.6546	0.3273	381.2
	1600	0.7419	0.3709	386.1
	1800	0.7851	0.3925	388.6
	2000	0.8264	0.4132	390.5
73	1200	0.5219	0.2609	354.5
	1600	0.5998	0.2999	360.5
	1800	0.6364	0.3182	361.5
	2000	0.6824	0.3412	364.1
66	1200	0.3184	0.1592	330.8
	1600	0.3637	0.1818	335.6
	1800	0.3829	0.1914	336.7
	2000	0.3953	0.1976	337.8
59	1200	1.8930	0.0946	325.4
	1600	0.2267	0.1133	328.1
	1800	0.2518	0.1259	330.2
	2000	0.2842	0.1421	327.6

Mode of transfer reaction of N-(ferrocenyl methyl)-2-nitro aniline on Pt RIE

To find the oxidation reaction mechanism of N-(ferrocenyl methyl)-2-nitro aniline to ferrocenium cation at Pt rotating indicator electrode, we plotted the variations in the intensity of the limit current as a function as the square root of angular velocity $I_{lim} = f(\sqrt{\omega})$, in each case we obtained a straight line passes by the origin which indicates that the oxidation reaction is controlled by diffusion process.

cyclic voltammogram of N-(ferrocenyl methyl)-2-nitro aniline on Pt fixed electrode at scan rates 25, 50, 75, 100 and 150 mV/s, the polarogram of ferrocenyl methyl aniline on Pt rotating electrode at angular velocities 1200, 1600, 1800 and 2000 rpm, $I_P = f(\sqrt{v})$ plot and $I_{lim} = f(\sqrt{\omega})$ plot of N-(ferrocenyl methyl)-2-nitro aniline in aqueous ethanol (90 %,81%, 73%, 66%, 59%) on Pt indicator electrode in potential

window of 0-600 mV (Vs/SCE), at 25 ^{0}C, are presented in figure III-34 to figure III-38.

Cyclic voltammograms of N-(ferrocenyl methyl)-2-nitro aniline on Pt fixed electrode	$I_P = f(\sqrt{v})$
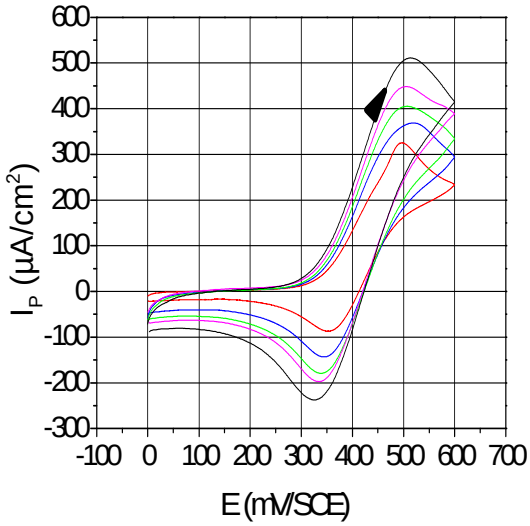	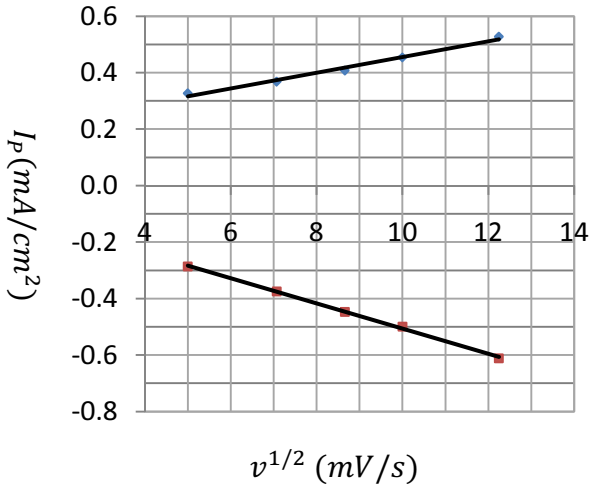
polarograms of N-(ferrocenyl methyl)-2-nitro aniline on Pt rotating electrode	$I_{lim} = f(\sqrt{\omega})$
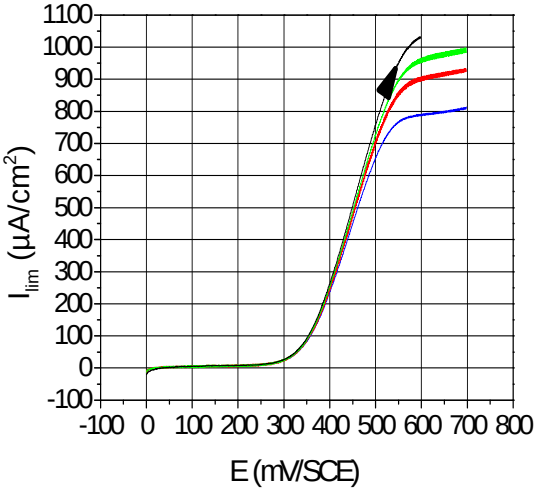	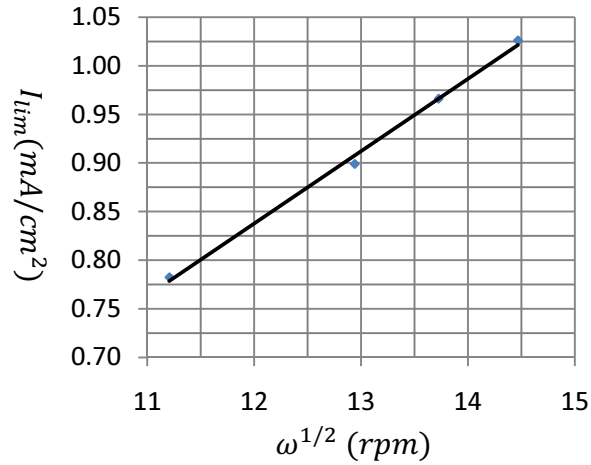

Figure III- 34 : cyclic voltammogram of N-(ferrocenyl methyl)-2-nitro aniline on Pt fixed electrode at scan rates 25, 50, 75, 100 and 150 mV/s, the polarogram of ferrocenyl methyl aniline on Pt rotating electrode at angular velocities 1200, 1600, 1800 and 2000 rpm, $\boldsymbol{I_P = f(\sqrt{v})}$ plot and $\boldsymbol{I_{lim} = f(\sqrt{\omega})}$ plot of N-(ferrocenyl methyl)-2-nitro aniline in aqueous ethanol (90 %)on Pt indicator electrode in potential window of 0-600 mV (Vs/SCE), at 25 ^{0}C.

Cyclic voltammograms of N-(ferrocenyl methyl)-2-nitro aniline on Pt fixed electrode	$I_P = f(\sqrt{v})$
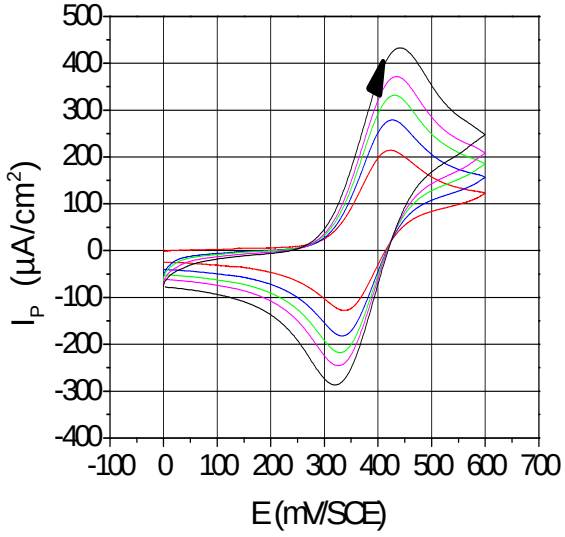	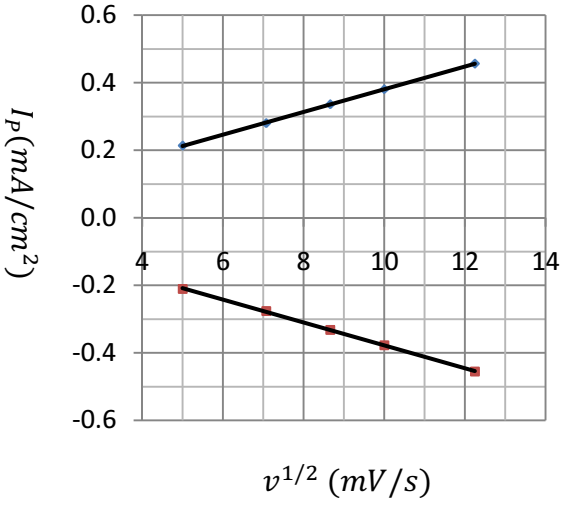
polarograms of N-(ferrocenyl methyl)-2-nitro aniline on Pt rotating electrode	$I_{lim} = f(\sqrt{\omega})$
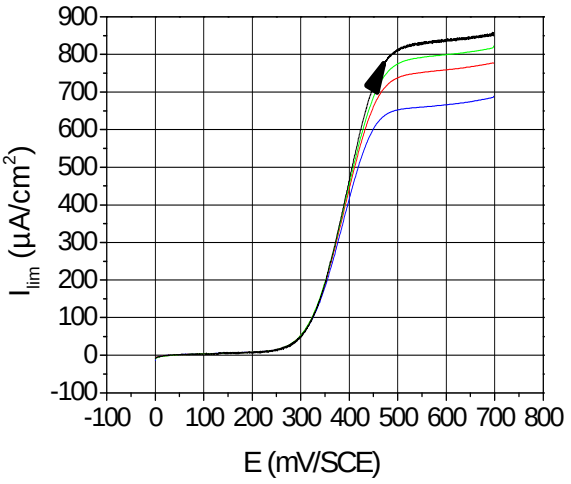	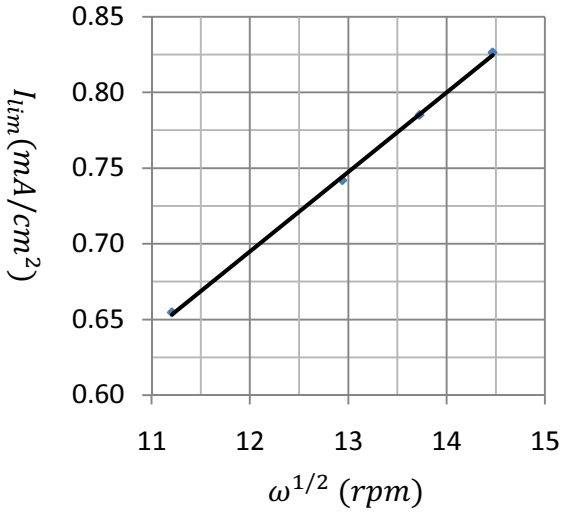

Figure III- 35: cyclic voltammogram of N-(ferrocenyl methyl)-2-nitro aniline on Pt fixed electrode at scan rates 25, 50, 75, 100 and 150 mV/s, the polarogram of ferrocenyl methyl aniline on Pt rotating electrode at angular velocities 1200, 1600, 1800 and 2000 rpm, $\boldsymbol{I_P = f(\sqrt{v})}$ plot and $\boldsymbol{I_{lim} = f(\sqrt{\omega})}$ plot of N-(ferrocenyl methyl)-2-nitro aniline in aqueous ethanol (81 %)on Pt indicator electrode in potential window of 0-600 mV (Vs/SCE), at 25 ^{0}C.

Cyclic voltammograms of N-(ferrocenyl methyl)-2-nitro aniline on Pt fixed electrode	$I_P = f(\sqrt{v})$
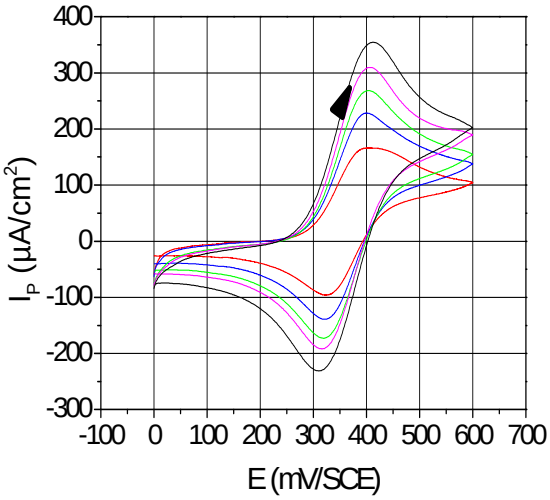	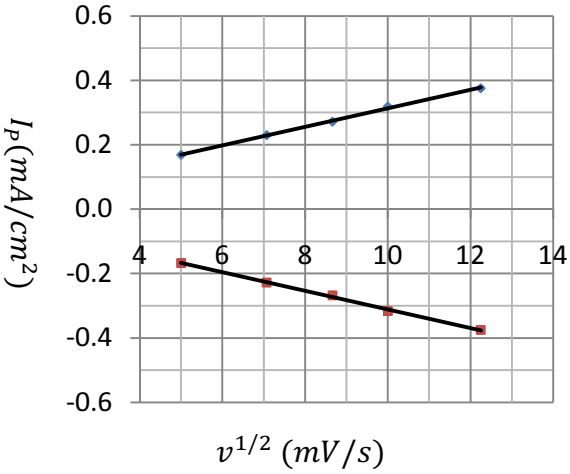
polarograms of N-(ferrocenyl methyl)-2-nitro aniline on Pt rotating electrode	$I_{lim} = f(\sqrt{\omega})$
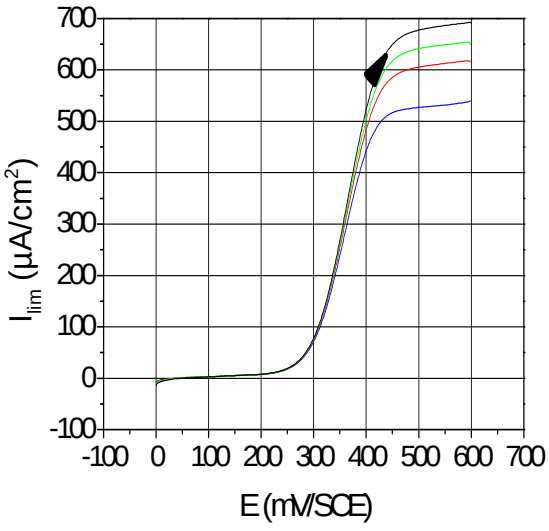	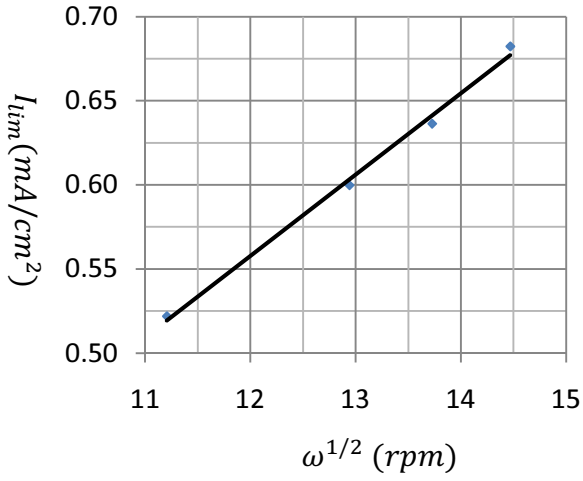

Figure III- 36 : cyclic voltammogram of N-(ferrocenyl methyl)-2-nitro aniline on Pt fixed electrode at scan rates 25, 50, 75, 100 and 150 mV/s, the polarogram of ferrocenyl methyl aniline on Pt rotating electrode at angular velocities 1200, 1600, 1800 and 2000 rpm, $\boldsymbol{I_P = f(\sqrt{v})}$ plot and $\boldsymbol{I_{lim} = f(\sqrt{\omega})}$ plot of N-(ferrocenyl methyl)-2-nitro aniline in aqueous ethanol (73 %) on Pt indicator electrode in potential window of 0-600 mV (Vs/SCE), at 25 ^{0}C.

Cyclic voltammograms of N-(ferrocenyl methyl)-2-nitro aniline on Pt fixed electrode	$I_P = f(\sqrt{v})$
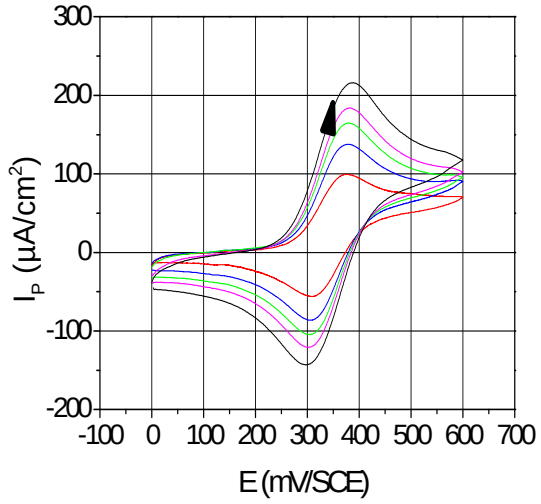	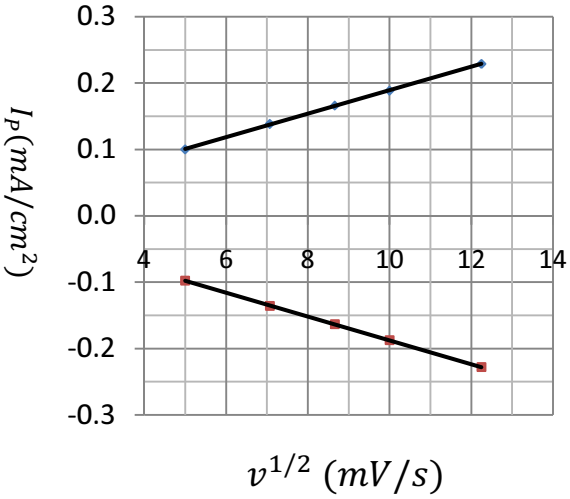
polarograms of N-(ferrocenyl methyl)-2-nitro aniline on Pt rotating electrode	$I_{lim} = f(\sqrt{\omega})$
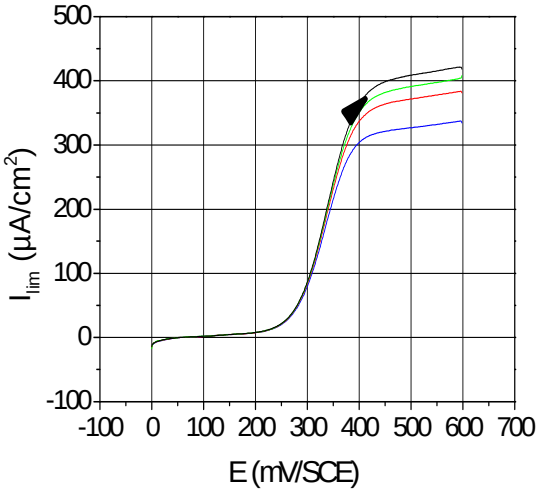	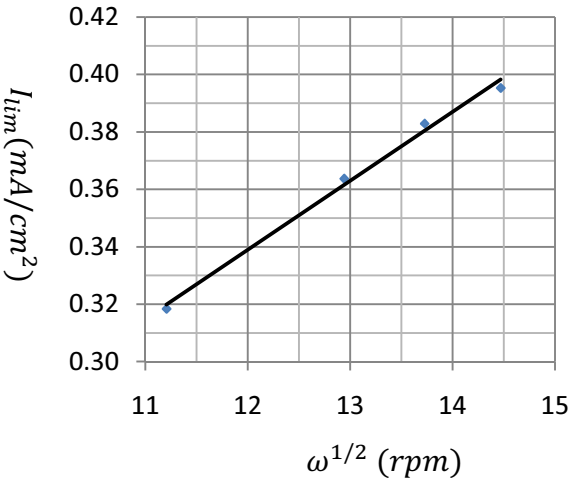

Figure III- 37 : cyclic voltammogram of N-(ferrocenyl methyl)-2-nitro aniline on Pt fixed electrode at scan rates 25, 50, 75, 100 and 150 mV/s, the polarogram of ferrocenyl methyl aniline on Pt rotating electrode at angular velocities 1200, 1600, 1800 and 2000 rpm, $\boldsymbol{I_P = f(\sqrt{v})}$ plot and $\boldsymbol{I_{lim} = f(\sqrt{\omega})}$ plot of N-(ferrocenyl methyl)-2-nitro aniline in aqueous ethanol (66 %) on Pt indicator electrode in potential window of 0-600 mV (Vs/SCE), at 25 ^{0}C.

Cyclic voltammograms of N-(ferrocenyl methyl)-2-nitro aniline on Pt electrode	$I_P = f(\sqrt{v})$
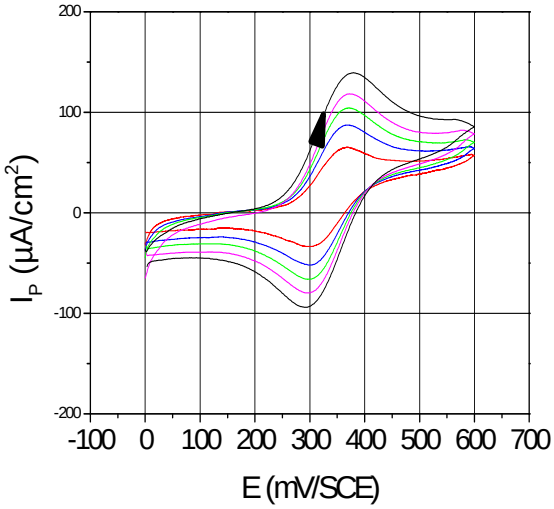	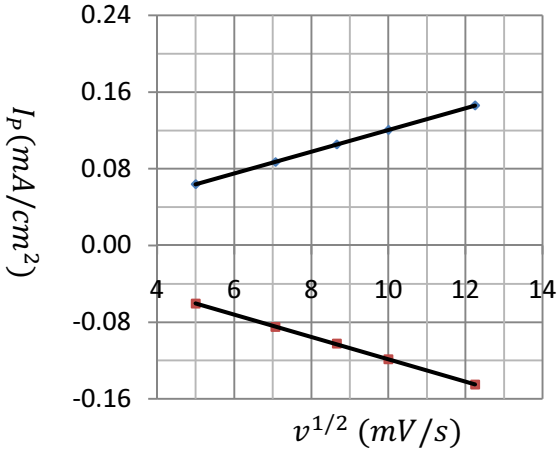
Polarograms of N-(ferrocenyl methyl)-2-nitro aniline on Pt rotating electrode	$I_{lim} = f(\sqrt{\omega})$
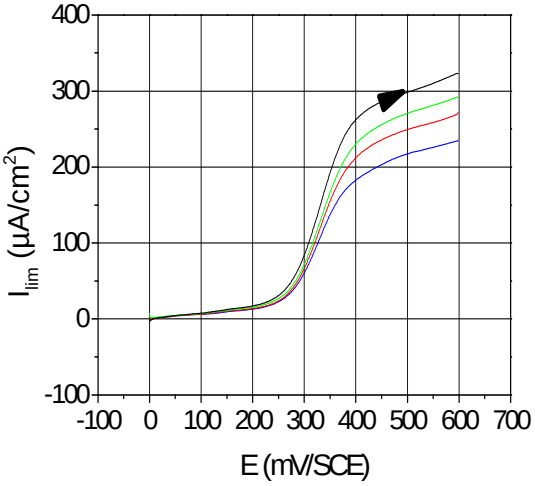	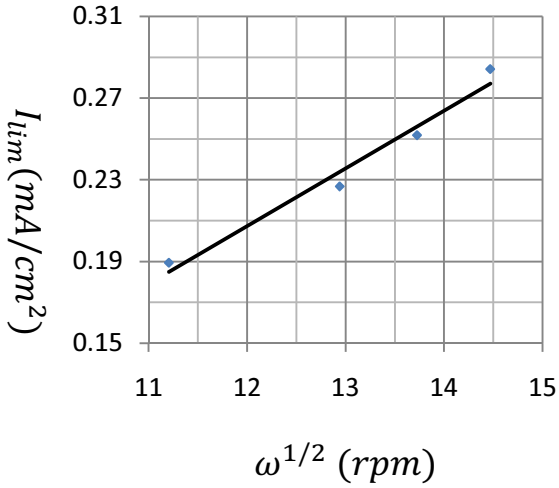

Figure III- 38: cyclic voltammogram of N-(ferrocenyl methyl)-2-nitro aniline on Pt fixed electrode at scan rates 25, 50, 75, 100 and 150 mV/s, the polarogram of ferrocenyl methyl aniline on Pt rotating electrode at angular velocities 1200, 1600, 1800 and 2000 rpm, $\boldsymbol{I_P = f(\sqrt{v})}$ plot and $\boldsymbol{I_{lim} = f(\sqrt{\omega})}$ plot of N-(ferrocenyl methyl)-2-nitro aniline in 59 % aqueous ethanol on Pt indicator electrode in potential window of 0-600 mV (Vs/SCE), at 25 ^{0}C.

On glassy carbon (GC) fixed indicator electrode

Before the study of the electrochemical behavior of N-(ferrocenyl methyl)-2-nitro aniline in aqueous ethanol in different percentages, on GC indicator electrode, the reactivity and the stability of the electroactive molecule must be confirmed, the reactivity of N-(ferrocenyl methyl)-2-nitro aniline in window potential of 0-600mV is confirmed with the obtaining of a cyclic voltammogram presents an anodic peak at 0.510mV and an cathodic peak at 0.330 mV (fig III-39 (A)), those two peaks are corresponded to the oxidation and to the reduction of ferrocenyl group/ferrocenium couple , and the superposed of multi-cycles voltammograms (in our case 05 cycles), indicates that the system is stable and do not change with the variation of the time (fig III-39 (B)).

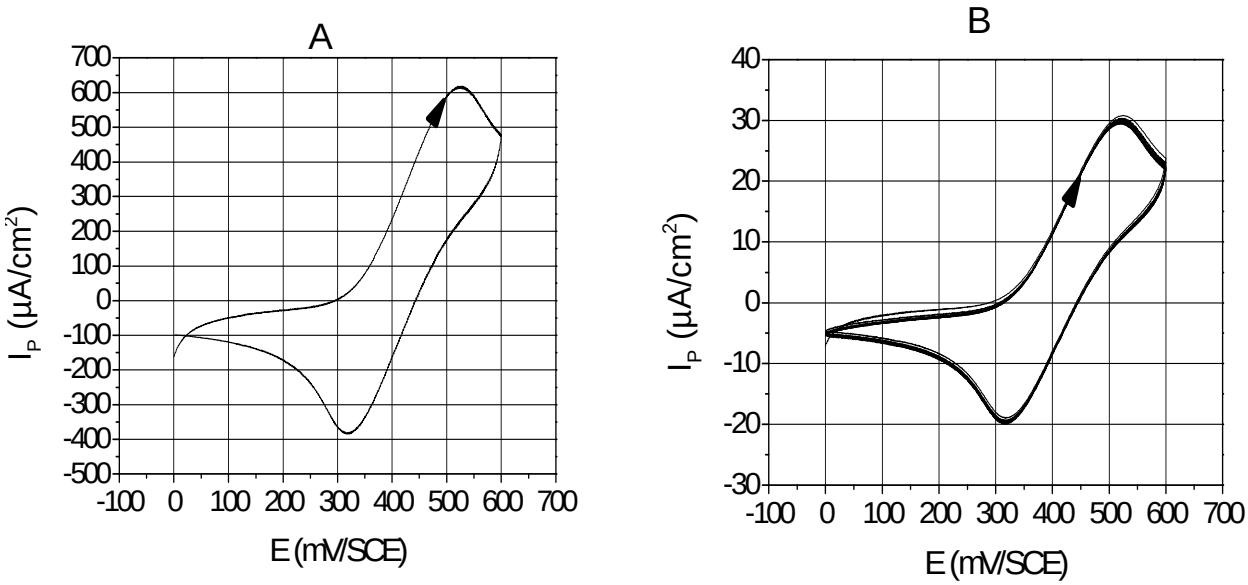

Figure III- 39: cyclic voltammogram of N-(ferrocenyl methyl)-2-nitro aniline in aqueous ethanol (90%), on GC indicator electrode in window potential of 0-600 mV (Vs/SCE), at 25 ^{0}C.

The multi-cycles voltammograms of N-(ferrocenyl methyl)-2-nitro aniline in aqueous ethanol (81%, 73%, 66%, and 59%) on GC indicator electrode are presented in the appendix.

The electrochemical parameters of N-(ferrocenyl methyl)-2-nitro aniline /ferrocenium couple obtained on GC fixed indicator electrode are summarized in the table III-37.

Table III- 37 : analysis data obtained from cyclic voltammograms of N-(ferrocenyl methyl)-2-nitro aniline in aqueous ethanol at different percentages on GC FIE

Aqueous ethanol %	**Scan rate** mV/s	E_a mV	E_c mV	$E_{1/2}$ mV	I_a mA/cm^2	I_c mA/cm^2	$\lvert I_a/I_c \rvert$
90	25	489.3	344.1	416.70	3.49E-02	-3.46E-02	1.0068
	50	505.1	332.7	418.90	4.59E-02	-4.57E-02	1.0047
	75	513.8	324.0	418.90	5.28E-02	-5.27E-02	1.0021
	100	525.7	319.1	422.40	6.13E-02	-6.11E-02	1.0036
	150	541.5	308.3	424.90	7.37E-02	-7.35E-02	1.0027
81	25	445.8	335.4	390.60	2.89E-02	-2.87E-02	1.0075
	50	444.2	330.0	387.10	3.76E-02	-3.74E-02	1.0036
	75	444.7	326.7	385.70	4.49E-02	-4.47E-02	1.0040
	100	449.1	323.5	386.30	5.02E-02	-5.00E-02	1.0052
	150	456.7	316.4	386.55	6.14E-02	-6.11E-02	1.0045
73	25	411.0	325.1	368.05	2.36E-02	-2.32E-02	1.0164
	50	414.8	322.9	368.85	3.38E-02	-3.36E-02	1.0066
	75	419.2	321.3	370.25	4.08E-02	-4.05E-02	1.0063
	100	427.9	318.6	373.25	4.89E-02	-4.85E-02	1.0084
	150	432.2	316.4	374.30	6.01E-02	-5.99E-02	1.0042
66	25	389.8	310.4	350.10	1.86E-02	-1.84E-02	1.0068
	50	386.5	308.8	347.65	2.53E-02	-2.51E-02	1.0096
	75	388.2	309.9	349.05	3.13E-02	-3.11E-02	1.0055
	100	390.9	308.3	349.60	3.65E-02	-3.63E-02	1.0049
	150	395.8	310.4	353.10	4.59E-02	-4.57E-02	1.0048
59	25	401.2	310.8	356.00	7.22E-02	-6.98E-02	1.0346
	50	389.8	311.9	350.85	1.09E-02	-1.07E-02	1.0183
	75	395.2	315.3	355.25	1.41E-02	-1.39E-02	1.0091
	100	393.6	317.5	355.55	1.59E-02	-1.58E-02	1.0054
	150	398	319.1	358.55	2.13E-02	-2.11E-02	1.0086

The values of $E_{1/2}$ are independents to scan rates variations, so the electrochemical reaction of N-(ferrocenyl methyl)-2-nitro aniline on GC fixed indicator electrode is a rapid and reversible.

Mode of transfer reaction of N-(ferrocenyl methyl)-2-nitro aniline on GC FIE

To find the electrochemical reaction mechanism of N-(ferrocenyl methyl)-2-nitro aniline / ferrocenium couple at the GC fixed indicator electrode, we plotted the intensity of the anodic and cathodic peaks current as a function of the square root of

scan rate $I_P = f(\sqrt{v})$, in each case we obtained a straight line passes by the origin which indicates that the electrochemical reaction on GC fixed indicator electrode is controlled by diffusion process.

On glassy carbon GC rotating indicator electrode

On the GC rotating indicator electrode, the electrochemical behavior of N-(ferrocenyl methyl)-2-nitro aniline presented a rapid, reversible and one electron transferred electrochemical reaction in potential window of 0-600 mV ,at scan rate equals to 100 mV/s at different angular velocities equal to 1200, 1600, 1800 and 2000 rpm .

Table III- 38 : analysis data obtained from polarograms of N-(ferrocenyl methyl)-2-nitro aniline in aqueous ethanol at different percentages on GC RIE

Aqueous ethanol %	**Angular velocities** rpm	I_{lim} mA/cm^2	$I_{lim/2}$ mA/cm^2	$E_{1/2}$ mV
90	1200	1.198	0.5990	460.4
	1600	1.350	0.6750	460.5
	1800	1.419	0.7095	462.1
	2000	1.480	0.7400	462.3
81	1200	0.946	0.4733	394.9
	1600	1.096	0.5480	401.9
	1800	1.192	0.5960	406.9
	2000	1.260	0.6300	410.7
73	1200	0.801	0.4009	364.2
	1600	0.908	0.4544	369.1
	1800	0.949	0.4747	371.2
	2000	0.978	0.4893	372.2
66	1200	0.523	0.2619	334.5
	1600	0.592	0.2964	337.6
	1800	0.622	0.3112	337.8
	2000	0.656	0.3282	338.3
59	1200	0.430	0.2151	396.6
	1600	0.444	0.2223	396.7
	1800	0.452	0.2261	396.8
	2000	0.463	0.2315	396.8

The electrochemical parameters of N-(ferrocenyl methyl)-2-nitro aniline obtained on GC rotating indicator electrode are summarized in the table III-38.

The values of $E_{1/2}$ are independents to angular velocities variations, so the oxidation reaction of N-(ferrocenyl methyl)-2-nitro aniline on GC rotating indicator electrode is a rapid and reversible.

Mode of transfer reaction of N-(ferrocenyl methyl)-2-nitro aniline on GC RIE

To find the oxidation reaction mechanism of N-(ferrocenyl methyl)-2-nitro aniline to ferrocenium cation at GC rotating indicator electrode, we plotted the variations in the intensity of the limit current as a function as the square root of angular velocity , $I_{lim} = f(\sqrt{\omega})$, in each case we obtained a straight line passes by the origin which indicates that the oxidation reaction is controlled by diffusion process.

Cyclic voltammogram of N-(ferrocenyl methyl)-2-nitro aniline on GC fixed electrode at scan rates 25, 50, 75, 100 and 150 mV/s, the polarogram of ferrocenyl methyl aniline on GC rotating electrode at angular velocities 1200, 1600, 1800 and 2000 rpm, $\boldsymbol{I_P = f(\sqrt{v})}$ plot and $\boldsymbol{I_{lim} = f(\sqrt{\omega})}$ plot of N-(ferrocenyl methyl)-2-nitro aniline in aqueous ethanol (90 %,81%, 73%, 66%, 59%) on GC indicator electrode in potential window of 0-600 mV (Vs/SCE), at 25 ^{0}C, are presented in figure III-40 to figure III-44.

Cyclic voltammograms of N-(ferrocenyl methyl)-2-nitro aniline on GC fixed electrode	$I_P = f(\sqrt{v})$
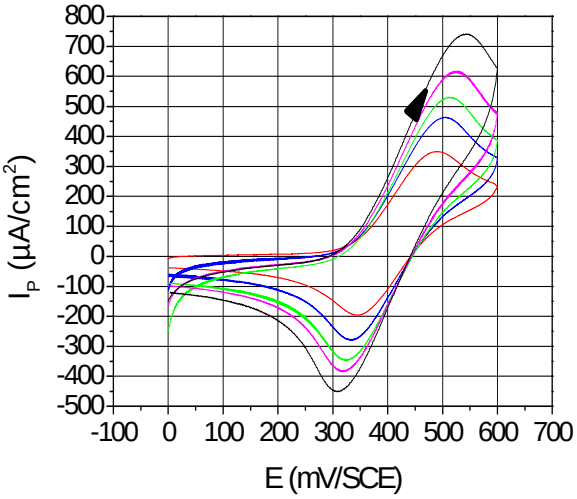	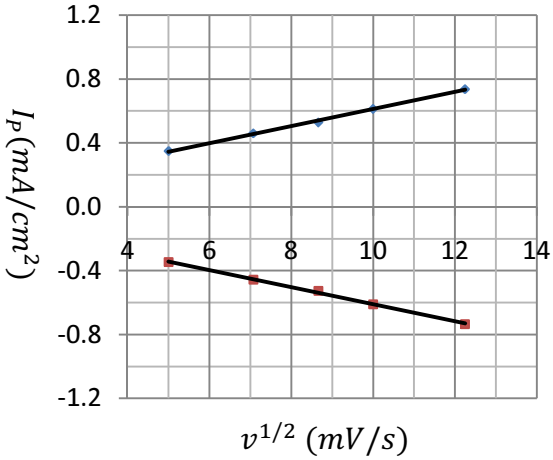
Polarograms of N-(ferrocenyl methyl)-2-nitro aniline on GC rotating electrode	$I_{lim} = f(\sqrt{\omega})$
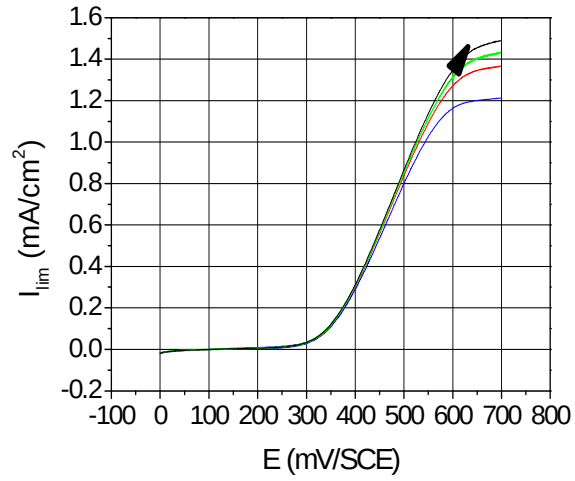	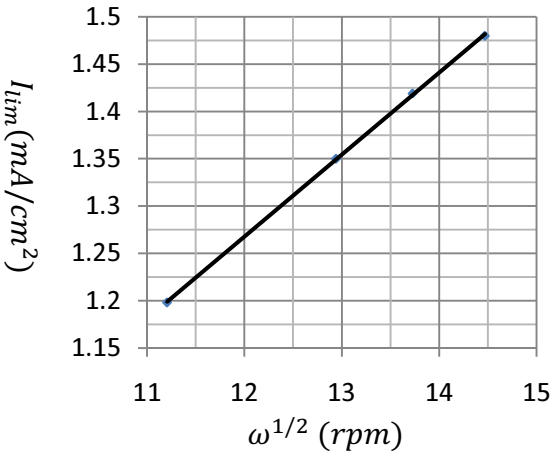

Figure III- 40: cyclic voltammogram of N-(ferrocenyl methyl)-2-nitro aniline on GC fixed electrode at scan rates 25, 50, 75, 100 and 150 mV/s, the polarogram of ferrocenyl methyl aniline on GC rotating electrode at angular velocities 1200, 1600, 1800 and 2000 rpm, $\boldsymbol{I_P = f(\sqrt{v})}$ plot and $\boldsymbol{I_{lim} = f(\sqrt{\omega})}$ plot of N-(ferrocenyl methyl)-2-nitro aniline in aqueous ethanol(90 %) on GC indicator electrode in potential window of 0-600 mV (Vs/SCE), at 25 ^{0}C.

Cyclic voltammograms of N-(ferrocenyl methyl)-2-nitro aniline on GC fixed electrode	$I_P = f(\sqrt{v})$
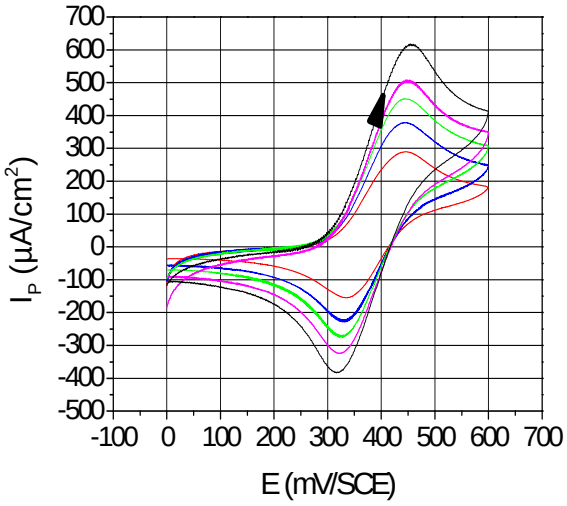	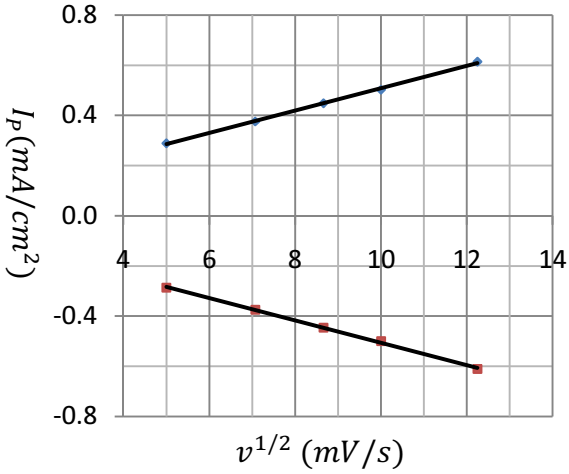
polarograms of N-(ferrocenyl methyl)-2-nitro aniline on GC rotating electrode	$I_{lim} = f(\sqrt{\omega})$
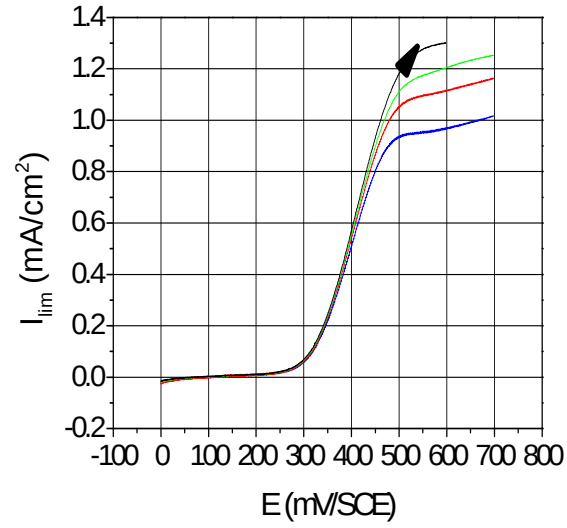	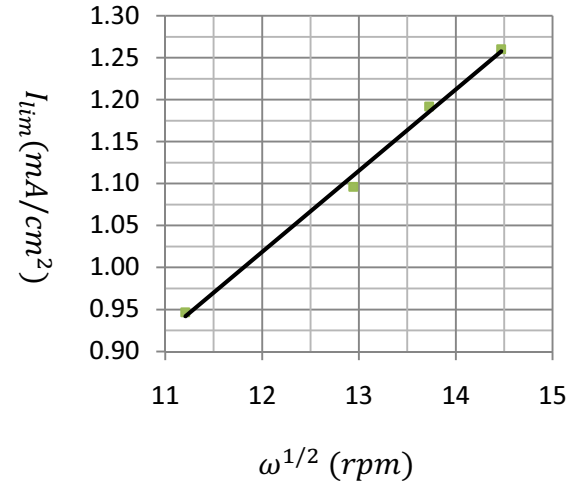

Figure III- 41: cyclic voltammogram of N-(ferrocenyl methyl)-2-nitro aniline on GC fixed electrode at scan rates 25, 50, 75, 100 and 150 mV/s, the polarogram of ferrocenyl methyl aniline on GC rotating electrode at angular velocities 1200, 1600, 1800 and 2000 rpm, $\boldsymbol{I_P = f(\sqrt{v})}$ plot and $\boldsymbol{I_{lim} = f(\sqrt{\omega})}$ plot of N-(ferrocenyl methyl)-2-nitro aniline in aqueous ethanol (81%) on GC indicator electrode in potential window of 0-600 mV (Vs/SCE), at 25 ^{0}C.

Cyclic voltammograms of N-(ferrocenyl methyl)-2-nitro aniline on GC fixed electrode	$I_P = f(\sqrt{v})$
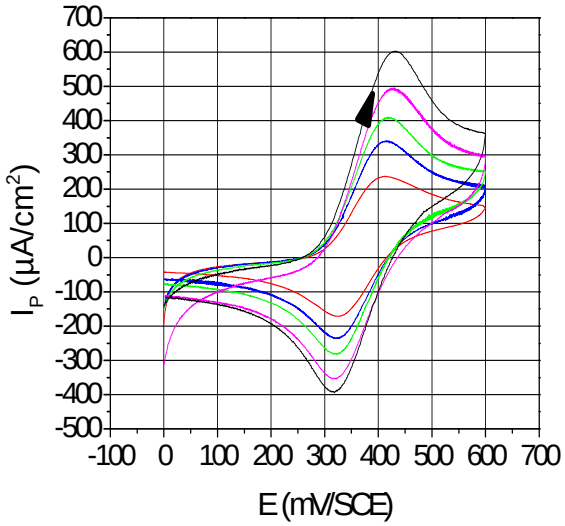	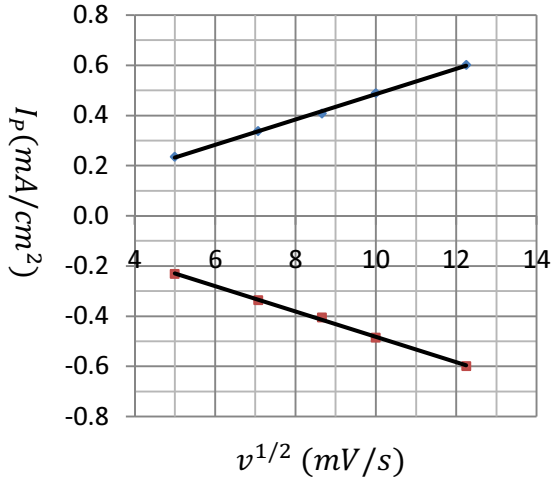
polarograms of N-(ferrocenyl methyl)-2-nitro aniline on GC rotating electrode	$I_{lim} = f(\sqrt{\omega})$
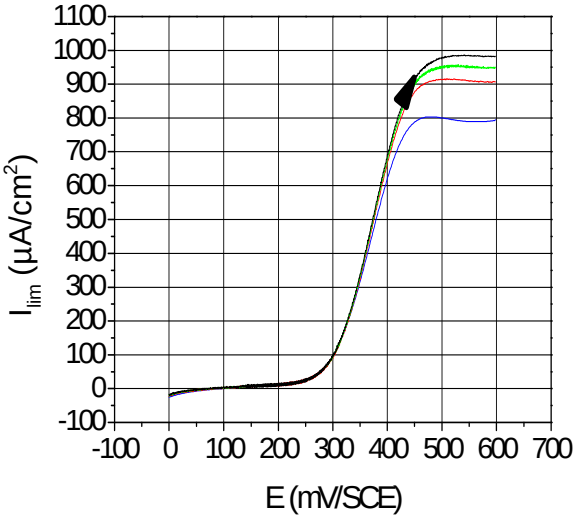	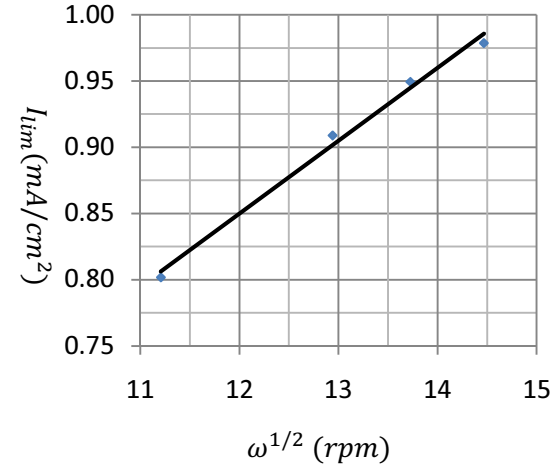

Figure III- 42: cyclic voltammogram of N-(ferrocenyl methyl)-2-nitro aniline on GC fixed electrode at scan rates 25, 50, 75, 100 and 150 mV/s, the polarogram of ferrocenyl methyl aniline on GC rotating electrode at angular velocities 1200, 1600, 1800 and 2000 rpm, $\boldsymbol{I_P = f(\sqrt{v})}$ plot and $\boldsymbol{I_{lim} = f(\sqrt{\omega})}$ plot of N-(ferrocenyl methyl)-2-nitro aniline in aqueous ethanol (73 %) on GC indicator electrode in potential window of 0-600 mV (Vs/SCE), at 25 ^{0}C.

Cyclic voltammograms of N-(ferrocenyl methyl)-2-nitro aniline on GC fixed electrode	$I_P = f(\sqrt{v})$
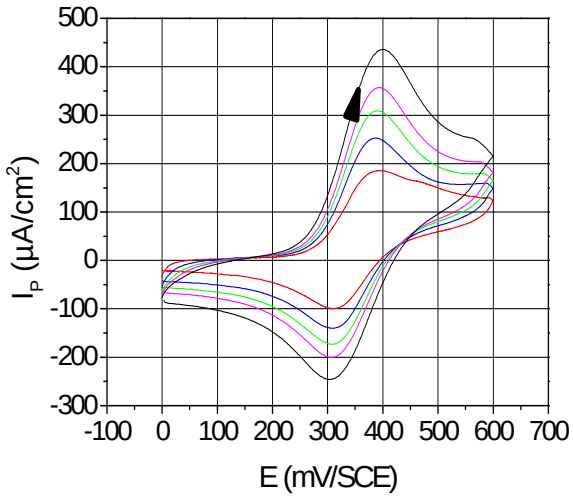	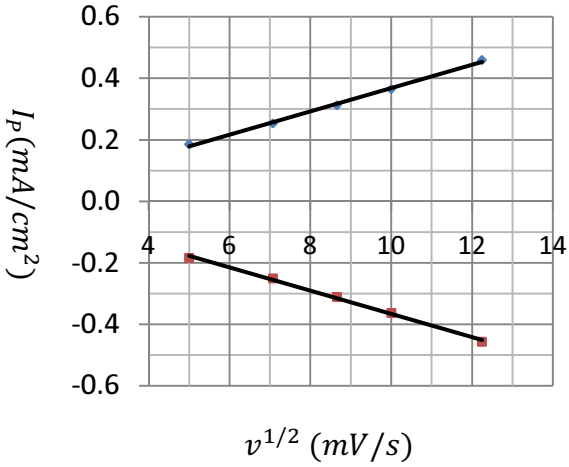
Polarograms of N-(ferrocenyl methyl)-2-nitro aniline on GC rotating electrode	$I_{lim} = f(\sqrt{\omega})$
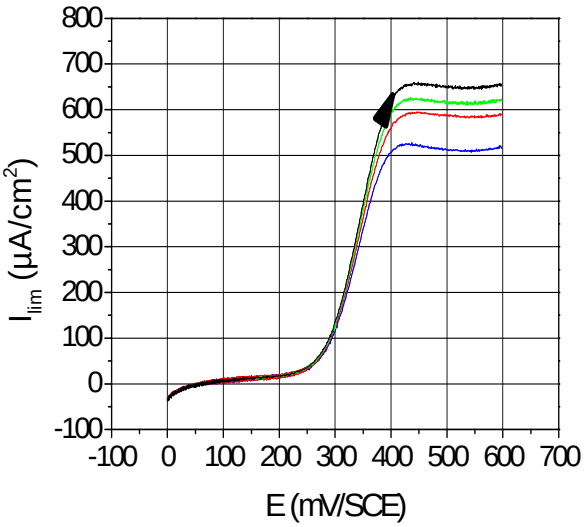	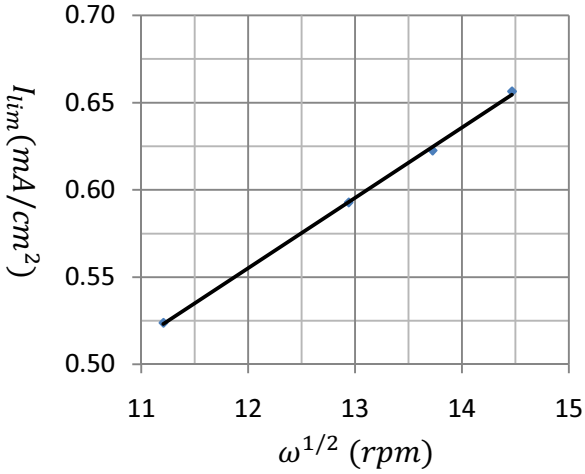

Figure III- 43: cyclic voltammogram of N-(ferrocenyl methyl)-2-nitro aniline on GC fixed electrode at scan rates 25, 50, 75, 100 and 150 mV/s, the polarogram of ferrocenyl methyl aniline on GC rotating electrode at angular velocities 1200, 1600, 1800 and 2000 rpm, $\boldsymbol{I_P = f(\sqrt{v})}$ plot and $\boldsymbol{I_{lim} = f(\sqrt{\omega})}$ plot of N-(ferrocenyl methyl)-2-nitro aniline in aqueous ethanol (66 %)on GC indicator electrode in potential window of 0-600 mV (Vs/SCE), at 25 ^{0}C.

Cyclic voltammograms of N-(ferrocenyl methyl)-2-nitro aniline on GC fixed electrode	$I_P = f(\sqrt{v})$
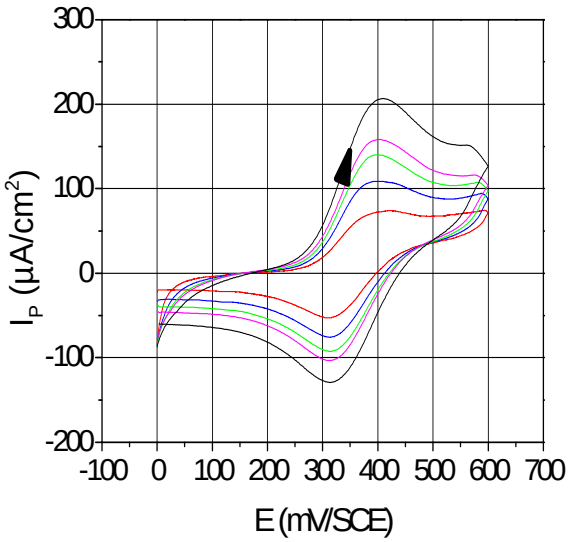	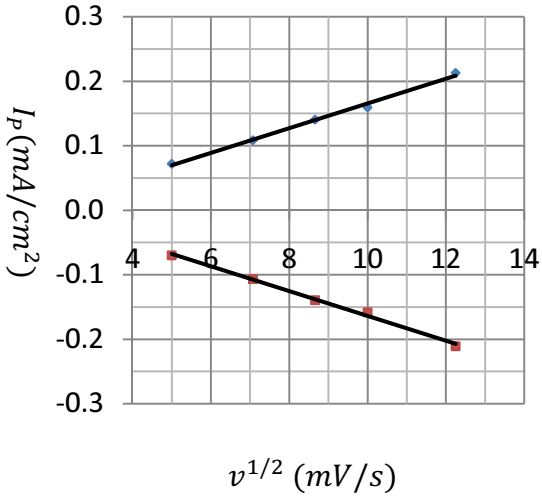
polarograms of N-(ferrocenyl methyl)-2-nitro aniline on GC rotating electrode	$I_{lim} = f(\sqrt{\omega})$
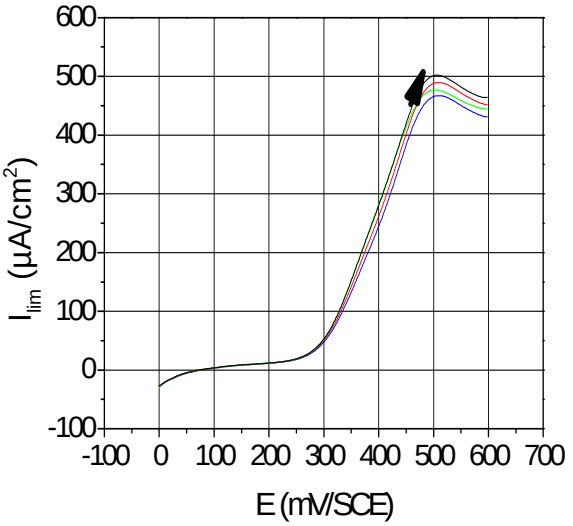	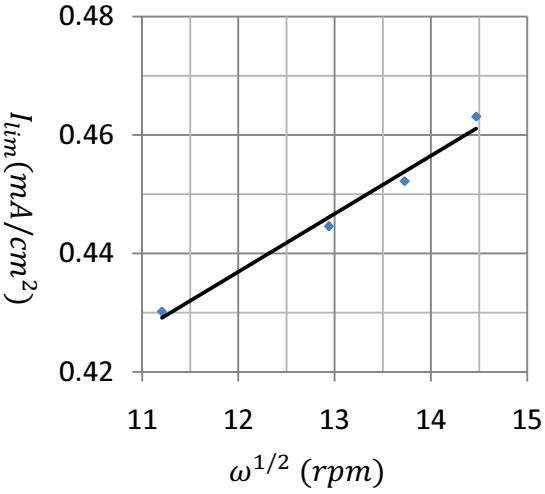

Figure III- 44 : cyclic voltammogram of N-(ferrocenyl methyl)-2-nitro aniline on GC fixed electrode at scan rates 25, 50, 75, 100 and 150 mV/s, the polarogram of ferrocenyl methyl aniline on GC rotating electrode at angular velocities 1200, 1600, 1800 and 2000 rpm, $\boldsymbol{I_P = f(\sqrt{v})}$ plot and $\boldsymbol{I_{lim} = f(\sqrt{\omega})}$ plot of N-(ferrocenyl methyl)-2-nitro aniline in aqueous ethanol (59 %) on GC indicator electrode in potential window of 0-600 mV (Vs/SCE), at 25 ^{0}C.

5.4.2. Calculation of diffusion coefficient of N-(ferrocenyl methyl)-2-nitro aniline /ferrocenium couple and diffusion layer thicknesses

On fixed Pt, GC indicator electrodes

The electrochemical reaction of N-(ferrocenyl methyl)-2-nitro aniline / ferrocenium couple on Pt and GC fixed indicator electrodes is a rapid, reversible and one electron transferred electrochemical reaction, controlled by diffusion process .the same VBA program was used to calculate the diffusion coefficients.

The diffusion coefficients of N-(ferrocenyl methyl)-2-nitro aniline /ferrocenium couple in aqueous ethanol at different percentages, obtained on Pt fixed indicator electrode are summarized in the table III-39, and the results are reported with 02 decimals.

Table III- 39 : The diffusion coefficients of N-(ferrocenyl methyl)-2-nitro aniline /ferrocenium couple in aqueous ethanol at different percentages obtained on Pt FIE

Aqueous ethanol %	**Concentration** (mol/l)	**The slope**	D_{m3} (m^2/s)	**The slope**	D_{Fc^+} (m^2/s)
90	$2{,}70.10^{-3}$	0.00277	1.45E-09	0.00279	1.45E-09
81	$2{,}43.10^{-3}$	0.00338	2.67E-09	0.00336	2.67E-09
73	$2{,}19.10^{-3}$	0.00288	2.39E-09	0.00288	2.39E-09
66	$1{,}97.10^{-3}$	0.00177	1.12E-09	0.00179	1.12E-09
59	$1{,}77.10^{-3}$	0.00113	5.63E-10	0.00116	5.63E-10

The diffusion layer thicknesses of N-(ferrocenyl methyl)-2-nitro aniline in aqueous ethanol solution at different percentages obtained on Pt fixed indicator electrode are summarized in the table III-40.

The diffusion coefficients of N-(ferrocenyl methyl)-2-nitro aniline /ferrocenium couple obtained on GC fixed indicator electrode are summarized in the table III-41, and the results are reported with 02 decimals.

Table III- 40: the diffusion layer thicknesses N-(ferrocenyl methyl)-2-nitro aniline in aqueous ethanol solution at different percentages on Pt FIE

Aqueous ethanol%	C (mol/l)	D (m^2/s)	t (s)	$\delta = \sqrt{Dt}$ (cm)
90	$2.70 .10^{-3}$	$1.45. 10^{-9}$	1	0.003808
			2	0.005385
			3	0.006595
			4	0.007616
			5	0.008515
			6	0.009327
81	$2.43.10^{-3}$	$2.67. 10^{-9}$	1	0.005167
			2	0.007308
			3	0.008950
			4	0.010334
			5	0.011554
			6	0.012657
73	$2.19.10^{-3}$	$2.39. 10^{-9}$	1	0.004889
			2	0.006914
			3	0.008468
			4	0.009778
			5	0.010932
			6	0.011975
66	$1.97.10^{-3}$	$1.12. 10^{-9}$	1	0.003347
			2	0.004733
			3	0.005797
			4	0.006693
			5	0.007483
			6	0.008198
59	$1.77.10^{-3}$	$5.63. 10^{-10}$	1	0.007503
			2	0.010611
			3	0.012996
			4	0.015007
			5	0.016778
			6	0.018379

Table III- 41 : The diffusion coefficients of N-(ferrocenyl methyl)-2-nitro aniline /ferrocenium couple in aqueous ethanol at different percentages on GC FIE

Aqueous ethanol %	**Concentration** (mol/l)	**The slope**	D_{m_3} (m^2/s)	**The slope**	D_{Fc^+} (m^2/s)
90	$2{,}70.10^{-3}$	0.00535	5.43E-09	0.00530	5.43E-09
81	$2{,}43.10^{-3}$	0.00447	4.68E-09	0.00446	4.68E-09
73	$2{,}19.10^{-3}$	0.00506	7.38E-09	0.00506	7.38E-09
66	$1{,}97.10^{-3}$	0.00378	5.09E-09	0.00377	5.09E-09
59	$1{,}77.10^{-3}$	0.00191	1.61E-09	0.00193	1.61E-09

Table III- 42: the diffusion layer thicknesses N-(ferrocenyl methyl)-2-nitro aniline in aqueous ethanol solution at different percentages on GC FIE

Aqueous ethanol%	$\boldsymbol{C}$ $(\boldsymbol{mol/l})$	$\boldsymbol{D}$ $(\boldsymbol{m^2/s})$	$\boldsymbol{t}$ $(\boldsymbol{s})$	$\boldsymbol{\delta = \sqrt{Dt}}$ $(\boldsymbol{cm})$
90	$2.70 .10^{-3}$	5.43E-09	1	0.007369
			2	0.010421
			3	0.012763
			4	0.014738
			5	0.016477
			6	0.018050
81	$2.43.10^{-3}$	4.68E-09	1	0.006841
			2	0.009675
			3	0.011849
			4	0.013682
			5	0.015297
			6	0.016757
73	$2.19.10^{-3}$	5.09E-09	1	0.007134
			2	0.010090
			3	0.012357
			4	0.014269
			5	0.015953
			6	0.017476
66	$1.97.10^{-3}$	1.61E-09	1	0.004012
			2	0.005675
			3	0.006950
			4	0.008025
			5	0.008972
			6	0.009829
59	$1.77.10^{-3}$	4.07E-09	1	0.006380
			2	0.009022
			3	0.011050
			4	0.012759
			5	0.014265
			6	0.015627

The diffusion layer thicknesses of N-(ferrocenyl methyl)-2-nitro aniline in aqueous ethanol solution at different percentages obtained on GC fixed indicator electrode are summarized in the table III-42.

On Pt, GC rotating indicator electrodes

Table III-43 : The diffusion coefficients of N-(ferrocenyl methyl)-2-nitro aniline in aqueous ethanol at different percentages on Pt RIE

Aqueous ethanol %	**Concentration** (mol/l)	**The slope**	D_{m3} (m^2/s)
90	$2{,}70.10^{-3}$	0.00745	2.48E-08
81	$2{,}43.10^{-3}$	0.00525	1.83E-08
73	$2{,}19.10^{-3}$	0.00484	1.98E-08
66	$1{,}97.10^{-3}$	0.00240	8.32E-09
59	$1{,}77.10^{-3}$	0.00282	1.27E-08

Table III- 44: diffusion layer thicknesses N-(ferrocenyl methyl)-2-nitro aniline in aqueous ethanol solution at different percentages on Pt RIE

Aqueous ethanol %	C (mol/cm^3)	D (m^2/s)	ν_{sol} **(25 ^{0}C)** (cm^2/s)	ω (rad/s)	δ (cm)
90	$2.70.10^{-6}$	$2.48.10^{-8}$	$3.91\ .10^{-5}$	125.60	0.001033
				167.46	0.000894
				188.40	0.000843
				209.33	0.000800
81	$2.43.10^{-6}$	$1.83.10^{-8}$	$5.10.10^{-5}$	125.60	0.000976
				167.46	0.000845
				188.40	0.000797
				209.33	0.000756
73	$2.19.10^{-6}$	$1.98.10^{-8}$	$6.04.10^{-5}$	125.60	0.001030
				167.46	0.000892
				188.40	0.000841
				209.33	0.000798
66	$1.97.10^{-6}$	$8.32.10^{-9}$	$6.73.10^{-5}$	125.60	0.000786
				167.46	0.000680
				188.40	0.000641
				209.33	0.000609
59	$1.77.10^{-6}$	$1.27.10^{-8}$	$7.24.10^{-5}$	125.60	0.000916
				167.46	0.000793
				188.40	0.000748
				209.33	0.000709

The reaction of oxidation of N-(ferrocenyl methyl)-2-nitro aniline to ferrocenium on Pt and GC rotating indicator electrodes is a rapid, reversible and one electron transferred electrochemical reaction, controlled by process, the same VBA program was used to calculate the diffusion coefficients.

The diffusion coefficients of N-(ferrocenyl methyl)-2-nitro aniline in aqueous ethanol at different percentages, obtained on Pt rotating indicator electrode are summarized in the table III-43, and the results are reported with 02 decimals.

The diffusion layer thicknesses of N-(ferrocenyl methyl)-2-nitro aniline in aqueous ethanol solution at different percentages obtained on Pt rotating indicator electrode are summarized in the table III-44.

Table III- 45 : the diffusion coefficients of N-(ferrocenyl methyl)-2-nitro aniline in aqueous ethanol at different percentages on GC RIE

Aqueous ethanol %	**Concentration** (mol/l)	**The slope**	D_{m3} (m^2/s)
90	$2{,}70.10^{-3}$	0.00868	3.12E-08
81	$2{,}43.10^{-3}$	0.00969	4.60E-08
73	$2{,}19.10^{-3}$	0.00551	2.40E-08
66	$1{,}97.10^{-3}$	0.00403	1.81E-08
59	$1{,}77.10^{-3}$	0.00098	2.60E-09

Table III- 46: diffusion layer thicknesses of N-(ferrocenyl methyl)-2-nitro aniline in aqueous ethanol solution at different percentages on GC RIE

Aqueous ethanol %	C (mol/cm^3)	D (m^2/s)	ν_{sol} (25 ^{0}C) (cm^2/s)	ω (rad/s)	δ (cm)
90	$2.70.10^{-6}$	$3.12.10^{-8}$	$3.91\ .10^{-5}$	125.60	0.001115
				167.46	0.000966
				188.40	0.000910
				209.33	0.000864
81	$2.43.10^{-6}$	$4.60.10^{-8}$	$5.10.10^{-5}$	125.60	0.001326
				167.46	0.001149
				188.40	0.001083
				209.33	0.001027
73	$2.19.10^{-6}$	$2.40.10^{-8}$	$6.04.10^{-5}$	125.60	0.001098
				167.46	0.000951
				188.40	0.000897
				209.33	0.000851
66	$1.97.10^{-6}$	$1.81.10^{-8}$	$6.73.10^{-5}$	125.60	0.001018
				167.46	0.000882
				188.40	0.000831
				209.33	0.000789
59	$1.77.10^{-6}$	$2.60.10^{-9}$	$7.24.10^{-5}$	125.60	0.000540
				167.46	0.000467
				188.40	0.000441
				209.33	0.000418

The diffusion coefficients of N-(ferrocenyl methyl)-2-nitro aniline in aqueous ethanol at different percentages obtained on GC rotating indicator electrode are summarized in the table III-45, and the results are reported with 02 decimals.

The diffusion layer thicknesses of N-(ferrocenyl methyl)-2-nitro aniline in aqueous ethanol solution at different percentages obtained on GC rotating indicator electrode are summarized in the table III-46.

6. Discussion of results

Table III- 47: the diffusion coefficients of ferrocene, ferrocenyl methyl aniline, N-(ferrocenyl methyl)-2 nitro aniline in aqueous ethanol at different percentages on fixed indicator electrodes

Aqueous ethanol %	C (mol/l)	$\nu_{solution}$ (25 ^{0}C) (cm^2/s)	$D_{Fr}(Pt)$ (m^2/s)	$D_{Fr}(GC)$ (m^2/s)	$D_{m2}(Pt)$ (m^2/s)	$D_{m2}(GC)$ (m^2/s)
90	2,70.10^{-3}	3,91.10^{-5}	2,30 E-9	4,05E-9	3,55E-9	5,30E-9
81	2,43.10^{-3}	5,10.10^{-5}	2,77 E-9	3,56 E-9	3,15E-9	6,06E-9
73	2,19.10^{-3}	6,04.10^{-5}	2,64 E-9	4,79 E-9	2,90E-9	5,30E-9
66	1,97.10^{-3}	6,73.10^{-5}	2,32 E-9	4,86 E-9	2,73E-9	4,07E-9
59	1,77.10^{-3}	7,24.10^{-5}	2,39 E-9	4,04 E-9	2,46E-9	7,09E-9

Aqueous ethanol %	$D_{m3}(Pt)$ (m^2/s)	$D_{m3}(GC)$ (m^2/s)	$D_{Fc^+}(Pt)$ (m^2/s)	$D_{Fc^+}(GC)$ (m^2/s)	$D_{Fc^+m2}(Pt)$ (m^2/s)
90	1.45E-09	5.43E-09	2.30E-09	4.05E-09	3.55E-09
81	2.67E-09	4.68E-09	2.77E-09	3.56E-09	3.15E-09
73	2.39E-09	7.38E-09	2.64E-09	4.79E-09	2.90E-09
66	1.12E-09	5.09E-09	2.32E-09	4.86E-09	2.73E-09
59	5.63E-10	1.61E-09	2.39E-09	4.04E-09	2.46E-09

Aqueous ethanol %	$D_{Fc^+m2}(GC)$ (m^2/s)	$D_{FC^+m3}(Pt)$ (m^2/s)	$D_{Fc^+m3}(GC)$ (m^2/s)
90	5.30E-09	1.45E-09	5.43E-09
81	6.06E-09	2.67E-09	4.68E-09
73	5.30E-09	2.39E-09	7.38E-09
66	7.09E-09	1.12E-09	5.09E-09
59	4.07E-09	5.63E-10	1.61E-09

The diffusion coefficients of ferrocene/ferrocenium, ferrocenyl methyl aniline/ferrocenium, N-(ferrocenyl methyl)-2 nitro aniline/ferrocenium couples in

aqueous ethanol at different percentages on Pt, GC fixed indicator electrodes are summarized in the table III-47.

The diffusion coefficients of ferrocene, ferrocenyl methyl aniline and N-(ferrocenyl methyl)-2 nitro aniline in aqueous ethanol at different percentages on Pt, GC rotating indicator electrodes are summarized in the table III-48.

Table III- 48 : the diffusion coefficients of ferrocene, ferrocenyl methyl aniline, N-(ferrocenyl methyl)-2 nitro aniline in aqueous ethanol at different percentages on rotating indicator electrodes

Aqueous ethanol %	**C** $(\mathbf{mol/l})$	$\boldsymbol{\nu_{solution}}$ **(25 ^{0}C)** $(\mathbf{cm^2/s})$	$\mathbf{D_{Fr}(Pt)}$ $(\mathbf{m^2/s})$	$\mathbf{D_{Fr}(GC)}$ $(\mathbf{m^2/s})$	$\mathbf{D_{m2}(Pt)}$ $(\mathbf{m^2/s})$
90	$2{,}70.10^{-3}$	$3{,}91.10^{-5}$	4.06E-08	4.60E-08	2.19E-08
81	$2{,}43.10^{-3}$	$5{,}10.10^{-5}$	2.43E-08	4.56E-08	2.43E-08
73	$2{,}19.10^{-3}$	$6{,}04.10^{-5}$	2.11E-08	3.46E-08	2.42E-08
66	$1{,}97.10^{-3}$	$6{,}73.10^{-5}$	2.03E-08	3.47E-08	1.80E-08
59	$1{,}77.10^{-3}$	$7{,}24.10^{-5}$	1.92E-08	2.60E-08	8.73E-09

Aqueous ethanol %	$\mathbf{D_{m2}(GC)}$ $(\mathbf{m^2/s})$	$\mathbf{D_{m3}(Pt)}$ $(\mathbf{m^2/s})$	$\mathbf{D_{m3}(GC)}$ $(\mathbf{m^2/s})$
90	4.36E-08	2.48E-08	3.12E-08
81	2.37E-08	1.83E-08	4.60E-08
73	3.19E-08	1.98E-08	2.40E-08
66	4.86E-08	8.32E-09	1.81E-08
59	2.15E-08	1.27E-08	2.60E-09

The diffusion coefficients of ferrocene/ferrocenium, ferrocenyl methyl aniline /ferrocenium, N (ferrocenyl methyl)-2-nitro aniline/ferrocenium couples in aqueous ethanol at different percentages, calculated using cyclic voltammetry and rotating disc electrode voltammetry, on the same indicator electrode, are nearly equals. But those obtained on GC indicator electrode are best than those obtained on Pt indicator electrode because of its broad potential window and low background current in comparison with platinum electrode. So, the indicator electrode material has an effect on diffusion coefficients. In descending classifying the diffusion coefficients calculated with cyclic voltammetry are those of ferrocenyl methyl aniline, ferrocene and N-(ferrocenyl methyl)-2-nitro aniline respectivelly. The diffusion coefficients calculated with rotating disc electrode voltammetry obtained are those of ferrocene, ferrocenyl methyl aniline and N-(ferrocenyl methyl)-2-nitro aniline respectivelly.

The voltammetry technique (cyclic, hydrodynamic) used has an effect on the diffusion coefficients. In cyclic voltammetry the diffusion layer thickness is a function of time parameter, but in hydrodynamic technique it is not.

The fluid is replenished by a flow normal to the surface. The RDE can be viewed as a pump that draws a fresh solution up from the bulk solution which keeps the diffusion layer thickness invariant.

The diffusion layer thicknesses on rotating disc electrode are smaller than those obtained on fixed indicator electrode. So, the diffusion coefficients calculated with hydrodynamic voltammetry are best then those calculated with cyclic voltammetry.

With rotating electrode voltammetry, the diffusion coefficients in descending classifying obtained are those of: ferrocene, ferrocenyl methyl aniline, and N-(ferrocenyl methyl)-2-nitro aniline respectivelly. The movement of the electrode with an angular velocity gives fluid a movement which facilitates the mass transfer. So, the molecule which has the lighter weight will have the best diffusion coefficient.

At another side ,the diffusion coefficients in descending classifying calculated with cyclic voltammetry are those of ferrocenyl methyl aniline, ferrocene, and N-(ferrocenyl methyl)-2-nitro aniline respectivelly, so the electroactive molecule which has the best solubility in aqueous ethanol will have the best diffusion coefficient.

The variation of the kinematic viscosity from medium to medium is not significant. The properties of the ethanol and of the distilled water are closes .The effect of the kinematic viscosity of medium on the diffusion of studied couples in aqueous ethanol at different percentages is not significant, elucidated that the diffusion coefficients obtained on the same indicator electrode are nearly equals.

in the boundary layer, the diffusion layer (Nernst layer)is separated from electrode surface/solution interface where the kinematic viscosity has the most effect on all phenomena of transfer (mass ,heat and momentum quantity) by the Helmholtz layer(inner, outer Helmholtz layer),(figure III-45).

So we can conclude that the nearly properties of ethanol and of distilled water and Helmholtz layer reduce the effect of kinematic viscosity on the diffusion of ferrocene/ferrocenium, ferrocenyl methyl aniline/ferrocenium and N-(ferrocenyl methyl)-2-nitro aniline/ferrocenium couples in aqueous ethanol at different percentages .

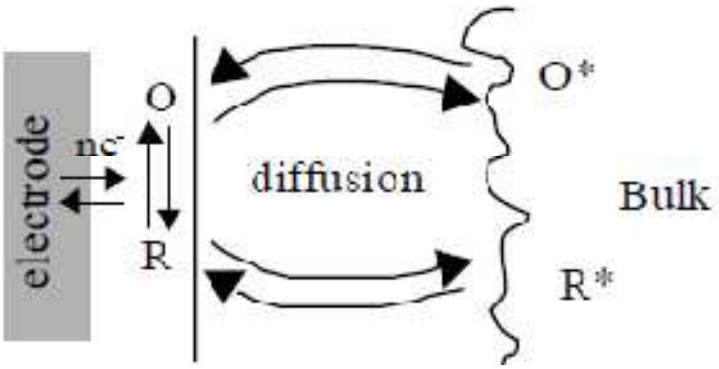

Figure III- 45 : separation of Nernst layer and the interface electrode/solution by Helmholtz layers.

7. Conclusion

The diffusion coefficients of ferrocene/ferrocenium, ferrocenyl methyl aniline/ferrocenium and (ferrocenyl methyl)-2-nitro aniline/ferrocenium couples in aqueous ethanol at different percentages are influenced by several factors, such as the indicator electrode material, the voltammetry technique used in the study of the electrochemical behavior of the electroactive molecule.

The variation of the kinematic viscosity from medium to medium is not significant because of the properties of the ethanol and of the distilled water are closes.

The kinematic viscosity of the medium has not a significant effect on the diffusion coefficients of studied couples in aqueous ethanol at different percentages because of the nearly properties of the ethanol and of the distilled water in side, on the other hand the Helmholtz layer in the electrical double layer separates the diffusion layer (Nernst layer) and the indicator electrode surface/solution interface where the viscosity has the most important influence on phenomena of transfer (mass, heat and momentum quantity).

So, the nearly of the properties of ethanol and of water and the separation of Nernst layer and the electrode/solution interface by Helmholtz layer, decrease the influence of the kinematic viscosity of the medium on the diffusion coefficients of the studied electroactive species.

Conclusion

The obtained diffusion coefficients of ferrocene/ferricenium, ferrocenyl methyl aniline/ferricenium and N-(ferrocenyl methyl)-2-nitro aniline/ferricenium couples in aqueous ethanol at different percentages on two different indicator electrode (GC, Pt) materials elucidate that the material of the indicator electrode has an effect on the diffusion coefficients as well as the voltammetry techniques used in the analysis of the studied molecules behavior; cyclic, rotating disc electrode.

The diffusion coefficients obtained on glassy carbon indicator electrode are best than those obtained on platinum indicator electrode, because of its broad potential window and low background current in comparison with platinum electrode. The diffusion coefficients obtained using rotating disc electrode voltammetry are best than those obtained using cyclic voltammetry. The fluid is replenished by a flow normal to the surface. The RDE can be viewed as a pump that draws a fresh solution up from the bulk solution which keeps the diffusion layer thickness invariant. The diffusion layer thicknesses on rotating disc electrodes are smaller than those obtained on fixed indicator electrodes.

The kinematic viscosity of the medium has not a significant effect on the diffusion coefficients of the studied electroactive molecules in aqueous ethanol at different percentages. The nearly properties of the ethanol and of the distilled water make the variation of the kinematic viscosity from medium to medium not significant. The separation of the electrode surface /solution interface where the kinematic viscosity has its effect on phenomena of transfer (mass, heat and momentum quantity) and the diffusion layer (Nernst layer) by the Helmholtz layer (inner and outer Helmholtz layer), decrease the effect of the kinematic viscosity of the medium on the diffusion coefficients of the studied electroactive molecules.

Bibliography

[1] Kosuke Izutsu, Electrochemistry in Nonaqueous Solutions, second revised and enlarged edition, by Wiley-VCH Verlag GmbH & Co. KGa. A. 2010

[2] D. Astruc, Electron transfer and radical processes in transition metal chemistry, VCH publishers Inc. New York, 1995.

[3] Joseph Wang, Analytical electrochemistry, Third edition, Wiley-VCH 2006.

[4] A.M Bond, Broadening electrochemical horizons principles and illustration of voltammetric and related techniques, Oxford University press. 2002

[5] Richard G Compton and Craig E banks, Understanding voltammetry, World Scientific Publishing 2007.

[6] Adrian W. Bott, Practical problems in voltammetry, reference electrodes for voltammetry. BIOANALYTICAL SYSTEMS, INC. 2, 2008. P. 64-68.

[7] David K. Gosser, Cyclic voltammetry simulation and analysis of reaction mechanisms by wiley-VCH. 1993

[8] Allen.J. Bard, Larry R. Folkner, Electrochemical methods fundamental and applications second edition John Wiley & Sons, Inc; 2001.

[9] Kosuke Izutsu, Electrochemistry in Nonaqueous Solutions. Wiley-VCH Verlag GmbH & Co. 2002

[10] Conway B.E, Theory and principles of electrode processes. Ronald Press New York, 1965.

[11] Paul Mank, Fundamental of electroanalytical chemistry (Analytical techniques in the sciences), John Wiley & Sons Ltd, 2001.

[12] Philip H. Rieger, Electrochemistry second edition, Chapman & Hall New York, 1994.

[13] Michael J. Weaver, H. Y. Liu, Yong joo Kim, The role of the supporting electrolyte cation in the kinetics of outer-sphere electrochemical redox

processes involving metal complexes. Canadian Journal of Chemistry 1981. P. 1944-1953

[14] Van Benschoten, J. J., Lewis, J. Y., Heineman, W. R., Roston, D. A., Kissinger, P. T., J Chem. Educ 60, 1983. P. 772-776.

[15] Orlando Tapia, and Juan Bertran, Solvent effects and chemical reactivity (Understanding Chemical Reactivity), Kluwer Academic Publishers, 2002.

[16] Matsumiya, M., Terazono, M., Tokuraku, K., Electrochim. Acta, 51, 2006. P. 1178-1183,.

[17] M.F. Bento, M.D. Geraldo, and M.I., Effect of the medium composition on the current of steady state voltammograms of neutral and charged species in dimethylformamide/toluene mixtures. Analytica Chimica Acta 1999 Volume 385, Issues 1-3, P. 365-371.

[18] Trémillon B., Electrochimie Analytique et réactions en solution, Tome 2 - Réactions et méthodes électrochimiques, éd. Masson (Paris), 1993.

[19] Van Stam J., Depaemelaere S., De Schryver F.C. J. Chem. Educ., 1998.

[20] Cristophe Nourry, Extraction electrochimique des lanthanides des milieux de fluorures fondue par formation d'alliages, Université de Paul Sabatier, Toulouse. 2007.

[21] Paul M.S monk, Bioanalytical Systems West Lafayette, Current Separations, John Weily, 1995.

[22] M. Albert Vannice, Solutions manual for kinetics of catalytic reactions, Springer sciences + business media, 2005.

[23] Diran Basmadjian, mass transfer principles and application, Taylor & Francise-Library, 2005.

[24] Richard Ghez, A primer of diffusion problems, by John Wiley & Sons, Inc., 1988.

[25] E.L Cussler, diffusion mass transfer in fluid system, second edition, Cambridge university press, 1997.

[26] Sawhney-I.K, Heat and mass transfer, international publishing house, 2008.

[27] Arvind Varma, Mass and heat transfer analysis of mass contactors and heat exchangers, Purdue University, Cambridge university press, volume 10, 2008.

[28] Ettiene Guyon, Jean Pierre Hulin, Luc Petit, hydrodynamique physique, CNRS Edition et EDP Sciences, 2001.

[29] Kenneth A.jackson, Kinitic process, crystal growth diffusion and phase transitions in material, WILEY-VCH Verlag GmbH & Co. KGaA, Weinheim, 2004.

[30] Helmut mehrer, diffusion in solids , Fundamentals methods materials, Diffusion-Controlled Processes, clarendon press, Springer-Verlag Berlin Heidelberg, 2007.

[31] Ross Taylor R. Karishna, multicompenent mass transfer, John Wiley & Sons, Inc, 1993.

[32] Cameron Tropea, Alexender L.Yarin John F Foss, Hand book of experimental fluid mechanics, volume 01, Springer, 2007.

[33] E.L Cussler, Eykamp, W., Koros, WJ, Riely RL, Diffusion mass transfer in fluid system, third edition, Cambridge university press, 1997.

[34] M. Thirumaleshwar, fundamentals of heat and mass transfer, Dorling Kindersley (india), 2006.

[35] Frank P. Incorpera, David P. Dewitt, Theodore L. Bergman, fundamentals of heat and mass transfer, John Weily, 2011.

[36] Hans Dieter Baehr, Karl Stephane, Heat and mass transfer, Springer Verlag Berlin, 2006.

[37] Herbert Oertel, Prandtl essential of fluid mechanic third edition, Springer Science, Business Media, 2010.

[38] Fundamentals of heat and mass transfer, C.P Kothandaraman, S. Subramanyan, new age international, 2006.

[39] R. Hughes, Hydrodynamics mass and heat transfer in chemical engineering, University of Salford, UK, Taylor & Francis, 2002.

[40] Dabir s. Viswanath, tushar k. Ghosh, Dasika h. L. Prasad, Nidamarty. K. Dutt, kalipatnapu y. Rani, Viscosity of liquids, theory, estimation, experiment and data, Springer, 2007.

[41] Johnson, K. E., *J. Electrochem. Soc. Interface,* 16, 38, 2007.

[42] L. Gary Leal, Advanced transport phenomena fluid mechanics and convection process, Cambridge University Press, 2007.

[43] Albert Ernest Dunstan, D. Sc, and Ferdinand Bernard Thole, Viscosity of liquids, green and co. 39 paternoster row, London, New York Bombay and Calcutta, 1914.

[44] ML Kijevkanin, viscosity of binary non-electrolyte liquid mixtures: prediction and correlation, Chemical Industry & Chemical Engineering Quarterly, 2008.

[45] E. Poling, John M. Prausnitz, John P. O'Connell, Properties of Gases and Liquids, Fifth Edition, Bruce, the McGraw-Hill Companies, 2004.

[46] Jürgen Millat,John H. Dymond,C. A. Nieto de Castro ,Transport properties of fluid: their correlation, prediction and estimation , press syndicate of the university of Cambridge, 1996.

[47] G. Latini,R. Cocci Grifoni,G. Passerini, transport properties of organic liquids, WIT press, 2006 .

[48] Paiming Wing, Anderzej Anderco, Robert D Youn, Modeling viscosity of concentrated and mixed solvent electrolyte system, elseiver, 2004.

[49] Etienne Guyon, Jean Pierre Hulin, hydrodynamique physique, EDP sciences, 2001.

[50] Satish G. Kandlikar, Masahiro Shoji V0.K.Dhir Hand book of phase change boiling, condensation, Taylor Francis, 1999.

[51] Rowe R.C, interactions in ternary powder system microcrystalline, cellulose, magnesium stearate and colloidal silica: a solubility parameter approach, international journal of pharmaceutics, 1988 b, 45, p.259-261.

[52] Rowe R.C interactions in coloured powders and tablets formulations: a theoretical approach based solubility parameter, international journal of pharmaceutics, 1989, 53, p .47-51.

[53] G. Wilkinson, M. Rosenblum, M.C. Whiting, and R.B. Woodward. *J. Am. Chem. Soc.* 1952, 74, 2125- 2126.

[54] G. Wilkinson. *J. Am. Chem. Soc.*, 1952, 74, 6149-6150.

[55] E.O. Fischer and W.Z. Pfab. *Naturforsch.*, 1952, 76, 377-379.

[56] T.J. Kealy and P.L. Pauson. *Nature*, 1951, 168, 1039-1040.

[57] S.A. Miller, J.A. Tebboth, and J.F. Tremaine. *J. Chem. Soc., (London)* 1952, 632-635.

[58] K. L. Rinchart, et coll, J. Am. Chem. Soc. 1960, 82, 4111.

[59] J. M. Osgerby and P. L. Pauson. Ferrocene derivatives. Part VIII. Tetrahydropyridoferrocenes. J. Chem. Soc., 1961, p 4600.- 4604

[60] Rahim O.K, synthèse et étude photochimique, électrochimique et structural de quelques N-ferrocenyl methyl anilines substitutes. Laboratoire VPRS. Université d'Ouargla. 2010.

[61] Carl L. yaws, Thermophysical properties of chemicals and hydrocarbon, William Andrew Inc, 2008.

[62] S. Koneshan, Jayendran C. Rasaiah, R. M. Lynden-Bell, and S. H. Lee, Solvent Structure, Dynamics, and Ion Mobility in Aqueous Solutions at 25^0C, *Pusan 608-736, Korea,1998.*

[63] J. P. Oliver, J. Marchand, L. O. Nilsson, Méthodologie de prévision de pénétration des ions chlore par diffusion dans le béton. Proceedings of the international RILEM (The Internationnal Union of Testing and Research Laboratories for Materials and Structures) 1998, p. 166-191

[64] M. Mosbach, T. Laurell , J. Nilsson, E. Csöregi, et W. Schuhmann, Biosensors & Bioelectronics 2001, 16, 611.

[65] A. Simenel , Y. V. Kuzmenko, E. A. Morozova, M. M. Ilyin, I. F. Gun'ko, L. V. Snegur, Journal of Organometallic Chemistry 2003, 688, 138.

[66] M. Vilas-Boas, E.M. Pereira, C. Freire , A.R. Hillman, Journal of, Electroanalytical Chemistry 2002, 538, 47.

Appendix

Table A- 1: conversion factors between various dynamic viscosity units [46]

Multiply by	**To**						
From	**Poiseuille (pas.s)**	**Poise Dyne.s/cm^2= g/cm.s**	**centipoise**	**Kg/m.h**	**Lb$_f$ .s/ft^2**	**Lb/ft.s**	**Lb/ft.h**
Poiseuille (pas.s)	1	10	10^3	$3.63\ 10^3$	$2.09\ 10^{-2}$	0.672	$2.42\ 10^3$
Poise Dyne.s/cm^2 =g/cm.s	0.1	1	100	360	$2.09\ 10^{-3}$	$6.72\ 10^{-2}$	242
centipoise	0.001	0.1	1	3.6	$2.9\ 10^{-5}$	$6.72\ 10^{-4}$	2.42
Kg/m.h	$2.78\ 10^{-4}$	$2.78\ 10^{-3}$	$2.78\ 10^{-1}$	1	$5.8\ 10^{-6}$	$1.87\ 10^{-4}$	0.672
Lb$_f$ .s/ft^2	4.79	479	$4.79\ 10^4$	$1.72\ 10^5$	1	32.2	$1.16\ 10^5$
Lb/ft.s	1.49	14.9	$1.49\ 10^3$	$5.36\ 10^3$	$3.11\ 10^{-2}$	1	$3.6\ 10^3$
Lb/ft.h	$4.13\ 10^{-4}$	$4.13\ 10^{-3}$	0.413	1.49	$6.62\ 10^{-6}$	$2.78\ 10^{-4}$	1

Table A-2: conversion factors between various kinematic viscosity units[45]

Multiply by	**To**					
From	**stocks**	**Centistoks**	**m^2/s**	**m^2/h**	**ft^2/s**	**ft^2/h**
stocks	1	100	10^{-4}	$3.6\ 10^{-1}$	$1.076\ 10^{-3}$	3.875969
Centistocks	0.01	1	10^{-6}	$3.6\ 10^{-3}$	$1.08\ 10^{-5}$	0.03876
m^2/s	10^4	10^6	1	$3.6\ 10^3$	$1.08\ 10^1$	$3.88\ 10^4$
m^2/h	2.78	$2.78\ 10^2$	$2.78\ 10^{-4}$	1	$2.99\ 10^{-3}$	$1.08\ 10^1$
ft^2/s	929	$9.29\ 10^4$	$9.29\ 10^{-2}$	$3.34\ 10^2$	1	$3.60\ 10^3$
ft^2/h	0.258	25.8	$2.58\ 10^{-5}$	$9.28\ 10^{-2}$	$2.78\ 10^{-4}$	1

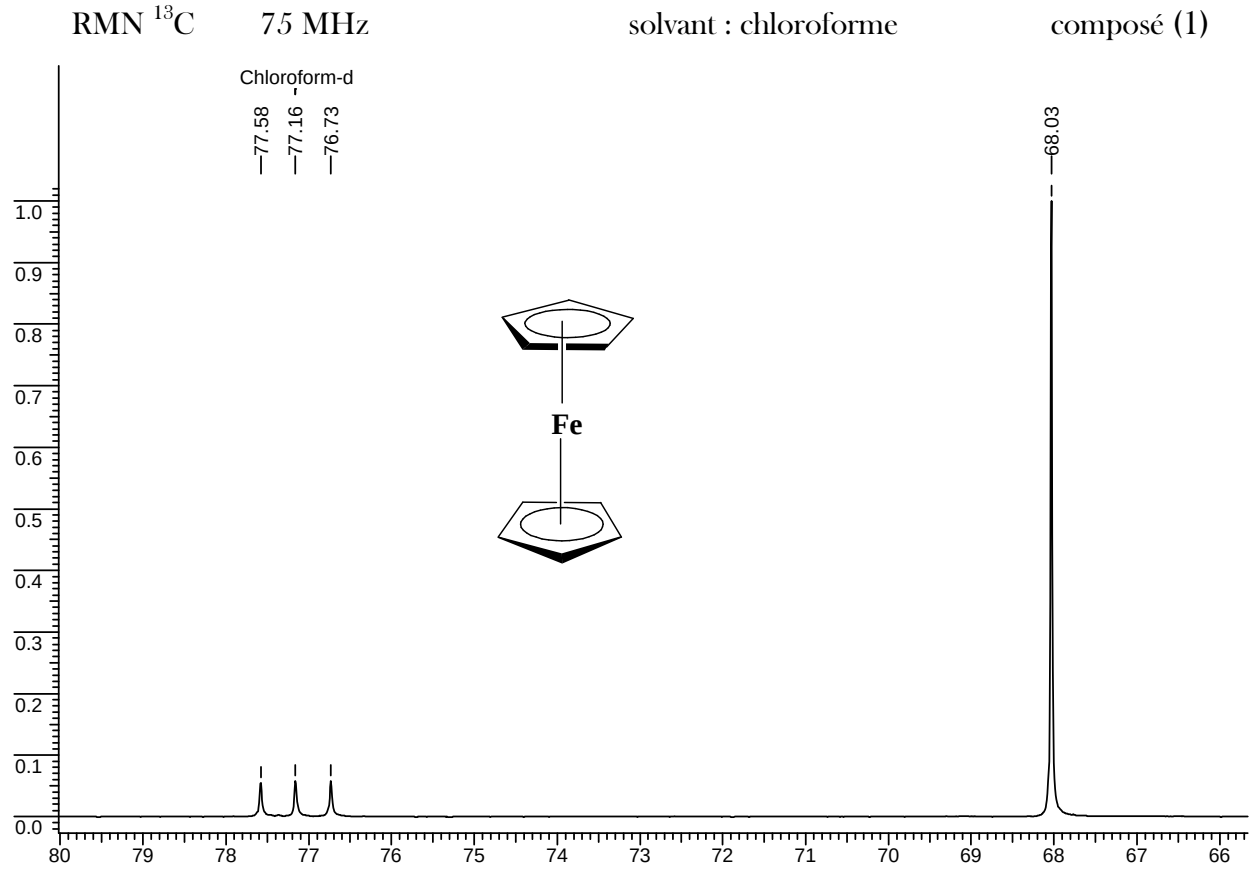

Figure A- 1 : The spectrum of ferrocene in chloroform by RMN^{13}C.

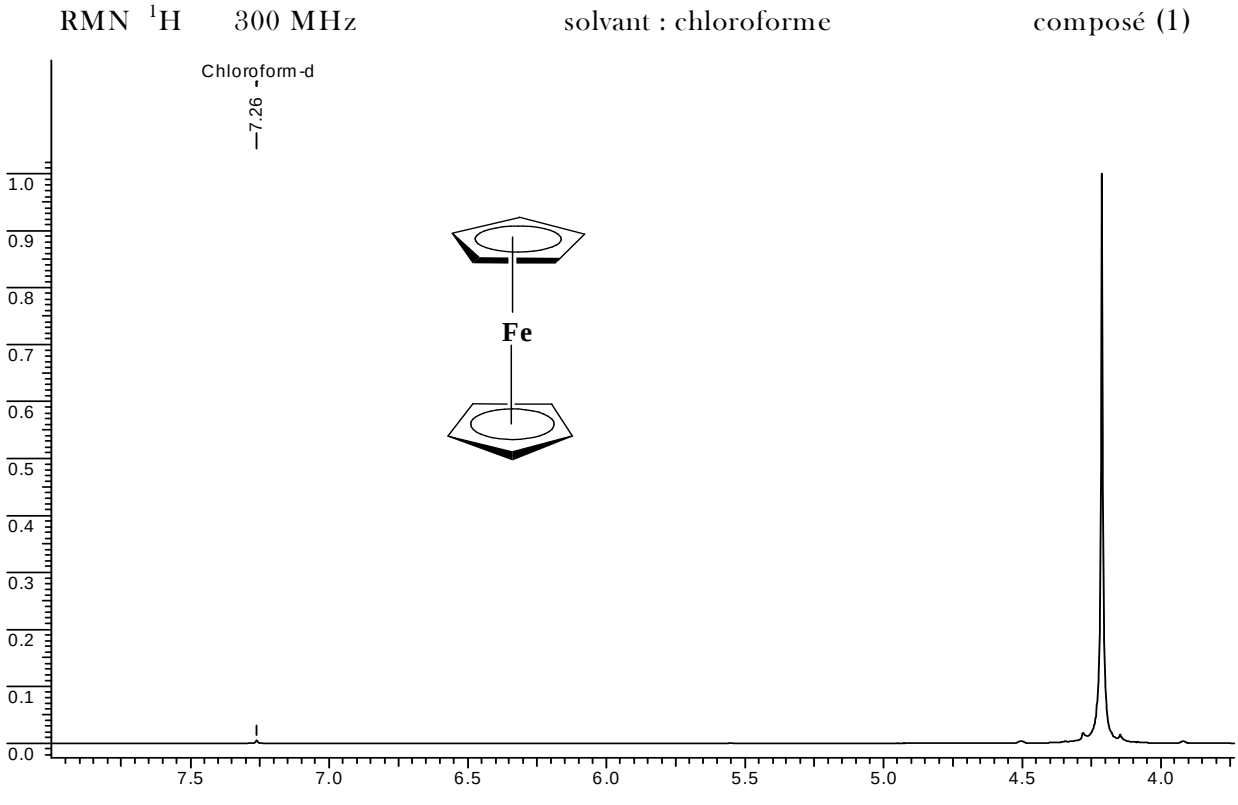

Figure A- 2: The spectrum of ferrocene in the chloroform by RMN^{1}H.

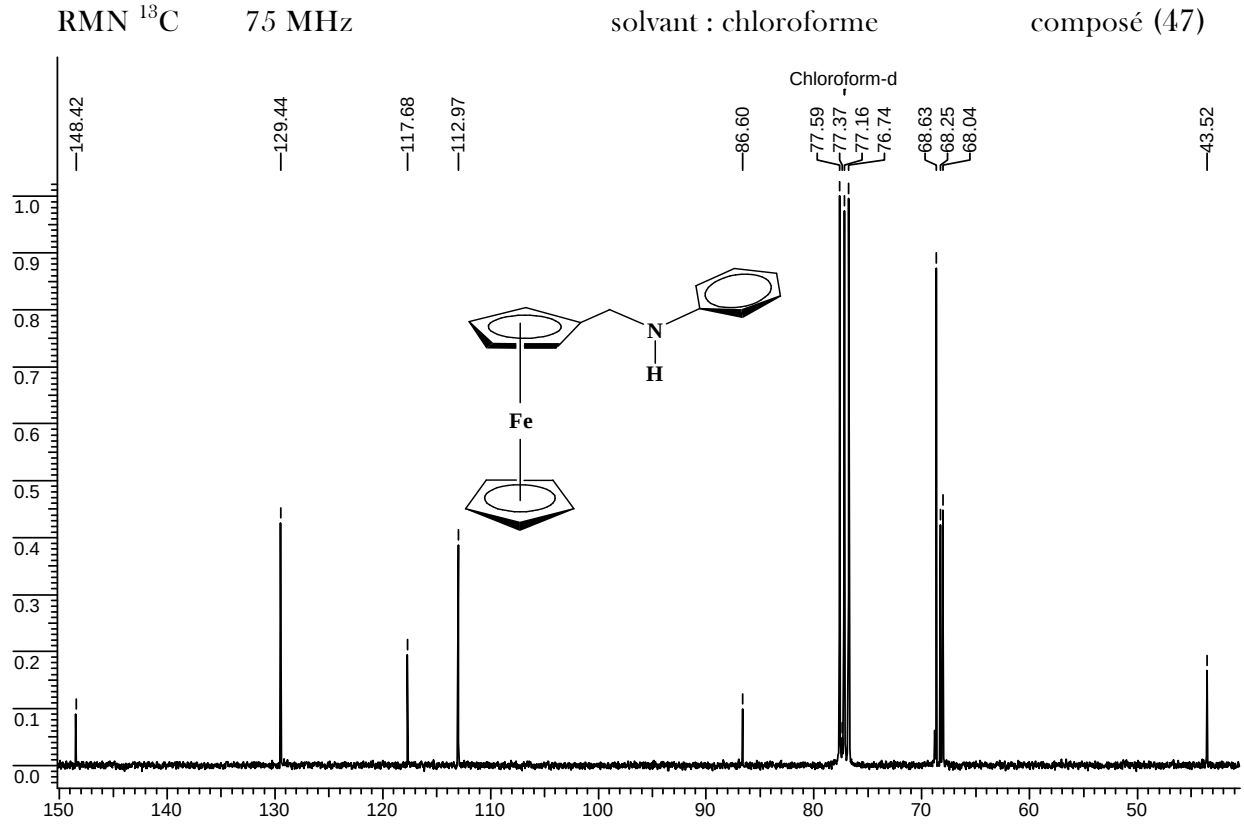

Figure A- 3 : The spectrum of ferrocenyl methyl aniline in the chloroform by RMN^{13}C.

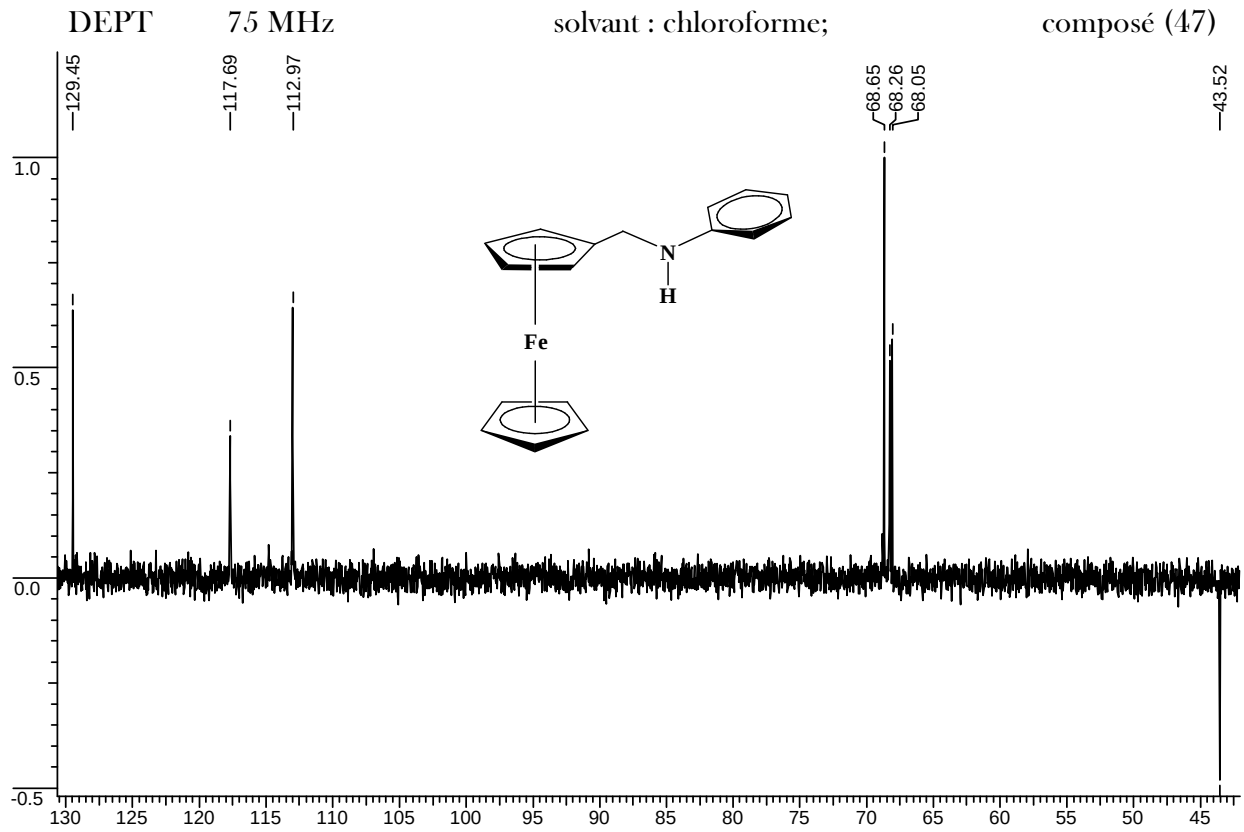

Figure A- 4 : the spectrum of ferrocenyl methyl aniline by DEPT.

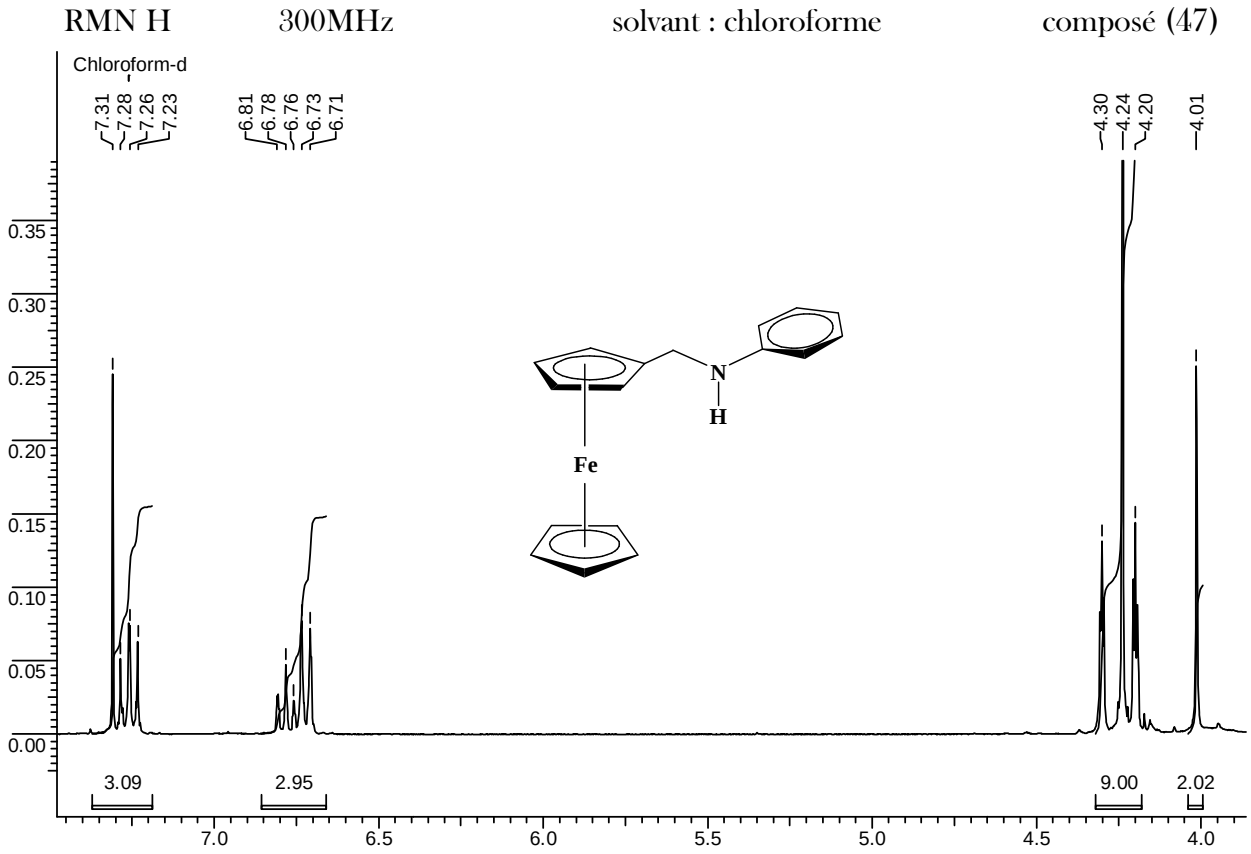

Figure A- 5 : the spectrum of ferrocenyl methyl aniline by RMN^{1}H.

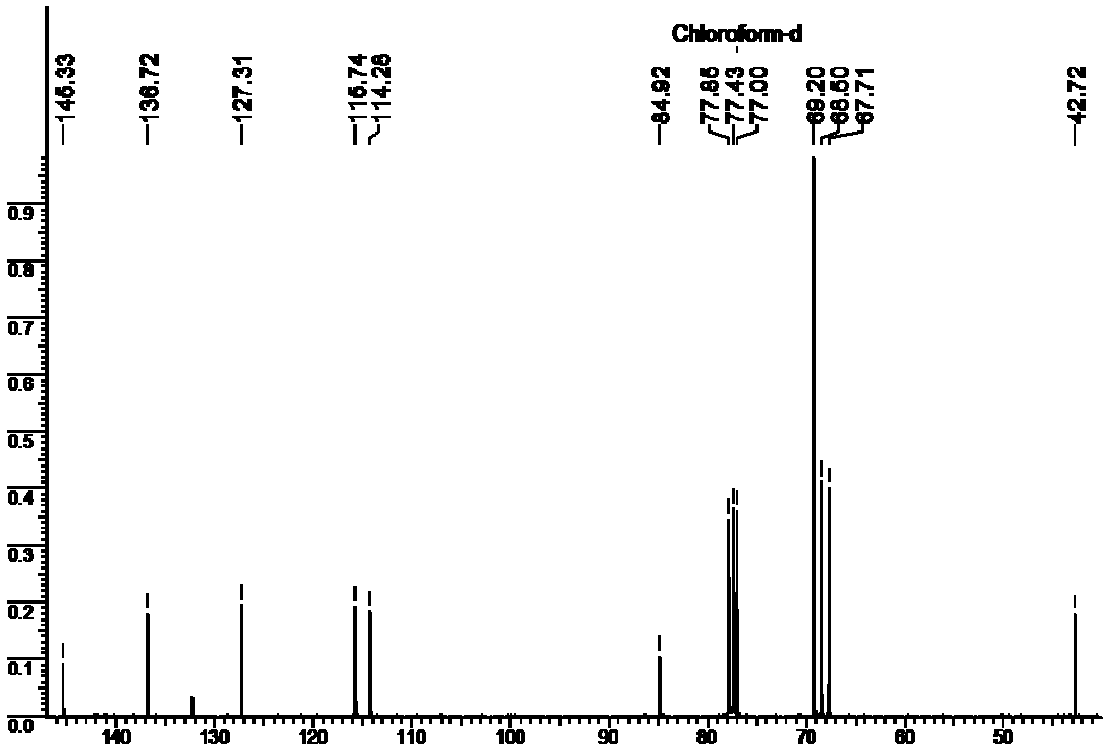

Figure A- 6 : The spectrum of N-(ferrocenyl methyl)-2-nitro aniline.

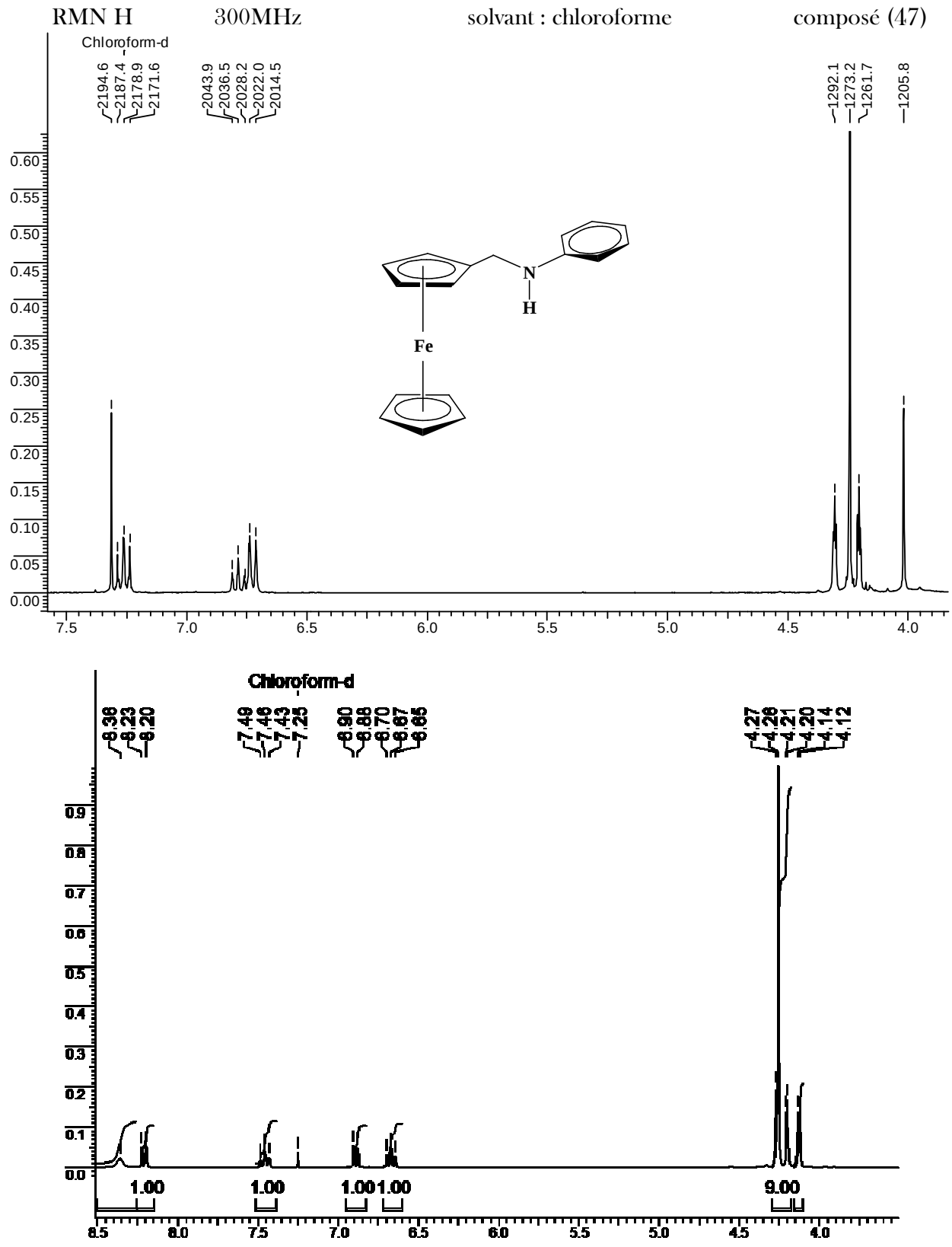

Figure A- 7 : The spectrum of ferrocenyl methyl aniline by RMN^{1}H.

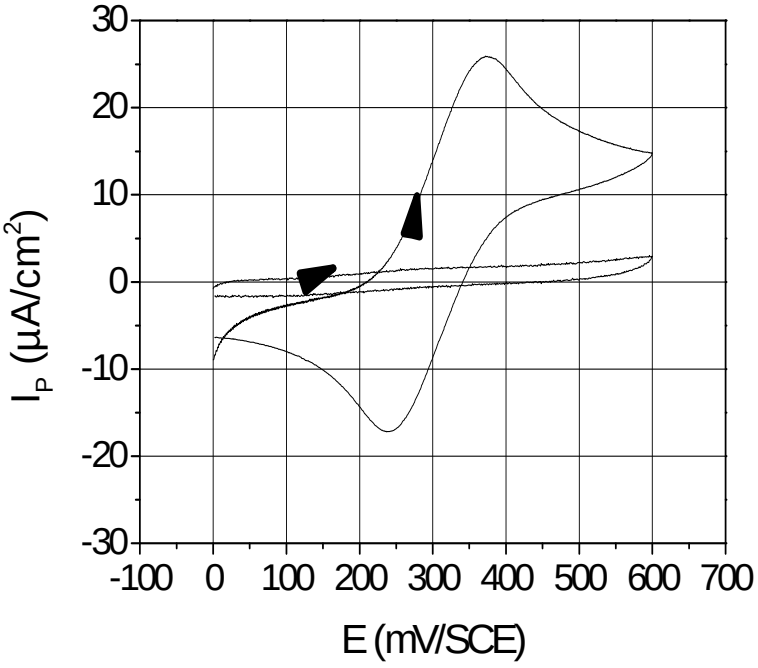

Figure A- 8 : the overlays of the volatammogram of the supporting electrolyte and the volatammogram of ferrocene at100 mV/s, in aqueous ethanol (81%) in window potential of 0-600 mV.

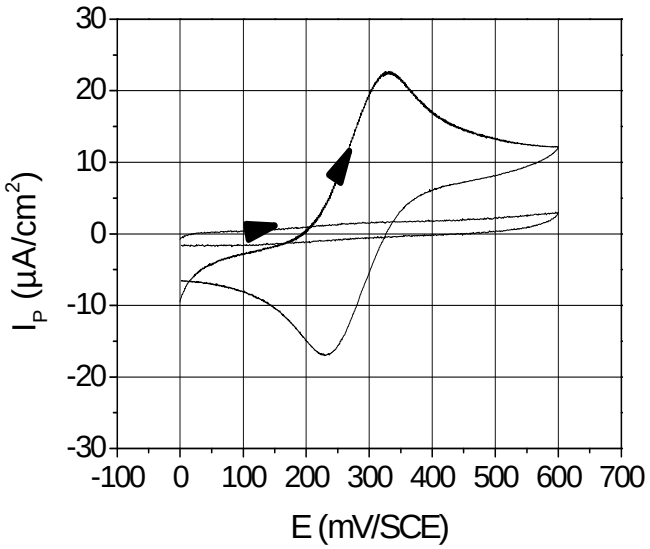

Figure A- 9 : the overlays of the volatammogram of the supporting electrolyte and the volatammogram of ferrocene at100 mV/s, in aqueous ethanol (73%) in window potential of 0-600 mV.

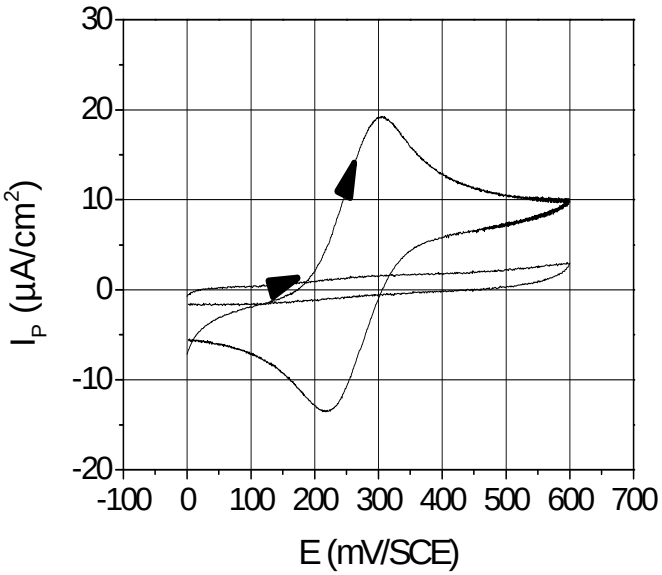

Figure A- 10: the overlays of the volatammogram of the supporting electrolyte and the volatammogram of ferrocene at100 mV/s, in aqueous ethanol (66%) in window potential of 0-600 mV.

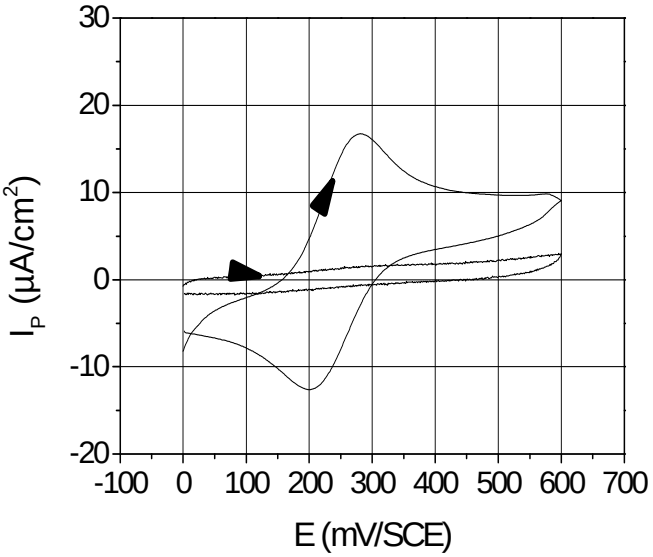

Figure A- 11 : the overlays of the volatammogram of the supporting electrolyte and the volatammogram of ferrocene at100 mV/s, in aqueous ethanol (59%) in window potential of 0-600 mV.

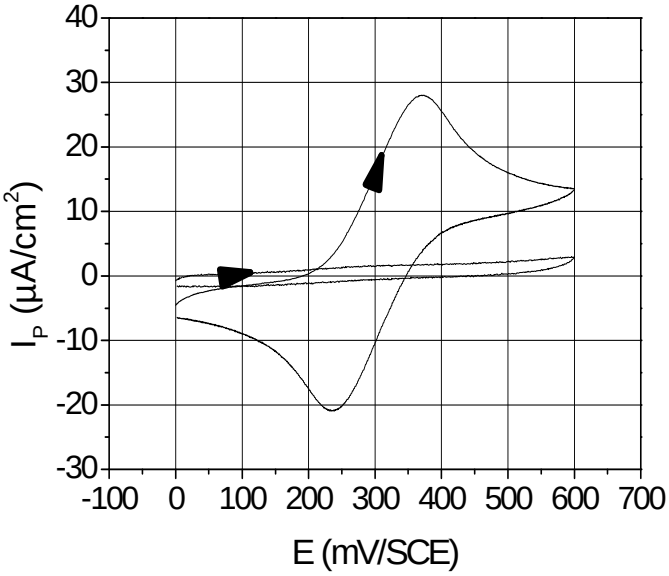

Figure A- 12 : the overlays of the volatammogram of the supporting electrolyte and the volatammogram of ferrocenyl methyl aniline at100 mV/s, in aqueous ethanol (81%) in window potential of 0-600 mV, (Vs/SCE), 25 ^{0}C.

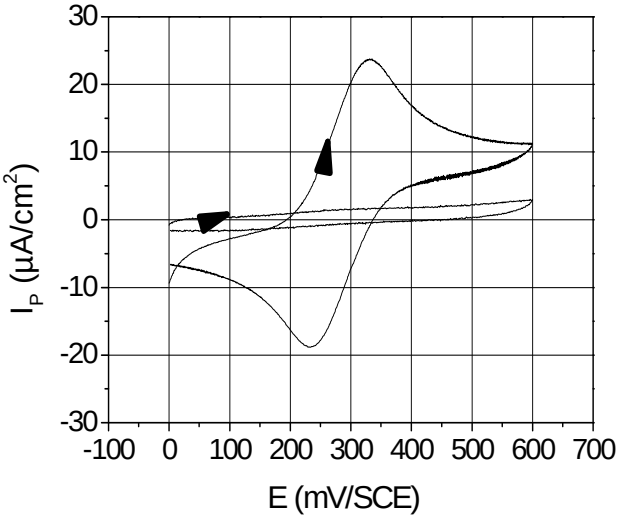

Figure A- 13 : the overlays of the volatammogram of the supporting electrolyte and the volatammogram of ferrocenyl methyl aniline at100 mV/s, in aqueous ethanol (73%) in window potential of 0-600 mV, (Vs/SCE), 25 ^{0}C.

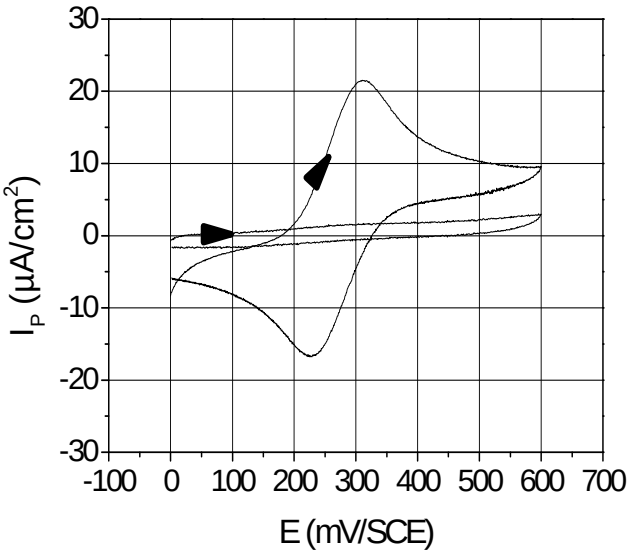

Figure A- 14 : the overlays of the volatammogram of the supporting electrolyte and the volatammogram of ferrocenyl methyl aniline at100 mV/s, in aqueous ethanol (66%) in window potential of 0-600 mV, (Vs/SCE), 25 ^{0}C.

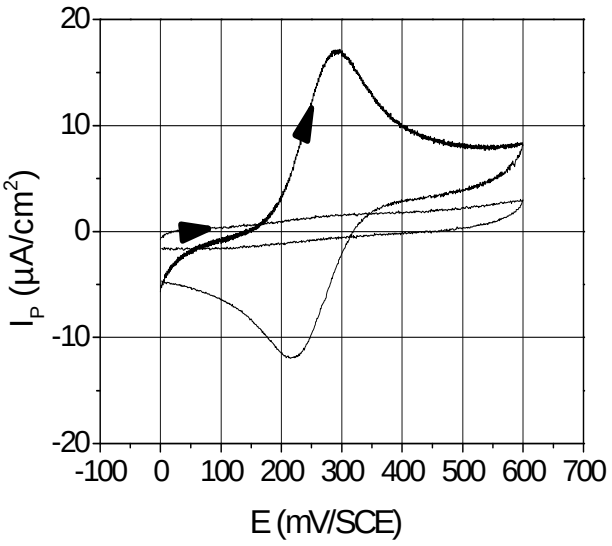

Figure A- 15 : the overlays of the volatammogram of the supporting electrolyte and the volatammogram of ferrocenyl methyl aniline at100 mV/s, in aqueous ethanol (59%) in window potential of 0-600 mV, (Vs/SCE), 25 ^{0}C.

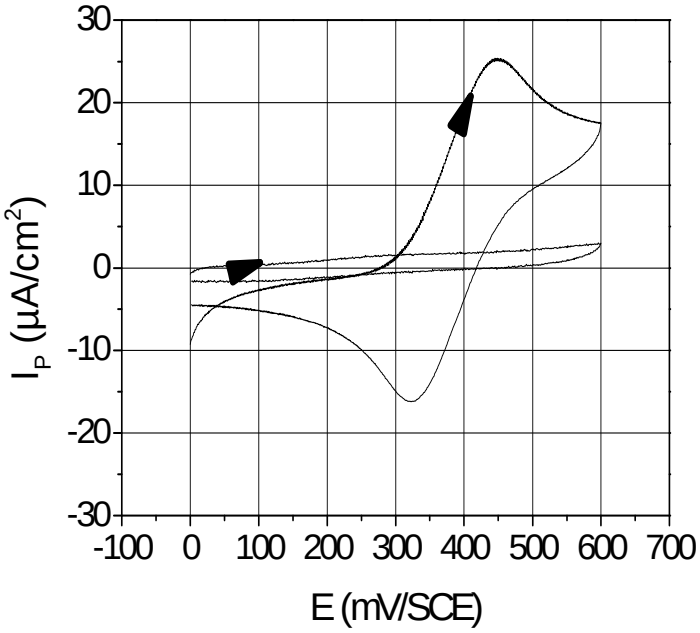

Figure A- 16 : the overlays of the volatammogram of the supporting electrolyte and the volatammogram of N-(ferrocenyl methyl)-2-nitro aniline at100 mV/s, in aqueous ethanol (81%) in window potential of 0-600 mV, (Vs/SCE), 25 ^{0}C.

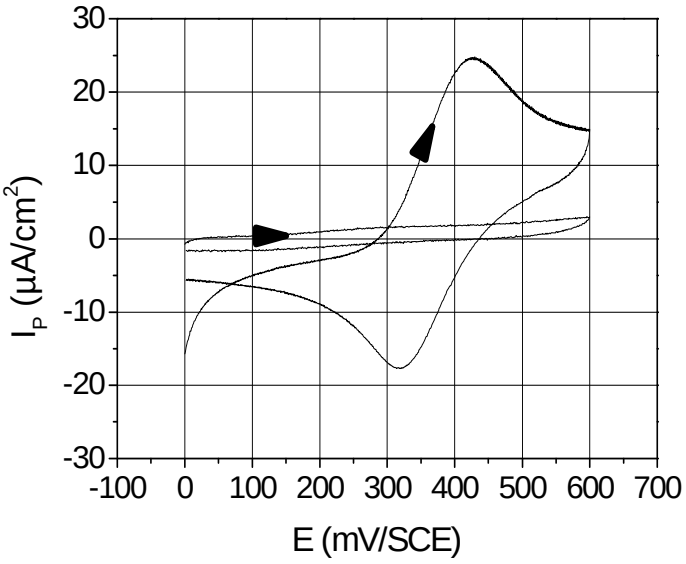

Figure A- 17 : the overlays of the volatammogram of the supporting electrolyte and the volatammogram of N-(ferrocenyl methyl)-2-nitro aniline at100 mV/s, in aqueous ethanol (73%) in window potential of 0-600 mV, (Vs/SCE), 25 ^{0}C.

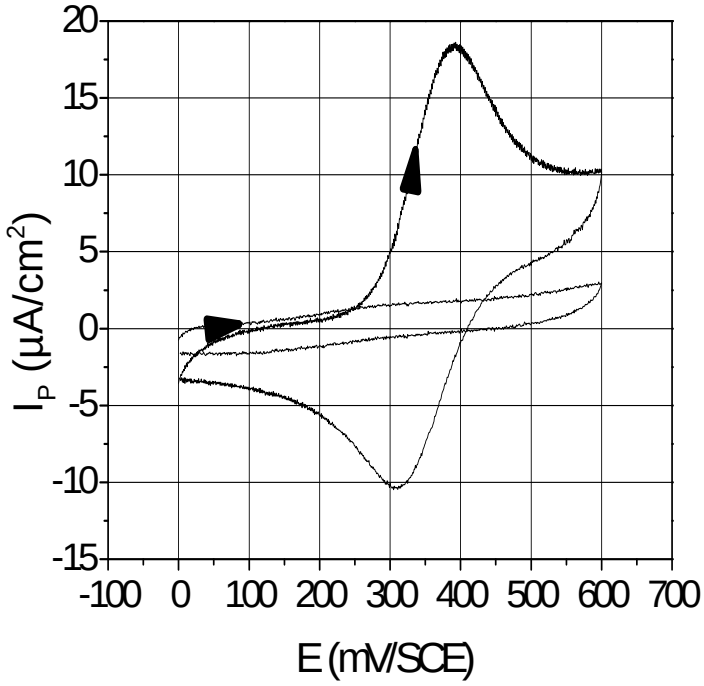

Figure A- 18 : the overlays of the volatammogram of the supporting electrolyte and the volatammogram of N-(ferrocenyl methyl)-2-nitro aniline at100 mV/s, in aqueous ethanol (66%) in window potential of 0-600 mV, (Vs/SCE), 25 ^{0}C.

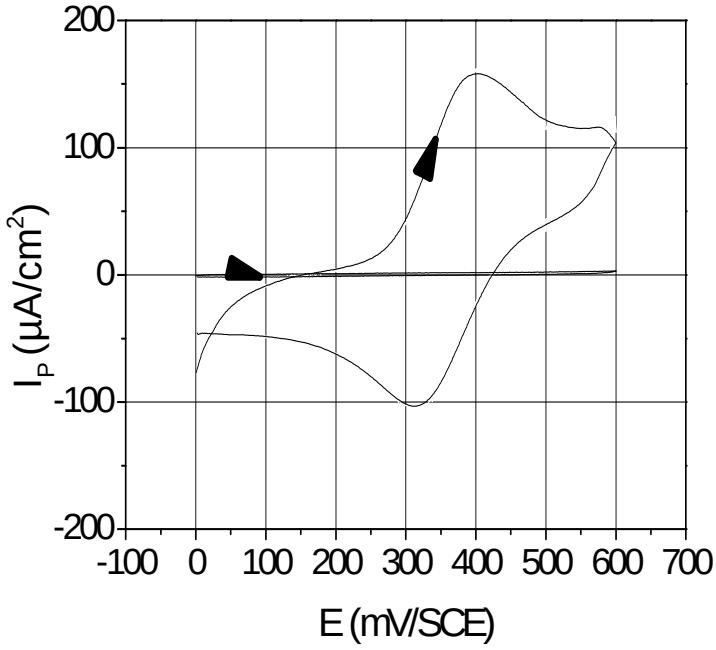

Figure A- 19 : the overlays of the volatammogram of the supporting electrolyte and the volatammogram of N-(ferrocenyl methyl)-2-nitro aniline at100 mV/s, in aqueous ethanol (59%) in window potential of 0-600 mV, (Vs/SCE), 25 ^{0}C.

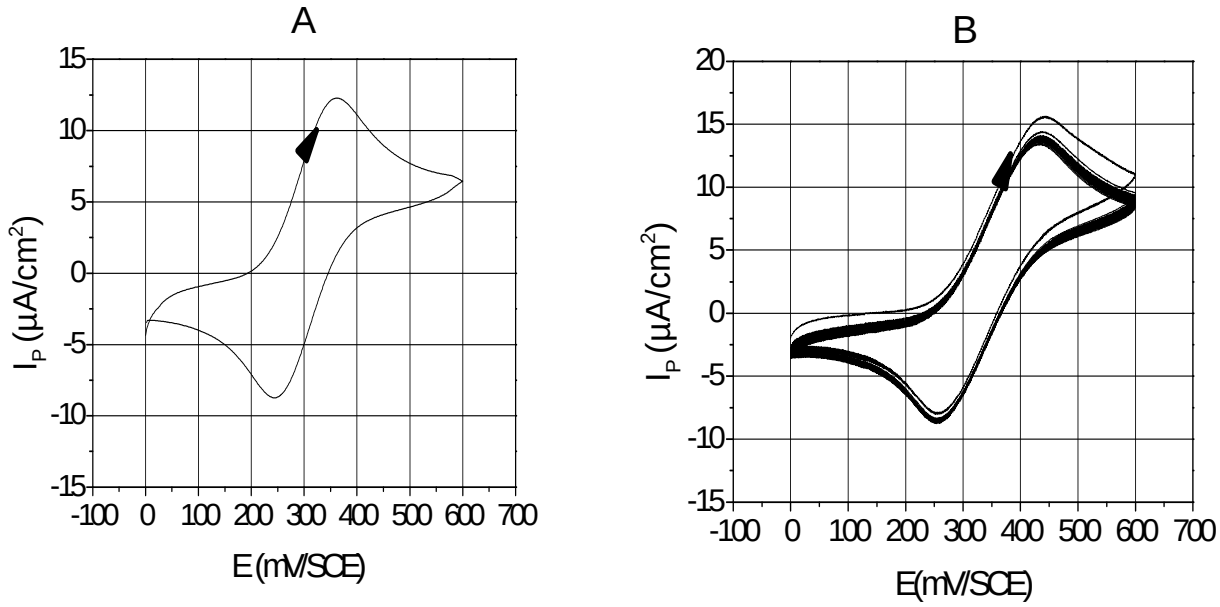

Figure A- 20 : cyclic voltammogram of ferrocene in aqueous ethanol (81%), at100 mV/s, on Pt indicator electrode (A) one cycle, (B) five cycles, (Vs/SCE), 25 ^{0}C.

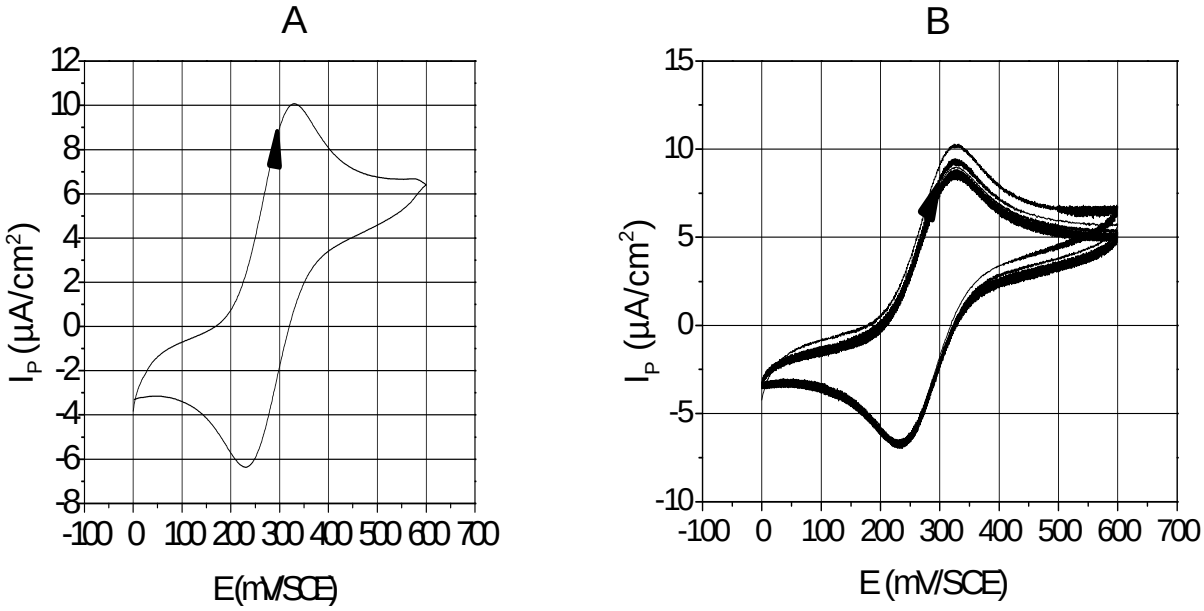

Figure A- 21 : cyclic voltammogram of ferrocene in aqueous ethanol (73%), at100 mV/s, on Pt indicator electrode (A) one cycle, (B) five cycles, (Vs/SCE), 25 ^{0}C.

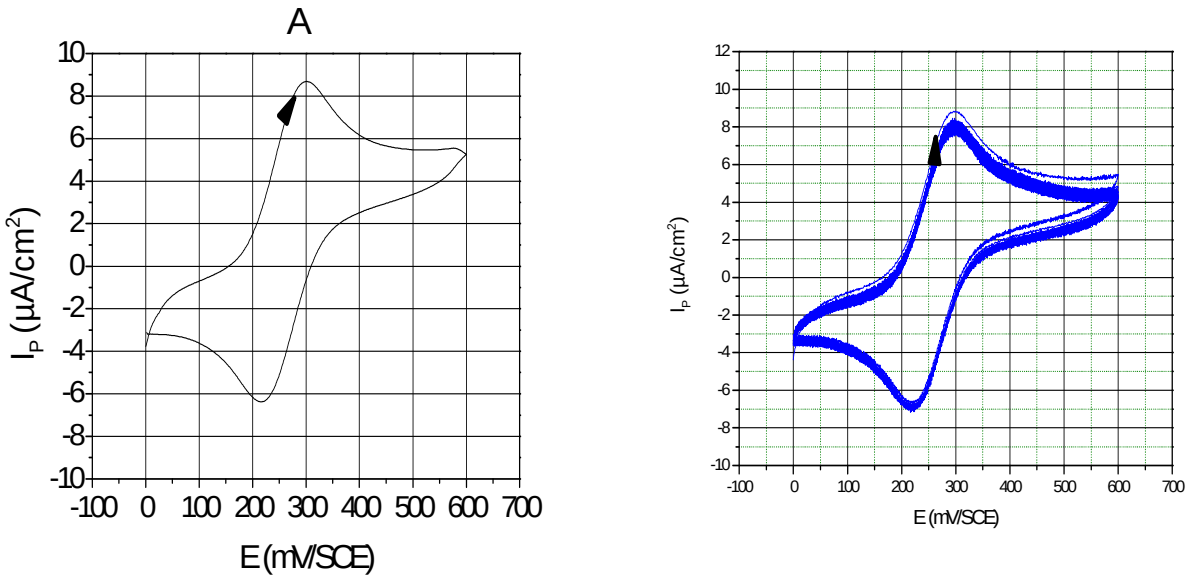

Figure A- 22 : cyclic voltammogram of ferrocene in aqueous ethanol (66%), at100 mV/s, on Pt indicator electrode (A) one cycle, (B) five cycles, (Vs/SCE), 25 ^{0}C.

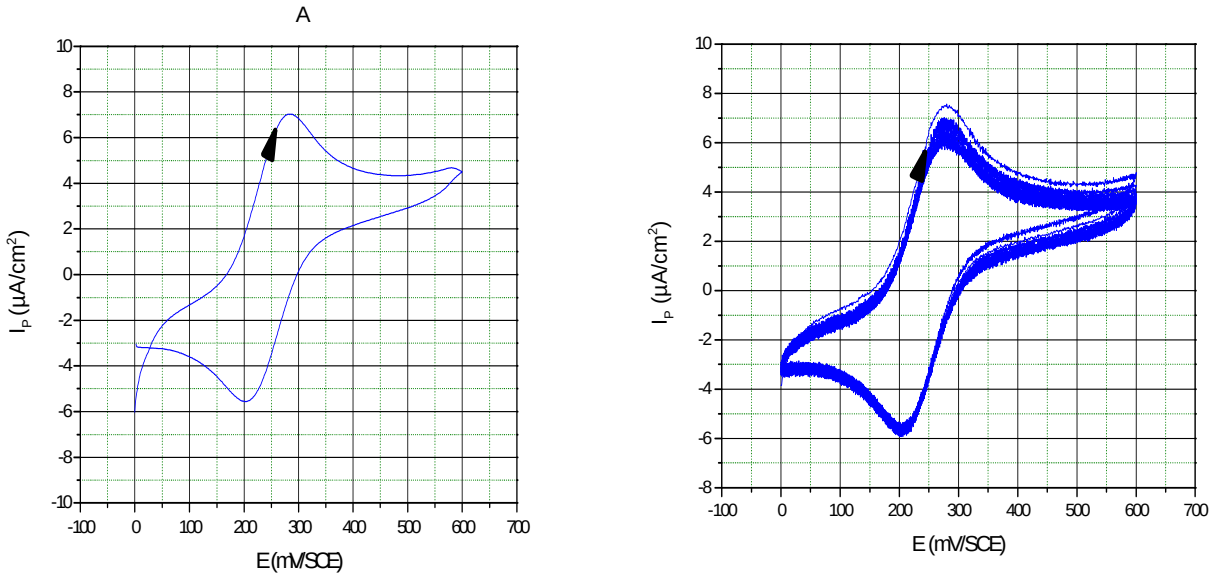

Figure A- 23 : cyclic voltammogram of ferrocene in aqueous ethanol (59%), at100 mV/s, on Pt indicator electrode (A) one cycle, (B) five cycles, (Vs/SCE), 25 ^{0}C.

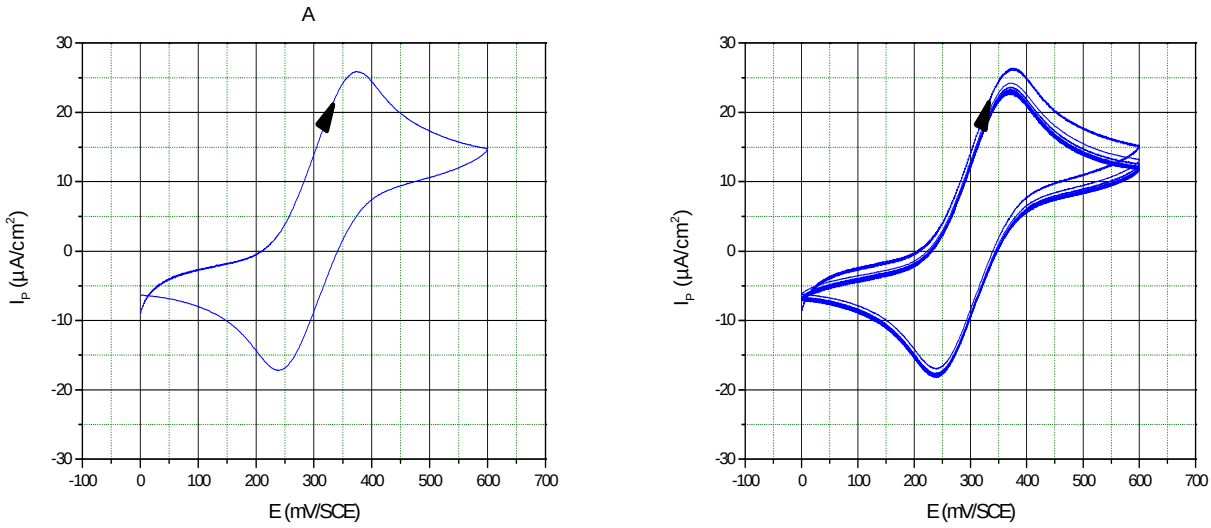

Figure A- 24: cyclic voltammogram of ferrocene in aqueous ethanol (81%), at100 mV/s, on GC indicator electrode (A) one cycle, (B) five cycles, (Vs/SCE), 25 ^{0}C.

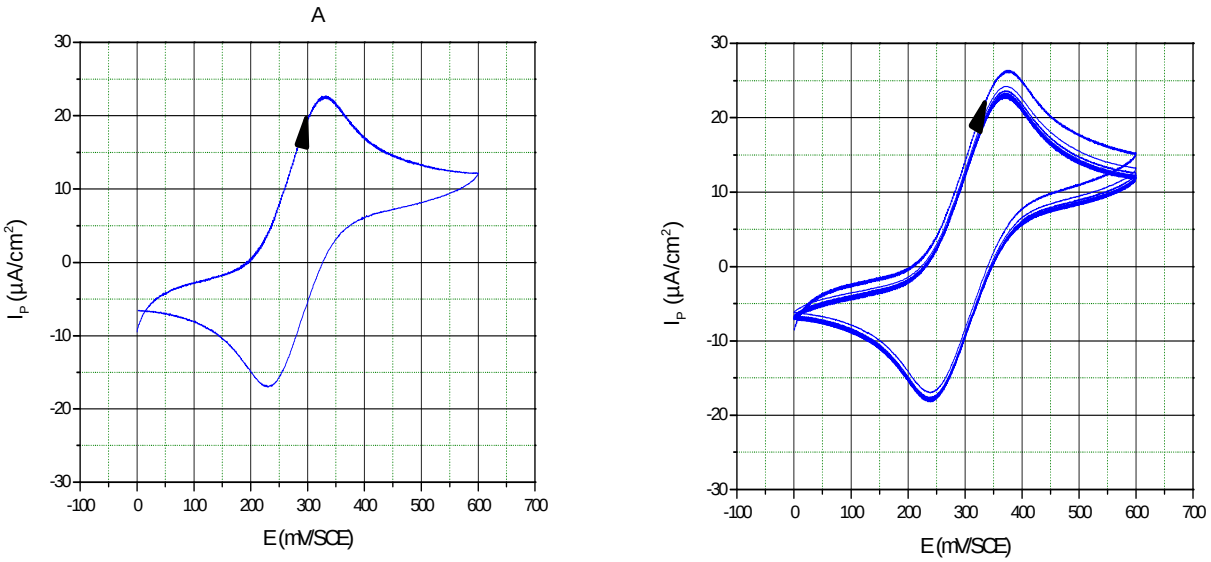

Figure A- 25 : cyclic voltammogram of ferrocene in aqueous ethanol (73%), at100 mV/s, on GC indicator electrode (A) one cycle, (B) five cycles, (Vs/SCE), 25 ^{0}C.

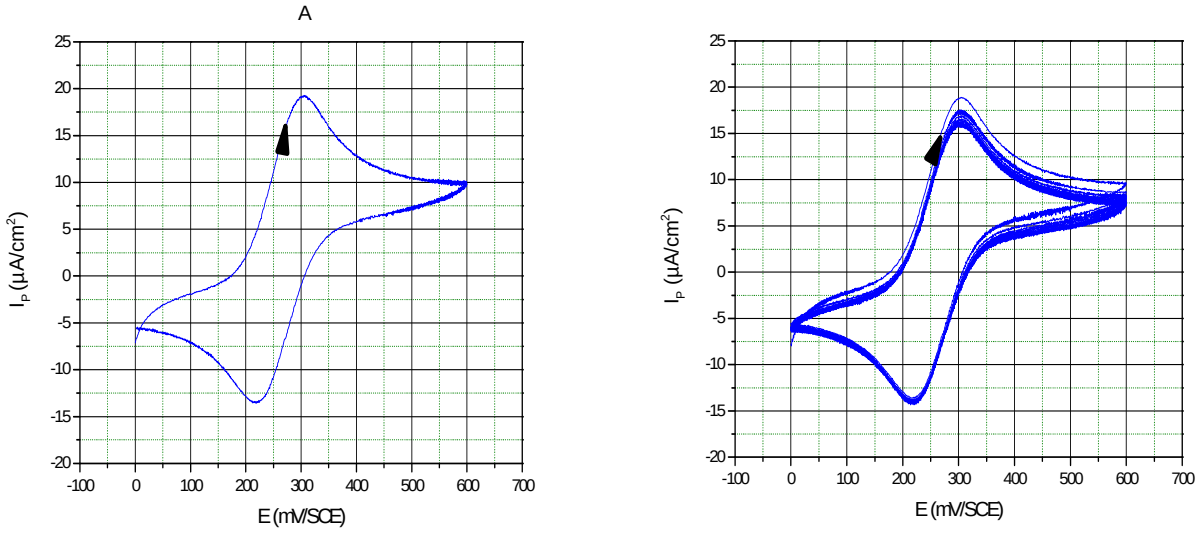

Figure A- 26 : cyclic voltammogram of ferrocene in aqueous ethanol (66%), at100 mV/s, on GC indicator electrode (A) one cycle, (B) five cycles, (Vs/SCE), 25 ^{0}C.

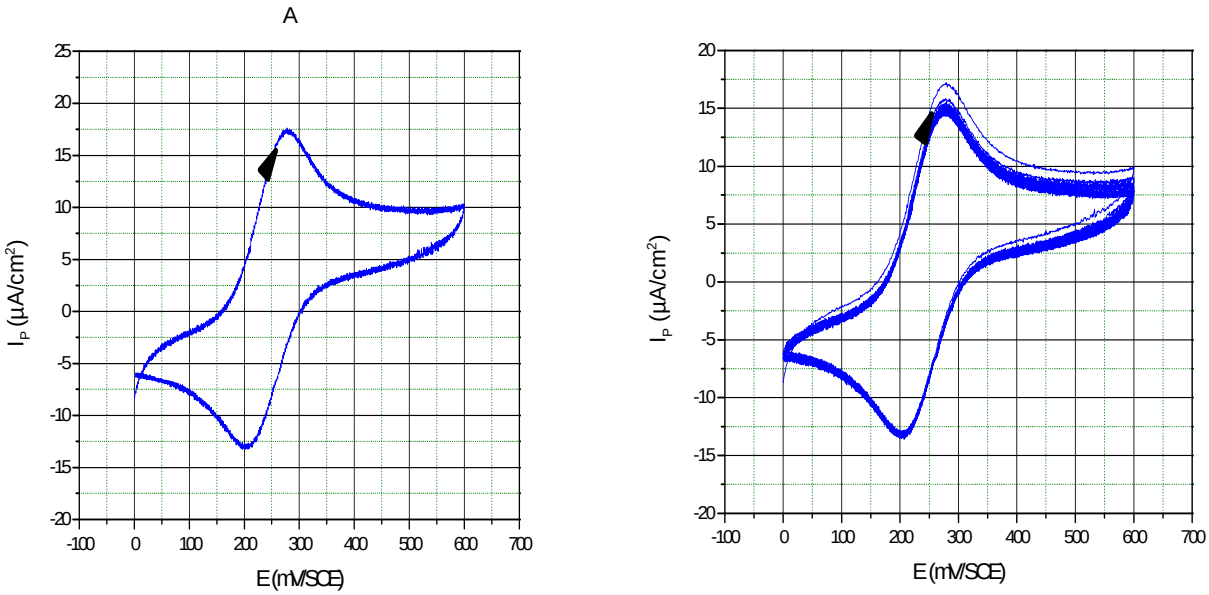

Figure A- 27 : cyclic voltammogram of ferrocene in aqueous ethanol (59%), at100 mV/s, on GC indicator electrode (A) one cycle, (B) five cycles, (Vs/SCE), 25 ^{0}C.

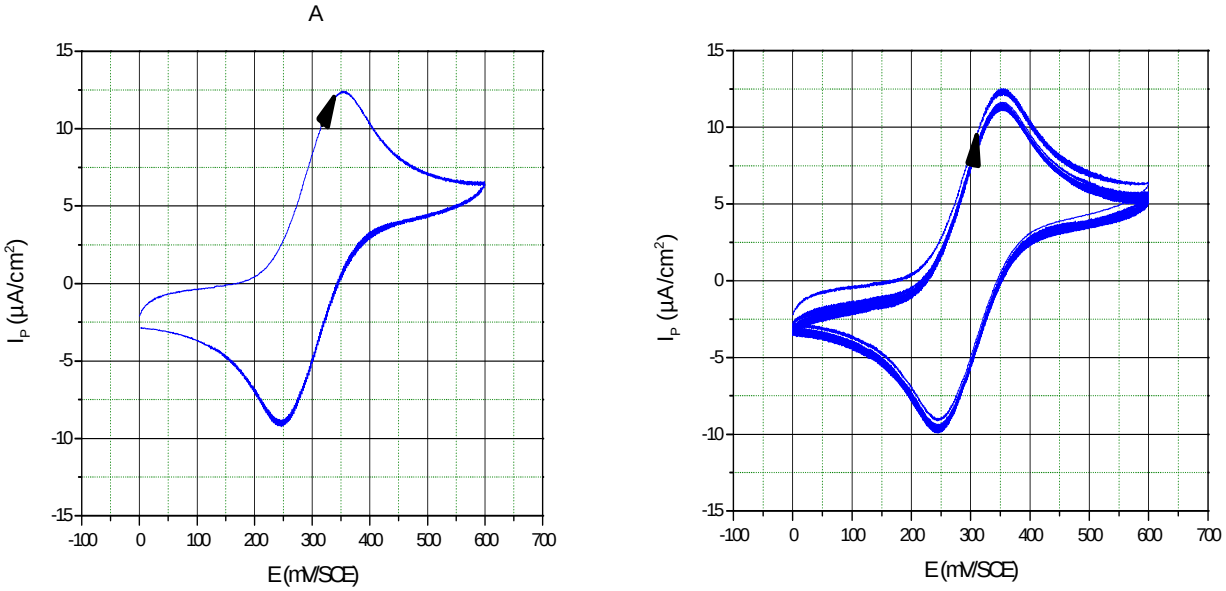

Figure A- 28 : cyclic voltammogram of ferrocenyl methyl aniline in aqueous ethanol (81%), at100 mV/s, on Pt indicator electrode (A) one cycle, (B) five cycles, (Vs/SCE), 25 ^{0}C.

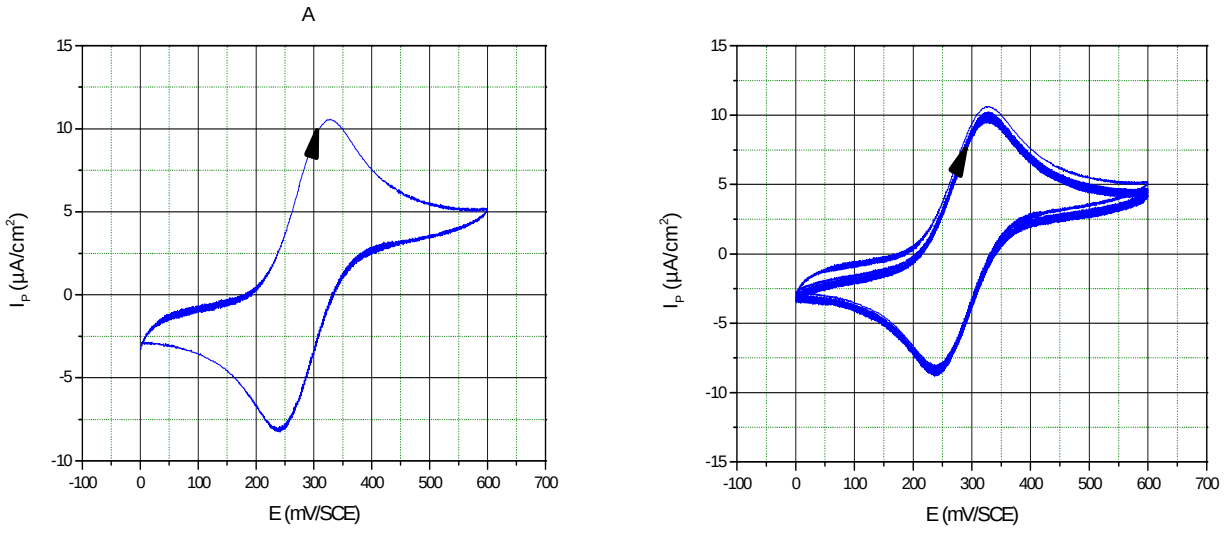

Figure A- 29 : cyclic voltammogram of ferrocenyl methyl aniline in aqueous ethanol (73%), at100 mV/s, on Pt indicator electrode (A) one cycle, (B) five cycles, (Vs/SCE), 25 ^{0}C.

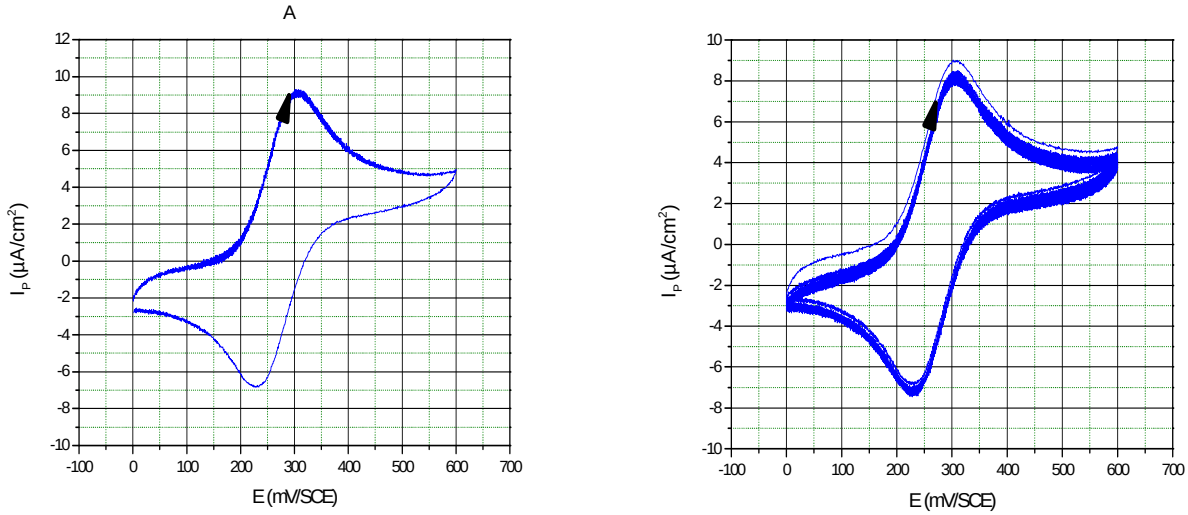

Figure A- 30 : cyclic voltammogram of ferrocenyl methyl aniline in aqueous ethanol (66%), at100 mV/s, on Pt indicator electrode (A) one cycle, (B) five cycles, (Vs/SCE), 25 ^{0}C.

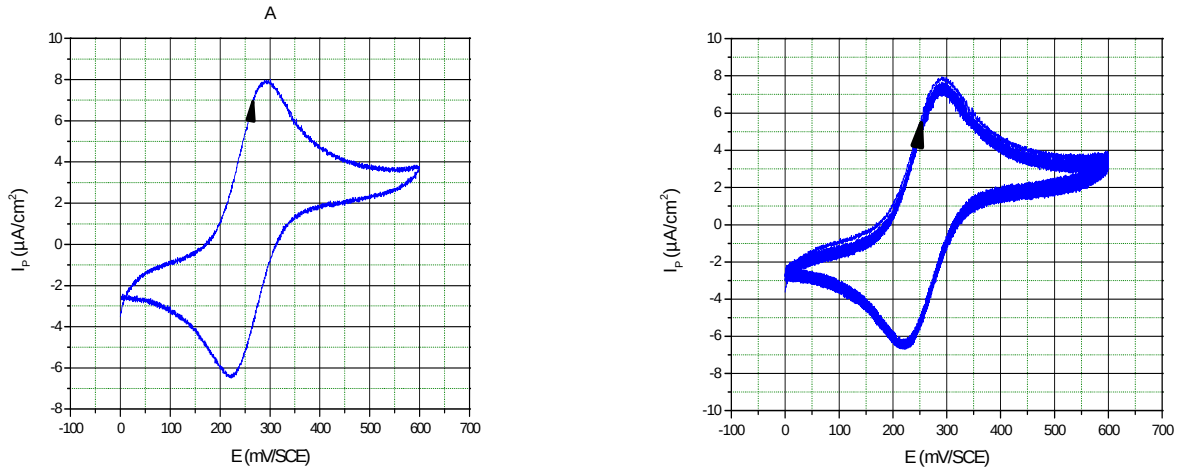

Figure A- 31 : cyclic voltammogram of ferrocenyl methyl aniline in aqueous ethanol (59%), at100 mV/s, on Pt indicator electrode (A) one cycle, (B) five cycles, (Vs/SCE), 25 ^{0}C.

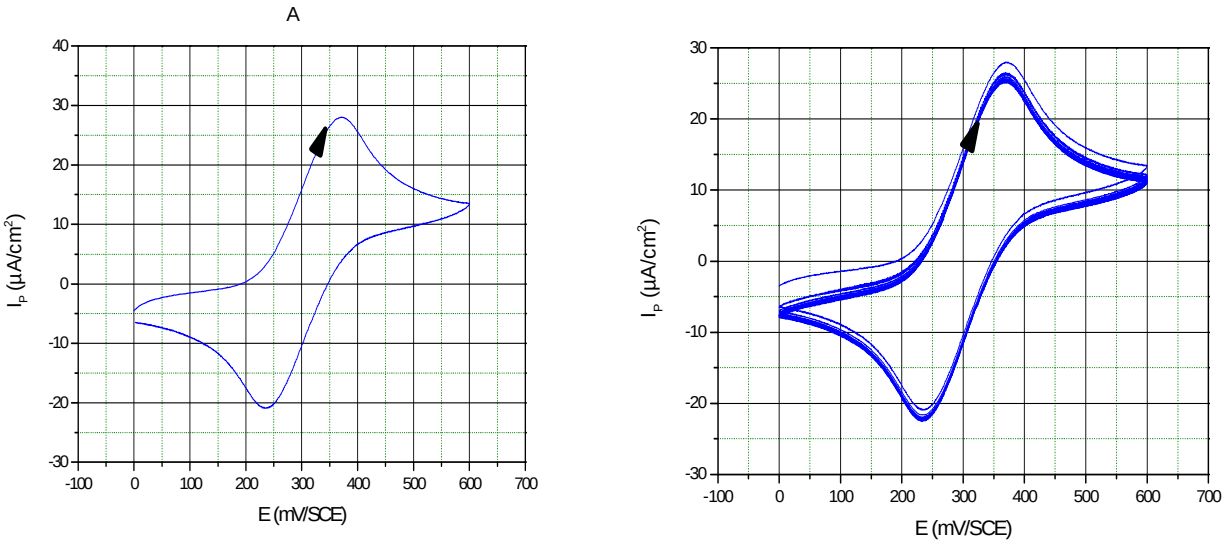

Figure A- 32 : cyclic voltammogram of ferrocenyl methyl aniline in aqueous ethanol (81%), at100 mV/s, on GC indicator electrode (A) one cycle, (B) five cycles, (Vs/SCE), 25 ^{0}C.

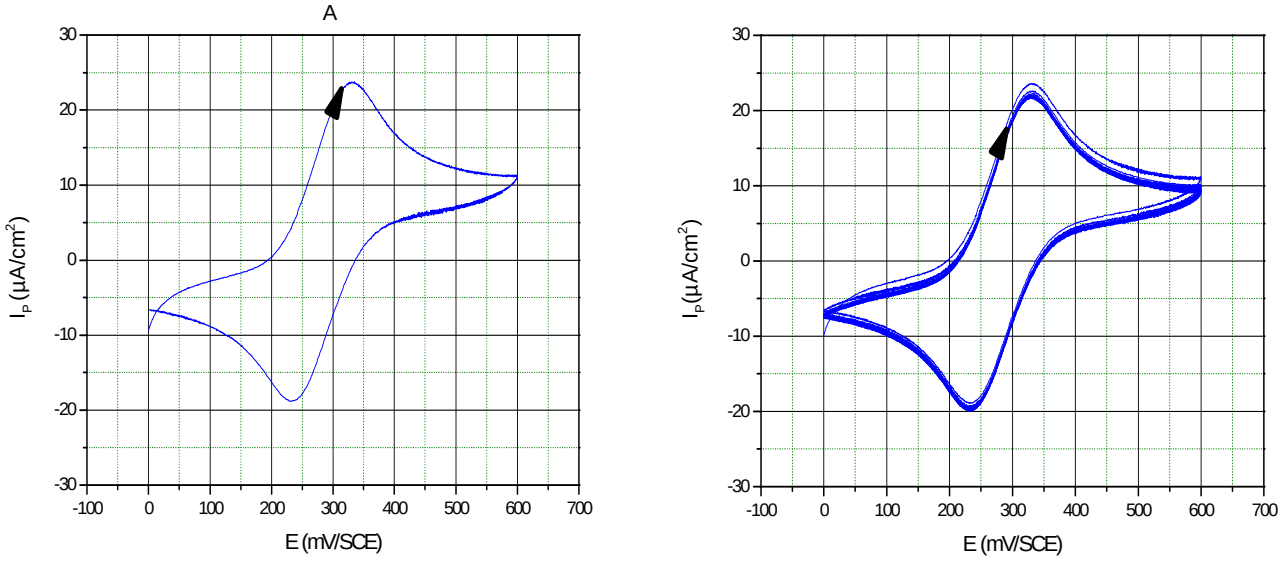

Figure A- 33 : cyclic voltammogram of ferrocenyl methyl aniline in aqueous ethanol (73%), at100 mV/s, on GC indicator electrode (A) one cycle, (B) five cycles, (Vs/SCE), 25 ^{0}C.

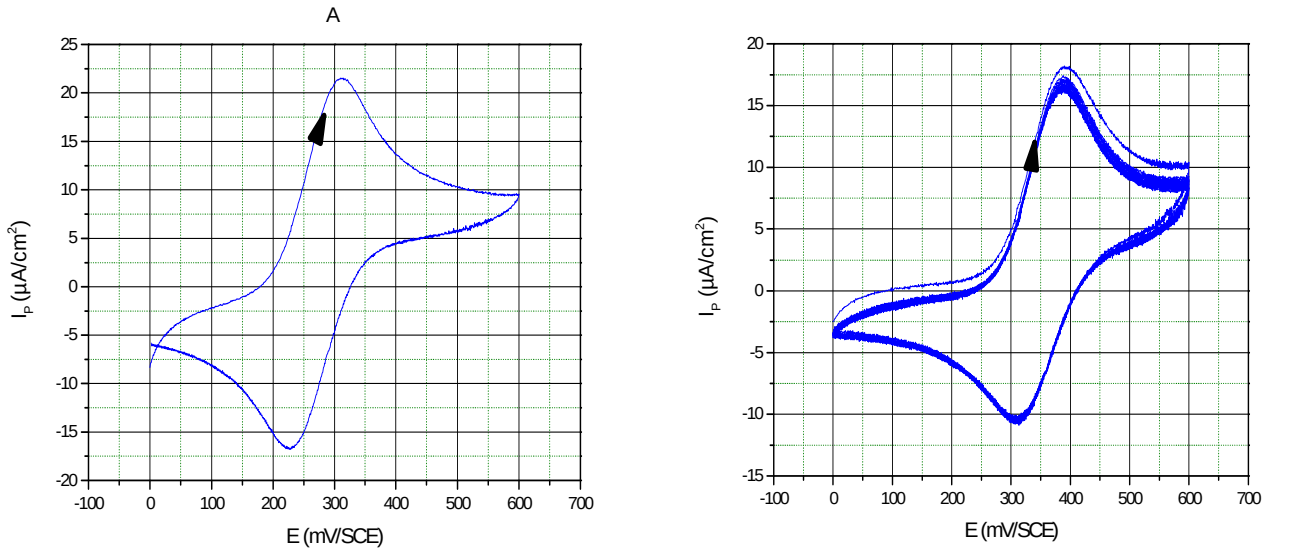

Figure A- 34 : cyclic voltammogram of ferrocenyl methyl aniline in aqueous ethanol (66%), at100 mV/s, on GC indicator electrode (A) one cycle, (B) five cycles, (Vs/SCE), 25 ^{0}C.

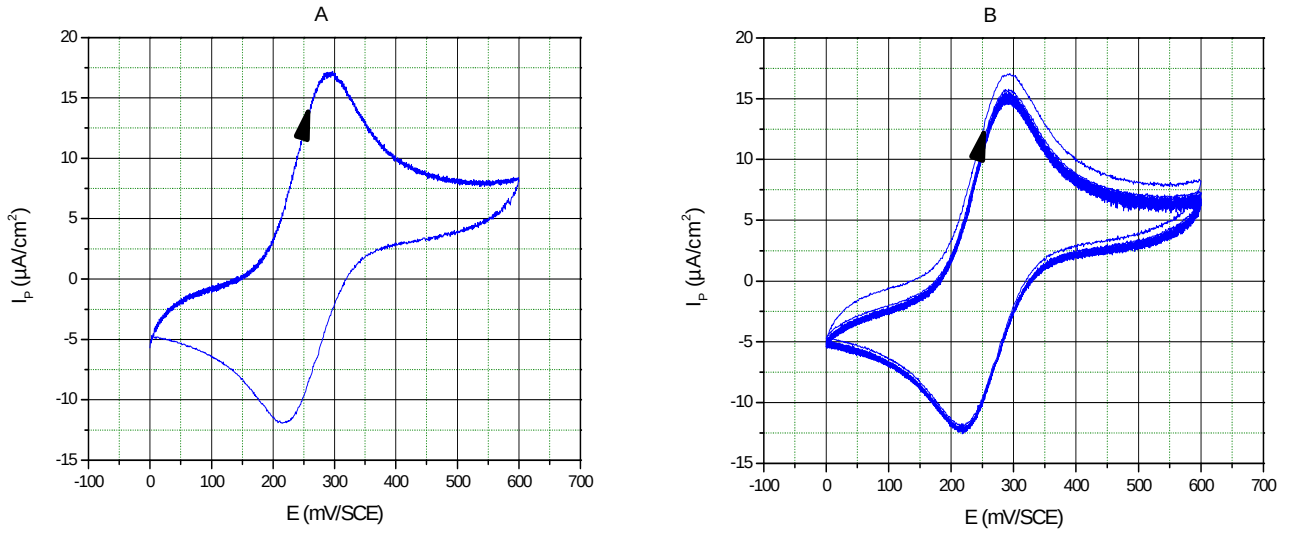

Figure A- 35 : cyclic voltammogram of ferrocenyl methyl aniline in aqueous ethanol (59%), at100 mV/s, on GC indicator electrode (A) one cycle, (B) five cycles, (Vs/SCE), 25 ^{0}C.

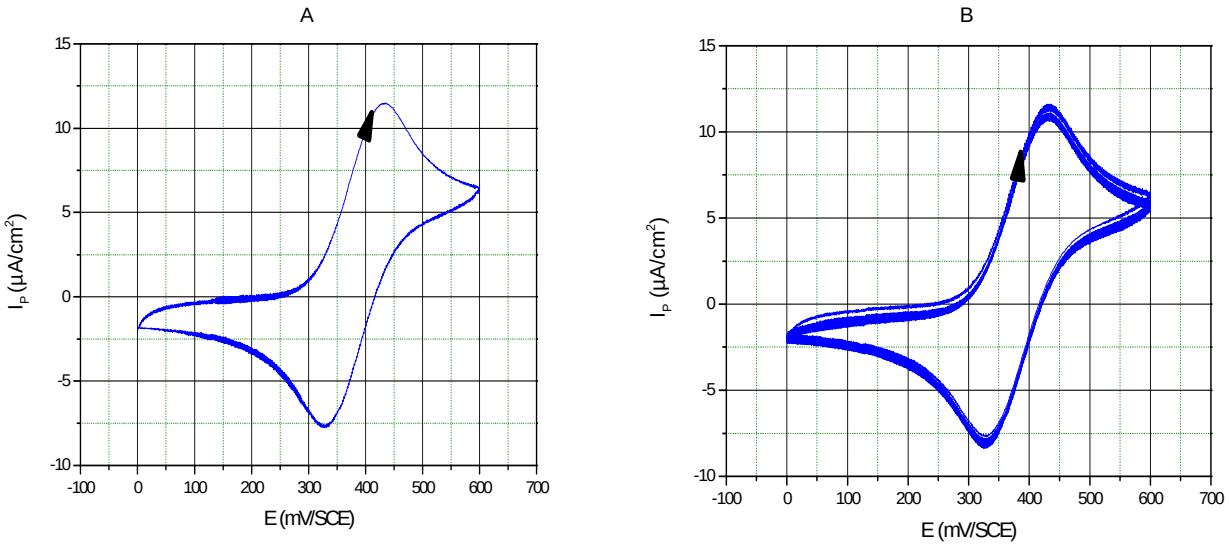

Figure A- 36: cyclic voltammogram of N-(ferrocenyl methyl)-2-nitro aniline in aqueous ethanol (81%), at100 mV/s, on Pt indicator electrode (A) one cycle, (B) five cycles, (Vs/SCE), 25 ^{0}C.

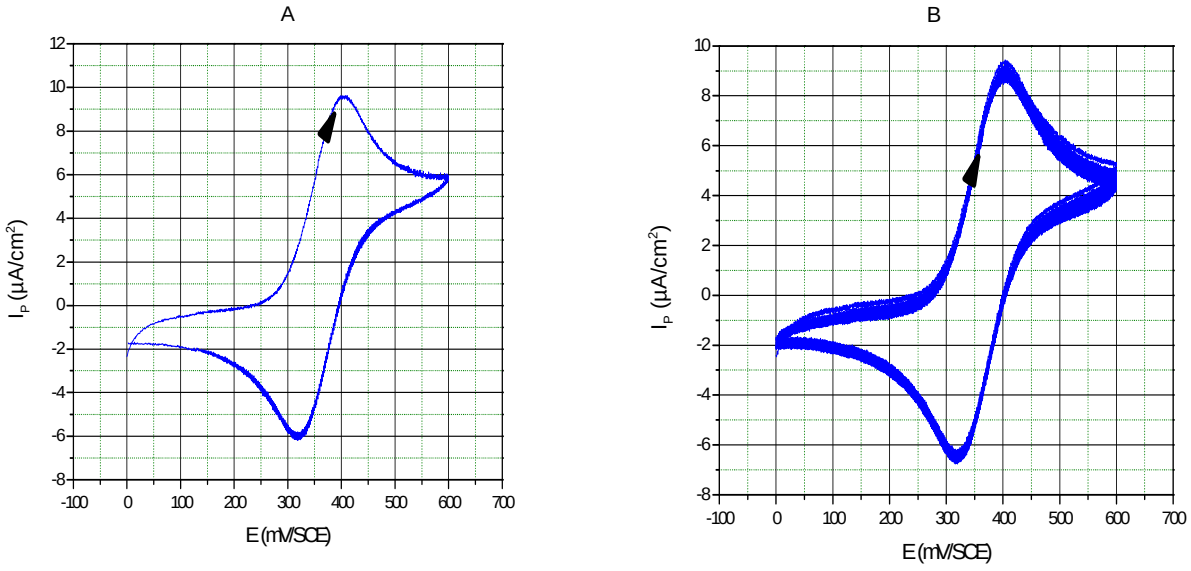

Figure A- 37 : cyclic voltammogram of N-(ferrocenyl methyl)-2-nitro aniline in aqueous ethanol (73%), at100 mV/s, on Pt indicator electrode (A) one cycle, (B) five cycles, (Vs/SCE), 25 ^{0}C.

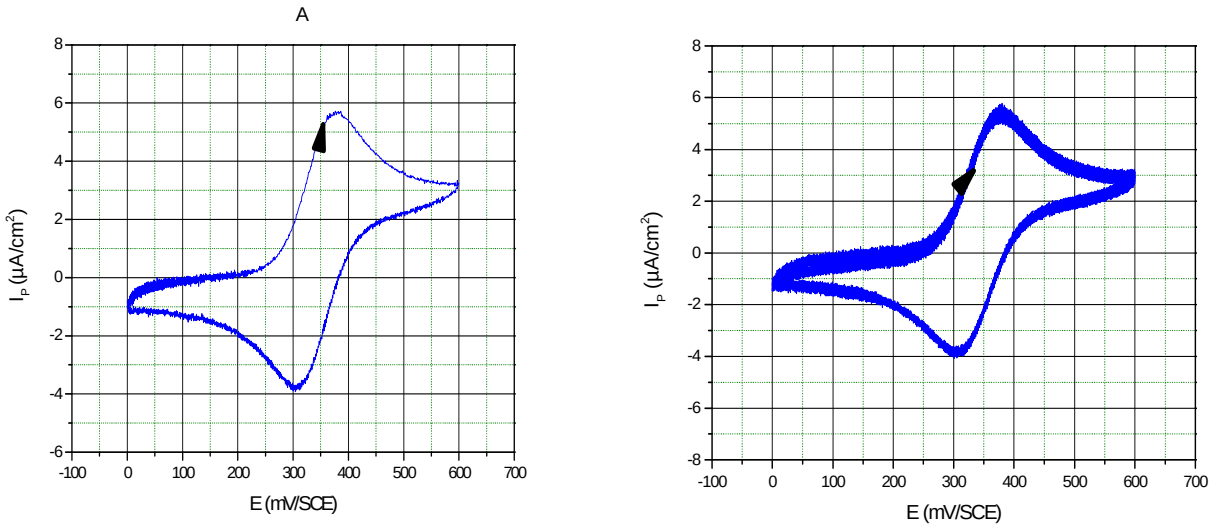

Figure A- 38 : cyclic voltammogram of N-(ferrocenyl methyl)-2-nitro aniline in aqueous ethanol (66%), at100 mV/s, on Pt indicator electrode (A) one cycle, (B) five cycles, (Vs/SCE), 25 ^{0}C.

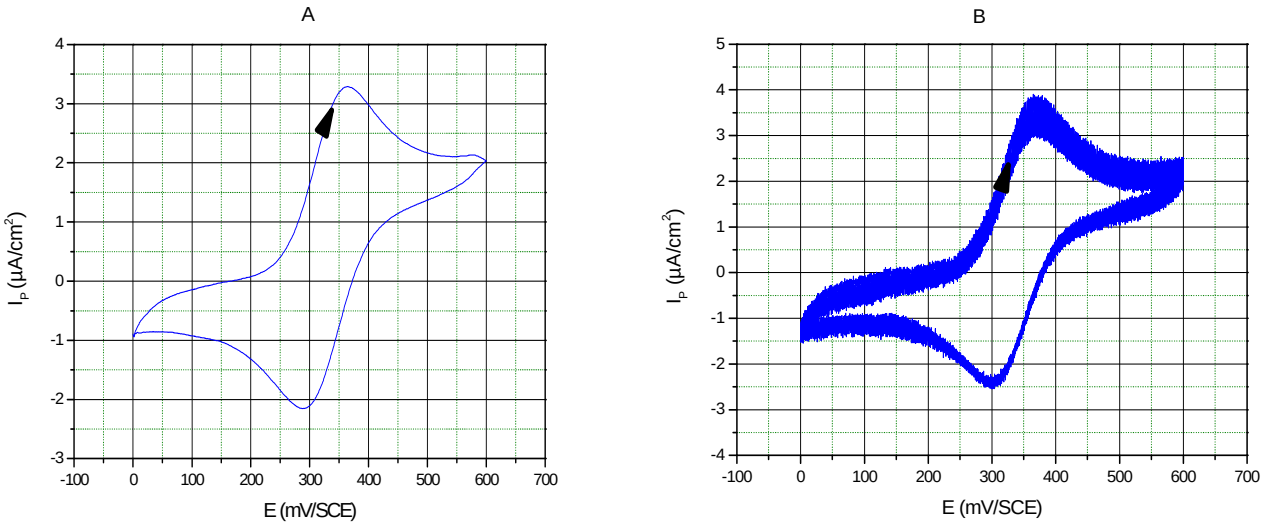

Figure A- 39: cyclic voltammogram of N-(ferrocenyl methyl)-2-nitro aniline in aqueous ethanol (59%), at100 mV/s, on Pt indicator electrode (A) one cycle, (B) five cycles, (Vs/SCE), 25 ^{0}C.

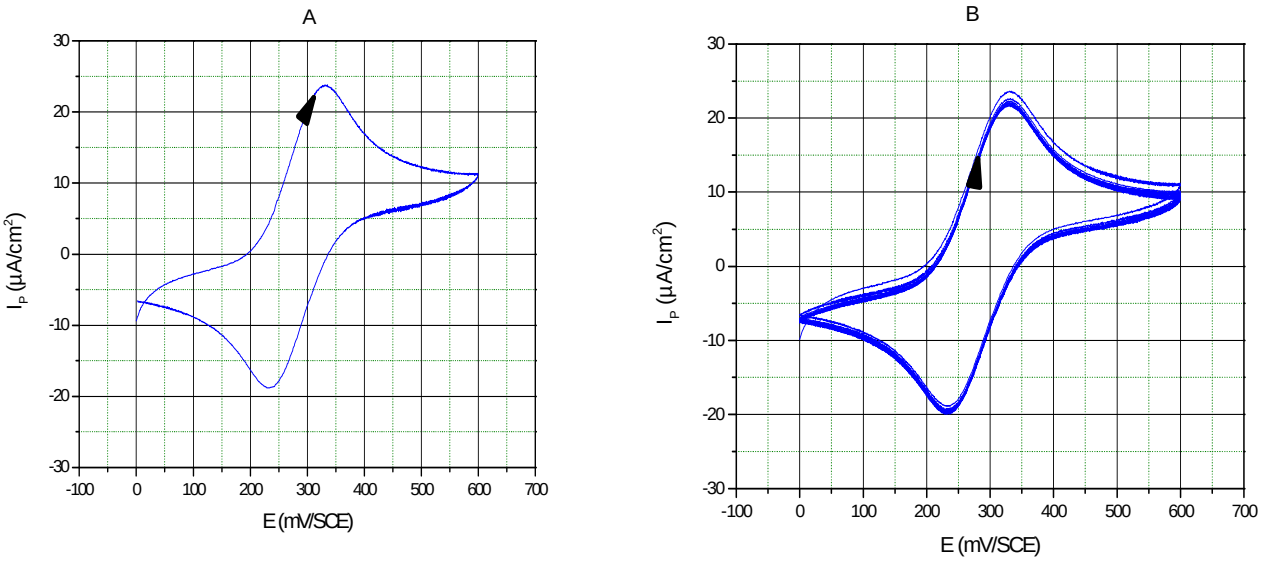

Figure A- 40 : cyclic voltammogram of N-(ferrocenyl methyl)-2-nitro aniline in aqueous ethanol (81%), at100 mV/s, on GC indicator electrode (A) one cycle, (B) five cycles, (Vs/SCE), 25 ^{0}C.

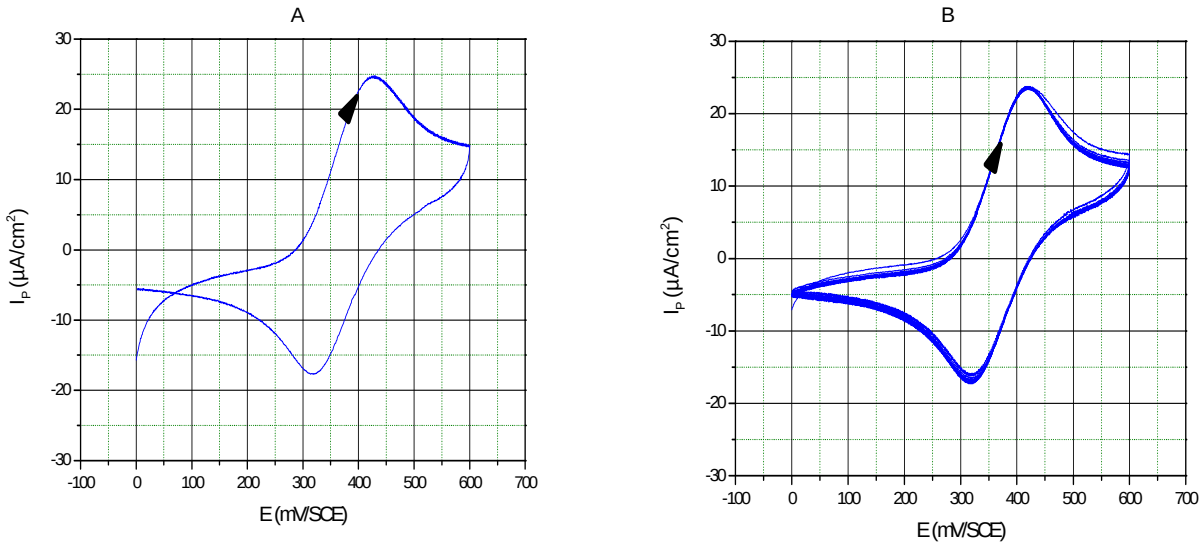

Figure A- 41 : cyclic voltammogram of N-(ferrocenyl methyl)-2-nitro aniline in aqueous ethanol (73%), at100 mV/s, on GC indicator electrode (A) one cycle, (B) five cycles, (Vs/SCE), 25 ^{0}C.

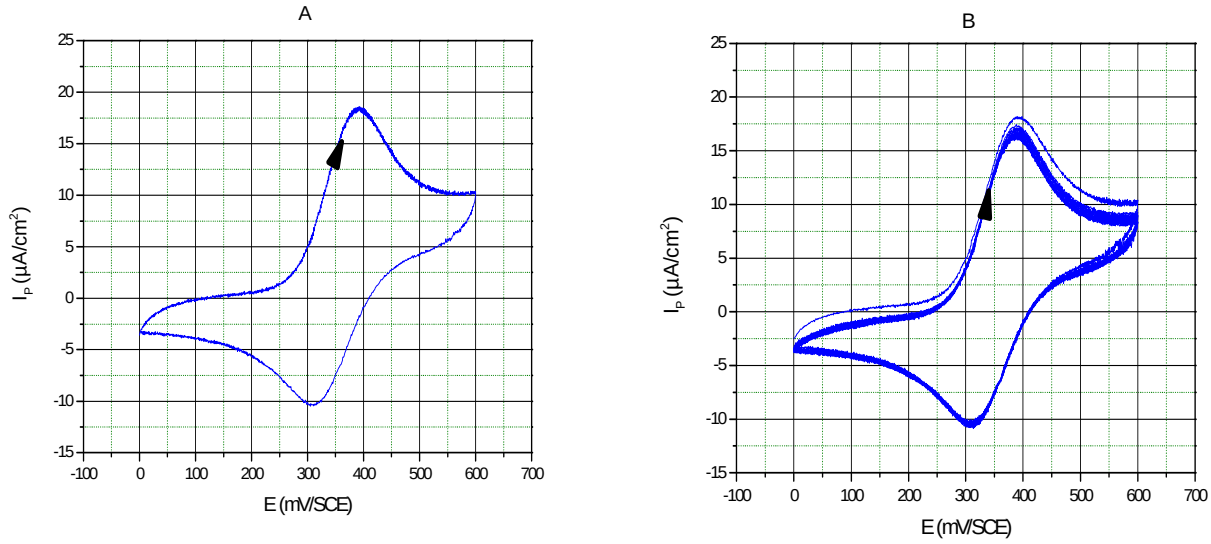

Figure A- 42 : cyclic voltammogram of N-(ferrocenyl methyl)-2-nitro aniline in aqueous ethanol (66%), at100 mV/s, on GC indicator electrode (A) one cycle, (B) five cycles, (Vs/SCE), 25 ^{0}C.

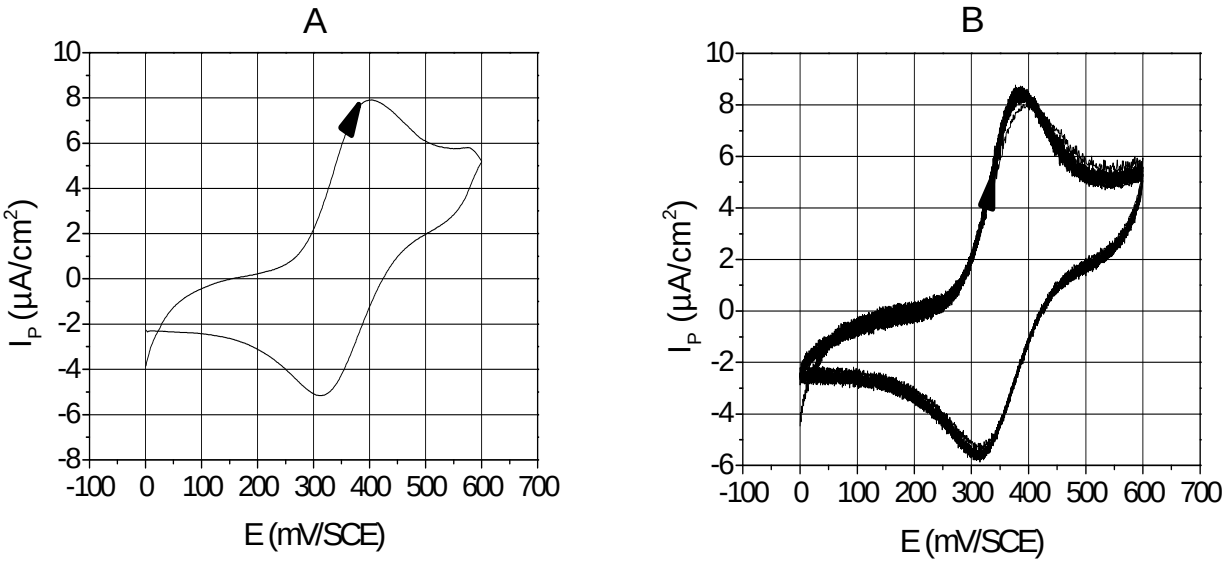

Figure A- 43 : cyclic voltammogram of N-(ferrocenyl methyl)-2-nitro aniline in aqueous ethanol (59%), at100 mV/s, on GC indicator electrode (A) one cycle, (B) five cycles, (Vs/SCE), 25 ^{0}C.